ไดอะซีแพมโซลิดลิปิดนาโนพาทิเคิล
โดยใช้กลีเซอรอล บีฮีเนท ด้วยกระบวนการโฮโมจีไนเซชันอุณหภูมิสูง

นาง อมรรัตน์ วิริยะโรจน์

สถาบันวิทยบริการ
จุฬาลงกรณ์มหาวิทยาลัย

วิทยานิพนธ์นี้เป็นส่วนหนึ่งของการศึกษาตามหลักสูตรปริญญาเภสัชศาสตรมหาบัณฑิต
สาขาวิชาเภสัชอุตสาหกรรม ภาควิชาเภสัชอุตสาหกรรม
คณะเภสัชศาสตร์ จุฬาลงกรณ์มหาวิทยาลัย
ปีการศึกษา 2544
ISBN 974-03-1031-1
ลิขสิทธิ์ของจุฬาลงกรณ์มหาวิทยาลัย

DIAZEPAM SOLID LIPID NANOPARTICLES USING GLYCEROL BEHENATE PRODUCED BY HOT HOMOGENIZATION PROCESS

Mrs. Amornrat Viriyaroj

สถาบันวิทยบริการ
จุฬาลงกรณ์มหาวิทยาลัย

A Thesis Submitted in Partial Fulfillment of the Requirements
for the Degree of Master of Science in Pharmacy
Department of Manufacturing Pharmacy
Faculty of Pharmaceutical Sciences
Chulalongkorn University
Academic Year 2001

ISBN 974-03-1031-1

Thesis Title	Diazepam solid lipid nanoparticles using glycerol behenate produced by hot homogenization process
By	Mrs. Amornrat Viriyaroj
Field of Study	Industrial Pharmacy
Thesis Advisor	Associate Professor Garnpimol C. Ritthidej, Ph.D.

Accepted by the Faculty of Pharmaceutical Sciences, Chulalongkorn University in Partial Fulfillment of the Requirements for the Master's Degree

……..Dean of Faculty of Pharmaceutical Sciences
(Associate Professor Boonyong Tantisira, Ph.D.)

THESIS COMMITTEE

……..Chairman
(Associate Professor Poj Kulvanich, Ph.D.)

……..Thesis Advisor
(Associate Professor Garnpimol C. Ritthidej, Ph.D.)

……..Member
(Assistant Professor Sirisak Dumrongpisuthigul, M.Sc. in Pharm.)

……..Member
(Warangkana Warisnoicharoen, Ph.D.)

สถาบันวิทยบริการ
จุฬาลงกรณ์มหาวิทยาลัย

อมรรัตน์ วิริยะโรจน์ : ไดอะซีแพมโซลิดลิปิดนาโนพาทิเคิล โดยใช้กลีเซอรอล บีฮีเนท ด้วยกระบวนการโฮโมจีไนเซชันอุณหภูมิสูง. (DIAZEPAM SOLID LIPID NANOPARTICLES USING GLYCEROL BEHENATE PRODUCED BY HOT HOMOGENIZATION PROCESS) อ.ที่ปรึกษา: รศ.ดร. กาญจน์พิมล ฤทธิเดช, 225 หน้า. ISBN 974-03-1031-1.

วัตถุประสงค์ของงานวิจัยนี้เพื่อ เตรียมไดอะซีแพมโซลิดลิปิดนาโนพาทิเคิล และศึกษาปัจจัยที่มีผลต่อลักษณะทางเคมีกายภาพ เพื่อใช้เป็นแนวทางในการนำไปใช้เป็นยาฉีด การเตรียมโซลิดลิปิดนาโนพาทิเคิลโดยวิธีโฮโมจีไนเซชันอุณหภูมิสูง ประกอบด้วย 2 ขั้นตอนได้แก่ การทำให้เกิดอิมัลชันด้วยเครื่องปั่นผสมความเร็วสูง และการลดขนาดอนุภาคด้วยเครื่องปั่นผสมความดันสูง โดยใช้สารเพิ่มความคงตัวคือ พอลอกซาเมอร์ 188, พอลอกซาเมอร์ 407, ฟอสโฟไลปอน 80, เอปิคูลอน 200, ทวีน 20, ทวีน 80 จากการศึกษาพบว่า ชนิด และความเข้มข้นของสารเพิ่มความคงตัว คือปัจจัยสำคัญในการเตรียมโซลิดลิปิดนาโนพาทิเคิล พอลอกซาเมอร์ 188, พอลอกซาเมอร์ 407 และทวีน 20 ให้ความคงตัวไม่เพียงพอหลังจากการทำให้ไร้เชื้อโดยใช้หม้อนึ่งอัดไอน้ำ ฟอสโฟไลปอน 80 และ เอปิคูลอน 200 ไม่สามารถทำให้ตำรับคงตัว ตำรับที่ใช้ทวีน 80 สามารถเตรียมโซลิดลิปิดนาโนพาทิเคิลที่คงตัว หลังจากการทำให้ไร้เชื้อโดยใช้หม้อนึ่งอัดไอน้ำ เนื่องจากผลของสเทอริก โดยตำรับที่ใช้กลีเซอรอลบีฮีเนท 5 เปอร์เซ็นต์ และทวีน 80 ในความเข้มข้น 4% เปอร์เซ็นต์ ให้ขนาดอนุภาคที่เล็กที่สุด จากการวัดด้วยเครื่องโฟตอนคอร์รีเลชัน สเปกโทรสโกปี โดยขนาดอนุภาคเฉลี่ยก่อน และหลังการไร้เชื้อโดยใช้หม้อนึ่งอัดไอน้ำมีค่า 118.4 และ 122.0 นาโนเมตร ตามลำดับ ซึ่งไม่มีความแตกต่างอย่างมีนัยสำคัญทางสถิติ จากข้อมูลพบว่าขนาดอนุภาคของไดอะซีแพมโซลิดลิปิดนาโนพาทิเคิลในความเข้มข้น 0.1-0.9 เปอร์เซ็นต์ มีขนาดใหญ่กว่า ขนาดอนุภาคของโซลิดลิปิดนาโนพาทิเคิลที่ไม่มียา ทั้งก่อน และหลังการทำให้ไร้เชื้อโดยใช้หม้อนึ่งอัดไอน้ำ การวิเคราะห์ความแปรปรวนแบบสองทางพบว่า ปริมาณของไมโครพาทิเคิลขึ้นอยู่กับความดันของเครื่องปั่นผสมความดันสูง สามารถเตรียมไดอะซีแพมโซลิดลิปิดนาโนพาทิเคิล ที่มีการกระจายอนุภาคแคบ โดยใช้ความดัน 20,000 ปอนด์ต่อตารางนิ้ว จำนวน 5 รอบ ไดอะซีแพมโซลิดลิปิดนาโนพาทิเคิลสามารถควบคุมการปลดปล่อยตัวยาได้นานกว่า 60 ชั่วโมง กลไกการปลดปล่อยเป็นไปตามสมการฮิกูชิ จากการตรวจสอบโดยเทคนิคอินฟราเรดสเปกโทรสโกปี ไม่พบอันตรกริยาระหว่างไดอะซีแพมและส่วนประกอบอื่นในตำรับ ผลของดิฟเฟอเรนเชียลสแกนนิงคาลอริเมทรี และเอกซเรย์ดิฟแฟรกโทเมทรี แสดงให้เห็นว่าไดอะซีแพมที่อยู่ในเมทริกซ์ไขมันกระจายอยู่ในระดับโมเลกุล หรือ รูปอสัณฐาณ

ภาควิชา.....เภสัชอุตสาหกรรม.....ลายมือชื่อนิสิต.....

สาขาวิชา.....เภสัชอุตสาหกรรม.....ลายมือชื่ออาจารย์ที่ปรึกษา.....

ปีการศึกษา.....2544.....ลายมือชื่ออาจารย์ที่ปรึกษาร่วม.....

427 66079 33 : MAJOR MANUFACTURING PHARMACY
KEYWORD: DIAZEPAM/ SOLID LIPID NANOPARTICLES/ HOT HOMOGENIZATION/ GLYCEROL BEHENATE

AMORNRAT VIRIYAROJ : DIAZEPAM SOLID LIPID NANOPARTICLES USING GLYCEROL BEHENATE PRODUCED BY HOT HOMOGENIZATION PROCESS. THESIS ADVISOR : ASSOC. PROF. GARNPIMOL C. RITTHIDEJ, Ph.D., 225 pp. ISBN 974-03-1031-1.

The purpose of this present study was to prepare diazepam loaded solid lipid nanoparticles (SLN) and to investigate factors affecting the physicochemical properties for parenteral applications. SLN was prepared by hot homogenization method. This method consisted of two processes; preparing the pre-emulsion using high speed homogenizer and reducing the particle size by high pressure homogenization. The stabilizers used were poloxamer 188, poloxamer 407, Phospholipon®80, Epikuron®200, tween 20 and tween 80. The results indicated that type and concentration of stabilizers were important factors for producing SLN. The poloxamer 188, poloxamer 407 and tween 20 provided insufficient stabilization after autoclaving. Phospholipon®80 and Epikuron®200 could not stabilize SLN. The formulation composed of tween 80 could form stable autoclaved SLN conceivably by steric stabilization. The SLN containing 5% glycerol behenate and 4% tween 80 yielded the smallest particle size. The mean particle sizes of such formulation detected by photon correlation spectroscopy before and after autoclaving were 118.4 and 122.0 nm, respectively, which were insignificantly different ($p>0.05$, t-test). It was found that mean particle sizes of 0.1-0.9% diazepam loaded SLN were larger than those of drug free formulation both before and after autoclaving. Two-way ANOVA test revealed that the content of microparticles was depended upon homogenization pressure. Diazepam loaded SLN with narrow size distribution could be prepared under pressure of 20,000 psi and 5 recycle times. The release profiles of diazepam loaded SLN could be controlled for more than 60 hours. Their release kinetics followed Higuchi model. The IR spectra showed that there was no interaction between diazepam and other components. The DSC thermograms and X-ray diffractograms demonstrated that diazepam in lipid matrix was in either molecularly dispersed or amorphous form.

Department…Manufacturing Pharmacy.. Student's signature……...
Field of study….Industrial Pharmacy….. Advisor's signature…….…….
Academic year……2001……. Co-advisor's signature……..

ACKNOWLEDGEMENTS

Many people have contributed to accomplish this study of which I sincerely appreciate their advice and kind cooperation. First, I would like to express my sincere thanks and gratitude to my thesis advisor, Associate Professor Garnpimol C. Ritthidej, Ph.D., for her invaluable advice, guidance, encouragement and understanding throughout this study. Her kindness and cheerfulness are also deeply appreciated.

I would like to acknowledge the thesis committee for their valuable scrutinizing and discussion.

Special thanks are given to the Graduate School of Chulalongkorn University and the Ministry of University Affairs for granting partial financial support to fulfill this study.

My sincere gratitude is extended to National Metal and Material Technology center (MTEC), Ministry of Science, Technology and Environment, Thailand for partial support in particle size, zeta potential and powder X-ray diffractometry analysis.

I wish to thank staffs, my friends and colleagues in Department of Manufacturing Pharmacy and other persons whose names have not been mentioned here for their assistance and encouragement.

My appreciation is also extended to Dr. Vichit Viriyaroj, my husband, for his warm friendship, encouragement, understanding all the time of my study.

Above all, I would like to express my thanks to my parents, sister and brothers for their assistance, cheerfulness, and endless love throughout my life.

CONTENTS

Page

Thai Abstract……iv
English Abstract……v
Acknowledgements……..vi
List of Tables……..viii
List of Figures……xvi
List of Abbreviations……xxiv
Chapter
I Introduction……1
II Literature Review……...4
III Materials and Methods…….35
IV Results and Discussion…….50
V Conclusions…..……..124
References……..126
Appendices…….139
Vita…….225

สถาบันวิทยบริการ
จุฬาลงกรณ์มหาวิทยาลัย

LIST OF TABLES

Table **Page**

1 Lipids used for preparation of SLN……6

2 Stabilizers and methods used for preparation of SLN……8

3 Composition and source of commercially available lecithins……..10

4 Examples of drugs incorporated in SLN……..15

5 The range of inside diameters of 20-25 hypodermic gauge size……..32

6 The composition of SLN……..……...38

7 The physical appearances of SLN containing various amounts of poloxamer 188……..54

8 The physical appearances of SLN containing various amounts of poloxamer 407……..55

9 The physical appearances of SLN containing various amounts of Phospholipon® 80…….…56

10 The physical appearances of SLN containing various amounts of tween 80…….……..58

11 Particle sizes of SLN containing 1-5 % tween 80 both before and after autoclaving analyzed by PCS and LD (a) before autoclaving (b) after autoclaving…….59

12 The pH, zeta potential, osmolality of SLN containing various amounts of tween 80……...64

13 Particle sizes of SLN containing 5 % glycerol behenate and 4% tween 80 (a) after autoclaving (b) storage at room temperature (c) storage at 4 ºC for 1, 3 and 6 months analyzed by PCS and LD……...69

14 The pH, osmolality and zeta potential of SLN containing 5% glycerol behenate and 4% tween 80 over storage time……..…….70

15 Particle sizes of SLN containing different ratios of glycerol behenate to tween 80 (a) before autoclaving (b) after autoclaving……..71

16 The pH, zeta potential, osmolality of SLN containing different ratios of glycerol behenate to tween 80…….…….73

LIST OF TABLES (cont.)

Table **Page**

17 Particle sizes of 0.1–0.9 % diazepam loaded SLN both before and after autoclaving analyzed by PCS and LD (a) before autoclaving (b) after autoclaving…….80

18 The pH, zeta potential, osmolality of 0.1–0.9 % diazepam loaded SLN ……..……...83

19 Entrapment efficiency of diazepam in SLN after autoclaving……..86

20 The coefficient of determinations of diazepam release in different models calculated from total amount of diazepam in formulation……89

21 Conditions used in 0.5% diazepam loaded SLN…….…….…..99

22 Particle sizes of 0.5% diazepam loaded SLN after autoclaving analyzed by PCS and LD…….100

23 Statistical analysis of the percentage of particle larger than 5 μm in 0.5% diazepam loaded SLN……...101

24 Particle sizes of 0.3% and 0.5% diazepam loaded SLN after autoclaving analyzed by PCS and LD (a) operating at 10,000 psi (b) operating at 20,000 psi……104

25 Effect of pressure on pH, zeta potential and osmolality in formulation of 0.3% and 0.5% diazepam loaded SLN after autoclaving (a) operating at 10,000 psi (b) operating at 20,000 psi……..……..…107

26 Entrapment efficiency of diazepam in formulations of 0.3% and 0.5% diazepam loaded SLN prepared under pressure of 20,000 psi…….…...109

27 The coefficient of determinations of diazepam release- from (a) total amount in formulation (b) total amount in solid lipids in formulations- of 0.3% and 0.5% diazepam loaded SLN prepared under pressure of 20,000 psi using different models……110

LIST OF TABLES (cont.)

Table **Page**

28 Particle sizes of 0.3% and 0.5% diazepam loaded SLN after autoclaving analyzed by PCS and LD (a) before storage under accelerated condition, (b) after storage under accelerated condition……..…..…..117

29 Effect of accelerated condition on pH, zeta potential and osmolality in formulation of 0.3% and 0.5% diazepam loaded SLN (a) before storage under accelerated condition, (b) after storage under accelerated condition……..…....118

30 The physical appearances of SLN containing various amounts of tween 20……..……...119

31 Particle sizes of SLN containing 0.5–5 % tween 20 after autoclaving analyzed by PCS and LD…….120

32 Effect of tween 20 on pH, zeta potential and osmolality in SLN containing 5% glycerol behanate……..123

b1 Solubility of diazepam…….……..148

b2 The relationship between absorbance and concentrations of diazepam in pH 7.4 phosphate buffer at wavelength of 230 nm….……...149

b3 Accuracy data of diazepam…….……...….152

b4 Data of within run precision of diazepam assayed by HPLC method…….…..…...154

b5 Data of between run precision of diazepam assayed by HPLC method….……..…154

b6 Data for a calibration curve of standard solutions of diazepam ranging from 1 to 25 mcg/ml……..…….…..156

b7 Data for a calibration curve of standard solutions of diazepam ranging from 50 to 1,000 ng/ml……..…….…..158

b8 Resolution of diazepam standard solution at concentration of 20 mcg/ml……..…….159

b9 Tailing factor of diazepam and lorazazepam at concentration of 10 and 15 mcg/ml……..…….160

LIST OF TABLES (cont.)

Table **Page**

c1 Release of diazepam from saturated solution…..……...161

c2 Release of diazepam from 0.1% diazepam loaded SLN prepared under pressure of 10,000 psi 5 cycles…….……..…162

c3 Release of diazepam from 0.3% diazepam loaded SLN prepared under pressure of 10,000 psi 5 cycles……..……163

c4 Release of diazepam from 0.5% diazepam loaded SLN prepared under pressure of 10,000 psi 5 cycles……...…164

c5 Release of diazepam from 0.7% diazepam loaded SLN prepared under pressure of 10,000 psi 5 cycles……..165

c6 Release of diazepam from 0.9% diazepam loaded SLN prepared under pressure of 10,000 psi 5 cycles……..166

c7 Release of diazepam from 0.3% diazepam loaded SLN prepared under pressure of 20,000 psi 5 cycles……..167

c8 Release of diazepam from 0.5% diazepam loaded SLN prepared under pressure of 20,000 psi 5 cycles……..……168

c9 Release of diazepam from supernatant of formulation 0.3% diazepam loaded SLN calculated from total amount of diazepam in formulation…….…….……..169

c10 Release of diazepam from supernatant of formulation 0.5% diazepam loaded SLN calculated from total amount of diazepam in formulation…….……..…….170

d1 Particle size distribution of formulation of 5 GB + 1 TW80 before autoclaving…….……..…173

d2 Particle size distribution of formulation of 5 GB + 1 TW80 after autoclaving…….174

d3 Particle size distribution of formulation of 5 GB + 2 TW80 before autoclaving…….……175

d4 Particle size distribution of formulation of 5 GB + 2 TW80 after autoclaving…….……...176

LIST OF TABLES (cont.)

Table **Page**

d5 Particle size distribution of formulation of 5 GB + 3 TW80 before autoclaving……..……177

d6 Particle size distribution of formulation of 5 GB + 3 TW80 after autoclaving……..……..…....178

d7 Particle size distribution of formulation of 5 GB + 4 TW80 before autoclaving……..……..…..179

d8 Particle size distribution of formulation of 5 GB + 4 TW80 after autoclaving……..……...180

d9 Particle size distribution of formulation of 5 GB + 5 TW80 before autoclaving……..……...….181

d10 Particle size distribution of formulation of 5 GB + 5 TW80 after autoclaving……..……...182

d11 Particle size distribution of formulation 5 GB + 4 TW80 after autoclaving stored at room temperature for 1 month……183

d12 Particle size distribution of formulation 5 GB + 4 TW80 after autoclaving kept in refrigerator for 1 month……..184

d13 Particle size distribution of formulation 5 GB + 4 TW80 after autoclaving stored at room temperature for 3 months……..185

d14 Particle size distribution of formulation 5 GB + 4 TW80 after autoclaving kept in refrigerator for 3 months……...186

d15 Particle size distribution of formulation 5 GB + 4 TW80 after autoclaving stored at room temperature for 6 months……..187

d16 Particle size distribution of formulation 5 GB + 4 TW80 after autoclaving kept in refrigerator for 6 months……188

d17 Particle size distribution of formulation 1 GB + 4 TW80 before autoclaving……189

d18 Particle size distribution of formulation 1 GB + 4 TW80 after autoclaving……190

d19 Particle size distribution of formulation 3 GB + 4 TW80 before autoclaving……191

LIST OF TABLES (cont.)

Table **Page**

d20 Particle size distribution of formulation 3 GB + 4 TW80 after autoclaving……192

d21 Particle size distribution of formulation 7 GB + 4 TW80 before autoclaving……193

d22 Particle size distribution of formulation 7 GB + 4 TW80 after autoclaving……194

d23 Particle size distribution of formulation 9 GB + 4 TW80 before autoclaving……195

d24 Particle size distribution of formulation 9 GB + 4 TW80 after autoclaving……196

d25 Particle size distribution of formulation 0.1 DI + 5 GB + 4 TW80 before autoclaving……197

d26 Particle size distribution of formulation 0.1 DI + 5 GB + 4 TW80 after autoclaving……198

d27 Particle size distribution of formulation 0.3 DI + 5 GB + 4 TW80 before autoclaving……199

d28 Particle size distribution of formulation 0.3 DI + 5 GB + 4 TW80 after autoclaving……200

d29 Particle size distribution of formulation 0.5 DI + 5 GB + 4 TW80

before autoclaving……201

d30 Particle size distribution of formulation 0.5 DI + 5 GB + 4 TW80 after autoclaving……202

d31 Particle size distribution of formulation 0.7 DI + 5 GB + 4 TW80 before autoclaving……203

d32 Particle size distribution of formulation 0.7 DI + 5 GB + 4 TW80 after autoclaving……204

d33 Particle size distribution of formulation 0.9 DI + 5 GB + 4 TW80 before autoclaving……205

d34 Particle size distribution of formulation 0.9 DI + 5 GB + 4 TW80 after autoclaving……206

LIST OF TABLES (**cont**.)

Table **Page**

d35 Particle size distribution of diazepam powder……207

d36 Particle size distribution of formulation of 0.5 DI + 5 GB + 4 TW80 prepared under pressure of 10,000 psi 7 cycles……208

d37 Particle size distribution of formulation of 0.5 DI + 5 GB + 4 TW80 prepared under pressure of 10,000 psi 9 cycles……209

d38 Particle size distribution of formulation of 0.5 DI + 5 GB + 4 TW80 prepared under pressure of 15,000 psi 5 cycles……210

d39 Particle size distribution of formulation of 0.5 DI + 5 GB + 4 TW80 prepared under pressure of 15,000 psi 7 cycles……211

d40 Particle size distribution of formulation of 0.5 DI + 5 GB + 4 TW80 prepared under pressure of 15,000 psi 9 cycles……212

d41 Particle size distribution of formulation of 0.5 DI + 5 GB + 4 TW80 prepared under pressure of 20,000 psi 5 cycles……213

d42 Particle size distribution of formulation of 0.5 DI + 5 GB + 4 TW80

prepared under pressure of 20,000 psi 7 cycles……214

d43 Particle size distribution of formulation of 0.5 DI + 5 GB + 4 TW80

prepared under pressure of 20,000 psi 9 cycles……215

d44 Particle size distribution of formulation of 0.3 DI + 5 GB + 4 TW80

prepared under pressure of 20,000 psi 5 cycles……216

d45 Particle size distribution of formulation of 0.3 DI + 5 GB + 4 TW80

after storage under accelerated condition……217

d46 Particle size distribution of formulation of 0.5 DI + 5 GB + 4 TW80

after storage under accelerated condition……218

d47 Particle size distribution of formulation of 5 GB + 0.5 TW20

after autoclaving……219

d48 Particle size distribution of formulation of 5 GB + 1 TW20

after autoclaving……220

d49 Particle size distribution of formulation of 5 GB + 2 TW20

after autoclaving……221

LIST OF TABLES (cont.)

Table **Page**

d50 Particle size distribution of formulation of 5 GB + 3 TW20

after autoclaving……222

d51 Particle size distribution of formulation of 5 GB + 4 TW20

after autoclaving……223

d52 Particle size distribution of formulation of 5 GB + 5 TW20

after autoclaving……224

LIST OF FIGURES

Figure **Page**

1 EmulsiFlex® C5……17

2 The schematic of static homogenizing valve (left) and dynamic homogenizing valve (right)……..17

3 Schematic procedure of hot and cold homogenization techniques for SLN production……..19

4 Proposed models for the internal structure of SLN……..27

5 Partitioning effects on drug during the production of SLN by the hot homogenization technique ……28

6 Construction of Cryo-SEM……..42

7 Asymmetrical chromatographic peak……..47

8 Effect of tween 80 concentration on the particle size of SLN containing 5% glycerol behenate analyzed by PCS……....60

9 Effect of tween 80 concentration on the particle size of SLN containing 5% glycerol behenate analyzed by LD…….…….60

10 Effect of tween 80 concentration on the polydispersity index of SLN containing 5% glycerol behenate analyzed by PCS…….……61

11 Effect of tween 80 concentration on the uniformity of SLN containing 5% glycerol behenate analyzed by LD……..61

12 Effect of tween 80 concentration of the percentage of particle larger than 1, 5, 10 μm of SLN containing 5% glycerol behenate after autoclaving analyzed by LD…….……...62

13 The pH of dispersion of SLN containing 5% glycerol behenate and 1-5 % tween 80…….…….63

14 The zeta potential of SLN containing 5% glycerol behenate and 1-5 % tween 80…….…….65

15 The osmolality of SLN containing 5% glycerol behenate and 1-5 % tween 80…….…..…66

16 The Cryo-SEM photomicrograph of SLN containing 5% glycerol behenate and 4% tween 80…….…..….67

17 The Cryo-SEM photomicrograph of distill water…….……..…….67

LIST OF FIGURES (cont.)

Figure **Page**

18 Infrared spectra of (A) glycerol behenate, (B) tween 80, (C) glycerol behenate SLN……..……..76
19 DSC thermograms of (A) glycerol behenate, (B) glycerol behenate SLN…..77
20 X-ray diffractograms of (A) glycerol behenate, (B) glycerol behenate SLN..78
21 Effect of drug loading on the particle size in diazepam loaded SLN analyzed by PCS…….…….……..81
22 Effect of drug loading on the polydispersity index in diazepam loaded SLN analyzed by PCS…….…….……..82
23 Effect of drug loading on uniformity in diazepam loaded SLN analyzed by LD…….……..….82
24 The pH of 0.1-0.9% diazepam loaded SLN both before and autoclaving…….84
25 Effect of drug loading on zeta potential in diazepam loaded SLN…….…….84
26 Effect of drug loading on osmolality in diazepam loaded SLN……..….85
27 The Cryo-SEM photomicrograph of 0.7% diazepam SLN after aytoclaving……..…….86
28 The release profile of diazepam from saturated solution…….……..88
29 The release profiles of diazepam from 0.1-0.9% diazepam loaded SLN……89
30 Infrared spectra of (A) glycerol behenate SLN, (B) diazepam, (C) 0.1% diazepam loaded SLN, (D) 0.3% diazepam loaded SLN……92
31 Infrared spectra of (A) 0.5% diazepam loaded SLN, (B) 0.7% diazepam loaded SLN, (C) 0.9% diazepam loaded SLN…….……..…..93
32 DSC thermograms of (a) glycerol behenate SLN, (b) diazepam, (c) 0.1% diazepam loaded SLN, (d) 0.3% diazepam loaded SLN…….……..…..….94

LIST OF FIGURES (cont.)

Figure **Page**

33 DSC thermograms of (a) 0.5% loaded diazepam loaded, (b) 0.7% diazepam loaded SLN, (C) 0.9% diazepam loaded SLN…….……..…...95

34 X ray diffractograms of (A) glycerol behenate, (B) diazepam, (C) physical mixing of diazepam and glycerol behenate in the same quantity of 0.3% diazepam loaded SLN, (D) physical mixing of diazepam and glycerol beheante in the same quantity of 0.5% diazepam loaded SLN……...…..96

35 X-ray diffractograms of (A) glycerol behenate SLN, (B) diazepam, (C) 0.1% diazepam loaded SLN, (D) 0.3% diazepam loaded SLN……..……97

36 X-ray diffractograms of (A) 0.5% diazepam loaded SLN, (B) 0.7% diazepam loaded SLN, (C) 0.9% diazepam loaded SLN……..……..……..98

37 Interactions of homogenization pressure and cycle of homogenization on percentage of particle larger than 5 μm of 0.5% diazepam loaded SLN…….....101

38 Effect of pressure on the percentage of particle larger than 1, 5 and 10 μm in formulation of 0.3% and 0.5% diazepam loaded SLN…….…….103

39 Effect of pressure on the polydispersity index in formulation of 0.3% and 0.5% diazepam loaded SLN……..105

40 Effect of pressure on the uniformity in formulation of 0.3% and 0.5% diazepam loaded SLN……..105

41 Particle size distribution of formulation of 0.3% diazepam loaded SLN prepared under pressure of 20,000 psi analysed by LD…….…….106

42 Particle size distribution of formulation of 0.5% diazepam loaded SLN prepared under pressure of 20,000 psi analysed by LD……..106

LIST OF FIGURES (cont.)

Figure **Page**

43 The Cryo-SEM photomicrograph of 0.3% diazepam loaded SLN prepared under pressure of 20,000 psi……...108

44 The Cryo-SEM photomicrograph of 0.5% diazepam loaded SLN prepared under pressure of 20,000 psi……..……108

45 The release profiles of diazepam from saturated solution, 0.3 and 0.5% diazepam loaded SLN prepared under pressure of 20,000 psi and supernatant of both preparations……..……..111

46 The release profiles of diazepam from 0.3 and 0.5% diazepam loaded SLN prepared under pressure of 10,000 psi and 20,000 psi……...111

47 Infrared spectra of (A) 0.3% diazepam loaded SLN –10,000 psi, (B) 0.3% diazepam loaded SLN –20,000 psi, (C) 0.5% diazepam loaded SLN –10,000 psi, (D) 0.5% diazepam loaded SLN –20,000 psi……..……...113

48 DSC thermograms of (A) 0.3% diazepam loaded SLN - 10,000 psi, (B) 0.3% diazepam loaded SLN- 20,000 psi (C) 0.5% diazepam loaded SLN- 10,000 psi, (D) 0.5% diazepam loaded SLN- 20,000 psi……..……...114

49 X-ray diffractograms of (A) 0.3% diazepam loaded SLN - 10,000 psi, (B) 0.3% diazepam loaded SLN- 20,000 psi (C) 0.5% diazepam loaded SLN- 10,000 psi, (D) 0.5% diazepam loaded SLN- 20,000……..115

50 Effect of tween 20 concentration on the particle size of SLN containing 5% glycerol behenate analyzed by LD…….121

51 Effect of tween 20 concentration on the percentage of particle larger than 1, 5, 10 μm of SLN containing 5% glycerol behenate analyzed by LD…….……121

b1 The UV spectrum of diazepam in pH 7.4 phosphate buffer solution…….……..148

b2 A representation of calibration curve of diazepam in pH 7.4 phosphate buffer at 230 nm……149

LIST OF FIGURES (cont.)

Figure **Page**

b3 HPLC chromatograms of (A) diazepam (B) lorazepam (C) phosphate buffer (D) supernatant from the formulation of 5% glycerol behenate and tween 80 (E) tween 80……151

b4 HPLC chromatograms of the standard solutions of diazepam and its internal standard in range of 1-25 mcg/ml……..155

b5 A representation of calibration curve of standard solutions of diazepam ranging from 1 to 25 mcg/ml…….156

b6 HPLC chromatograms of the standard solutions of diazepam and its internal standard ranging from 50 to 1,000 ng/ml……..157

b7 A representation of calibration curve of standard solutions of diazepam ranging from 50 to 1,000 ng/ml……..……158

d1 Particle size distribution of formulation of 5 GB + 1 TW80 before autoclaving……173

d2 Particle size distribution of formulation of 5 GB + 1 TW80 after autoclaving……174

d3 Particle size distribution of formulation of 5 GB + 2 TW80 before autoclaving……175

d4 Particle size distribution of formulation of 5 GB + 2 TW80 after autoclaving……176

d5 Particle size distribution of formulation of 5 GB + 3 TW80 before autoclaving……177

d6 Particle size distribution of formulation of 5 GB + 3 TW80 after autoclaving……178

d7 Particle size distribution of formulation of 5 GB + 4 TW80 before autoclaving……179

d8 Particle size distribution of formulation of 5 GB + 4 TW80 after autoclaving……180

d9 Particle size distribution of formulation of 5 GB + 5 TW80 before autoclaving……181

LIST OF FIGURES (cont.)

Figure **Page**

d10 Particle size distribution of formulation of 5 GB + 5 TW80 after autoclaving……182
d11 Particle size distribution of formulation 5 GB + 4 TW80 after autoclaving stored at room temperature for 1 month……183
d12 Particle size distribution of formulation 5 GB + 4 TW80 after autoclaving kept in refrigerator for 1 month……184
d13 Particle size distribution of formulation 5 GB + 4 TW80 after autoclaving stored at room temperature for 3 months……185
d14 Particle size distribution of formulation 5 GB + 4 TW80 after autoclaving kept in refrigerator for 3 months……186
d15 Particle size distribution of formulation 5 GB + 4 TW80 after autoclaving stored at room temperature for 6 months……187
d16 Particle size distribution of formulation 5 GB + 4 TW80 after autoclaving kept in refrigerator for 6 months……188
d17 Particle size distribution of formulation 1 GB + 4 TW80 before autoclaving……189
d18 Particle size distribution of formulation 1 GB + 4 TW80 after autoclaving……190
d19 Particle size distribution of formulation 3 GB + 4 TW80 before autoclaving……191
d20 Particle size distribution of formulation 3 GB + 4 TW80 after autoclaving……192

d21 Particle size distribution of formulation 7 GB + 4 TW80 before autoclaving……193

d22 Particle size distribution of formulation 7 GB + 4 TW80 after autoclaving……194

d23 Particle size distribution of formulation 9 GB + 4 TW80 before autoclaving……195

d24 Particle size distribution of formulation 9 GB + 4 TW80 after autoclaving……196

LIST OF FIGURES (cont.)

Figure **Page**

d25 Particle size distribution of formulation 0.1 DI + 5 GB + 4 TW80 before autoclaving……197

d26 Particle size distribution of formulation 0.1 DI + 5 GB + 4 TW80 after autoclaving……198

d27 Particle size distribution of formulation 0.3 DI + 5 GB + 4 TW80 before autoclaving……199

d28 Particle size distribution of formulation 0.3 DI + 5 GB + 4 TW80 after autoclaving……200

d29 Particle size distribution of formulation 0.5 DI + 5 GB + 4 TW80 before autoclaving……201

d30 Particle size distribution of formulation 0.5 DI + 5 GB + 4 TW80 after autoclaving……202

d31 Particle size distribution of formulation 0.7 DI + 5 GB + 4 TW80 before autoclaving……203

d32 Particle size distribution of formulation 0.7 DI + 5 GB + 4 TW80 after autoclaving……204

d33 Particle size distribution of formulation 0.9 DI + 5 GB + 4 TW80

before autoclaving……..……..205

d34 Particle size distribution of formulation 0.9 DI + 5 GB + 4 TW80 after autoclaving……..……..206

d35 Particle size distribution of diazepam powder……....……..207

d36 Particle size distribution of formulation of 0.5 DI + 5 GB + 4 TW80 prepared under pressure of 10,000 psi 7 cycles……208

d37 Particle size distribution of formulation of 0.5 DI + 5 GB + 4 TW80 prepared under pressure of 10,000 psi 9 cycles……209

d38 Particle size distribution of formulation of 0.5 DI + 5 GB + 4 TW80 prepared under pressure of 15,000 psi 5 cycles……210

d39 Particle size distribution of formulation of 0.5 DI + 5 GB + 4 TW80 prepared under pressure of 15,000 psi 7 cycles……211

LIST OF FIGURES (cont.)

Figure **Page**

d40 Particle size distribution of formulation of 0.5 DI + 5 GB + 4 TW80 prepared under pressure of 15,000 psi 9 cycles……..…212

d41 Particle size distribution of formulation of 0.5 DI + 5 GB + 4 TW80 prepared under pressure of 20,000 psi 5 cycles……213

d42 Particle size distribution of formulation of 0.5 DI + 5 GB + 4 TW80 prepared under pressure of 20,000 psi 7 cycles……214

d43 Particle size distribution of formulation of 0.5 DI + 5 GB + 4 TW80 prepared under pressure of 20,000 psi 9 cycles……215

d44 Particle size distribution of formulation of 0.3 DI + 5 GB + 4 TW80 prepared under pressure of 20,000 psi 5 cycles……216

d45 Particle size distribution of formulation of 0.3 DI + 5 GB + 4 TW80 after storage under accelerated condition……..……217

d_{46} Particle size distribution of formulation of $_{0.5}$ DI $_{+ 5}$ GB $_{+ 4}$ TW_{80} after storage under accelerated condition……218

d_{47} Particle size distribution of formulation of $_{5}$ GB $_{+ 0.5}$ TW_{20} after autoclaving……219

d_{48} Particle size distribution of formulation of $_{5}$ GB $_{+ 1}$ TW_{20} after autoclaving……220

d_{49} Particle size distribution of formulation of $_{5}$ GB $_{+ 2}$ TW_{20} after autoclaving……221

d_{50} Particle size distribution of formulation of $_{5}$ GB $_{+ 3}$ TW_{20} after autoclaving……222

d_{51} Particle size distribution of formulation of $_{5}$ GB $_{+ 4}$ TW_{20} after autoclaving……223

d_{52} Particle size distribution of formulation of $_{5}$ GB $_{+ 5}$ TW_{20} after autoclaving……224

สถาบันวิทยบริการ
จุฬาลงกรณ์มหาวิทยาลัย

LIST OF ABBREVIATIONS

AFM	=	atomic force microscopy
AUC	=	area under the curve
ºC	=	degree Celsius
Cryo-TEM	=	Cryo-Transmission electron microscopy
Cryo-SEM	=	Cryo-Scanning electron microscopy
df	=	degree of freedom
DI	=	diazepam
DSC	=	differential scanning calorimetry
i.e.	=	id est (that is)
IR	=	infrared spectroscopy
e.g.	=	exampli gratia (for example)
et al.	=	et alii (and others)
EP200	=	Epikuron®200
EPR	=	electron paramagnetic resonance
FDA	=	food and drug administration
FF-TEM	=	Freeze-Fracture Transmission electron microscopy
FTIR	=	Fourier Transform Infrared Spectroscopy
HLB	=	hydrophilic lipophilic balance
g	=	gram (s)
GB	=	glycerol behenate
^{1}H NMR	=	proton nuclear magnetic resonance spectroscopy
HPH	=	high pressure homogenization
hr	=	hour (s)
km/hr	=	kilometer per hour
LD	=	laser diffractometry
LDA	=	laser doppler anemometry
L/hr	=	liter (s) per hour
NMR	=	nuclear magnetic resonance
nm	=	nanometer (s)
mOsm/L	=	milliosmols per liter
max.	=	maximun

สถาบันวิทยบริการ
จุฬาลงกรณ์มหาวิทยาลัย

LIST OF ABBREVIATIONS (cont.)

min.	=	minimum
ml	=	milliliter (s)
ng	=	nanogram (s)
nm	=	nanometer (s)
No.	=	number of sample
O/W	=	oil in water emulsion
P188	=	poloxamer 188
P407	=	poloxamer 407
PCS	=	photon correlation spectroscopy
pH	=	the negative logarithym of the hydrogen ion concentration
PI	=	polydispersity index
PL80	=	Phospholipon® 80
psi	=	pound (s) per square inch
R^2	=	coefficient of determination
rpm	=	revolution (s) per minute
µg	=	microgram (s)
µm	=	micrometer (s)
µl	=	microliter (s)
SD	=	standard deviation
SLN	=	solid lipid nanoparticle
TEM	=	Transmission electron microscopy
TW20	=	Tween 20
TW80	=	Twen 80
w/w	=	weight by weight
%	=	percentage
>	=	more than
<	=	less than
α	=	alpha
β	=	beta
β′	=	beta prime

สถาบันวิทยบริการ
จุฬาลงกรณ์มหาวิทยาลัย

CHAPTER I
INTRODUCTION

Solid lipid nanoparticle (SLN) represents an alternative colloidal drug delivery system. The use of solid lipids as matrix materials for drug delivery is well-known from lipid pellets for oral drug delivery. Nanoparticles made from solid lipids are attractively increasing attention during recent years. The idea to use solid lipids instead of liquid oils is a very attractive idea to achieve controlled drug release because drug mobility in a solid lipid should be considerably low compared with in liquid oil (Mehnert and Mäder, 2001). The SLN can be employed for any purpose for which nanoparticles have distinct advantages. The advantages are the possibility of incorporating drugs for controlled drug release, the low cytotoxicity due to its composition of physiological compound and the possibility for loading both lipophilic and hydrophilic drugs into solid matrix. The solid matrix can also protect incorporated active ingredients against chemical degradation (Müller, Mehnert et al., 1995).

Many researchers have studied the preparation of SLN. Several techniques have been developed to obtain nanometer size range with narrow size distribution. The lipid nanopellets were prepared by dispersing a melted lipid in a surfactant solution by stirring or sonication. However, dispersion quality is often compromised by the present of microparticles. Sjöström and Bergenståhl (1992) described a production method to prepare nanoparticle dispersions by solvent-emulsification method. The narrow size distribution in nanometer could be achieved by this technique. However, disadvantage is the need to use organic solvent. To overcome these problems, high pressure homogenization (HPH) was used to prepare SLN. Under optimized production conditions, SLN can be produced with a quality acceptable for parenteral administration. SLN with mean particle diameter less than 5 μm could be used for intravenous application (Müller, Lippacher, and Gohla, 2000). Yang, Lu et al. (1999) prepared camptothecin loaded SLN using high pressure homogenizer. They found that SLN was a promising sustained release and drug targeting system after intravenous injection. In addition, incorporation of the drug into SLN might reduce irritancy compared to injecting drug microparticles.

Many drugs are formulated for controlled release in several dosage forms such as tablets, capsules and suspensions. Since controlled release drug delivery has distinct therapeutic advantages. The advantages include increase of dosing compliance, avoidance both of the unnecessarily high and the too low drug levels, reduction of dosing frequency without compromising the effectiveness of the treatment, minimizing systemic toxicity and maximizing of effectiveness by directly into the affected region (Senior, 2000).

Diazepam is one of most widely used benzodiazepaines in general practice for treatment of anxiety states, acute alcoholic withdrawal, excitation states, skeletal muscle spasm, premedication for surgical procedures, status epilepticus and other convulsive disorders (Gustafson et al., 1981). Available dosage forms are tablet, syrup, emulsion, gel suppository, solution suppository and parenteral dosage form. The usual oral or rectal dosage for adults ranges between 4 and 40 mg daily. Therefore diazepam is generally prescribed to be taken as divided doses 2-4 times a day. Hence, the controlled release diazepam capsule has been developed to achieve in one administration. The controlled release preparation contains the active constituent enclosed in a floating capsule which remains in the stomach for a prolonged period, thus permitting slow and reliable gastric absorption (Sheth and Tossouian, 1984). The diazepam controlled release capsule (15mg/capsule) is indicated for the management of anxiety disorders. The usual daily dose is 1 or 2 capsules once daily in adults depending upon severity of symptoms (Hulbert, 1995). Diazepam controlled release is also a useful adjunct for the relief of skeletal muscle spasm due to reflex spasm to local pathology such as inflammation of the muscles or joints, spasticity caused by upper motor neuron disorders such as cerebral palsy and paraplegia. Moreover, diazepam controlled release provides the advantage that a single dose given the night before surgery produced both night sedation and also anxiolysis extending to the preoperative period (Eastley, Fell, and Smith, 1986). Several studies have shown that the blood concentration of diazepam is maintained throughout the day after single dose of controlled release capsule so that the desired effect is stabilized without the patient having to take repeat doses during the day (Montandon et al., 1986).

The development of a controlled release formulation of diazepam offers a number of advantages over ordinary conventional dosage forms such as increase of

patient compliance, reduction of the fluctuation in plasma concentration and decrease of dosing frequency (Dollery, 1999). Furthermore, there was no observable difference in the severity and duration of drowsiness between the conventional tablet (t.i.d) and the controlled release capsule (o.d) (Wills, 1984). In treatment of status epilepticus or convulsive status, a parenteral mode of administration is preferable for patients whom oral administration is not feasible. However, there is no study that investigates a controlled release of diazepam for parenteral administration. SLN was a promising carrier for possibility of controlled drug release owing to its aforementioned advantages. Consequently, The objective of this study was to prepare diazepam loaded SLN using hot homogenization method and study drug release profile. Glycerol behenate was chosen to be lipid carrier due to its physiological compound. Poloxamer 188, poloxamer 407, Phospholipon® 80, Epikuron® 200, tween 20 and tween 80 were used as stabilizer in concentration of 1-5% which can be used in parenteral products (Nema, Washkuhn, and Brendel, 1997).

Objectives

The aims of this study were as following:

1. To study the process of preparation and the physicochemical characteristics of SLN.

2. To investigate the effects of type and amount of stabilizers on the stability of SLN.

3. To study the effects of pressure and number of cycle of homogenization on the particle size of diazepam loaded SLN.

4. To study drug release profiles and determine the release kinetics of diazepam from SLN.

CHAPTER II
LITERATURE REVIEW

Solid lipid nanoparticle (SLN)

Solid lipid nanoparticle represents an alternative colloidal drug carrier system with mean particle diameter ranging from 50 up to 1,000 nm. SLN is characterized as lipid based carrier system of solid physical state. It consists of biodegradable lipids and physiologically acceptable additives. These carriers provide sufficient loading capacity for lipophilic and possibly also hydrophilic drugs. SLN can be administered by parenteral, transdermal and oral route. By varying production parameters and the excipients, a desired mean particle size can be produced in a controlled way (Westesen and Siekmann, 1996).

Solid lipid as matrix material for drug delivery is well-known from lipid pellet for oral drug delivery. The first attempts to develop SLN dated back to decades ago when the first parenteral lipid emulsions became commercially available. The use of solid lipid as carrier matrix can combine the advantages of polymeric nanoparticles and lipid emulsions. SLN possesses obvious advantages which is superior than other carriers. Their benefits are (i) biocompatibility and biodegradability of lipid carriers (ii) the possibility of controlled drug release and drug targeting (iii) avoidance of physical instability (iv) reduction of drug leakage (v) avoidance of the toxic residues (vi) no problem with respect to sterilization by autoclaving (vii) increasing of drug resistance to hydrolysis or oxidation (vii) possibility to administer drugs through most routes of administration including parenteral, oral, trandermal and pulmonary (Schwarz et al., 1994).

However, the difficulty in formulation, difficulty in manufacturing production and reproducibility problem are the obstacles that limit the development plans in particulated drug delivery systems. Therefore, the study of the process of preparation, characteristics and drug release of SLN is currently increasing attention during recent years (Floyd and Jain, 1996).

Excipient and formulation consideration

In general, SLN includes therapeutic agent, pharmaceutical acceptable lipid matrix, stabilizer, other additives and water. Special attention should be given into two major ingredients in SLN formulation, lipid matrix and stabilizer, especially in preparation intended for parenteral application. Potential toxicity, physical stability, chemical incompatibility and physicochemical property must be taken into consideration.

1. Lipid matrix

The variety of lipid matrices used in the formulation of SLN include fatty acids, partial glycerides, triglycerides, steroids, waxes which are solid at room temperature. Lipids consist of different chemical structures that have the melting ranging from approximately 30-120 ºC. Some lipids used for preparation of SLN are shown in Table 1 (Danisco, 2001, Freitas and Müller, 1998, Heiati, Tawashi et al. 1996, Lukowski et al. 2000, Zimmermann, Müller, and Mädder, 2000)

Using the hot homogenization, it has been found that the average particle size of SLN dispersions increased with higher melting lipid. These results are in agreement to the general theory of high pressure homogenization and can be explained by the higher viscosity of the dispersed phase. In addition, other critical parameters for nanoparticle formation will be different for different lipids. The reasons include the velocity of lipid crystallization, lipid hydrophilicity, the shape of the lipid crystals and the surface area. It is also noteworthy that most of the lipids used represent a mixture of several chemical compounds. The composition might therefore vary from different suppliers and might even vary for different batches from the same supplier. However, small differences in the lipid composition might considerably impact on the quality of SLN dispersion e.g. by changing the zeta potential, retarding crystallization process. For example, lipid nanodispersions made with cetyl palmitate from different suppliers had different particle sizes and storage stabilities (Mehnert and Mäder, 2001). The influence of lipid composition on particle size was also confirmed on SLN produced via high shear homogenization. The average particle size of Witepsol W 35 SLN was found to be significantly smaller (117.0±1.8 nm) than

Table 1 Lipids used for preparation of SLN

Lipids	Melting range (°C)	Tradename (Manufacturer)
Glycerides		
● Glyceryl tricaprinate	31-32	Tricaprin® (Fluka)
● Glyceryl trilaurate	46.5	Trilaurin® (Fluka)
● Glyceryl trimyristate	55-58	Dynasan® 114(CONDEA)
● Glyceryl tripalmitate	61-65	Dynasan® 116 (CONDEA)
● Glyceryl tristearate	70-73	Dynasan® 118 (CONDEA)
● Glyceryl palmitostearate	53-57	Precirol® ATO 5 (Gattefossé)
● Glyceryl monostearate	54-64	Imwitor® 900 (CONDEA)
● Glyceryl behenate	69-74	Compritol® 888 ATO (Gattefossé)
● Hydrogenated coco-glyceride	42-44	Softisan® 142 (CONDEA)
● Hydrogenated coco-glyceride	33.5-35.5	Witepsol® W 35 (CONDEA)
● Hydrogenated coco-glyceride	33.5-35.5	Witepsol® H 35 (CONDEA)
● Hydrogenated coco-glyceride	41-43	Witepsol® H 42 (CONDEA)
● Hydrogenated coco-glyceride	42-44	Witepsol® E 48 (CONDEA)
● Monostearate monocitrate diglyceride	64	Grindsted CITREM® N12 (Danisco)
Fatty acids		
● Palmitic acid	63-64	Palmitic acid (Fluka)
● Stearic acid	69-71	Stearic acid (Fluka)
● Behenic acid	77-80	Behenic acid (Fluka)
Waxes		
● Cetyl palmitate	46-51	Cutina® CP (Cognis)
Other fat types		
● Propylene glycol monosterate	34-37.5	Monosteol® (Gattefossé)
● Polyethyleneglycol-6 stearate	33-37	Superpolystate® (Gattefossé)
● Mixture of glycerol tribehenate and calcium behenate	105-115	Syncrowax® HRSC (Nettetal)

the size of Dynasan 118 SLN (175.1±1.8 nm). Witepsol W 35 contains shorter fatty acid chains and considerable amounts of monoglycerides and diglycerides which possess surface active properties.

Previous work has indicated that the stability of SLN after autoclaving depended on the nature of lipid. It was found that poloxamer 188 was the most efficient for stabilizing cetyl palmitate SLN, but little effective in syncrowax® HRC SLN (Müller et al., 1995). Mühlen, Schwarz, and Mehnert (1998) have pointed out that controlled adjustment of drug release could be achieved by modification of chemical nature of lipid matrix.

Lipids exhibit a pronounced polymorphism. Depending on the conditions, glycerides may crystallize in three different polymorphic foms- alpha (α), beta prime (β′) and beta (β). These polymorphic modifications characterized by the particular carbon chain packing may differ significantly in their properties such as solubility, melting point and thermal stability. The β form, a triclinic subcell structure, is the most themodynamically stable polymorph. Where as α is the least stable with a loosely packed hexagonal subcell structure. The α form therefore has a tendency to be quickly transformed to a form with a better chain packing β′ and β (Eldem, Speiser, and Altorfer, 1991). This transformation is accompanied by a change of physicochemical properties. Early study has revealed that the polymorphic transition in glycerol behenate SLN changed from β′ into β after continuation of the drying process (Jenning, Schäfer-Korting, and Gohla, 2000).

2. Stabilizer

Natural and synthetic agents have been considered for use as possible stabilizers because none of oils typically employed form a spontaneous emulsion when mixed with water. Many stabilizers have shown a high potential to stabilize SLN in a long period of time. The choice of the stabilizers and their concentrations is of great impact on the quality of the SLN dispersion. Table 2 demonstrates stabilizers and methods used for production of SLN (Almeid, Runge, and Müller, 1997, Cavalli, Marengo et al., 1996, Floyd, 1999, Morel, Terreno et al., 1998, Siekmann and Westesen, 1996).

Table 2 Stabilizers and methods used for preparation of SLN

Stabilizers	Methods
Natural stabilizers	
● Soybean lecithin	Hot homogenization/ Microemulsion
● Egg lecithin	Hot homogenization/ Microemulsion
Synthetic stabilizers	
● Poloxamer 188	Hot homogenization/ Cold homogenization
● Poloxamer 182	Cold homogenization
● Poloxamer 407	Hot homogenization
● Poloxamine 908	Hot homogenization
● Tyloxapol	Hot homogenization /Solvent emulsification and evaporation
● Polysorbate 20	Microemulsion
● Polysorbate 60	Microemulsion
● Polysorbate 80	Hot homogenization/ Cold homogenization
● Sodium cholate	Cold homogenization
● Sodium glycocholate	Hot homogenization/ Cold homogenization /Solvent emulsification and evaporation
● Taurocholic acid sodium salt	Microemulsion
● Taurodeoxycholic acid sodium salt	Microemulsion
● Butanol	Microemulsion
● Butyric acid	Microemulsion
● Dioctyl sodium sulfosuccinate	Microemulsion
● Monooctylphosphoric acid sodium	Microemulsion

Only the limited number of stabilizers is commonly regarded as safe to use for parenteral administration of which the most important is lecithin. Lecithin, the most commonly used emulsifier in lipid emulsions, is defined as a mixture of triglycerides of stearic, palmitic, and oleic acid, linked to the choline ester of phosphoric acid. It has been obtained from both animal (egg yolk) and vegetable (soybean) sources. Lecithin can be totally biodegraded and metabolized since it is an integral part of biological membranes. It is regarded as a well tolerated and non-toxic compound which is expressed by Generally Recognised As Safe (GRAS) approved by the FDA, making it suitable for long term and large dose infusion.

The production of SLN is similar to that of lipid emulsions. During the preparation of SLN by hot homogenization method, an emulsion of the lipid melt in the aqueous phase is intermediately created before the lipid droplets solidify to form solid lipid nanoparticles. However, it has been observed that the preparation of lecithin stabilized tripalmitate SLN with a composition similar to lipid emulsions resulted in the formation of gel. Westesen and Siekmann (1997) reported that melt-homogenized tripalmitate dispersions containing exclusively the phosphatidylcholine rich soybean lecithin product, Lipoid® S100, as a stabilizer became semisolid immediately on cooling of the hot emulsion. Whereas dispersions stabilized by the egg lecithin, Lipoid® E80, formed gels within several hours after preparation. In tripalmitate suspensions stabilized by the cruder soybean lecithin, Lipoid® S75, transformation into semisolid product was obviously retarded but not prevented. The less pronounced gelation tendency of the Lipoid® S75 stabilized systems compared to those stabilized by Lipoid® S100 or Lipoid® E80 may be explained an improved but still not sufficient steric or electrostatic stabilization caused by the minor components of the cruder lecithin mixtures, such as glycolipids. According to the manufacturer of Lipoid® S75, the lecithin may contain up to 15% glycolipids. The different commercially available lecithins are shown in Table 3.

However, the gel formation in the preparation of lecithin stabilized tripalmitate SLN can be avoided by the addition of a cosurfactant such as glycocholate or tyloxapol. These observations point to basic physicochemical difference between similarly composed lipid emulsions and solid lipid nanoparticles.

Table 3 Composition and source of commercially available lecithins

Components	Lipoid® S100	Lipoid® S75	Lipoid® E80
Phosphatidylcholine	min.94.0	66.0-70.0	80.0-85.0
Phosphatidylethanolamine	n. sp.	7.0-10.0	7.0-9.5
N-Acyl-phosphatidylethanolamine	max. 1.0	n. sp.	n. sp.
Phosphatidylinositol	max. 0.1	max. 0.5	n. sp.
Lysophospholipids	max. 3.0	max. 3.5	max. 3.5
Triglycerides	max. 2.0	max. 3.0	max. 3.0
Free fatty acids	max. 0.5	max. 0.5	max. 0.05
Sphingomyelin	n. sp.	n. sp.	2.0-3.0
Cholesterol	n. sp.	n. sp.	max. 1.5
DL-α-Tocopherol	0.15-0.25	0.1-0.2	0.05-0.1
Source	soybean	soybean	egg yolk

In contrast to Westesen and Siekmann, Ugazio et al. (2000) stated that SLN using lecithin (Epikuron® 200) as emulsifier could be prepared by microemulsion method. They also found that the mean diameters of SLN were in nanometer range and the mean particle sizes after autoclaving showed similar results to those before autoclaving. The difference in SLN product using lecithin as stabilizer resulted from differently experimental condition e.g. lecithin source, method of preparation, type of lipid matrix and quantity of lecithin in formulation.

Recently, many synthetic stabilizers continue to receive attention. The group of nonionic materials that has shown promises as stabilizers for parenteral applications is the poloxamers. Poloxamers consist of neutral synthetic polyoxyethylene-polyoxypropylene block co-polymers. Poloxamer 188 are well suited for small volume parenterals but large volumes or long term administration are associated with overloading syndrome. Jumaa and Müller (1998) demonstrated that the using of poloxamer 188 as stabilizer was superior to other nonionic stablilzers including polyoxyethylene glycol sorbitan monooleate (tween 80), polyoxyethylene 660 hydroxy stearate (Solutol® H 15) and polyoxyethylene 35 ricinoleate (Cremophore® EL) upon autoclaving. They explained the results on basic of high

cloud point of poloxamer 188, resulting in more resistance against dehydration during autoclaving and subsequently no stabilizer damage.

Other investigators continue to study the fatty acid esters of sorbitans (various types of spans) and polyoxyethylene sorbitans (various types of tweens) that are approved by the various pharmacopoeias for parenteral administration and have been included in parenteral formulation (Nema et al., 1997). Both tween 20 and tween 80 are used as pharmaceutical exipients in available commercial parenteral products – Calcijex® and Codarone® X IV, respectively. Many studies revealed that using a combination of stabilizers are superior to those formed using single stabilizer. The combination stabilizer can produce more flexible interfacial films necessary to form stable system. Lundberg (1994) found that a suitable stabilizer is the mixture of purified egg yolk phosphatidylcholine and tween 80 in ratio of 4:0.12.

Investigating the influence of the stabilizer concentration on the particle size of glycerol behenate SLN dispersions, Mühlen (1998) obtained best results with 5% sodium cholate or poloxamer 188. Batches produced with lower concentrations of the stabilizer contained higher amounts of microparticles.

Different stabilizer compositions might require different homogenization parameters. For example, the maximum degree of dispersing was obtained with 500 bar and three cycles for poloxamer 188 stabilized systems. Homogenization with pressures of 1,000 or 1,500 bar did not result in further reduction of the particle. In contrast, pressures of 1,500 bar proved to be the best for lecithin (Lipoid® S75) stabilized systems. A possible explanation for this observation is the different velocity of the coverage of the new lipid surfaces.

3. Aqueous phase

The dispersion medium of SLN may contain one or more of following additive: isotonic agent, preservative, antiflocculant, cryoprotectant.

Isotonic agent

Normally, emulsified oil exerts no osmotic effect, hence isotonic adjustment is needed to adjust the physiological tonicity for large volume parenterals. The osmolarity should be in range of 280-300 mOsmol/L in order to prevent any hemolysis, pain, irritation and tissue damage at the site of administration. Glycerol has been proved to be very efficient in this respect. While sorbitol and xylitol are also used as isotonic agents. Siekmann and Westesen (2001) found that the use of glycerol could promote the stability of SLN. Nevertheless, this consideration may not pay much attention in small volume parenterals.

Preservative

All colloidal dispersions for small volume parenterals should include an antimicrobial agent because the aqueous is most vulnerable to inadvertent contamination. These agents can be dissolved in the aqueous phase prior to emulsification. Suggested preservatives include the methyl and butyl derivatives of *p*-hydroxybenzoic acid. Quaternary ammonium compounds are useful because of their high aqueous solubility and limited tendency to partition into the oil phase. Thimerosal in concentration of 0.01% was used as preservative for SLN (Floyd, 1999).

Cryoprotectant

Previous study has been shown that particle sizes of aqueous SLN dispersions might be stable over 12-36 months. However, this stability is not a general feature of SLN dispersions and in most cases, an increase in particle size will be observed in a shorter period of time. Lyophilization is one approach to increase chemical and physical SLN stability over extended periods of time. However, the addition of cryoprotectors is necessary to decrease SLN aggregation and to obtain a better redispersion of the dry product. Typical cryoprotective agents are sorbitol, lactose, mannose, trehalose, glucose, and polyvinylpyrrolidone. Schwarz and Mehnert (1997) investigated the lyophilization of SLN in great detail. Best results were obtained with the cryoprotectors glucose, manose, maltose and trehalose in concentrations between

10 and 15%. The observations were in agreement with the results of Müller et al.(1995) in that glucose and trehalose were proved to be the most suitable cryoprotectant.

4. Drug

Many different drugs have been incorporated in SLN, examples are given in Table 4. A very important point to judge the suitability of a drug carrier system is its loading capacity. Factors determining the loading capacity of drug in lipid are (i) solubility of drug in melted lipid (ii) miscibility of drug melt and lipid melt (iii) chemical and physical structure of solid lipid matrix (iv) polymorphic state of lipid material. The prerequisite to obtain a sufficient loading capacity is a sufficiently high solubility of the drug in the lipid melt. Typically, the solubility should be higher than required because it decreases when cooling down the melt and might even be lower in the solid lipid. To enhance the solubility in the lipid melt one can add solubilizers. In addition, the presence of monoglycerides and diglycerides in the lipid used as matrix material promotes drug solubilization. The chemical nature of the lipid is also important because lipids which from highly crystalline particles with a perfect lattice such as monoacid triglycerides lead to drug expulsion (Westesen, Bunjes, and Koch, 1997). More complex lipids being mixtures of monoglycerides, diglycerides and triglycerides and also containing fatty acids of different chain length form less perfect crystals with many imperfections offering space to accommodate the drugs.

Crystalline structure is a key factor to decide in determining whether a drug will be expelled or firmly incorporated in the long term. Therefore, for a controlled optimization of drug incorporation and drug loading, intensive characterization of the physical state of lipid particles by nuclear magnetic resonance (NMR) and X-ray powder diffractometry is highly essential.

The polymorphic form is also a parameter determining drug incorporation. Crystallization of the lipid in nanoparticles is different to the bulk material, lipid nanoparticles recrystallize at least partially in the α form, whereas bulk lipids tend to recrystallize preferentially in the β′ modification and transforming rapidly into the β form (Westesen, Siekmann, and Koch, 1993). With increasing formation of the more

stable modifications the lattice is getting more perfect and the number of imperfections decreases, that means the β′→ β transition promotes drug expulsion. In general the transformation is slower for long chain than for short chain triglycerides (Bunjes, Westesen, and Koch, 1996).

SLN production

Many researchers have prepared solid lipid nanoparticle by various techniques.

1. High shear homogenization and ultrasound

The lipid nanopellets developed by Speiser (1989) are produced by dispersing a melted lipid in a surfactant solution by high shear homogenization and ultrasound. Both methods are widespread and easy to handle. However, dispersion quality is often compromised by the presence of microparticles. Furthermore, metal contamination has to be considered if ultrasound is used. By using ultrasonication, Speiser obtained lipid nanopellets in range of 80-800 nm constituted mainly of fatty acids and glycerides. To preferentially obtain nanoparticles, relatively high surfactant concentrations are employed. However, during the production of lipid particles, surfactant is also incorporated into the lipid phase. The more surfactant is present, the more it is incorporated leading to a reduced crystallinity of the lipid particles. Higher surfactant concentrations might be acceptable for oral administration but might cause some problems for other administration routes such as intravenous.

2. High pressure homogenization

High pressure homogenization (HPH) has emerged as a reliable and powerful technique for the preparation of SLN. The high pressure homogenizers may in principle be attributed to either one of two types according to the geometry of the interaction device (i) machines with a ring-shapeed gap valve and (ii) machines based on an interaction chamber where two liquid streams are forced to interact with each other. Homogenizers of different sizes are commercially available from several

Table 4 Examples of drugs incorporated in SLN (Cavalli, Morel et al.,1995, Cavalli, Piera et al., 1999, Heiati, Phillips et al., 1996, Jenning, Gysler et al., 2000, Morel, Ugazio et al.,1996, Morel, Terreno et al., 1998, Westesen, Bunjes et al., 1997, Yang, Zhu et al., 1999, Zhang, et al., 2000,)

Drug	Research group
● Deoxycorticosterone ● Doxorubicin ● Gadolinium (III) complexes ● Hydrocortisone ● Idarubicin ● Paclitaxel ● Pilocarpine ● Progesterone ● Thymopentin ● Timolol	Gasco
● Coenzyme Q10 ● Retinol ● Retinyl palmitate ● Vitamin A palmitate	Gohla
● Prednisolone ● Tetracaine ● Etomidate	Mehnert
● Cyclosporin	Müller
● 3′-Azido-3′deoxythymidine palmitate	Phillips
● Betamethasone valerate ● Cortisone ● Menadione ● Oxazepam ● Prednisolone ● Retinol	Westesen
● Camptothecin	Yang
● Cyclosporin A	Nagai

manufacturers e.g. Micron Lab 40, Gaulin lab 60, Microfluidizer 110, Nanojet, Kavitator (Brandl, 1998). HPH has been used for years for the production of lipid emulsions for parenteral nutrition. In contrast to other techniques, scaling up represents no problem in most cases. High pressure homogenizers push a liquid with high pressure through a narrow gap in range of a few microns. The fluid accelerates on a very short distance to very high velocity over which is 1,000 km/hr. Very high shear stress and cavitation forces disrupt the particles down to the submicron range. Typical lipid contents are in the range 5-10% and represent no problem to the homogenizer. Even higher lipid concentrations up to 40% have been homogenized to lipid nanodispersions (Lippacher, Müller, and Mäder, 2000).

In this study, The EmulsiFlex® C5 (Avestin, Canada) used to prepare SLN is shown in Figure 1. It has a capacity of 1-5 liter/hr. A sample as 7 ml can be processed with a hold back volume of less than 2 ml. The homogenizing pressure can be adjusted from 500 to 30,000 psi. The aqueous dispersion is pushed by a high pressure pump which is connected compressed air supply line. The EmulsiFlex® C5 consisted of two different homogenizing valves as shown in Figure 2. The static valve's pressure is controlled by varying the flow rate through the homogenizing valve. The greater the flow rate, the greater the pressure is. The clogging might occur during operation. However, the static valve can easily be disassembled for cleaning and inspection. While dynamic homogenizing valve is fully adjustable through its maximum homogenizing pressure range. Pressure is independent from flow rate and will remain at the set value over the process time. During homogenization the process is discontinuous, therefore the system needs to be dismantled and the dispersion poured back into the cylinder body for next homogenizing cycle. For multiple cycling, the particle size distribution becomes narrower which is due to the effect reducing the coarse material (Avestin, 2000).

Two general approaches of the homogenization step, The hot and cold homogenization techniques can be used for the production of SLN. In both cases, a preparatory step involves the drug incorporation into the bulk lipid by dissolving or dispersing the drug in the lipid melt. Schematic procedure of hot and cold homogenization techniques for SLN production is shown in Figure 3.

Figure 1 EmulsiFlex® C5

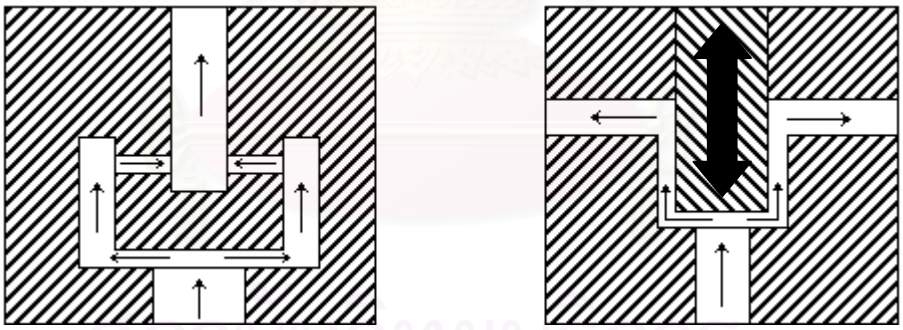

Figure 2 The schematic of static homogenizing valve (left) and dynamic homogenizing valve (right)

2.1 Hot homogenization

Hot homogenization is carried out at temperatures above the melting point of the lipid and can therefore be regarded as the homogenization of an emulsion. A pre-emulsion of the drug loaded lipid melt and the aqueous phase at the same temperature is obtained by high shear mixing device e.g. Ultra-Turrax®. The obtained coarse pre-emulsion is then homogenized using high pressure homogenizer. Cooling

down of this emulsion to room temperature will lead to lipid crystallization and formation of the solid lipid nanoparticle. The hot homogenization technique can be applied to lipophilic and insoluble drugs. Many heat sensitive drugs can be processed because the exposure time to higher temperatures is relatively short. However, in case of highly temperature sensitive compounds the cold homogenization technique can be applied. The hot homogenization technique is not suitable for incorporating hydrophilic drugs into SLN. During the homogenization of the melted lipid phase the drug will partition to the water phase resulting in a too low entrapment efficiency (Siekmann and Westesen, 2001).

The quality of the pre-emulsion affects the quality of the final product to a large extent and it is desirable to obtain droplets in the size range of few micrometers. HPH of the pre-emulsion is carried out at temperatures above the melting point of the lipid. In general, higher temperatures result in lower particle sizes due to the decreased viscosity of the inner phase. However, high temperatures may also increase the degradation rate of the drug and the carrier. The homogenization step can be repeated several times. Typically, HPH increases the temperature of the sample approximately 10ºC for 500 bar. In most case, 3-5 homogenization cycles at 500-1500 bar are sufficient (Jahnke, 1998). Furthermore, it was found that the small particle size and the presence of stabilizers, lipid crystallization may be highly retarded and the sample may remain as a supercooled melt for several months (Bunjes, Siekmann, and Westesen, 1998).

2.2 Cold homogenization

Cold homogenization has been developed to overcome the following problems (i) temperature-induced drug degradation (ii) drug distribution into the aqueous phase during homogenization (iii) complexity of the crystallization step of the emulsion leading to several modifications and/or supercooled melts. In the first preparatory step, the drug is dissolved in the melt lipid. The drug containing melt lipid is solidified in dry ice or liquid nitrogen and milled using a mortar mill or ball mill. The high cooling rate flavors a homogeneous distribution of the drug within the lipid matrix. Typical particle sizes obtained by means of mortar mill or ball mill are in range 50-100 microns. Then the obtained lipid microparticles are dispersed in a cold

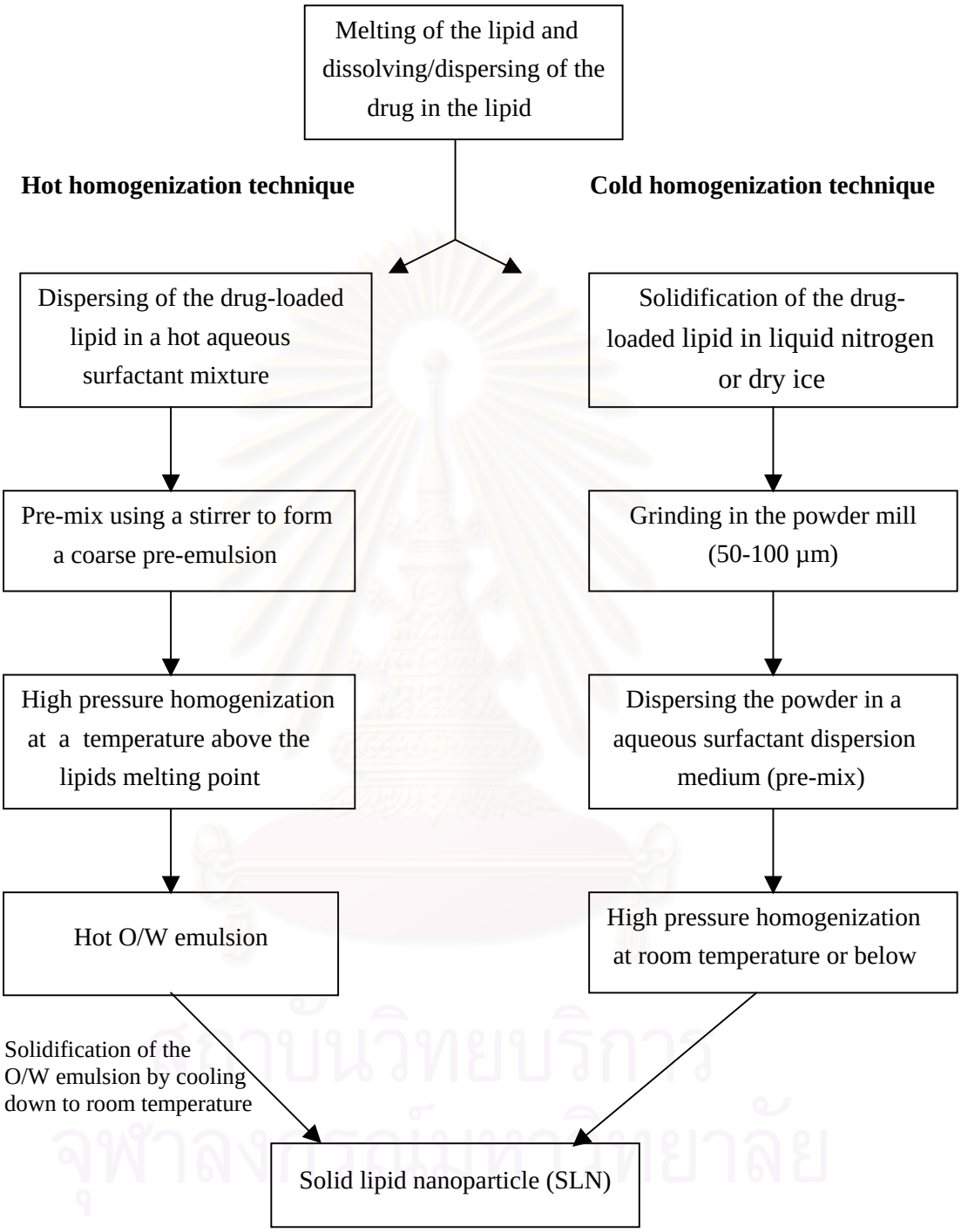

Figure 3 Schematic procedure of hot and cold homogenization techniques for SLN production

aqueous surfactant solution and the dispersion is homogenized at room temperature or below. The cavitation and shear forces in the homogenizing gap are sufficiently high to break the microparticles and to yield solid lipid nanoparticles. In general, compared to hot homogenization, larger particle sizes and a broader size distribution are observed in cold homogenized samples of the same lipid at identical homogenization parameters. To further reduce the mean particle size and to minimize the size distribution, a higher number of homogenization cycles can be applied. The method of cold homogenization minimizes the thermal exposure of the sample, but it does not avoid it due to the melting of the lipid/drug-mixture in the initial step.

3. Microemulsion

Gasco (1993) developed SLN preparation techniques which are based on the dilution of microemulsions. Microemulsions are clear or slightly bluish solutions being composed of a lipophilic phase, surfactant, co-surfactant and water. To form a microemulsion with a lipid being solid at room temperature, the microemulsion needs to be produced at a temperature above the melting point of the lipid. The lipid is melted, a mixture of water, the surfactant and co-surfactant are heated to the same temperature as the lipid and added under mild stirring to the lipid melt. A transparent, thermodynamically stable system is formed when the compounds are mixed in the correct ratio for microemulsion formation. This microemulsion is then dispersed in a cold aqueous medium (2-3ºC) under mild mechanical mixing, thus ensuring that the small size of the particles is due to the precipitation and not mechanically induced by a stirring process. Surfactants include lecithin, polysorbate 20, polysorbate 60, taurodeoxycholate sodium salt and co-surfactants consist of butanol, sodium monooctylphosphate (Morel et al., 1998). Typical volume ratios of the hot microemulsion to cold water are in the range of 1:25 to 1:50. The dilution process is critically determined by the composition of the microemulsion.

Considering microemulsions, the temperature gradient and the pH value fix the product quality in addition to the composition of the microemulsion. High temperature gradients facilitate rapid liquid crystallization and prevent aggregation (Cavalli, Marengo et al., 1996). Large scale production of SLN by the microemulsion technique also appears feasible and is at present under development at Vectorpharma

(Trieste, Italy). The microemulsion is prepared in a large, temperature-controlled tank and then pumped from this tank into a cold water tank for the precipitation step (Müller, Mäder, and Gohla, 2000).

4. Solvent emulsification and evaporation (precipitation in o/w emulsions)

Sjöström and Bergenståhl (1992) described a production method to prepare nanoparticle dispersions precipitation in O/W emulsions. The lipophilic material is dissolved in a water-immiscible organic solvent e.g. cyclohexane, chloroform, methylene chloride, diethyl ether, petroleum ether. This solution is then emulsified in an aqueous phase. Upon evaporation of the solvent a nanoparticle dispersion is formed by precipitation of the lipid in the aqueous medium. The mean diameter of the obtained particles was 25 nm with cholesterol acetate as model drug and by using a lecithin/sodium glycocholate blend as emulsifier. The reproducibility of these results is confirmed by Siekmann and Westesen (1996). They prepared nanoparticles of tripalmitin by dissolving the triglyceride in chloroform. This solution was emulsified in an aqueous phase by HPH. The organic solvent was removed from emulsion by evaporation under reduced pressure. The mean particle size ranges from approximately 30 to 100 nm depending on the lecithin/co-surfactant blend. Particles with average diameters as small as 30 nm were obtained by using sodium glycocholate as co-surfactant. The advantage of this procedure over the homogenization process is the avoidance of any thermal stress. However, a clear disadvantage is the use of organic solvent.

Analytical characterization of SLN

An adequate characterization of SLN is a necessity for the control of the quality of the product. The characterization methods should be sensitive to the key parameters of SLN performance and should avoid artifacts. However, characterization of SLN is serious challenge due to the colloidal size of the particles and the complexity of the system, which includes also dynamic phenomena. Many analytical tools do not permit direct measurement in the undiluted SLN dispersion. Possible artifacts caused by sample preparation e.g. the removal of stabilizer from particle

surface by dilution, the induction of crystallization processes, the changes of lipid modifications. Therefore, several parameters have to be considered.

1. Particle size and shape

Photon correlation spectroscopy (PCS) and laser diffraction (LD) are the most powerful techniques for routine measurements of particle size. PCS measured the fluctuation of the intensity of the scattered light which was caused by particle movement. Since small particles suspended in a fluid exhibit random Brownian motion as a consequence of molecular bombardment. The more massive the particle, the less significant this effect is. Thus measurement of the random motion can yield size (Jone, 1999). This method covered a size range from a few nanometers to about 3 μm. However, PCS was not able for detection of larger particles. Larger particles can be visualized by means of laser diffraction measurement. This method was based on the dependency of the diffraction angle on particle radius. Smaller particles caused more intense scattering at high angles compared to the larger one. The advantage of LD was the coverage of a broad size range from nanometer to the lower millimeter range (Müller et al., 2000). However laser diffractometry yielded a volume distribution which weighed large volume particle more intensively. Therefore size data were generally higher compared to data from photon correlation spectroscopy (Krause and Müller, 2001). In this study, the z average, mean particle size from PCS, was used to compare mean of the bulk population. The percentage of particle larger than 1, 5 and 10 μm calculated from LD was used to assess the formulation intended for parenteral applications. The D(v,0.5) was the volume diameter 50% obtained from LD, that mean 50% of the particle are below the given size. The polydispersity index (PI) and uniformity described the width of the distribution. The PI ranged from zero (monodisperse particle) to 0.5 (broad spectrum), values above 0.5 did not allow allocation to a logarithmic normal distribution to the PI. The PI value about 0.1 meant that particle size distribution was narrow. However, both methods are not direct particle measurement. They detect light scattering effects which are used to calculate particle sizes. Furthermore, difficulties may arise both in PCS and LD measurements for samples which contain several populations of different size. Therefore, additional techniques might be useful.

Light microscopy is recommended, although it is not sensitive to the nanometer size range. It gives a fast indication of the presence and character of microparticle. For example, the microparticles are in unit form or consist of aggregates of smaller particles.

Electron microscopy provides, in contrast to PCS and LD, direct information on the particle shape and size. However, the investigator should pay special attention to possible artifacts which may be caused by the sample preparation. Transmission electron microscopy (TEM) can be used for direct examination of particle in the size range 1 nm-5 μm. Both Freeze-Fracture Transmission electron microscopy (FF-TEM) and Cryo-Transmission electron microscopy (Cryo-TEM) were used to investigate particle shape and size of SLN (Cavalli, Gasco et al., 2001, Sznitowska et al., 2001, Zhang et al., 2000). Scanning electron microscopy (SEM) has also been reported to study the surface morphology of lipid micropellets (Eldem, Speiser, and Alfoter, 1991). In this study, Cryo-Scanning electron microscopy (Cryo-SEM) was used to investigate particle shape of SLN. Cryo-SEM is provided with two stages– a specimen treatment stage in the Cryo-chamber and a cooling stage in the SEM specimen chamber. Both stages are constantly cooled with liquid nitrogen. A fracture knife, an etching heater and an evaporator are built into the Cryo chamber. The Cryo-SEM construction diagram is shown in Chapter 3. The Cryo-SEM method is to physically fix water (i.e., freeze into ice). After The sample is transferred to cooling stage, the specimen was fractured with the built-in knife. The particle shape and size can be observed.

Sznitowska et al (2001) investigated cetyl palmitate SLN stabilized by alkyl glucoside (Plantacare® 2000) by TEM. The electron micrographs suggest the spherical form of particles. On contrary, different SLN shapes such as platelet-like pattern were reported for SLN made of triglycerides with high purity (Siekmann and Westesen, 1998). The chemically homogenous lipid tends to form more or less perfect crystals with the typical platelet-like pattern of the β modification. The use of chemically heterogeneous lipids in combination with heterogeneous surfactants favors the formation of ideally spherical lipid nanoparticles.

2. Zeta potential

The measurement of the zeta potential allows predictions about the storage stability of colloidal dispersion. Generally particle aggregation is less likely to occur for charged particles due to electric repulsion. A reduction in the electrical charge is known to increase the rate of flocculation and coalescence (Floyd and Jain, 1996). However, this rule cannot strictly applied for systems which contain steric stabilizers because the adsorption of steric stabilizer will decrease the zeta potential due to the shift in the shear plane of the particle. In this observation, zeta potentials were determined using a ZetaSizer 4. In ZetaSizer 4, zeta potential measurements are performed using a laser doppler anemometry (LDA). LDA allows fast determination of the electrophoretic mobility using laser light scattering. The zeta potential is calculated from the electrophoretic mobility, the electric field strength applied, the viscosity and the dielectric constant of the dispersion medium at a given temperature.

3. Degree of crystallinity and lipid modification

Special attention must be paid to the characterization of the degree of lipid crystallinity and the modification of the lipid, because these parameters are strongly correlated with drug incorporation and release rates.

Differential scanning calorimetry (DSC) is a method which measures the difference in energy between a reference and a sample. It is widely used to investigate the status of the lipid because different lipid modifications possess different melting points and melting enthalpies (Byrn, Pfeiffer, and Stowell, 1999). Freitas and Müller (1999) studied the correlation between long-term stability of solid lipid nanoparticles and crystallinity of the lipid phase using DSC. They found that the destabilizing factors light, temperature and shear forces cause a distinct increase in the recrystallization index by transformation of the lipid to the β′ modification being accompanied by gel formation. In addition, the crystalline and amorphous nature of drug dispersed in SLN can be determined using DSC (Clas, Dalton, and Hancock, 1999). Cavalli, Peira et al. (1999) found that hydrocortisone and progesterone are dispersed in lipid matrix in an amorphous form.

X-ray diffractometry is widely used to study for the identification of solid phases. The X-ray diffraction pattern of every crysrtalline form of a compound is unique, making this technique particularly suited for the identification of the polymorphic forms of a compound (Suryanarayanan, 1995). The X-ray diffraction pattern also allows to differentiate between crystalline and amorphous meterial. Using the X-ray diffractometry and ^{1}H NMR, Bunjes, Siekmann et al. (1998) revealed that dispersed trimyristin in SLN remained in liquid and does not form a solid amorphous phase at room temperature. However, the colloidally dispersed trimyristin could crystallize by cooling down the temperature below its critical temperature.

Infrared spectroscopy (IR) is very useful for analysis of solid. It is extremely sensitive to the structure and thus is a powerful method for the characterization and identification of different solid forms. In SLN, IR was used to study chemical interaction occurred between the lipid matrix and drug. Zhang et al. (2000) found that no any shift after encapsulation of cyclosporin A to stearic acid. Hence, there was no chemical reaction occurred in cyclosporin A loaded stearic acid SLN.

4. Coexistence of additional colloidal structures

The coexistence of additional colloidal structures e.g. micelles, liposomes, mixed micelles, supercooled melts has to be taken into account for all SLN dispersions. Unfortunately, this aspect has been ignored in the majority of the SLN literature. Stabilizing agents are not localized exclusively on the lipid surface, but also in the aqueous phase. Therefore, micelle forming surfactant molecules will be present in three different forms (i) on the lipid surface (ii) as micelle (iii) as surfactant monomer. Lecithin will form liposomes, which have also been detected in lipid emulsions for parenteral nutrition. Mixed micelles have to be considered in glycocholate/lecithin stabilized and related systems. The characterization and quantification are a conscientious challenge due to the similarities in size combined with the low resolution of PCS to detect multimodal distributions. Anyway, nuclear magnetic resonance (NMR) and electron paramagnetic resonance (EPR) are powerful tools for investigating dynamic phenomena and the characteristics of nanocompartments in colloidal lipid dispersions.

Simple ^{1}H NMR spectrosopy permits an easy and rapid detection of supercooled melts due to the low linewidths of the lipid protons. This method is based on the different proton relaxation times in the liquid state give sharp signals with high signal amplitudes, while semisolid/solid protons give weak and broad NMR signals under these circumstances.

EPR spectroscopy was used to investigate the incorporation of drugs into SLN in order to establish their location, the entrapment efficiency and to follow the stabilization of SLN dispersion during storage. Ahlin et al. (2000) synthesized spin-labelled derivertives of fatty acid as the model lipophillic drug for their study. They have shown that model lipophilic drug distribute between the solid glyceride core and the phospholipid layers and the distribution depends on the type of lipid matrix and on the phospholipid concentration.

5. Drug incorporation and drug release

A large number of drugs have been studied with regard to their incorporation into SLN as shown in Table 4. Drug loading might result in strong changes of the SLN characteristics – particle size distribution, zeta potential, lipid modification. The modification of drug and lipid could be characterized by DSC, X-ray diffractometry and NMR. However, there are distinctly less data available about drug release especially information about the release mechanisms. Due to the colloidal size, release studies are not trivial experiment. The choice of a suitable model of drug release nanoparticles is still problematic. Membrane diffusion technique is the most widely used to study the *in vitro* drug release from SLN (Yang et al., 1999). The USP paddle method and flow-though diffusion Franze cell have also been employed to determine the release kinetics from SLN (Jenning, Thünemann, and Gohla, 2000, Müller, Mehnert et al., 1995). The release experiments were conducted under several conditions. Therefore, it is not easy to compare the results.

At the beginning of SLN development, burst release was observed. It seemed that the system is not feasible for a prolonged drug release. The breakthrough was in developing the first SLN, which showed a prolonged *in vitro* drug release up to 5-6 weeks. To develop controlled release SLN, the understanding of the drug release is

necessity. Müller, Lippacher et al. (2000) proposed four different models of internal structure SLN to explain the drug release profiles.

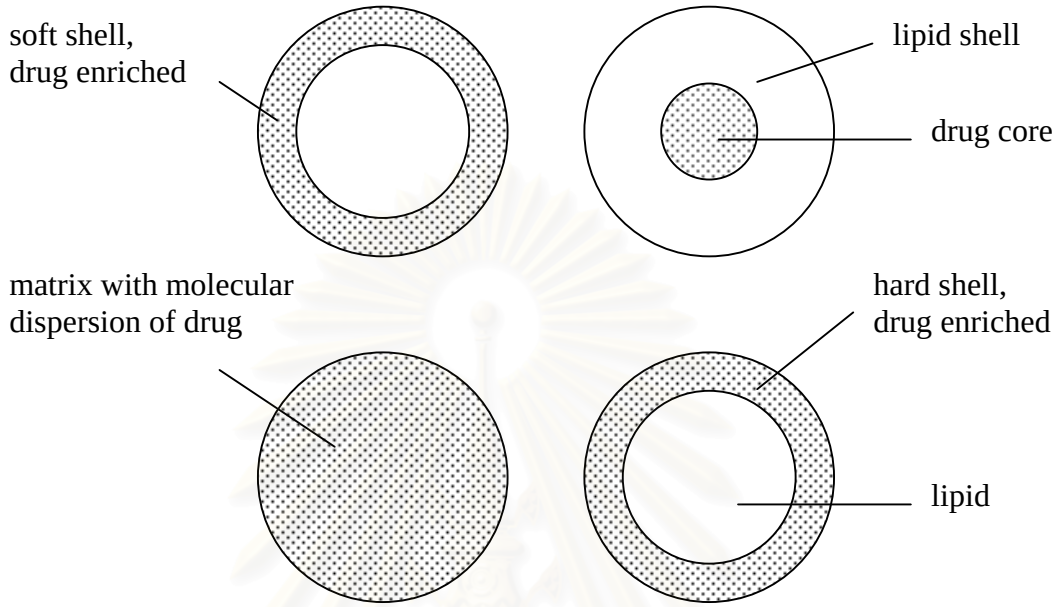

Figure 4 Proposed models for the internal structure of SLN: (1) Soft drug-containing shell surrounding a lipid core (upper left) (2) Homogeneous particle matrix with molecular dispersion of drug (lower left) (3) A drug core surrounded by a lipid shell being drug-free or of low drug content (upper right) (4) Drug-free lipid core surrounded by a hard shell composed of lipid –drug mixture (lower right)

1. Soft drug-containing shell core model

Mühen et al. (1998) studied the release profile of drugs from SLN. They found that the burst release was observed when incorporating tetracaine and etomidate into SLN. It was also found that the burst release diminished with increasing particle size and prolonged release could be obtained when particles were sufficiently large i.e. lipid microparticles. From the data, it was concluded that the drug was enriched in an outer shell of the particles. The drug has a relatively short distance of diffusion and will be released in a burst. The formation of the shell is explained by the stepwise crystallization process of the drug-lipid mixture. After the hot homogenization step the produced O/W emulsion is cooled, the lipid precipitates first forming a more or less drug-free lipid core. The remaining liquid drug-lipid mixture will enrich

continuously in drug content until the eutecticum is reached. Reaching the eutecticum leads to the simultaneously crystallization of lipid and drug, forming an outer shell surrounding the drug-free lipid core as depicted in Figure 5. The soft drug-containing shell core model is shown in Figure 4, upper left.

In addition, it must be considered that surfactant is present. This surfactant will interact with the outer shell and affect its structure. The existence of a shell can be proven by atomic force microscopy (AFM) measurements. With special technique, noncontact imaging, the hardness of the particle is determined by pressing the cantilever of the AFM instrument into the particle. The force required to press the cantilever into the particle is a measure of the viscosity of the particle matrix. It can be shown that there is an outer shell of relatively low viscosity that is composed of lipid, drug, and partially incorporated surfactant (Mühlen, Mühlen et al., 1996).

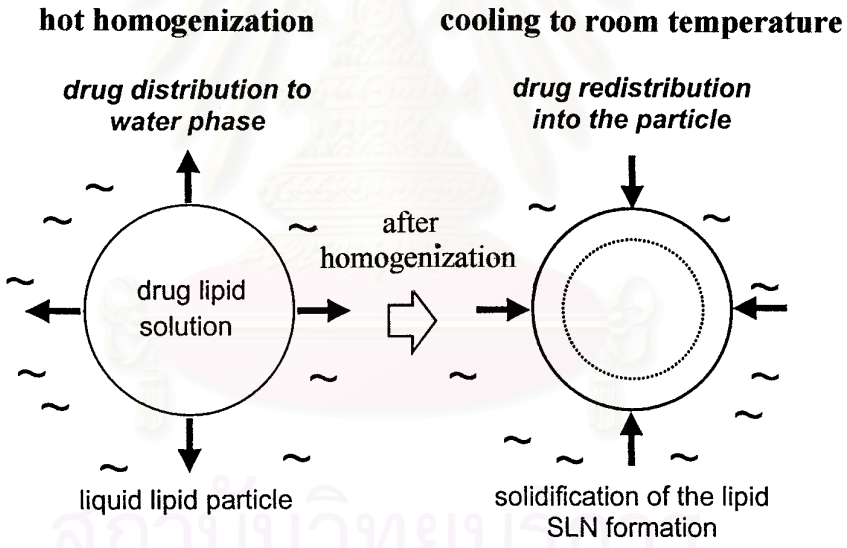

Figure 5 Partitioning effects on drug during the production of SLN by the hot homogenization technique. Left: Partitioning of drug from the lipid phase to the water phase at increased temperature. Right: Re-partitioning of the drug to the lipid phase during cooling of the produced O/W emulsion.

2. Solid dispersion model

In contrast, the prolonged release over a period of 5 weeks was observed from prednisolone loaded glyceryl behenate SLN (Mühlen, Schwarz et al., 1998). The SLN system was produced by cold homogenization method. The prolonged release can be explained by molecular distribution of the drug in the lipid matrix. This is very likely because cooling the drug-containing lipid will lead to the formation of a solid dispersion. This solid dispersion was just milled by high pressure homogenization, which means that no or limited melting occurred. The particles were just broken down and retained their structure of a solid dispersion. Although, there will be a warming up of the dispersion by approximately 20ºC. However, this does not lead to a melting in lipid because melting point of the lipid is sufficient high. Based on these results, the solid dispersion model was proposed as depicted in Figure 4, lower left.

3. Drug core/ lipid shell model

A drug-enriched core will be found in case the drug precipitates first before the lipid recrystallizes. This should be obtained when dissolving a drug in the lipid melt at or close to its saturation solubility. Cooling of the emulsion will lead to a supersaturation of drug in the melted lipid and subsequently to drug crystallization prior to lipid crystallization. Further cooling will finally lead to the recrystallization of the lipid surrounding the drug core as a membrane. This lipid membrane will contain only drug in such a concentration corresponding to the saturation solubility of the drug at the recrystallization temperature of lipid. That means it will result in a drug-enriched core surrounded by a lipid shell as shown in Figure 4, upper right.

4. Drug-free core/ hard drug-containing shell model

Recently, it was discovered that there is additionally the hard shell core model of SLN. Within an industrial product development, the SLN was loaded with coenzyme Q10. The coenzyme Q10 loaded SLN was routinely investigated by contact AFM. It was assumed that a solid dispersion of coenzyme Q10 in lipid would be present. Contact AFM revealed that there was an outer shell of increased rigidity, the core was distinctly less rigid. The coenzyme Q10 was released relatively fast. Possibly coenzyme Q10 and the lipid had structural properties such that they fitted together very well to form a solid structure like brick layers. It could be possible that

the molecule coenzyme Q10 fitted into the imperfections of the lipid, leading to a more solid structure. Due to the location of coenzyme Q10 in the outer shell, the drug release was fast but the presence of coenzyme Q10 led to a more solid state of the lipid leading to a firm outer shell. The proposed model of drug-free lipid core surrounded by a hard shell composed of lipid drug mixture is shown in Figure 4, lower right.

Applications of SLN for drug delivery

The applications of SLN are manifold. Basically, the SLN can be employed for any purpose for which nanoparticles have a distinct advantage. The application range from topical to parenteral.

1. Topical administration

Regarding the regulatory aspect, topical application is relatively unproblematic. The major advantages for topical products are the protective properties of SLN for chemically labile drugs against degradation and the occlusion effect due to film formation on the skin. Stability enhancement was reported for coenzyme Q10 and also for the very sensitive retinol. An enhancement of occlusiveness can be achieved by adding SLN of suitable composition to light O/W day creams, thus increasing the moisturing effect without having the glossiness of a night cream.

The parameter to assess the ability of a delivery system is its effect on active ingredient penetration into skin and consequently its therapeutic effect and in cosmetic applications the effect on skin appearance. A range of active ingredients e.g. coenzyme Q10, retinol, vitamin E and its derivatives have been incorporated into SLN. The skin caring properties of a commercial retinol cream have been compared to the same cream containing retinol loaded SLN, reference was untreated skin. Parameters assessed were skin elasticity, moisture state and skin roughness as standard read out parameters. The moisture level of the SLN containing formulation and SLN free cream were raised by 33% and 23%, respectively after a 1 week period of treatment compared to untreated skin. Besides this the cream containing retinol

loaded SLN improved the skin smoothness by 10.3%, the SLN free cream achieved only 4.1% (Müller, Mäder et al., 2000).

2. Peroral administration

The application of SLN as drug delivery by oral administration was presented by Yang, Zhu et al. (1999). They produced camptothecin containing SLN from stearic acid (2%), lecithin (1.5%) and poloxmer 188 (0.5%). The encapsulation efficiency of camptothecin was 99.6%. The plasma levels and body distribution were determined after administration of camptothecin loaded SLN versus a camptothecin solution. Two plasma peaks were observed after administration of camptothecin loaded SLN. The first peak was attributed to the presence of free drug, the second peak can be attributed to controlled release or potential gut uptake of SLN. These two peaks were also found in the total camptothecin concentration-time profiles of all measured organs. It was also found that the incorporation into SLN protected camptothecin from hydrolysis. The conclusion from this study was that SLN was the promising sustained release system for camptothecin and other lipophilic drugs after oral administration.

3. Parenteral administration

For parenteral applications, SLN had to be easily drawn into a syringe through a 20-25 gauge needle (syringeability) and readily ejected from syringe into the patient (injectability). The range of inside diameters of 20-25 hypodermic gauge size is shown in Table 5 (Terumo, 2001). However, the amount of microparticles is the limiting factor for SLN to be acceptable for intravenous administration by the regular authorities. The injection of the relatively high content of microparticles larger than 5 μm could bring about the danger of capillary blockage resulting in fat embolism. The pharmacopoeia differs very much regarding their specifications. The monographs regarding fat emulsions for intravenous administration might be a guideline to judge the SLN. The European Pharmacopoeia 1979 required that the particle diameter should not be larger than 5 μm, the German Pharmacopoeia demands only a determination of the particle size. There is a lack of obligatory precise specification. In addition, one has to consider that a toxicity study with the parenteral new product

has to be made. To formulate parenteral SLN, surfactants accepted for parenteral administration can be used e.g. lecithin, tween 80, poloxamer 188, polyvinyl pyrrolidone, span 85. For the intravenous route it is recommended to focus on the i.v. accepted surfactants e.g. lecithin, tween 80, poloxamer 188, sodium glycocholate (Müller, Mader et al., 2000).

Studies using intravenously administered SLN have been performed by various groups. Bocca et al. (1998) produced stealth and non-stealth solid lipid nanoparticles and studied them in cultures of macrophages and also after loading them with paclitaxel in vivo. The i.v. administered SLN led to higher and prolonged plasma levels of paclitaxel. Both non-stealth and stealth SLN showed a similar low uptake by the liver and the spleen macrophages, a very interesting point was the increased uptake observed in the brain. This study demonstrates the potential of SLN to achieve prolonged drug plasma levels. The observed similar low uptake by the liver and spleen macrophages might be explained by a similar low surface hydrophobicity of both types of particles avoiding the adsorption of any blood proteins mediating the uptake by liver and spleen macrophages. The uptake of the SLN by the brain might be explained by adsorption of a blood protein mediating the adherence to the endothelial cells of the blood brain barrier.

Table 5 The range of inside diameters of 20-25 hypodermic gauge size

Gauge size	**Designated metric size**	**Inside diameter of tubing (millimeters)**					
		Regular wall		**Thin wall**		**Ultra wall**	
		min.	**max.**	**min.**	**max.**	**min.**	**max.**
25 G	0.5	0.23	0.28	0.29	0.34	0.29	0.34
24 G	0.55	0.28	0.33	0.35	0.39	0.35	0.39
23 G	0.6	0.33	0.38	0.36	0.41	0.38	0.43
22 G	0.7	0.39	0.44	0.44	0.49	0.46	0.51
21 G	0.8	0.48	0.54	0.53	0.58	0.54	0.61
20 G	0.9	0.56	0.62	0.61	0.67	0.63	0.69

Pharmacokinetics studies of doxorubicin incorporated into SLN showed higher blood levels in comparison to a commercial drug solution after i.v. injection in

rats. Concerning the body distribution, SLN was found to cause higher drug concentrations in lung, spleen and brain, while the solution led to a distribution more into liver and kidneys (Zara et al., 1999).

Yang, Lu et al.(1999) reported on the pharmacokinetics and body distribution of camptothecin after i.v. injection in mice. In comparison to a drug solution, SLN was found to lead to much higher AUC/dose and mean residences time especially in brain, heart and reticuloendothelial cells containing organs. The highest AUC ratio of SLN to drug solution among the tested organs was found in the brain.

Toxicity aspects

The status and toxicity of SLN are a major issue for the use of a delivery system particularly in parenteral administration. For parenteral administration, information about the interaction of SLN with phagocytic cells is a prerequisite. Phagocytic cells such as mononuclear phagocytes and granulocytes which are the first cells that interact with particles in the blood stream and thereby represent the first line of defence of the immune system. (Schöler, Hahn et al., 2002). Interaction of phagocytic cells with foreign bodies such as drug delivery systems may result in phagocytic uptake and uncontrolled release of pro-inflammatory cytokines such as interleukin 1 (IL-1), interleukin 6 (IL-6), interleukin 12 (IL-12), tumor-necrosis-factor α (TNF- α) (Schöler, Olbrich et al., 2001). Uncontrolled secretion of these molecules may lead to a cascade of adverse reactions and subsequently cell death. In order to evaluate the performance and toxicological acceptance of drug delivery systems, knowledge on what causes change in the production of these pro-inflammatory cytokines is of utmost importance.

The interaction of SLN with phagocytizing cell has been studied in vitro on human granulocytes. A luminol-based chemiluminescence was use to compare SLN with polymer particles and to compare SLN composition on the phagocytosis rate. Müller, Maassen et al. (1997) found that phagocytosis rate of poloxamer stabilized glycerol behenate and cetyl palmitate SLN was lower in comparison to polystyrene nanoparticles. Furthermore, they also concluded that the cytotoxicity of the glyceride SLN was about 10-fold below the one of polylactide/glycolide nanoparticles. The

results of cytotoxicity studies assessed by the 3-(4,5-dimethylthiazol-2-yl)-2,5-diphenyl-tetrazolium bromide (MTT) test indicated that glycerol behenate and glyceryl myristate SLN were less toxic than polyalkylcyanoacrylate and polylactic/glycolic acid nanoparticles (Müller, Rühl et al, 1997). The cytotoxicity of SLN determined by viability measurements proved to be very low (Müller, Maassen et al., 1997). The viability of human granulocytes was 84% after incubation with 1.2% poloxamer 188 stabilized cetyl palmitate SLN and 72% after incubation with 5% poloxamer 188 stabilized glycerol behanate SLN. Poloxamer stabilized polylactide/polyglycolide particles reduced the cell viability to 50% at a concentration of 0.1%. Higher concentrations of polylactide/polyglycolide particles up to 0.5% led to complete cell death.

Recently, in vivo toxicity study with i.v. injected glycerol behenate and cetyl palmitate SLN was performed. Bolus injections of 1.33g lipid/kg body weight were administered every two days in mice, a total of six injections. Despite of the cetyl palmitate being a wax, these SLN were very well tolerated without increase in liver and spleen weight. Glycerol behenate SLN showed an increase in liver and spleen weight accompanied by histological changes e.g. infiltration of macrophages. However, these side effects were reversible and could be avoided by lowering the dose of glycerol behenate.

สถาบันวิทยบริการ
จุฬาลงกรณ์มหาวิทยาลัย

CHAPTER III
MATERIALS AND METHODS

Materials

The following materials were used as received.

- Compritol® 888 ATO (glycerol behenate) (Lot No. 24230, Gattefossé, France)
- Diazepam (Lot No. R1-43/00341, Tianjin Medicines, China)
- Epikuron® 200 (Batch No.1-0-9036, Lucas Meyer GmbH & Co., Germany)
- Lorazepam (Department of Medical Science, Thailand)
- Methanol AR grade (Labscan Asia Co., Ltd., Thailand)
- Nitrogen gas (Supplied by Namheng Oxygen Co., Ltd., Thailand)
- Phospholipon® 80 (Lot No. 90030, Nattermann Phospholipid GmbH, Germany)
- Poloxamer 188 (Lutrol® F 68) (Lot No. 37-0479, BASF, Germany)
- Poloxamer 407 (Lutrol® F 127) (Lot No. 49-0123, BASF, Germany)
- Potassium bromide (Lot No. 403125/1 43199, Fluka Chemika, Switzerland)
- Potassium dihydrogen phosphate (Lot No. 471687, Carlo Erbe, Italy)
- Sodium hydroxide pellets (Lot. No. 7708MVKK, Mallinckrodt Baker, Mexico)
- Standard buffer solution (Beckman, USA)
- Tween 20 (Distributed by Srichand Dispensary Co., Ltd., Thailand)
- Tween 80 (Distributed by B. L. Hua & Co., Ltd., Thailand)
- Water for injection (The Government Pharmaceutical Organization, Thailand)

Equipment

- Autoclave (Hirayama MFG. Corp., Japan)
- Analytical balance (Sartorius, A200S, Germany)
- Cryoscopic osmometer (Model Osmomat® 030-D, Gonotec, Germany)
- Differential scanning calorimeter (NETZCH DSC 200, Germany)
- Dissolution apparatus (Model DT 6R, Erweka, Germany)
- Fourier transform infrared spectrophotometer (FT-IR Spectrometer®, Perkin Elmer, USA)
- High speed homogenizer (Model D-7801, Ystral, Germany)
- High-performance liquid chromatography (HPLC) instrument equipped with the following
    - Liquid chromatograph pump (LC-10AD, Shimadzu, Japan)
    - UV-VIS detector (SPD-10A, Shimadzu, Japan)
    - Recorder (C-R6A Chromatopac, Shimadzu, Japan)
    - Microsyringe 100 µl (ITO Corporation, Japan)
    - C-18 Column (250 x 4.6 mm, 5 µ, Hypersil® BDS, England)
- High pressure homogenizer (Model EmulsiFlex C5®, Avestin, Canada)
- Hot air oven (Mammert, USA)
- Photon correlation spectrometer (Malvern 4700, Malvern Instruments Ltd., England)
- pH meter (Beckman, USA)
- Laser Diffractometer (Particle size analyzer, Mastersizer® S long bed Ver 2.11, Malvern Instruments Ltd., England)
- Scanning electron microscope (Model JSM-5410LV, JEOL, Japan)
- Transonic digital (Ultrasound ELMA® Model T900, Elma, Germany)
- Top to bottom rotator
- Ultracentrifuge® (Model L 80, Beckman, USA)
- UV visible spectrophotometer (Model UV-1601, Shimadzu, Japan)
- Ultrapure Water® equipped with filter system (Balson®, Balson Inc., USA), Boost pump, Option 3 water purifier, Maximum ultrapure water, and Reservoir (ELGA, USA)
- Vaccum filtration apparatus with sinter glass fiber No.3 (Waters, USA)
- Water bath (Model TBVS01, Hetomix and DT Hetotherm, Denmark)

- X-Ray diffractometer (JDX-3530 Diffractometer system, JEOL, Japan)
- ZetaSizer 4 (Malvern Instruments Ltd., England)

Glassware and Miscellaneous

- 0.22 and 0.45 μm membrane filter (Waters, USA)
- Aluminum foil (MMP Packaging, Thailand)
- Autopipette and disposable pipette tip (Socorex ISBA S.A, Switzerland)
- Beaker (Pyrex, USA)
- Cylinder (Pyrex, USA)
- Dialysis membrane (Lot No. 28H 0141, Sigma, USA)
- Disposable syringe and needle (Terumo, Thailand)
- Filter device (Swinnex®, Millipore, USA)
- Locking dialysis membrane clamp (MFPI, USA)
- Osmolality vessel (Gonotec, Germany)
- Parafilm (American National Can., USA)
- Polycarbonate centrifuge tube (Nalge Company, USA)
- Screwed-cap tube (Pyrex, USA)
- Transfering pipette (HBG, Western Germany)
- Vial type I glass with rubber cap and aluminum ring (Supplied by APPA Industried Co., Ltd., Thailand)

Methods

1 Formulation of solid lipid nanoparticle (SLN)

Solid lipid nanoparticle (SLN) was prepared by hot homogenization method. The high speed homogenizer and high pressure homogenizer were used to reduce particle size of emulsion. It was noteworthy that all formulations of SLN in the present study were prepared in % w/w. To study effect of types and amounts of stabilizer on the characteristics of SLN, Phospholipon® 80 (PL80), Epikuron®200 (EP200), poloxamer 188 (P188), poloxamer 407 (P407), tween 20 (TW20), and tween

80 (TW80) were used at the concentration ranging from 1 to 5 %. The ingredients used in the formulation are listed in Table 6.

Table 6 The composition of SLN

Chemicals	Concentration (%w/w)
Glycerol behenate	5
Stabilizer	1-5
Water for injection	to 100

The SLN was prepared by dissolving or dispersing stabilizer in aqueous phase. The aqueous and oil phases were separately heated up to 80°C. The temperature was controlled at 80±1°C using water bath. The aqueous phase was then added to the oil phase. In diazepam loaded SLN, oil phase consisted of mixture of 5% glycerol behenate and diazepam varying concentration from 0.1% to 0.9%. The high speed homogenizer was used to prepare coarse emulsion at the speed of 4,080 rpm for 10 minutes. The coarse emulsion was then homogenized to produce fine emulsion using EmulsiFlex® C-5 operating at 10,000 psi for 5 cycles (Wiwat Pichayakorn, 1999: 49-51). The obtained homogenization product was an O/W emulsion of melted lipid in the aqueous solution. Then this emulsion was filled into vials type I glass, purged with nitrogen gas for a few seconds before sealing with rubber caps and aluminum rings. All vials containing SLN were wrapped using aluminum foil to protect from light. Each preparation was evaluated for the particle size, zeta potential, pH and osmolality before sterilization. The rest of preparation were sterilized by autoclaving at 121°C, 15 psi for 15 minutes (British Pharmacopeia Comission, 1993) and were then allowed to stand at room temperature. The oil droplets solidified during cooling and formed SLN. The formulation after autoclaving was also determined for particle size, zeta potential, pH and osmolality.

1.1 Determination of type and amount of stabilizer

After sterilization, the preparations were allowed to room temperature and visually observed for any instabilities i.e. color change, coalescence, gel

formation. The optimum concentration of stabilizer that could produces stable SLN and the smallest particle size after autoclaving was chosen for further study.

1.2 Effect of storage temperature

The suitable formulation was kept at ambient temperature and 4°C. The particle size, pH, zeta potential and osmolality were assessed after storage for 1 month, 3 months and 6 months.

1.3 Effect of various amounts of glycerol behenate

After the optimal concentration of stabilizer in the formulation was determined, the concentration of glycerol behenate in quantity of 1 to 9% w/w was formulated. It was noticed that SLN were prepared under the same condition in order to study the effect of ratios of glycerol behenate to stabilizer on physicochemical properties. The particle size, pH, zeta potential and osmolality were evaluated.

1.4 Effect of various amounts of diazepam

According to percentage of stabilizer and glycerol behenate, the optimal composition of formulation was chosen to study the effect of drug concentration. Therefore, the concentration of diazepam varying from 0.1 to 0.9 % w/w of formulation was used to evaluate physicochemical properties and drug release profiles. It was noted that diazepam loaded SLN was initially prepared under pressure of 10,000 psi and 5 cycles.

1.5 Effect of homogenizing condition for 0.5% diazepam loaded SLN

The SLN containing 0.5% w/w of diazepam was chosen to determine the optimum homogenizing condition. The homogenization pressure of 10,000, 15,000 and 20,000 psi and the cycles of homogenization of 5, 7, 9 were studied to evaluated the optimum pressure and number of cycle of homogenization. The statistical analysis was undertaken using the two-way ANOVA (Analysis of Variance) test with SPSS® version 10 software program.

1.6 Stability testing

The stable SLN formulations after being sterilized were also observed under accelerated condition (heating and cooling cycle) by storing the sample at 4°C for 48 hours and 45°C for 48 hours for 6 cycles. The particle size and zeta potential were studied. Physical instability was also visually investigated.

2. Physicochemical characterizations of SLN

2.1 Determination of size

The particle size analysis was assessed within 24 hours after preparing.

2.1.1 Photon correlation spectroscopy (PCS)

A photon correlation spectrometer with He-Ne laser at a fixed wavelength of 632.8 nm as the light source at a single scattering angle of 90°, was used to determine particle size of SLN in nanometer size range. A SLN sample was dispersed in triple distilled water. The triple distilled water was filtered through 0.22 μm filter before use. A sample of dispersion was put in the quartz cuvette. The sample was then placed in the instrument and allowed to be temperature equilibrium between sample and sample holder at 30°C. From PCS measurements, the data were reported as both the average of particle size (z value) and polydispersity index (PI) which was a measure of the width of the distribution.

สถาบันวิทยบริการ
จุฬาลงกรณ์มหาวิทยาลัย

2.1.2 Laser diffractometry

A laser diffractometer with 300 RF mm range lens, 2.40 mm beam length was used for analyzing the content of nanoparticles and microparticles. The sample was dispersed with purified water by adding it to the instrument at a suitable concentration. The correct amount was adjusted by observing the obscuration. In case of the obscuration is too low. The sample concentration was adjusted by adding sample. If the obscuration is too high. The concentration was reduced by adding purified water. The bar on the obscuration monitor showed green with a value

reported between 10% and 40% indicated that the concentration was suitable. During analysis, temperature was controlled at 30°C. Particle size distribution was analyzed by the curve plotted between particle diameter versus percentage volume of particles. Cumulative frequency of volume diameter was calculated, and the volume mean diameter- D(4,3), the surface mean diameter- D(3,2), diameter of particles of 10%, 50%, and 90% volume percentile- D(v,0.1), D(v,0.5), D(v,0.9) respectively, were determined. The span and uniformity described the broadness of size distribution as defined in Appendix D. Higher value of both span and uniformity indicated broader particle size distribution. The percentage of the microparticles was calculated to assess the possibility for parenteral administration. The data obtained were the average of three determinations.

2.2 Determination of zeta potential

The zeta potential of SLN was determined by microelectrophoresis using cross beam laser doppler anemometry. SLN sample was diluted in triple distilled water. The triple distilled water was filtered through 0.22 µm membrane filter. The SLN are placed in an electric field by applying to the cell using 10-ml plastic syringe. During the measurement, the temperature was controlled at 30°C. The zeta potential was automatically calculated using Smolochowski equation. Each sample was carried out in tripicate.

2.3 pH measurement

The pH of SLN was measured at room temperature using a pH meter. The equipment was calibrated at pH 4 and 7 using Beckman standard buffer solution before used. Each sample was performed in triplicate.

2.4 Osmolality measurement

The osmolality of SLN was measured at room temperature using freezing point depression principle. Before the measurement of the osmolality of samples, the instrument had to be calibrated with water for injection. The SLN volume of 50 µl was filled in a clean and dry measuring vessel by means of a pipette,

avoiding the trapping of air bubbles. The measuring vessel was pushed on the measuring vessel holder to the upper limit and then let the holder down into the lower cooling system. The measuring result was automatically displayed as value for osmolality concentration in Osmol/kg. Each sample was measured in triplicate.

2.5 Scanning electron microscopy (SEM)

Particle size and shape of SLN were observed by scanning electron microscope. The SEM observation method SLN in this study was Cryo-SEM method. The basic construction diagram of Cryo-SEM is shown in Figure 6. The sample was dropped into the hole of stub and the specimen stub was set on the specimen holder. The specimen holder was screwed with the specimen exchange rod. The specimen stub was then freezed in liquid nitrogen which made the sample kept below 0°C. The sample holder was set in the Cryo-chamber through the air lock chamber. After the specimen was fractured with the built-in knife and was carried out sublimation(etching) by using etching heater about 1 minute, the sample was then transferred to cooling stage and observed particle shape and size (Observation of water-containing specimens SEM method, JEOL application note). The observation was performed in duplicate in each sample.

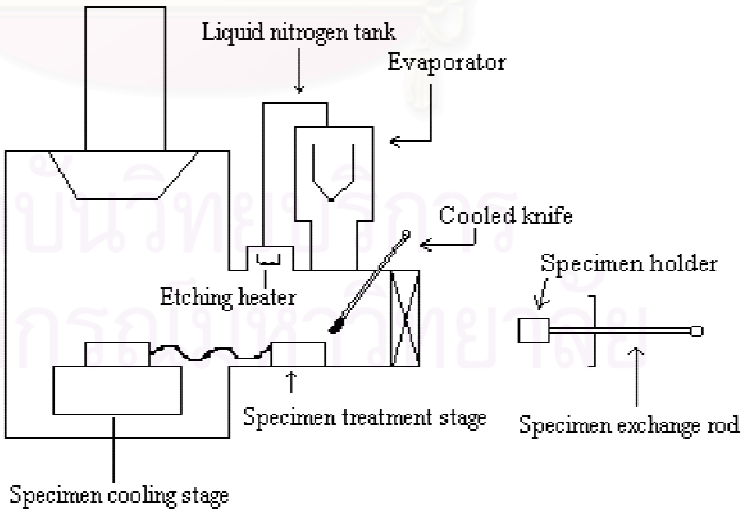

Figure 6 Construction of Cryo-SEM

2.6 Infrared Spectroscopy (IR)

Fourier transform infrared spectrophotomery (FT-IR), a high sensitivity of IR, was used to study interaction between drug and other exipients. The change of functional groups of triglyceride, drug and stabilizer was observed from the positions and intensities of IR spectra. The IR spectra of triglyceride, drug, stabilizer and solid lipid products after ultracentrifugation and drying in desiccator were acquired by potassium bromide disc method. The dried sample was mixed with potassium bromide in agate mortar and pestle by geometric dilution technique, then was placed using hydrolic press to a thin disc. The KBr disc was then measured within the wavenumbers of 400-4000 cm^{-1}.

2.7 Differential Scanning Calorimetry

The DSC analysis was used to investigate the crystalline structure of triglyceride, drug and solid lipid products (Cavalli, Caputo, and Gasco, 2000). The sample was weighed about 3 mg into a crimped aluminum pan with 1 pinhole and the empty pan was used as reference. DSC pattern was determine by using NETZSCH DSC 200 (Germany) with a heating rate of 10°C/min, in the temperature range from 0-250°C for all samples.

2.8 Powder X-ray Diffractometry

Powder X-ray diffractometry was used to study the change of crystallinity of triglyceride and drug after preparing process (Jenning, Schafter-Korting, and Gohla, 2000). The sample was made as fine as possible using an agate mortar and pestle. The proper amount of the sample was placed onto the acrylic plate containing rectangular window. After firmly pressed it down using another piece of glass plate, any surplus of sample was removed. The sample plate stuffed with the sample was mounted onto the sample holder. X-ray diffractogram was scanned with the diffraction angle increasing from 3° to 60°, 2θ angle, with a step angle of 0.04° and count time of 1 second.

2.9 *In-vitro* drug release

The *in vitro* drug release study of SLN was performed using dialysis technique.

The tubing dialysis membrane was immersed in deionized water for 12 hours, and was then rinsed with hot water to wash off any water soluble contaminants approximately 3 minutes. The membrane was soaked in release medium prior to use. The 2-ml SLN was filled into dialysis bag which was locked at the one end using locking clamp. The air bubbles were removed and dialysis bag was sealed at the other end. The SLN was immersed in 600 ml phosphate buffer, pH 7.4 at 37±0.5°C as release medium. The dissolution apparatus (Erweka, Germany) with paddle rotation at 50±2 rpm was used in this experiment. (Yang, Lu et al., 1999). Aliquot of 10 ml dissolution medium was withdrawn and the equal volume of fresh medium was added periodically. The amount of drug released was assayed by UV-VIS spectrophotometer and calculated from calibration curve. The cumulative percent release of dissolved drug was subsequently computed. The release profile was set up from these data.

Saturated solution of diazepam was determined for drug diffusion through dialysis membrane in order to compare drug release profiles of solution and dispersions containing SLN. The supernatant of preparation was also assayed for drug release in compensating the release of drug outside the solid lipid particles using HPLC assay.

Dissolution medium was pH 7.4 phosphate buffer (The United States Pharmacopeial Convention, 2000). A 8 L of medium was prepared using 54.4 g monobasic potassium phosphate and 12.48 g of sodium hydroxide, added purified water to adjust volume.

2.10 Entrapment efficiency

Diazepam SLN was separated from liquid medium using Ultracentrifugation® at 60,000 rpm, 4°C for 6 hours (Zhang et al. 1999). The entrapment efficiency was determined indirectly by measuring the concentration of

drug in supernatant after centrifugation. The triplicate observations were measured. The encapsulation efficiency was calculated from

$$\text{Entrapment efficiency} = \frac{[D]_{total} - [D]_{supernatant}}{[D]_{total}} \times 100$$

where $[D]_{total}$ = theoretical drug content per 1 ml of preparation and

$[D]_{supernatant}$ = drug content per 0.95 ml of supernatant found.

3 Solubility measurement

Excess amounts of diazepam powder were added to 5 ml deionized water or pH 7.4 phosphate buffer in sealed screwed-cap tube. Then, the sample was placed in top to bottom rotator. The temperature was controlled at 37±1°C. At 24 hours, the sample was withdrawn using spinal needle No.18, filtered through 0.45 membrane by filter device (Swinnex®). The sample was then diluted with mobile phase and assayed for drug concentration by HPLC at wavelength of 254 nm.

4 Method for quantitative analysis of drug

4.1 UV-visible assay for diazepam analysis

4.1.1 Calibration curve of diazepam in pH 7.4 phosphate buffer

The calibration curve of diazepam in pH 7.4 phosphate buffer was performed to calculate amount of drug dissolved in dissolution test. Diazepam of 200 mg was accurately weighed into 10 ml volumetric flask. Diazepam was completely dissolved with methanol AR grade. The stock solution was accurately diluted with pH 7.4 phosphate buffer to the concentration of 1, 2, 3, 4, 5 µg/ml, respectively. The absorbance of standard solutions was performed using UV visible spectrophotometer at wavelength of 230 nm. The relationship of diazepam concentration and absorbance was fitted using linear regression.

4.2 HPLC assay for diazepam analysis

The high performance liquid chromatography with ultraviolet detector was used to determine amount of drug dissolved in supernatant and solubility measurement.

Validation characteristics

4.2.1 Specificity

Under the chromatographic condition used, the peak of diazepam had be completely separated from the peaks of other components in the sample. Diazepam, lorazepam, tween 80, phosphate buffer and the supernatant of blank preparation were determined.

4.2.2 Accuracy

Three sets of the standard solutions of diazepam having concentrations of 1-25 µg/ml were prepared and injected. The percentage of analytical recovery of each standard solution was calculated.

4.2.3 Precision

a) Within run precision

The within run precision was determined by analyzing three sets of the five standard solutions of diazepam in the same day. Peak area ratios of diazepam to lorazepam were compared and the percentage coefficient of variation (% CV) for each concentration was determined.

b) Between run precision

The between run precision was determined by comparing each concentration of diazepam standard solutions prepared and injected on different days. The percentage coefficient of variation (% CV) of diazepam to lorazepam peak area ratios from three sets of standard solutions on different days was calculated.

4.2.4 Linearity

Linearity was determined by calculating a regression line by method of least squares of peak area ratios of diazepam to lorazepam and concentrations of diazepam in sample. The slope, intercept and coefficient of determination (R^2) were performed.

System suitability

System suitability tests were used to verify that the resolution and reproducibility of the chromatographic system were adequate for analysis to be done.

4.2.5 Resolution

The resolution was a function of column efficiency and was specified to ensure that diazepam was resolved from lorazepam. The resolution, R, is determined by the following equation

$$R = \frac{2\,(t_2 - t_1)}{W_2 + W_1}$$

in which t_2 and t_1 = the retention times of diazepam and lorazepam, respectively

W_2 and W_1 = the corresponding widths at the bases of the peaks obtained by extrapolating the relatively straight sides of the peak to the baseline as shown in Figure 7.

สถาบันวิทยบริการ
จุฬาลงกรณ์มหาวิทยาลัย

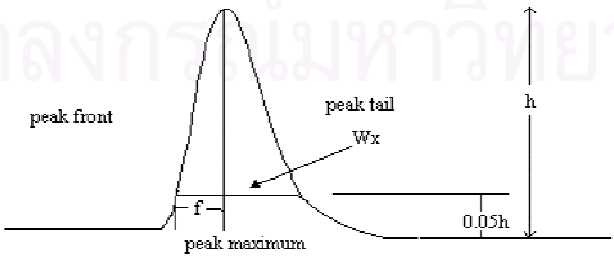

Figure 7 Asymmetrical chromatographic peak

4.2.6 Tailing factor

Tailing factor was performed by collecting data from injection standard curve. This test is determined by the equation

$$T = \frac{W_x}{2f}$$

in which W_x = the width of peak of diazepam or lorazepam at 5 % height

f = the distance from the peak maximum to the leading edge of the peak, the distance being measured at a point 5% of the peak height from the baseline as depicted Figure 7.

4.2.7 Calibration curve of diazepam

Lorazepam of 75 mg was accurately weighed into 100-ml volumetric flask. Lorazepam was completely dissolved with methanol HPLC grade. Diazepam of 50 mg was accurately weighed into 100-ml volumetric flask. Diazepam was completely dissolved with methanol HPLC grade. For the calibration curve of diazepam ranging from 1 to 25 µg/ml, stock solution of diazepam was diluted to 1, 5, 10, 15, 20 and 25 µg/ml, respectively. And stock solution of lorazepam was mixed to 15 µg/ml into each concentration of diazepam. Whereas in range of 50 to 1000 ng/ml, stock solution of diazepam was diluted to 50, 100, 250, 500, and 1,000 ng/ml, respectively. And stock solution of lorazepam was mixed to 300 ng/ml into each concentration of diazepam. Mobile phase was then added to adjust volume. The equation was calculated from the relationship between peak area ratios of diazepam to lorazepam and diazepam concentration.

HPLC conditions

The quantitative determination of diazepam was performed by reverse-phase high performance liquid chromatography. Concentration of diazepam was determined using a HPLC apparatus equipped with a 250 x 4.6 mm, 5 µ C-18 column and C-18 pre-column. The mobile phase was 70% methanol**:**30% water which was freshly prepared and filtered through a 0.45 µm membrane filter and was then

degassed by sonication about 30 minutes. The flow rate was set at 1 ml/minute. The volume of injected sample was 20 µl and detector wavelength was 254 nm. The attenuation was set at 64 and 8 for determining concentration of diazepam ranging from 1 to 25 µg/ml and 50 to 1,000 ng/ml, respectively (Lunn and Schmuff, 1997).

สถาบันวิทยบริการ
จุฬาลงกรณ์มหาวิทยาลัย

CHAPTER IV
RESULTS AND DISCUSSION

In this study, SLN was prepared by hot homogenization technique. This method consisted of two processes, preparing the pre-emulsion using high speed homogenizer and reducing the particle size by high pressure homogenizer.

Formulation of solid lipid nanoparticle (SLN)

SLN consisted of 5% glycerol behenate and 1-5% of various stabilizers. The stabilizers used to prepare SLN included poloxamer 188, poloxamer 407, Phospholipon® 80, Epikuron® 200, tween 20 and tween 80. The experiment was performed initially using homogenizing time for 10 minutes, pressure at 10,000 psi and 5 recycle times. The physical appearances of SLN are shown in Tables 7-10.

A Poloxamer

Poloxamers are nonionic surfactants composing of hydrophobic portions and hydrophilic portions. In O/W emulsions, the ethylene oxide chain of poloxamer would protrude into the aqueous side of the O/W interface while the propylene oxide chain of the emulsifier would be primarily locate in the oil side. The mechanism by which poloxamers acts as stabilizers is due to the bridging of the polymer between the surfaces of different particles called steric stabilization (Swarbrick, Rubino, and Rubino, 2000).

1 Polxamer 188

The visual observations of SLN containing 1-5% poloxamer 188 both before and after autoclaving are presented in Table 7. When 1% poloxamer 188 was used, the cooled lipid particles were large and occluded at the orifice during cycle 4 of homogenization. After autoclaving, coalescence occurred in all formulations. This indicated that solid lipids fused and agglomerated into large particles. The formulations containing poloxamer 188 had tendency to form gelation. Their viscosity

visibly increased. In most cases, gel formation was irreversible. This data showed that gel formation after autoclaving was faster than that of the same formulation which was not autoclaved. This might be resulted from high temperature exposure during autoclaving. Introduction of energy to the SLN systems accelerated particle growth and subsequently gelation. Solid lipids floated on the top of dispersion and later brought about larger particles after kept at room temperature. At low concentration of 1-3% poloxamer 188, a large surface area of the solid lipids was available for adsorption of stabilizer. Bridging between particles occurred as a result of the simultaneous adsorption of poloxamer 188 molecules onto the surfaces of different solid lipid particles. However, the number of particle-particle bridges was relative low. Therefore, these systems had uncovered lipid surface particles with could contact other particles and resulted gel formation. At higher concentrations of poloxamer 188 of 4-5%, the higher concentration of polymer on particle surface would prevent close attraction of the particles via the phenomenon of steric stabilization and therefore gel formation could be retarded. Similar result had been reported by Freitas and Müller (1998). They found that high temperatures and mechanical stress promoted gelation in SLN. In accordance with Chansiri et al. (1998), high temperature provided high kinetic energy and could affect the emulsifier film in lipid emulsions. The oil droplets would coalescence and increase in droplet size which could markedly be observed.

2 Polxamer 407

The physical appearances of SLN containing 1-5% poloxamer 407 both before and after sterilization are presented in Table 8. SLN containing poloxamer 407 of 1-5% could be prepared. White fluid dispersion could be observed. In formulation containing 1% poloxamer 407, the gelation obviously occurred after autoclaving under 6 months storage. Because insufficient quantity of poloxamer 407 film could not completely cover lipid surface droplets. Therefore, droplets could contact other which resulted in rigid network of gel structure. Poloxamer 407 possessed higher molecular weight and larger propylene oxide than poloxamer 188. The propylene portion imparted lipophilicity which located at the surface particles. More propylene portion caused higher strength of mechanical barriers which could resist alteration of the adsorbed layer of stabilizer. Therefore gel formation occurred slower than that from formulation of poloxamer 188 at the same concentration. However, the solid

lipids separated from dispersions containing 407 after autoclaving. Formulation containing 2-5% poloxamer 407 exhibited coalescence because droplets fused into large particles. The coalescence process might be resulted from high kinetic energy of system during autoclaving.

B Lecithin

Aqueous dispersions of SLN were prepared by hot homogenization using different available lecithin mixture.

3 Phospholipon® 80

SLN containing phospholipon® 80 could be prepared. Yellowish fluid dispersions were observed due to the color of lecithin. Their physical appearances are shown in Table 9. This experiment found that gel formation occurred in all preparations containing phospholipon® 80 after 1 month storage. This could be assumed that semisolid gel structures immobilized the complete aqueous phase amount to 90%. The formulation containing 1% Phospholipon® 80 formed gel structure within 6 months storage after autoclaving. This indicated that high energy during autoclaving could only retard gel formation but could not prevent the process. This might be explained that high energy upon autoclaving promoted disruption of the bilayers, reducing the diffusional pathways and accelerating the diffusion mobility. Thus the stabilizer could covered the interface of droplets and retarded gel formation in comparison to that before autoclaving.

The results were similar to previous works. Westesen and Siekmann (1997) revealed that phospholipid stabilized tripalmitate suspensions tended to form semisolid like-gels upon cooling of the hot tripalmitate-in-water emulsions. Gel formation could be explained by transformation of droplets. The change in particle shape with the increase in the particle surface during recrystallization resulted in a sudden local demand for additional emulsifier molecules at the particle surfaces in order to stabilize the freshly created surfaces. Phospholipids were not able to immediately cover these newly created interfaces during recrystallization. Therefore, the mobility of phospholipid vesicles was low

resulting in insufficient phospholipid molecules to counteract the sudden lack of emulsifier. Hence, particle aggregation could proceed via these unprotected lateral faces building up gel structure which was able to immobilize the aqueous phase.

4 Epikuron® 200

SLN containing Epikuron® 200 could not be prepared by hot homogenization method. Hot emulsions containing Epikuron® 200 as an emulsifier became semisolid immediately after addition of the heated aqueous phase to oil phase under shear forces by high speed homogenizer. This is indicated that the lecithin had not sufficient steric or electrostatic stabilization. This result agreed with previous research by Wetesen and Siekman (1998). They revealed that a high tendency to form gelation depended on the lecithin composition. The dispersions containing exclusively the phosphatidylcholine rich soya lecithin as stabilizer became semisolid immediately on cooling of hot emulsion whereas dispersions stabilized by the cruder lecithin mixture formed gels within several hours after preparation. However, Epikuron® 200 can be used as stabilizer for the production of SLN by microemulsion technique. The average diameter of SLN was in nanometer size range with narrow polydispersity index. (Cavalli, Caputo, Carlotti et al., 1997, Cavalli, Peira et al., 1999). The difference in SLN product using lecithin as stabilizer resulted from differently experimental condition e.g. lecithin source, method of preparation, type of lipid matrix, quantity of lecithin and coemulsifier in formulation. Despite obvious similarlities between solid lipid nanoparticles and O/W emulsions regarding the preparation method and chemical composition, the instability of SLN containing the same type and concentration of emulsifer as comparable O/W emulsions indicates that there are basic physicochemical differences between colloidal lipid emulsions and solid lipid nanoparticles (Siekmann and Westesen, 1998).

The SLN stabilized by both types of poloxamer and both types of lecithin showed instabilities. Therefore, all formulations were excluded for further particle size determination.

Table 7 The physical appearances of SLN containing various amounts of poloxamer 188

Formulation	Physical appearance	
	Before autoclaving	**After autoclaving**
5 GB + 1 P188	●White fluid dispersion ●Solid lipids floated on the top of dispersion† ●Gel formation after 6 months storage	●White fluid dispersion ●Gel formation after 1 month storage
5 GB + 2 P188	●White fluid dispersion ●Solid lipids floated on the top of dispersion† ●Gel formation after 6 months storage	●Coaleascence ●Gel formation after 1 month storage
5 GB + 3 P188	●White fluid dispersion ●Solid lipids floated on the top of dispersion† ●Gel formation after 6 months storage	●Coaleascence ●Gel formation after 1 month storage
5 GB + 4 P188	●White fluid dispersion ●Solid lipids floated on the top of dispersion† ●Gel formation after 6 months storage	●Coaleascence ●Gel formation after 3 months storage
5 GB + 5 P188	●White fluid dispersion ●Solid lipids floated on the top of dispersion† ●Gel formation after 6 months storage	●Coaleascence ●Gel formation after 3 months storage

† Solid lipids floated on the top of dispersion within 2 hours

Table 8 The physical appearances of SLN containing various amounts of poloxamer 407

Formulation	**Physical appearance**	
	Before autoclaving	**After autoclaving**
5 GB + 1 P407	●White fluid dispersion ●Solid lipids floated on the top of dispersion†	●White fluid dispersion ●Gel formation after 6 months storage
5 GB + 2 P407	●White fluid dispersion ●Solid lipids floated on the top of dispersion†	●White fluid dispersion ●Coalescence
5 GB + 3 P407	●White fluid dispersion ●Solid lipids floated on the top of dispersion†	●White fluid dispersion ●Coalescence
5 GB + 4 P407	●White fluid dispersion ●Solid lipids floated on the top of dispersion†	●White fluid dispersion ●Coalescence
5 GB + 5 P407	●White fluid dispersion ●Solid lipids floated on the top of dispersion†	●White fluid dispersion ●Coalescence

† Solid lipids floated on the top of dispersion within 2 hours

Table 9 The physical appearances of SLN containing various amounts of Phospholipon® 80

Formulation	**Physical appearance**	
	Before autoclaving	**After autoclaving**
5 GB + 1 PL80	●Yellowish fluid dispersion ●Gel formation after 1 month storage	●Yellowish fluid dispersion ●Solid lipids floated on the top of dispersion ●Gel formation after 6 months storage
5 GB + 2 PL80	●Yellowish fluid dispersion ●Gel formation after 1 month storage	●Yellowish fluid dispersion ●Solid lipids floated on the top of dispersion
5 GB + 3 PL80	●Yellowish fluid dispersion ●Gel formation after 1 month storage	●Yellowish fluid dispersion ●Solid lipids floated on the top of dispersion
5 GB + 4 PL80	●Yellowish fluid dispersion ●Gel formation after 1 month storage	●Yellowish fluid dispersion ●Solid lipids floated on the top of dispersion
5 GB + 5 PL80	●Yellowish fluid dispersion ●Gel formation after 1 month storage	●Yellowish fluid dispersion ●Solid lipids floated on the top of dispersion

C Tween

Tween is nonionic surfactant which stabilize the suspensions through a steric mechanism from two forces- (i) osmotic forces- nonionic surfactants usually contained the polyethylene chain or hydrophilic polymer chain as the hydrophilic portions. When two droplets come in close contact, the polymer chain would overlap and the region became more concentrate. This led to the osmotic gradient resulting in the dilution of the overlap area by water molecules and the solution forces occurred which pushed the droplets apart. (ii) Another force was called entropic effects. When the polymer chain overlapped, the entropy of the system was lost. This resulted in thermodynamically unfavorable condition which forced the droplets to be separated (Attwood and Florence, 1983, Duro et al., 1998).

5 Tween 80

5.1 Effect of concentration of tween 80

5.1.1 Particle size

The visual observations of SLN containing 1-5% tween 80 both before and after autoclaving are shown in Table 10. Their particle sizes of SLN both before and after autoclaving are listed in Table 11. In this study, the particle size measurement used both photon correlation spectrometer (PCS) and laser diffractometer (LD) simultaneously.

For the preparations containing 5% glycerol behenate and 1-5% tween 80, the mean particle sizes were in nanometer. The D(v,0.5) values were below 1 μm both before and after autoclaving as shown in Figure 9. The results from PCS confirmed that the mean particle sizes were lower than 1,000 nm both before and after autoclaving as shown in Figure 8. The mean particle sizes after autoclaving tended to be larger while the polydispersity indices and uniformity values were lower than those before autoclaving as shown in Figures 10 and 11. These results indicated that the distributions of mean particle size after autoclaving were lower. The decrease in particle size distribution was as a result from the decreasing surface area of dispersed

solid lipids with higher coverage of tween 80 at the interface. The percentage of particle larger than 1 μm, 5 μm and 10 μm also seemed to reduce after autoclaving. There was no particle larger than 5 μm and 10 μm in preparation of 5% glycerol behenate containing 1-4% tween 80 as shown in Figure 12. The results indicated that such formulations were suitable for carrier intended for parenteral applications. There were significant differences of mean particle sizes in SLN containing 1-5% tween 80 after autoclaving ($p<0.05$, ANOVA). The formulation containing 5% glycerol behenate and 4% tween 80 yielded the smallest particle size after autoclaving which was in agreement from both PCS and LD. The mean particle sizes of such formulation detected by PCS before and after autoclaving were 118.4 and 122.0 nm, respectively, which were insignificantly different ($p>0.05$, t-test). Increasing the concentration of tween 80 concentration beyond 4% w/w did not result in further decrease in the particle size of SLN. The increase of mean particle size, polydispersity index and uniformity in formulation of 5% glycerol behenate and 5% tween 80 could be a consequence of the formation of tween 80 multilayer on the particle surfaces.

Table 10 The physical appearances of SLN containing various amounts of tween 80

Formulation	**Physical appearance**	
	Before autoclaving	**After autoclaving**
5 GB + 1 TW80	●White fluid dispersion	●White fluid dispersion
5 GB + 2 TW80	●White fluid dispersion	●White fluid dispersion
5 GB + 3 TW80	●White fluid dispersion	●White fluid dispersion
5 GB + 4 TW80	●White fluid dispersion	●White fluid dispersion
5 GB + 5 TW80	●White fluid dispersion	●White fluid dispersion

Table 11 Particle sizes of SLN containing 1-5 % tween 80 both before and after autoclaving analyzed by PCS and LD (a) before autoclaving (b) after autoclaving

Formulation	PCS		LD						
	Mean particle size (nm)		Volume particle size (μm)				% Particle larger than		
	z value	PI	D(v,0.1)	D(v,0.5)	D(v,0.9)	uniformity	1 μm	5 μm	10 μm
5 GB + 1 TW80 (a)	308.9	0.417	0.19	0.40	1.17	8.45	13.02	1.90	0.75
5 GB + 1 TW80 (b)	319.2	0.355	0.24	0.44	1.10	0.62	12.54	0.00	0.00
5 GB + 2 TW80 (a)	199.5	0.319	0.17	0.33	0.64	0.74	1.85	0.10	0.05
5 GB + 2 TW80 (b)	200.2	0.290	0.20	0.35	0.66	0.44	2.16	0.00	0.00
5 GB + 3 TW80 (a)	141.6	0.316	0.21	0.30	0.46	2.15	0.15	0.15	0.15
5 GB + 3 TW80 (b)	137.2	0.189	0.17	0.32	0.59	0.43	0.36	0.00	0.00
5 GB + 4 TW80 (a)	118.4	0.342	0.36	0.39	0.92	2.38	8.75	2.53	2.20
5 GB + 4 TW80 (b)	122.0	0.157	0.18	0.30	0.47	0.33	0.30	0.00	0.00
5 GB + 5 TW80 (a)	132.3	0.329	0.17	0.41	18.82	12.47	26.30	15.46	13.16
5 GB + 5 TW80 (b)	145.3	0.177	0.15	0.37	29.41	19.65	31.33	23.34	19.61

สถาบันวิทยบริการ
จุฬาลงกรณ์มหาวิทยาลัย

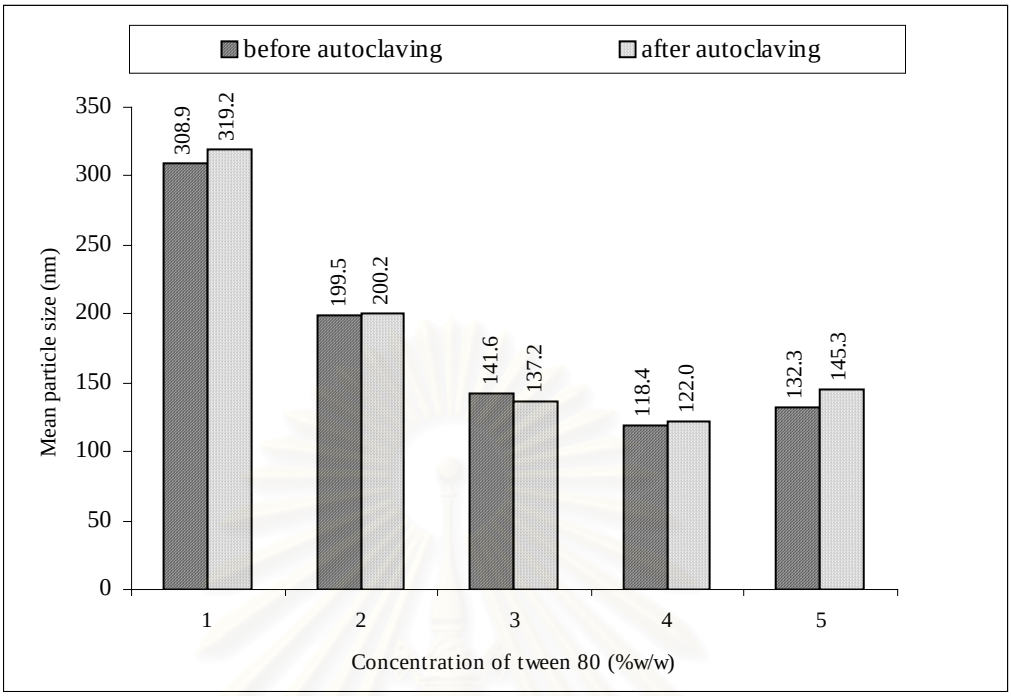

Figure 8 Effect of tween 80 concentration on the particle size of SLN containing 5% glycerol behenate analyzed by PCS

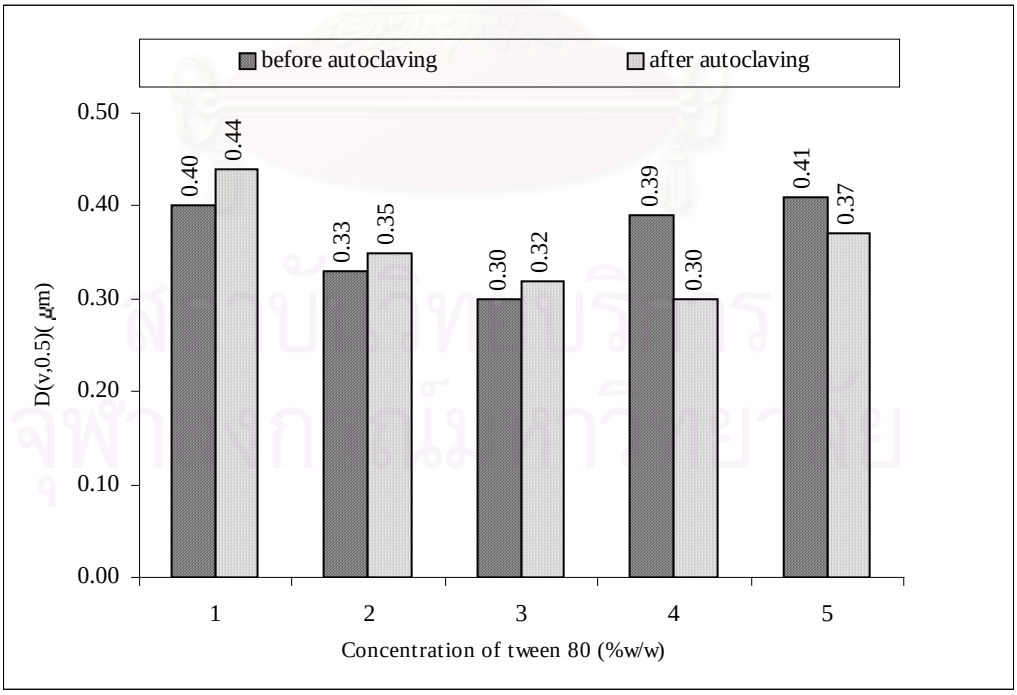

Figure 9 Effect of tween 80 concentration on the particle size of SLN containing 5% glycerol behenate analyzed by LD

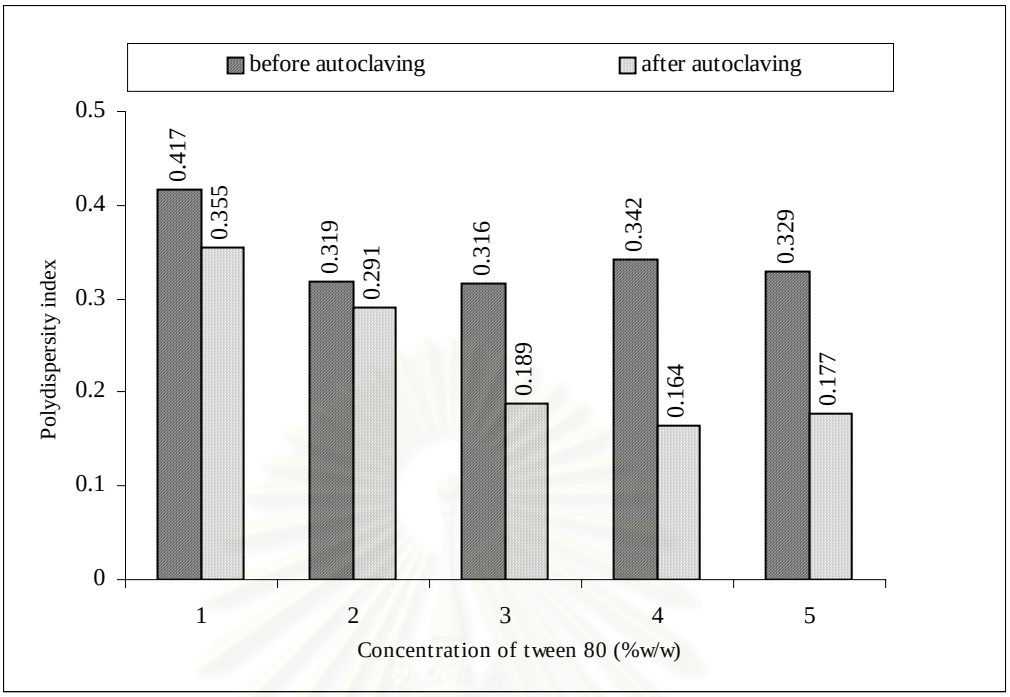

Figure 10 Effect of tween 80 concentration on the polydispersity index of SLN containing 5% glycerol behenate analyzed by PCS

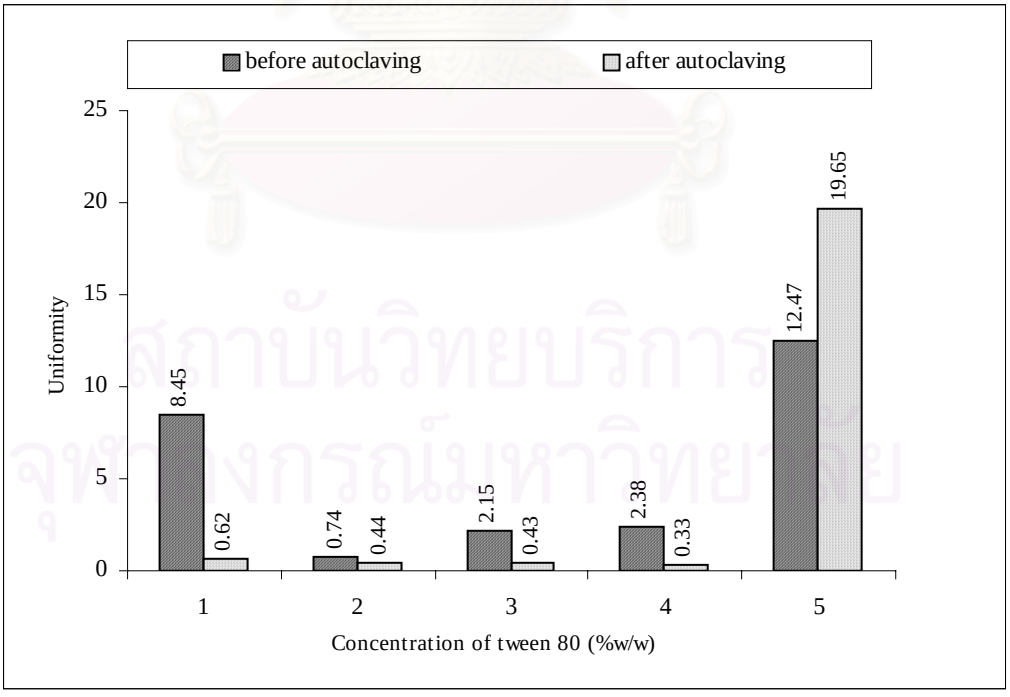

Figure 11 Effect of tween 80 concentration on the uniformity of SLN containing 5% glycerol behenate analyzed by LD

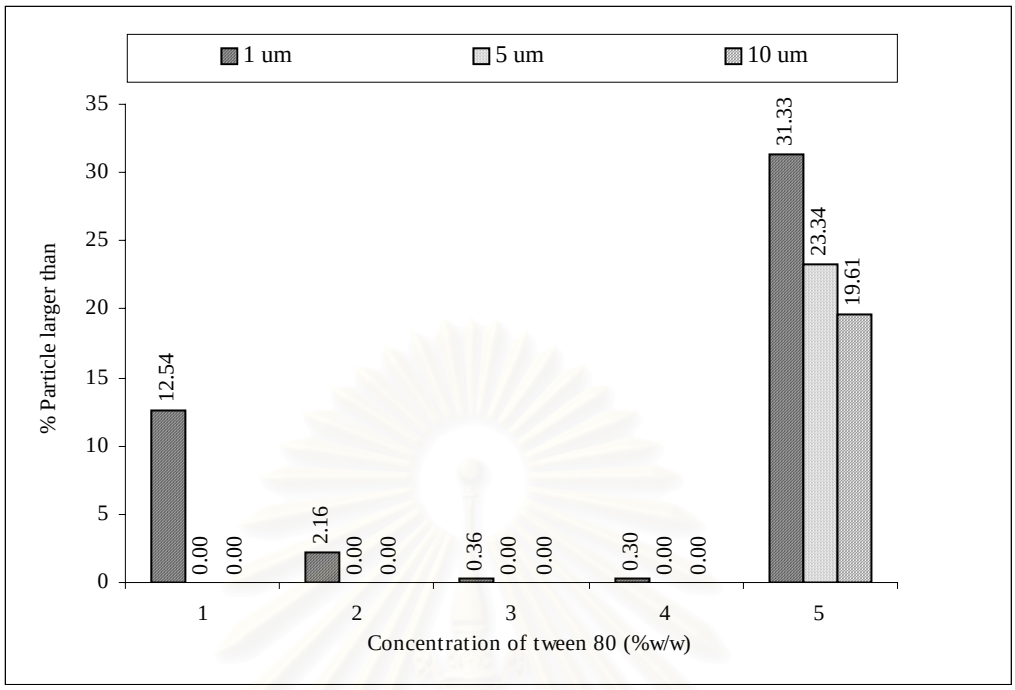

Figure 12 Effect of tween 80 concentration of the percentage of particle larger than 1, 5, 10 µm of SLN containing 5% glycerol behenate after autoclaving analyzed by LD

5.1.2 pH measurement

As shown in Table 12, all preparations were weakly acidic. After autoclaving, the pH of all formulations decreased as depicted in Figure 13. It was possible that the elevated temperature accelerated the hydrolysis of glycerol behenate leading to the formation of free fatty acids such as behenic acid, arachidonic acid, stearic acid which gradually reduced the pH of the system. The lowest pH was found in the formulation of 5% glycerol behenate and 1% tween 80. Increasing the amount of tween 80 could increase pH value. This might result from higher concentration of tween 80 caused higher surface coverage at interface therefore could reduce hydrolysis of glycerol behenate.

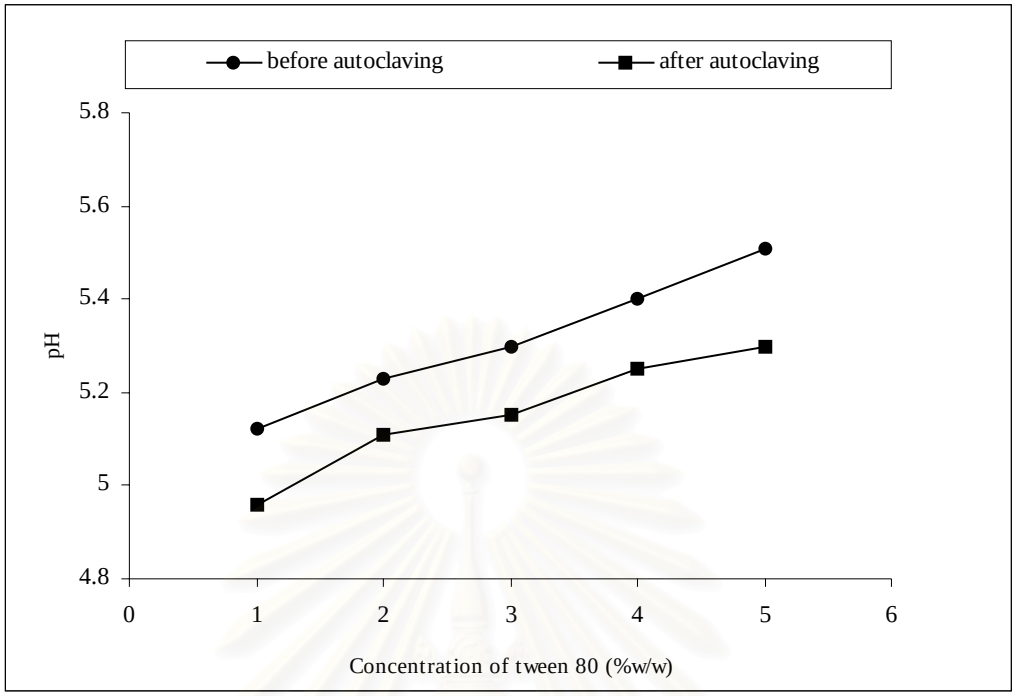

Figure 13 The pH of SLN containing 5% glycerol behenate and 1-5 % tween 80

5.1.3 Zeta potential

All preparations had negative zeta potential as shown in Figure 14. The zeta potential became more negative after autoclaving. This was possibly due to the hydrolysis of glycerol behenate resulting in pH lowering of bulk medium and more negative charge at the interface area of droplets of solid lipid. The zeta potential tended to negatively decrease with higher concentration of tween 80. This was due to higher uncharged polymer layer which was sufficient coverage at interface. The result was consistent with a previous study by Luck, Müller, and Müller (1990). The magnitude of zeta potential for the aqueous suspension decreased upon addition of polysorbate 80, which is attributable to the interfacial film formed having increased the distance between the shear surface and particle surface

Table 12 The pH, zeta potential, osmolality of SLN containing various amounts of tween 80

Formulation	Before autoclaving			After autoclaving		
	pH	**Zeta potential** (millivolt)	Osmolality (Osmol/kg)	pH	Zeta potential (millivolt)	Osmolality (Omol/kg)
5 GB + 1 TW80	5.12 (± 0.021)	-23.7 (± 1.0)	0.006 (± 0.001)	4.96 (± 0.012)	-25.4 (± 1.0)	0.010 (± 0.001)
5 GB + 2 TW80	5.23 (± 0.087)	-22.5 (± 0.4)	0.007 (± 0.001)	5.11 (± 0.052)	-24.0 (± 1.5)	0.011 (± 0.002)
5 GB + 3 TW80	5.30 (± 0.061)	-20.6 (± 0.5)	0.013 (± 0.004)	5.15 (± 0.015)	-21.0 (± 0.7)	0.013 (± 0.002)
5 GB + 4 TW80	5.40 (± 0.021)	-21.2 (± 1.4)	0.017 (± 0.002)	5.25 (± 0.080)	-23.8 (± 1.5)	0.017 (± 0.002)
5 GB + 5 TW80	5.51 (± 0.051)	-19.6 (± 2.5)	0.019 (± 0.001)	5.30 (± 0.015)	-20.1 (± 0.8)	0.019 (± 0.002)

สถาบันวิทยบริการ
จุฬาลงกรณ์มหาวิทยาลัย

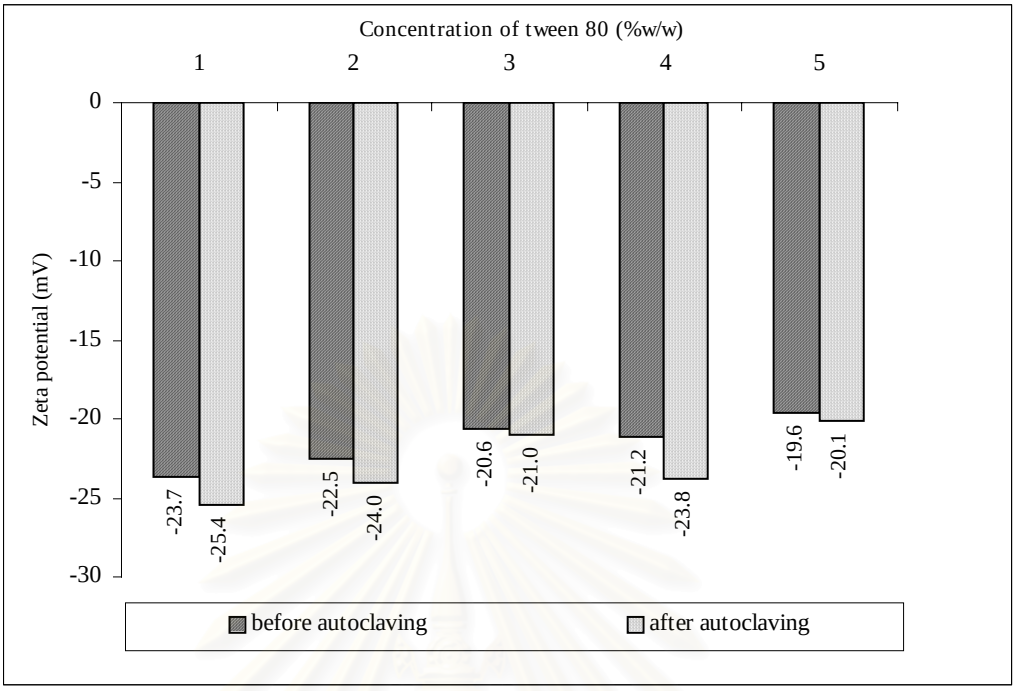

Figure 14 The zeta potential of SLN containing 5% glycerol behenate and 1-5 % tween 80

5.1.4 Osmolality

The osmolalities of SLN examined both before and after autoclaving were rather constant as listed in Table 12 and Figure 15. The osmolality was slightly affected by the composition of SLN. Increasing the percentage of tween 80 could slightly increase the osmolality. All data showed very low osmolality of these preparations. However the SLN was carrier matrix intended for small volume parenteral applications, hence low osmolality values of SLN were still acceptable.

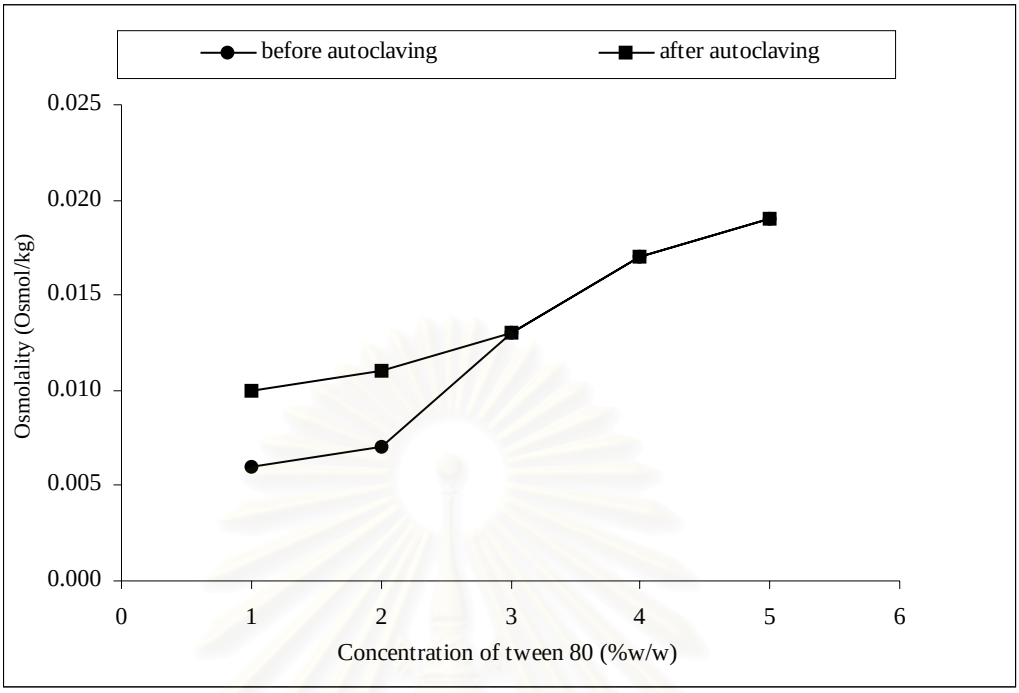

Figure 15 The osmolality of SLN containing 5% glycerol behenate and 1-5 % tween 80

5.1.5 Particle shape

The particle shape was observed by Cryo-scanning electron microscopy (Cryo-SEM). The photomicrograph of preparation containing 5% glycerol behenate stabilized by 4% tween 80 is shown in Figure 16. The Cryo-SEM analysis showed that the solid lipids were spherical in shape and all particles were in nanometer size range. Compared to the Cryo-SEM photomicrograph of distilled water in Figure 17, the Cryo-SEM analysis confirmed that spherical droplets were solid lipid particles.

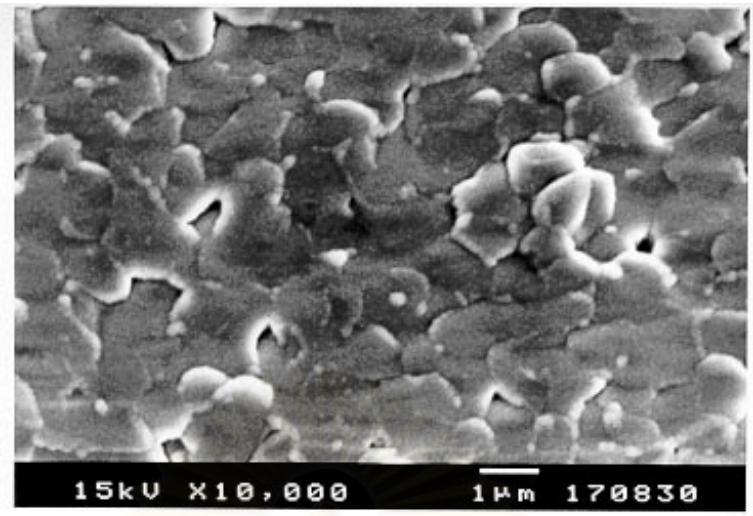

Figure 16 The Cryo-SEM photomicrograph of SLN containing 5% glycerol behenate and 4% tween 80

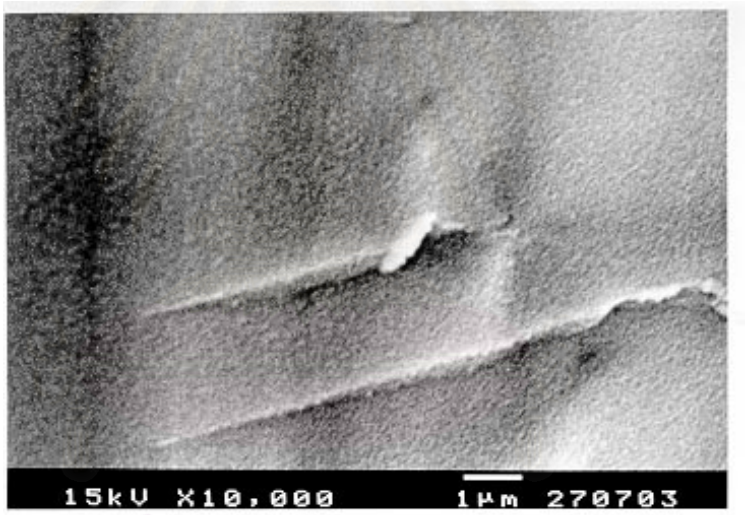

Figure 17 The Cryo-SEM photomicrograph of distilled water

5.2 Effect of storage time

The suitable preparation to be used in parenteral applications was the preparation of 5% glycerol behenate and 4% tween 80. Its particle size was sufficiently small to be used in subcutaneous, intramuscular and intravenous. Therefore, the preparation of 5% glycerol behenate and 4% tween 80 was kept at room temperature and 4˚C in refrigerator. The particle size, pH, zeta potential and

osmolality were evaluated after storage for 1 month, 3 months and 6 months as shown in Tables 13 and 14.

5.2.1 Effect of storage time on particle size

The SLN of 5% glycerol behenate and 4% tween 80 exhibited mean particle sizes in range of 122.0-133.9 nm which were relatively constant over the storage time as listed in Table 13. However, the mean particle size and D(v,0.5) of the formulation stored at 4˚C were larger than that of stored at room temperature. Furthermore, the percentage of particle size larger than 1 μm, 5 μm and 10 μm of the formulation stored at 4˚C was distinctly increased. At low temperature solid lipids had a low energy barrier, therefore had insufficient repulsive force. These might affect the tween 80 adsorption layer and caused partial collapse leading to particle aggregation. The data obtained indicated that the selected formulation should be stored at room temperature since there was no particle size larger than 5 μm after 6 months storage.

5.2.2 Effect of storage time on pH, zeta potential and osmolality

As shown in Table 14, the pH of SLN containing 5% glycerol behenate and 4% tween 80 decreased with time to weak acid. The decrease of pH was possibly resulted from the presence of free fatty acid liberated in system. The lowest pH of 4.55 was found in sample stored at room temperature for 6 months storage. The pH of such formulation stored at room temperature was more acidic compared to stored at 4˚C at each interval observation, which was significantly different ($p<0.05$, t-test). This result suggested that there were more free fatty acids liberated in system stored at room temperature than kept in 4˚C. The result agreed with a previous study by Herman and Grove (1992). They stated that the decrease pH resulted from the hydrolysis of some lipid in emulsions leading to the formation of free fatty acids which gradually reduced the pH of the system. The zeta potential was affected by alteration of pH. The zeta potential tended to increase over storage of time. The zeta potential of such formulation stored at room temperature became more negative higher than that stored at 4˚C. The osmolality values were rather constant. The range of osmolalities were of 0.017-0.019 Osmol/kg. This result indicated that the osmolality values seemed to be independent on storage time.

Table 13 Particle sizes of SLN containing 5 % glycerol behenate and 4% tween 80 (a) after autoclaving (b) storage at room temperature (c) storage at 4 ºC for 1, 3 and 6 months analyzed by PCS and LD

Condition	Formulation	PCS		LD						
		Mean particle size (nm)		Volume particle size (µm)				% Particle larger than		
		z value	PI	D(v,0.1)	D(v,0.5)	D(v,0.9)	Uniformity	1 µm	5 µm	10 µm
after autoclaving	5 GB + 4 TW80 (a)	122.0	0.157	0.18	0.30	0.47	0.33	0.30	0.00	0.00
1 month storage										
room temperature	5 GB + 4 TW80 (b)	133.7	0.195	0.12	0.26	0.48	0.43	0.00	0.00	0.00
4 ºC	5 GB + 4 TW80 (c)	133.9	0.149	0.15	0.33	15.81	16.11	24.12	16.28	13.10
3 months storage										
room temperature	5 GB + 4 TW80 (b)	129.1	0.175	0.12	0.27	0.62	0.94	7.67	0.00	0.00
4 ºC	5 GB + 4 TW80 (c)	129.5	0.155	0.24	0.46	56.30	31.84	42.57	36.13	31.00
6 months storage										
room temperature	5 GB + 4 TW80 (b)	123.7	0.201	0.15	0.29	0.50	0.35	0.00	0.00	0.00
4 ºC	5 GB + 4 TW80 (c)	126.3	0.211	0.16	0.30	0.57	0.58	3.17	0.00	0.00

สถาบันวิทยบริการ
จุฬาลงกรณ์มหาวิทยาลัย

Table 14 The pH, zeta potential and osmolality of SLN containing 5% glycerol behenate and 4% tween 80 over storage time

Condition	Formulation	pH	Zeta potential (millivolt)	Osmolality (Osmol/kg)
After autoclaving	5 GB + 4 TW80	5.25 ± 0.08	-23.8 ± 1.5	0.017 ± 0.002
1 month storage				
room temperature	5 GB + 4 TW80	5.16 ± 0.01	-21.4 ± 2.0	0.017 ± 0.002
4˚C	5 GB + 4 TW80	5.29 ± 0.01	-21.4 ± 0.9	0.017 ± 0.002
3 months storage				
room temperature	5 GB + 4 TW80	4.82 ± 0.01	-32.0 ± 1.2	0.017 ± 0.001
4˚C	5 GB + 4 TW80	5.19 ± 0.01	-31.1 ± 1.1	0.019 ± 0.001
6 months storage				
room temperature	5 GB + 4 TW80	4.55 ± 0.04	-24.9 ± 0.2	0.017 ± 0.001
4˚C	5 GB + 4 TW80	4.85 ± 0.05	-24.8 ± 0.8	0.018 ± 0.002

5.3 Effect of various amounts of glycerol behenate

5.3.1 Effect of various amounts of glycerol behenate on particle size

From the data obtained, the suitable concentration of tween 80 which could stabilize 5% glycerol behenate was 4% w/w in the formulation. To investigate the effect of ratio of glycerol behenate to tween 80 (GB:TW80 ratio) on their physicochemical properties, four SLN were formulated with increasing ratio of glycerol behenate to tween 80 ranging from 0.25 to 2.25. Four parameters were evaluated, particle size, pH, zeta potential, and osmolality. Table 15 illustrates particle size at different ratios both before and after autoclaving.

Table 16 The pH, zeta potential, osmolality of SLN containing different ratios of glycerol behenate to tween 80

Formulation	Ratio of GB to TW 80	Before autoclaving			After autoclaving		
		pH	Zeta potential (millivolt)	Osmolality (Osmol/kg)	pH	Zeta potential (millivolt)	Osmolality (Osmol/kg)
1 GB + 4 TW80	0.25	5.51 ± 0.04	-13.0 ± 1.2	0.014 ± 0.002	5.40 ± 0.02	-17.6 ± 1.4	0.015 ± 0.002
3 GB + 4 TW80	0.75	5.48 ± 0.01	-15.1 ± 1.5	0.017 ± 0.002	5.42 ± 0.02	-18.1 ± 0.6	0.017 ± 0.003
7 GB + 4 TW80	1.75	5.21 ± 0.01	-30.8 ± 1.2	0.021 ± 0.003	4.99 ± 0.02	-31.2 ± 1.2	0.021 ± 0.002
9 GB + 4 TW80	2.25	5.13 ± 0.01	-31.0 ± 0.1	0.023 ± 0.001	4.80 ± 0.02	-32.3 ± 0.3	0.022 ± 0.001

สถาบันวิทยบริการ
จุฬาลงกรณ์มหาวิทยาลัย

It was observed that there was a difference in effect of GB to TW80 ratio on the particle size of SLN. These SLN showed that mean particle sizes increased after autoclaving with the exception of the formulation containing 1% glycerol behenate and 4% tween 80 examined by PCS and LD. Such formulation showed macroscopic change due to oil separation after autoclaving. It was evident that increasing the GB:TW80 ratios further increased in particle size. Increasing the GB:TW80 ratios from 0.25 to 2.25 resulted in a four-fold increase in particle size analyzed by PCS. This result was found to be similar from the result reported by Jumaa and Müller (1998). They reported that increasing volume of castor oil for parenteral fat emulsion led to a remarkable increase in the mean particle size measured by PCS. Furthermore, the percentage of particle size larger than 1, 5 and 10 μm in GB:TW80 ratio of 1.75 and 2.25 was higher than that of 0.25 and 0.75. It was possible that higher concentration of glycerol behenate cause a much higher viscosity than the lower concentration. Therefore, the formulation containing higher concentration of glycerol behenate yielded mean particle size larger than that of lower concentration. In order to achieve smaller particle size and narrower particle size distribution, higher homogenization pressure was needed when increasing the ratio of glycerol behenate to tween 80. In the formulation containing 3% glycerol behenate and 4% tween 80, the percentage of solid lipids larger than 5 μm and 10 μm was reduced after autoclaving. This was probable that there was sufficient amount of tween 80 stabilized oil phase during steam sterilization.

5.3.2 Effect of various amounts of glycerol behenate on pH, zeta potential and osmolality

As shown in Table 16, it was observed that pH prominently reduced with increasing of GB:TW80 ratio. The negativity of zeta potential remarkably increased with higher amount of glycerol behenate. This result confirmed that the decrease of pH and the increase of zeta potential after autoclaving resulted from hydrolysis of glycerol behenate. The osmolality seemed to increase with increasing of GB:TW80 ratio. These above results indicated that the physicochemical properties were influenced by the ratio of glycerol behenate to tween 80.

Table 16 The pH, zeta potential, osmolality of SLN containing different ratios of glycerol behenate to tween 80

Formulation	Ratio of GB to TW 80	Before autoclaving			After autoclaving		
		pH	Zeta potential (millivolt)	Osmolality (Osmol/kg)	pH	Zeta potential (millivolt)	Osmolality (Osmol/kg)
1 GB + 4 TW80	0.25	5.51 ± 0.04	-13.0 ± 1.2	0.014 ± 0.002	5.40 ± 0.02	-17.6 ± 1.4	0.015 ± 0.002
3 GB + 4 TW80	0.75	5.48 ± 0.01	-15.1 ± 1.5	0.017 ± 0.002	5.42 ± 0.02	-18.1 ± 0.6	0.017 ± 0.003
7 GB + 4 TW80	1.75	5.21 ± 0.01	-30.8 ± 1.2	0.021 ± 0.003	4.99 ± 0.02	-31.2 ± 1.2	0.021 ± 0.002
9 GB + 4 TW80	2.25	5.13 ± 0.01	-31.0 ± 0.1	0.023 ± 0.001	4.80 ± 0.02	-32.3 ± 0.3	0.022 ± 0.001

สถาบันวิทยบริการ
จุฬาลงกรณ์มหาวิทยาลัย

5.4 Fourier Transform Infrared Spectroscopy

The infrared spectra of glycerol behenate, tween 80 and solid lipid prepared by ultracentrifugation of SLN containing 5% glycerol behenate and 4% tween 80 (glycerol behenate SLN) are shown in Figure 18. The principal peaks of glycerol behenate were observed at the wavenumbers of 3431, 2921, 2852, 1730, 1469, 1177, 721 cm^{-1}. The peak at 3421 cm^{-1} was O-H stretching. The sharp peaks at 2921 cm^{-1} and 2852 cm^{-1} were CH_2 symmetric and CH_2 asymmetric of aliphatic C-H stretching, respectively. The distinguished peak at 1730 cm^{-1} was the C=O stretching. The peaks of 1469 and 721 cm^{-1} were CH_2 bending and CH_2 rocking, respectively. The peak of 1177 cm^{-1} was C-O stretching (Bugay and Findlay, 1999).

The infrared spectrum of tween 80 showed peak of O-H stretching at 3442 cm^{-1}. The sharp peaks at 2924 and 2866 cm^{-1} were CH_2 symmetric and CH_2 asymmetric of aliphatic C-H stretching, respectively. The peak at 1737 cm^{-1} was the C=O stretching. The peak of 1462 cm^{-1} was CH_2 bending. The distinguished peak at 1100 cm^{-1} was C-O stretching (Fresenius et al., 1989).

The infrared spectrum of glycerol behenate SLN showed spectra corresponding to superimposition of their parent materials. The sharp peaks at 3436, 2918, 2851, 1737, 1472, 1113, 720 cm^{-1} were observed from the combination of both spectra. No new peak was observed from its mixture. The data indicated that no strong interaction and significant shift occurred between glycerol behenate and tween 80. It was assumed that there was no incompatibility occurred in glycerol behenate SLN.

5.5 Differential Scanning Calorimetry

The DSC thermograms of glycerol behenate and glycerol behenate SLN are presented in Figure 19. The DSC thermogram of glycerol behenate displayed a sharp melting endotherm. The onset of melting endotherm began from 69.6ºC to 74ºC which had the melting peak at 71.5ºC. And the DSC thermogram of glycerol behenate SLN

showed an endothermic peak at 71.9ºC. The melting endotherm presented between 68.9ºC to 74.1ºC. From this data, it can be concluded that no new peak occurred from its mixture.

5.6 Powder X-ray Diffractometry

The powder X-ray diffraction patterns of glycerol behenate and glycerol behenate SLN are shown in Figure 20. Glycerol behenate exhibited crystalline which showed the characteristic peak at 4.120º, 20.920º, 22.880º. The diffractogram of glycerol behenate SLN displayed weaker intensity of diffraction pattern than that of glycerol behenate. The sharp peaks at 4.470º, 20.790º, 21.190º were observed with additional peaks at 19.310º, 23.070º and 24.270º. These data indicated that the X-ray diffraction pattern of glycerol behenate SLN was considerably changed. A possible explanation for this difference may be as a result of polymorphic transition. This finding was similar to the result from previous investigation by Jenning, Schäfer-Korting et al. (2000). They found that there was polymorphic transformation in glycerol behenate SLN when compared to glycerol behenate. They stated that the diffraction pattern of glycerol behenate showed a typical pattern for orthorhombic β′ form of triglyceride whereas glycerol behenate SLN after 24 hours and drying at 32ºC reflected the characteristic for β_i polymorph which was triclinic or orthorhombic.

สถาบันวิทยบริการ
จุฬาลงกรณ์มหาวิทยาลัย

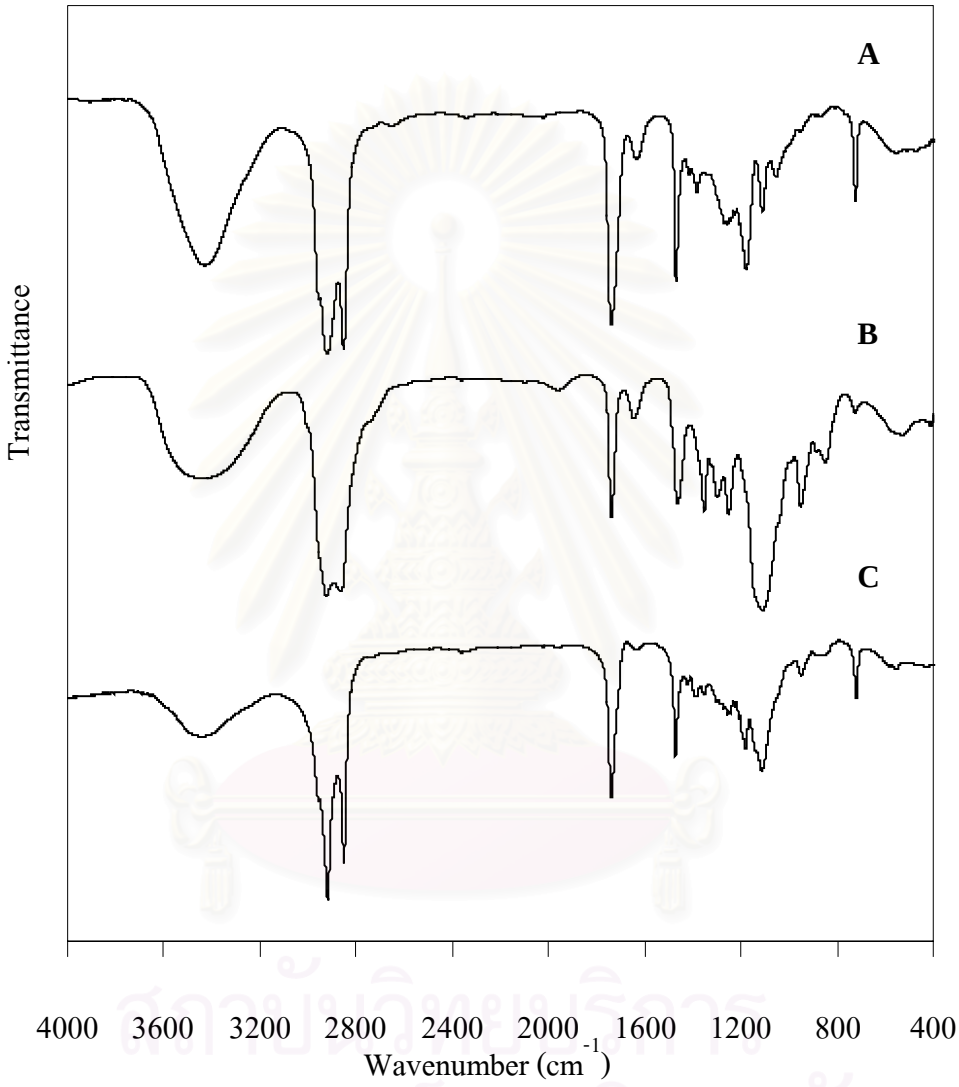

Figure 18 Infrared spectra of (A) glycerol behenate, (B) tween 80, (c) glycerol behenate SLN

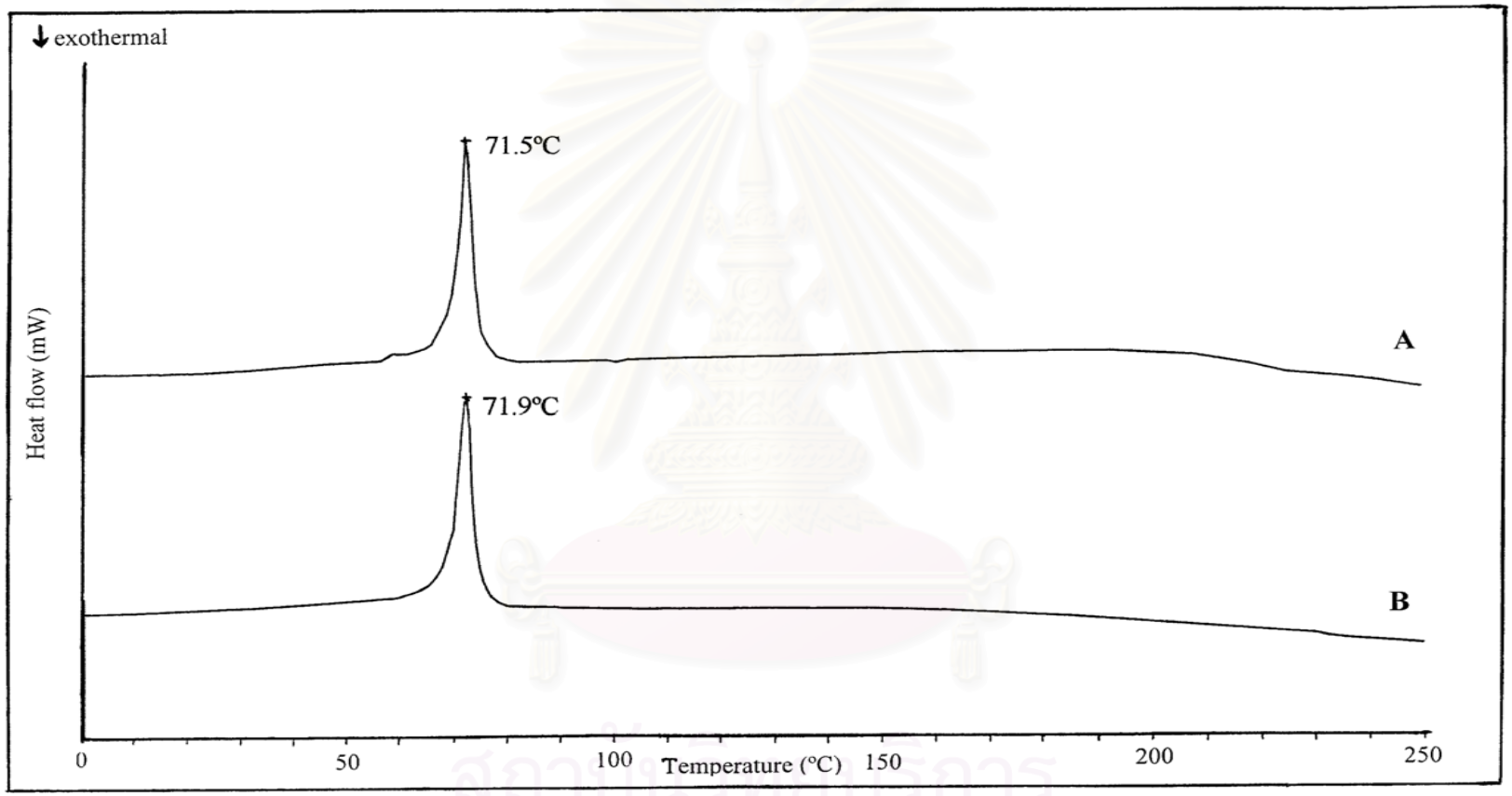

Figure 19 DSC thermograms of (a) glycerol behenate, (B) glycerol behenate SLN

สถาบันวิทยบริการ
จุฬาลงกรณ์มหาวิทยาลัย

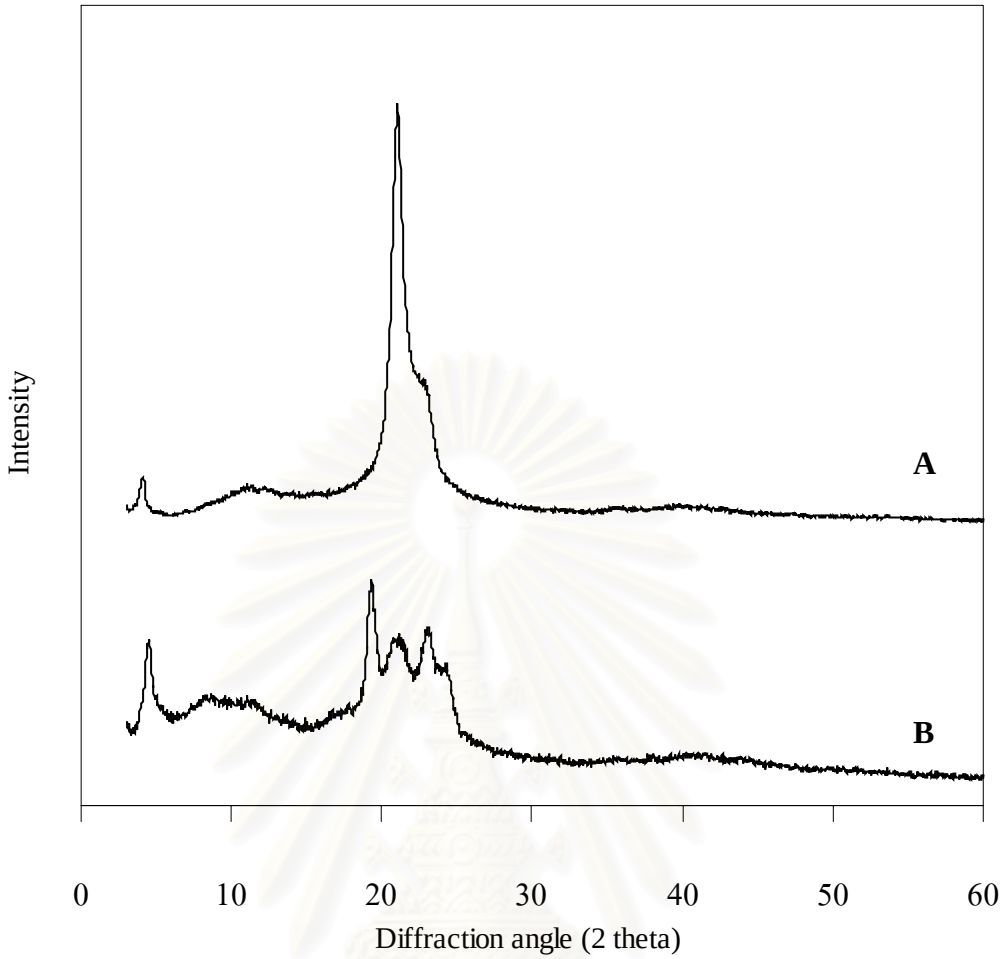

Figure 20 X-ray diffractograms of (A) glycerol behenate, (B) glycerol behenate SLN

5.7 **Effect of diazepam loading**

According to the percentage of stabilizer and glycerol behenate, it was found that the formulations containing ratios of glycerol behenate to tween 80 of 0.75 and 1.25 were suitable for parenteral application since there was no particle larger than 5 µm and 10 µm and no macroscopic change. However, higher amount of solid lipids served as higher drug loading. Therefore, the formulation containing 5% glycerol behenate and 4% tween 80 was chosen in order to study the effect of drug loading.

5.7.1 Physical appearance

Preparation of SLN containing 0.1-0.9% diazepam could be prepared using 4% tween 80 as stabilizer. White fluid dispersions were observed in SLN containing diazepam both before and after autoclaving.

5.7.2 Particle size

The particle sizes of SLN containing diazepam are shown in Table 17. The mean particle sizes of SLN containing 0.1-0.9% diazepam were higher than those of drug free preparation before and after autoclaving, analyzed by PCS. The z values of preparation containing diazepam after autoclaving were in range of 154.2-168.7 nm as depicted in Figure 21. Their D(v,0.5) values were lower than 1 μm. This indicated that bulk populations were in nanometer range. However the particle sizes larger than 5 μm were observed at high percentage (15.58-25.08%) in all formulations after autoclaving. It was possible that diazepam had a large particle size therefore diazepam loaded into lipid matrix induced particle aggregation. In addition, some drug could dissolve in dispersion medium and disturbed tween 80 layer. Thus the tween 80 diffused to the surface of the droplets slower than drug free preparation. Therefore, higher levels of particle in micrometer range were obtained in all diazepam loaded preparations. In contrast to PI, the uniformity of all preparations increased after autoclaving as depicted in Figures 22 and 23. These could explain by the increasing content of particles in micrometer size after autoclaving.

5.7.3 Effect of diazepam loading on pH, zeta potential and osmolality

The pH and osmolality of diazepam loaded SLN were rather constant when increasing the concentration of drug in the preparations as shown in Table 18. This indicated that low amount of diazepam was soluble in dispersion and slightly affected the pH of dispersion. While the pH values of diazepam loaded SLN after autoclaving were significantly decreased when compared to those before autoclaving as depicted in Figure 24 ($p<0.05$, t-test). This result agreed with the same explanation

Table 17 Particle sizes of 0.1–0.9 % diazepam loaded SLN both before and after autoclaving analyzed by PCS and LD (a) before autoclaving (b) after autoclaving

Formulation	PCS		LD						
	Mean particle size (nm)		Volume particle size (µm)				% Particle larger than		
	z value	PI	D(v,0.1)	D(v,0.5)	D(v,0.9)	uniformity	1 µm	5 µm	10 µm
0.1 DI + 5 GB + 4 TW80 (a)	127.8	0.205	0.09	0.25	11.05	19.54	19.05	13.66	10.50
0.1 DI + 5 GB + 4 TW80 (b)	154.2	0.142	0.14	0.35	55.47	52.30	30.65	25.08	22.14
0.3 DI + 5 GB + 4 TW80 (a)	146.1	0.203	0.15	0.32	6.28	10.67	13.59	10.47	8.81
0.3 DI + 5 GB + 4 TW80 (b)	156.2	0.161	0.15	0.33	35.72	31.62	26.95	22.03	18.77
0.5 DI + 5 GB + 4 TW80 (a)	150.6	0.208	0.15	0.36	26.20	24.68	25.20	17.22	14.09
0.5 DI + 5 GB + 4 TW80 (b)	152.4	0.163	0.16	0.37	56.24	39.00	34.04	28.08	24.84
0.7 DI + 5 GB + 4 TW80 (a)	162.8	0.189	0.21	0.38	12.09	17.51	22.52	12.93	10.55
0.7 DI + 5 GB + 4 TW80 (b)	168.7	0.179	0.17	0.36	47.07	35.06	31.25	25.37	22.14
0.9 DI + 5 GB + 4 TW80 (a)	163.3	0.207	0.19	0.36	2.54	3.36	17.30	6.35	3.10
0.9 DI + 5 GB + 4 TW80 (b)	162.3	0.198	0.17	0.34	19.22	23.59	22.16	15.58	12.84

สถาบันวิทยบริการ
จุฬาลงกรณ์มหาวิทยาลัย

in that the high temperature under steam sterilization could accelerate the hydrolysis of glycerol behenate resulting in free fatty acids. Then the decrease in pH could be ascribed to the hydrogen ions produced by its ionization. The negativity of zeta potential became increase after autoclaving. However, there was no significant difference in zeta potential values of all preparations after autoclaving ($p>0.05$, ANOVA) as depicted in Figure 25. This suggested that increasing diazepam concentration did not alter surface charge of solid lipid.

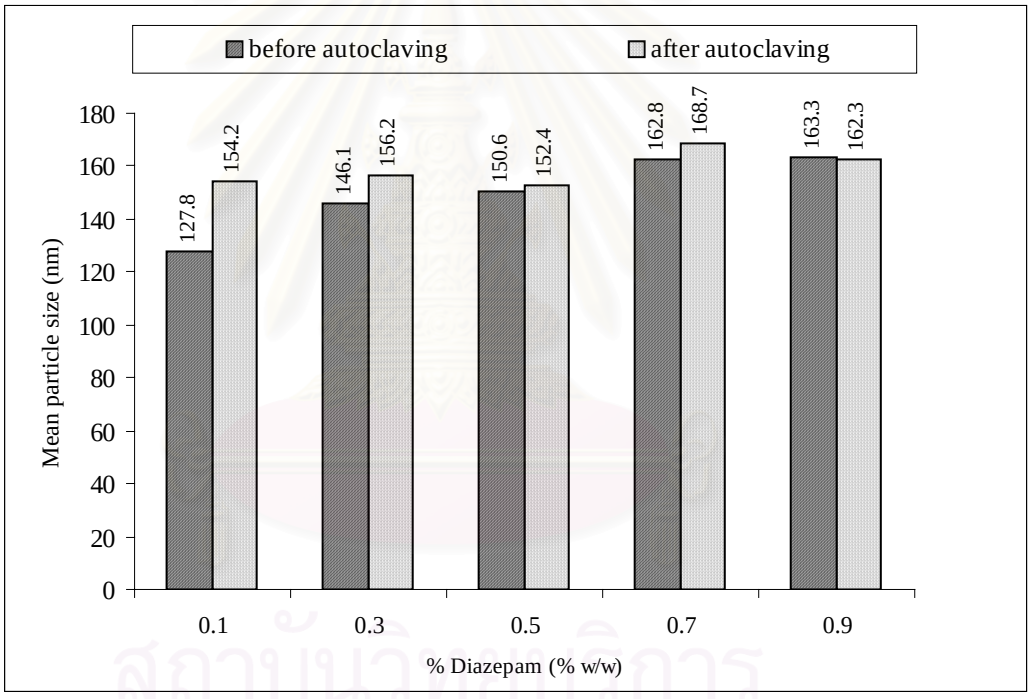

Figure 21 Effect of drug loading on the particle size in diazepam loaded SLN analyzed by PCS

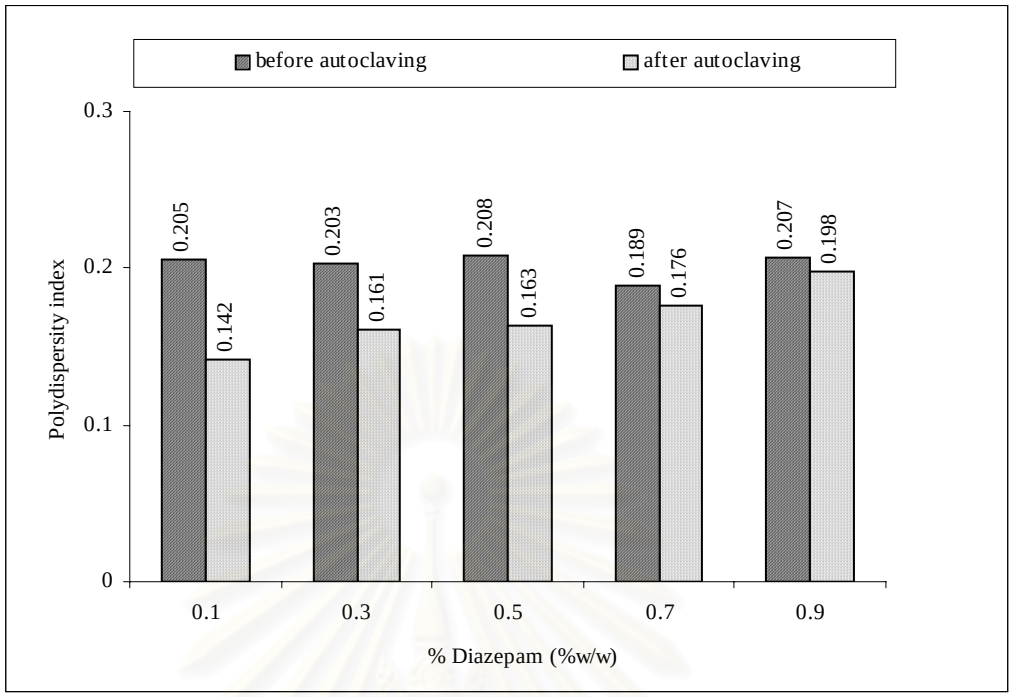

Figure 22 Effect of drug loading on polydispersity index in diazepam loaded SLN analyzed by PCS

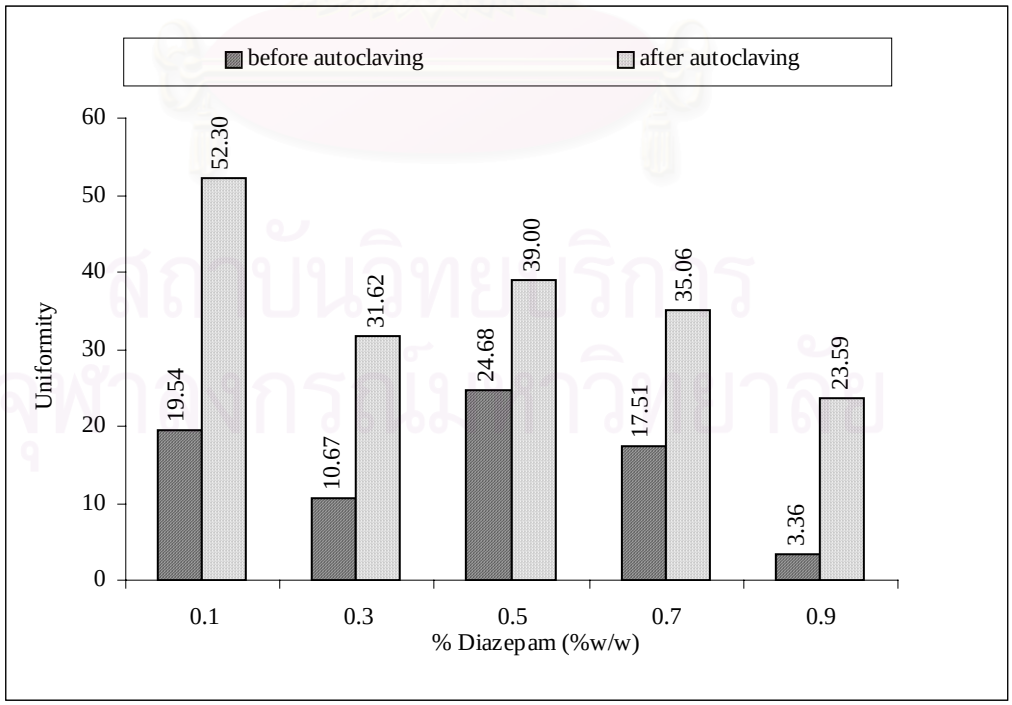

Figure 23 Effect of drug loading on uniformity in diazepam loaded SLN analyzed by LD

Table 18 The pH, zeta potential, osmolality of 0.1–0.9 % diazepam loaded SLN

Formulation	Before autoclaving			After autoclaving		
	pH	Zeta potential (millivolt)	Osmolality (Osmol/kg)	pH	Zeta potential (millivolt)	Osmolality (Osmol/kg)
0.1 DI + 5 GB + 4 TW80	5.42 ± 0.01	-22.4 ± 1.8	0.019 ± 0.001	5.09 ± 0.02	-22.6 ± 1.0	0.022 ± 0.002
0.3 DI + 5 GB + 4 TW80	5.47 ± 0.03	-20.6 ± 1.6	0.020 ± 0.002	5.17 ± 0.01	-21.0 ± 0.3	0.026 ± 0.001
0.5 DI + 5 GB + 4 TW80	5.47 ± 0.01	-17.1 ± 1.9	0.024 ± 0.003	5.16 ± 0.01	-21.9 ± 1.1	0.024 ± 0.001
0.7 DI + 5 GB + 4 TW80	5.46 ± 0.01	-19.8 ± 0.3	0.020 ± 0.001	5.12 ± 0.01	-20.9 ± 0.4	0.020 ± 0.001
0.9 DI + 5 GB + 4 TW80	5.47 ± 0.02	-16.1 ± 1.5	0.021 ± 0.001	5.15 ± 0.01	-19.9 ± 1.7	0.022 ± 0.001

สถาบันวิทยบริการ
จุฬาลงกรณ์มหาวิทยาลัย

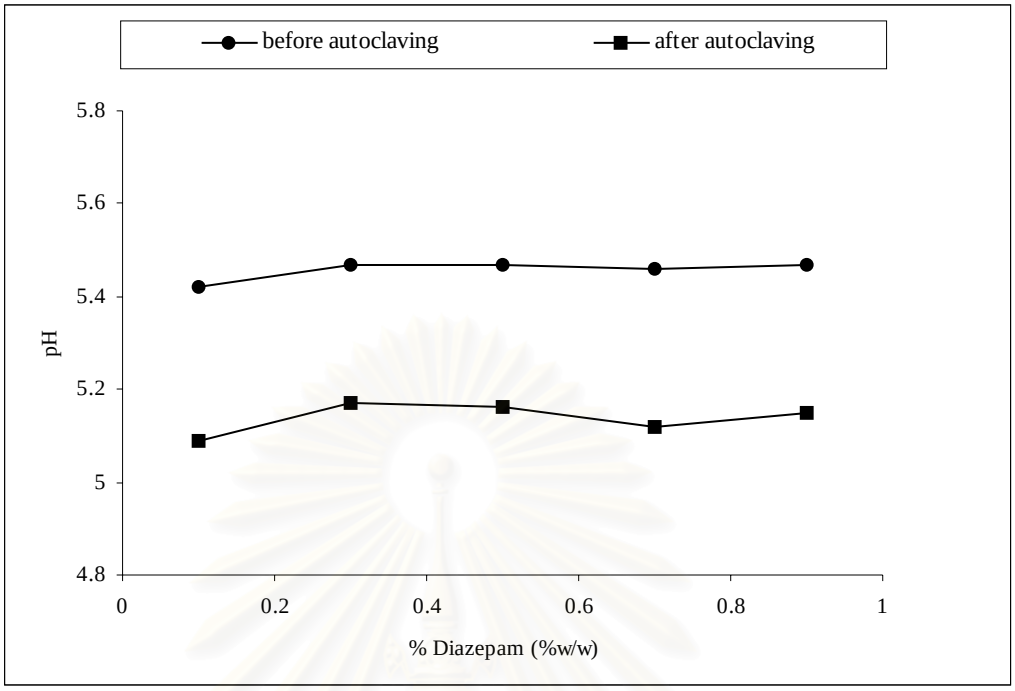

Figure 24 The pH of 0.1-0.9% diazepam loaded SLN both before and autoclaving

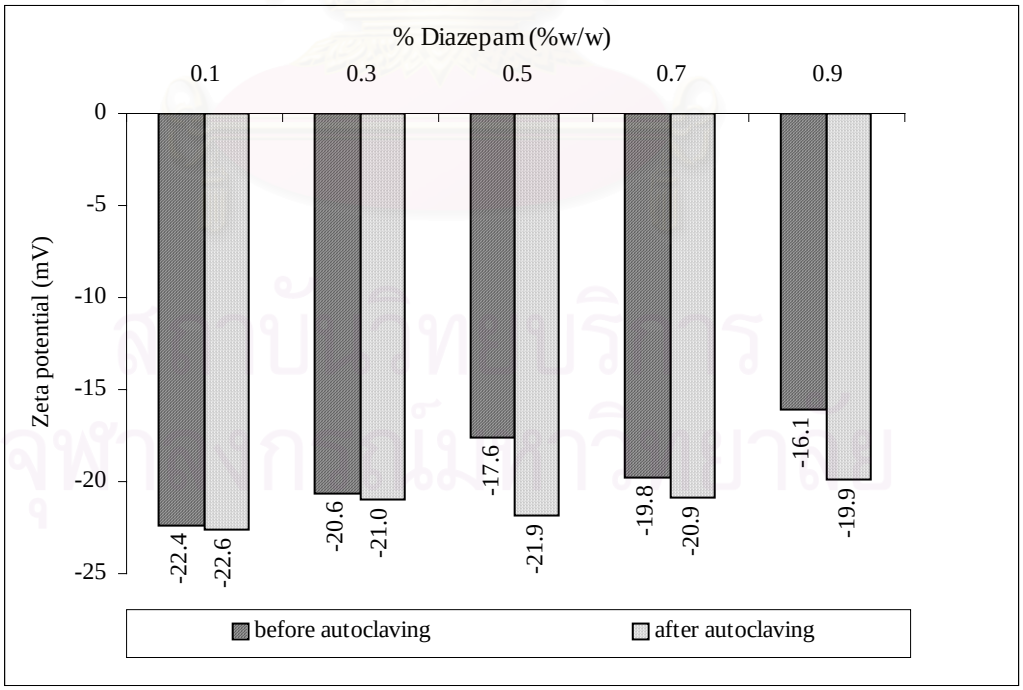

Figure 25 Effect of drug loading on zeta potential in diazepam loaded SLN

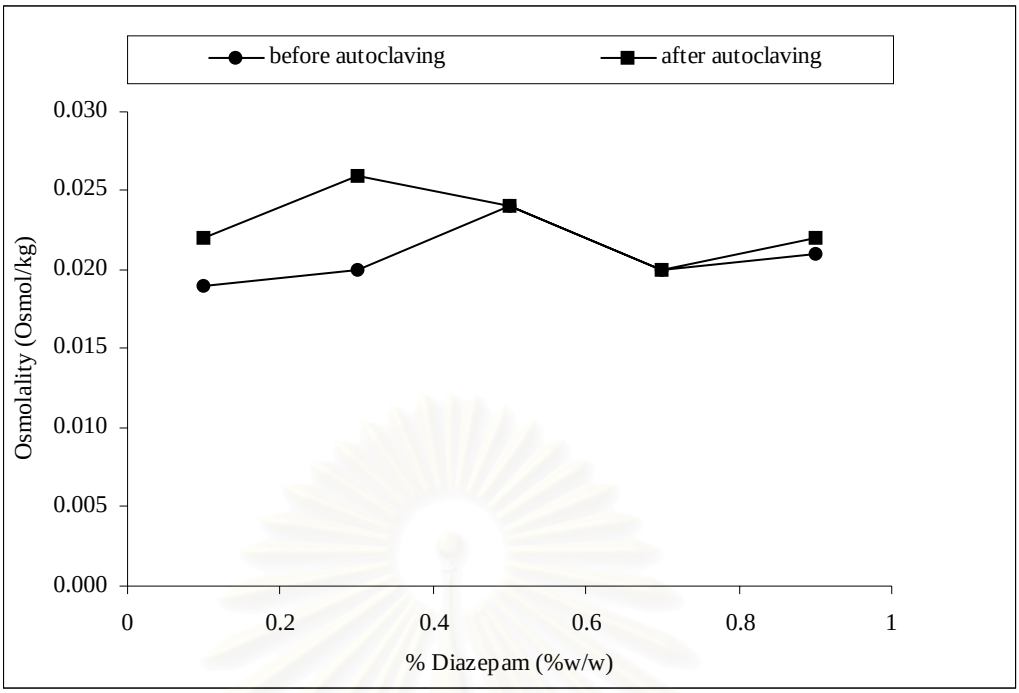

Figure 26 Effect of drug loading on osmolality in diazepam loaded SLN

5.7.4 Particle shape

The Cryo-SEM was used to investigate the particle shape and qualitatively confirmed the results from particle size analysis. The Cryo-SEM photomicrograph of diazepam loaded SLN showed spherical shape of solid lipids as depicted in Figure 27. Their sizes were in range of nanometer. Incorporation of diazepam in SLN did not change the physical appearance of drug free SLN. However, diazepam loaded SLN seems to be larger than drug free SLN. This result was in agreement of aforementioned report on the particle size analysis.

5.7.5 Entrapment efficiency

High entrapment efficiency was obtained in the preparations of SLN containing diazepam. Table 19 shows entrapment efficiency of the preparations. It was shown that diazepam, a water insoluble drug, could be loaded in high level. The percentage of entrapment was higher than 70% as observed in all preparations. It was also found that increasing the drug concentration would increase the entrapment efficiency.

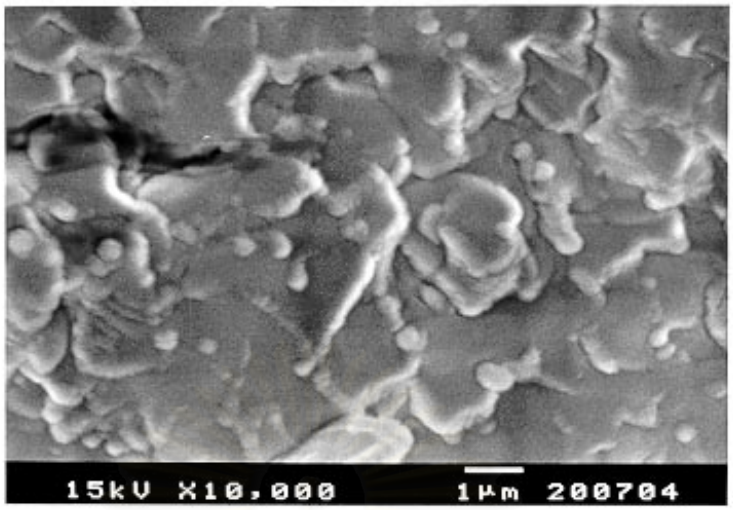

Figure 27 The Cryo-SEM photomicrograph of 0.7% diazepam SLN after autoclaving

Table 19 Entrapment efficiency of diazepam in SLN after autoclaving

Formulation	Percentage drug entrapment of diazepam loaded SLN			
	No. 1	No. 2	No. 3	Mean ± SD
0.1 DI + 5 GB + 4 TW80	73.83	72.19	73.01	73.01 ± 0.82
0.3 DI + 5 GB + 4 TW80	89.41	89.23	90.04	89.56 ± 0.43
0.5 DI + 5 GB + 4 TW80	93.25	93.30	93.41	93.32 ± 0.08
0.7 DI + 5 GB + 4 TW80	97.92	97.91	97.94	97.92 ± 0.02
0.9 DI + 5 GB + 4 TW80	94.29	94.36	94.29	94.31 ± 0.04

สถาบันวิทยบริการ
จุฬาลงกรณ์มหาวิทยาลัย

5.7.6 Drug release

In this study, five models of release kinetics: zero order, first order, Higuchi model, power expression, and Hixson-Crowell were used to assess the drug release model (Costa and Lobo, 2001). In zero order model, the relationship between the percentage of drug released versus time was plotted. For the first order model, the equation was expressed between natural logarithm of fraction of drug remaining and initial amount of drug against time. While Higuchi model, the relation was plotted

between the percentage of drug released and square root of time. Whilst in the power expression model, the equation was set between natural logarithm of fraction of drug released and total drug versus natural logarithm of time. And the Hixson-Crowell model, the relation was plotted between cube root of initial amount of drug minus cube root of remaining amount of drug and time. Linear regression was used to estimate the coefficient of determination (R^2). The model of dissolution profile was decided on which plot gave the higher coefficient of determination. The five models of release kinetics are determined as following equations

Zero order model: $Q = kt$

First order model: $\ln (Q_t/Q_o) = kt$

Higuchi model $Q = kt^{1/2}$

Power expression model $Q = kt^n$

or $\ln Q = \ln k + n \ln t$

Hixson-Crowell model $Q_o^{1/3} - Q_t^{1/3} = kt$

where Q = the amount of drug released at time t

Q_t = the amount of drug remaining at time t

Q_o = the initial amount of drug.

Diazepam saturated solution was rapidly diffused through dialysis membrane into pH 7.4 phosphate buffer. About 100% of diazepam was determined in release medium within 4 hours as shown in Figure 28. Diazepam loaded SLN showed slow release of drug for more than 60 hours. This indicated that solid lipid matrix could retard diazepam release. The reason explaining the drastic decrease in release rate of drug from the SLN was partition of drug. Diazepam had a high partition coefficient value. The partition coefficient (log P) of diazepam between 1-octanol and pH 7.4 phosphate buffer was 2.7 (Florey, 1972). This indicated that the diazepam

partition in favor of solid lipid could markedly reduce the aqueous drug concentration available for diffusion through the dialysis membrane. Figure 29 shows the dissolution profiles of SLN with different drug loading. The diazepam release rate was faster from the SLN with low drug loading (0.1% ,0.3% and 0.5% diazepam). This might be resulted from smaller mean particle size in formulation containing low drug loading resulting in much higher interfacial area. There was significant deference ($p<0.05$, ANOVA) in mean particle sizes between low drug loading (0.1% ,0.3% and 0.5% diazepam) and high drug loading (0.7% and 0.9% diazepam). Consequently, the release constant (k) was higher following Fick's first law in formulations with low drug loading. In addition, an increase in surface area led to an increase in the dissolution velocity according to the Noyes-Whitney equation. The elucidation of drug release kinetics is shown in Table 20. Diazepam loaded SLN in all formulations followed Higuchi model. The coefficient of determination was in nearly integral in all release profiles.

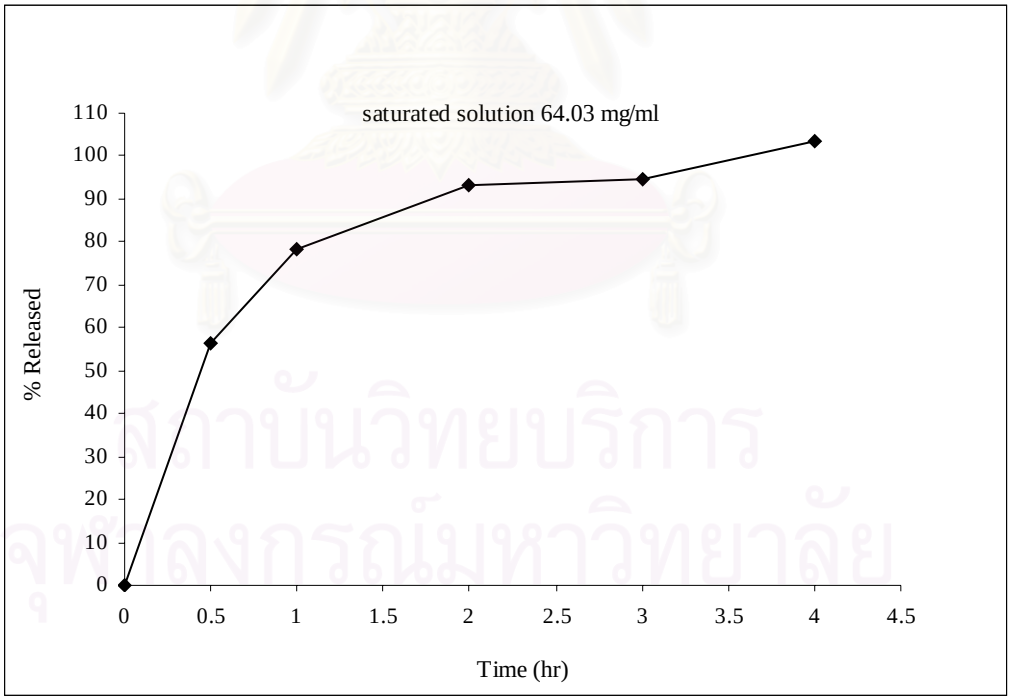

Figure 28 The release profile of diazepam from saturated solution

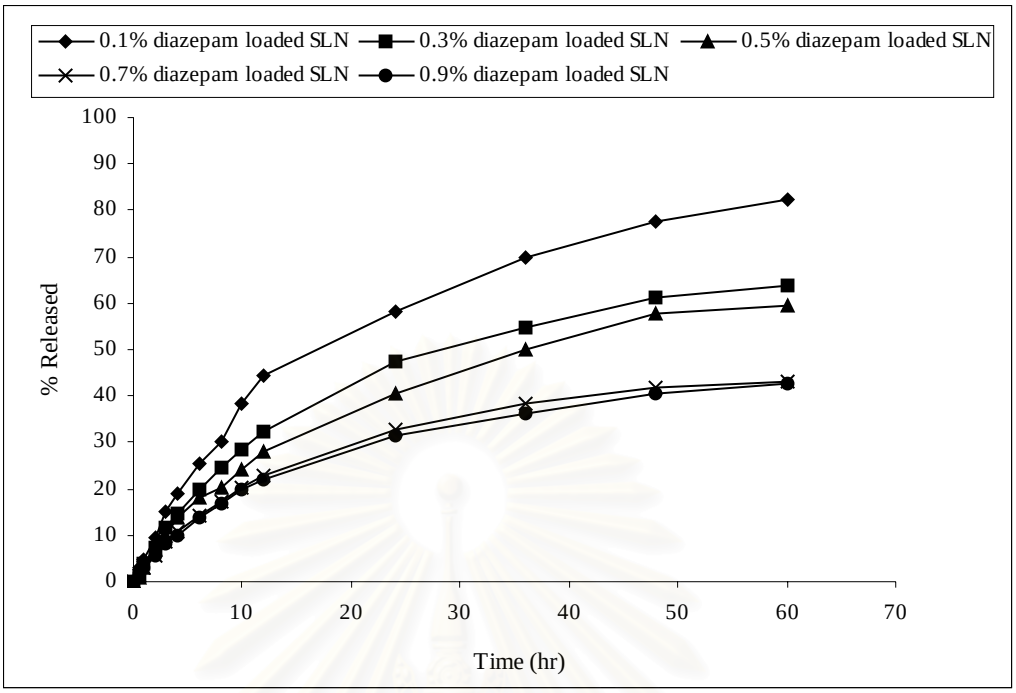

Figure 29 The release profiles of diazepam from 0.1-0.9% diazepam loaded SLN

Table 20 The coefficient of determinations of diazepam release in different models calculated from total amount of diazepam in formulation

Formulation	Coefficient of determination (R^2)				
	Zero order model	First order model	Higuchi model	Power expression	Hixson-Crowell model
0.1 DI + 5 GB+ 4 TW80	0.8834	0.9812	0.9836	0.9674	0.8834
0.3 DI + 5 GB+ 4 TW80	0.8860	0.9523	0.9846	0.9379	0.8860
0.5 DI + 5 GB + 4 TW80	0.9111	0.9634	0.9905	0.9316	0.9111
0.7 DI + 5 GB + 4 TW80	0.8722	0.9137	0.9811	0.9498	0.8722
0.9 DI + 5 GB + 4 TW80	0.8966	0.9354	0.9871	0.9718	0.8966

5.7.7 Fourier transform infrared spectroscopy

Figure 30 shows the IR sprectrum of diazepam. The FTIR pattern of diazepam showed strong peak at 3438 cm^{-1} for N-H stretching, the sharp peak 1682 cm^{-1} representing C=O stretching, the peak at 1612 cm^{-1} representing C=C cyclic stretching, the peak at 1131 cm^{-1} representing C-N stretching and the peak at 817 and 701 cm^{-1} representing =C-H out of plane bending (Wade, 1986, Florey, 1972).

The 0.1-0.9% diazepam loaded SLN obtained by ultracentrifugation presented the similar FTIR pattern with glycerol behenate SLN as shown in Figures 30 and 31. Diazepam loaded SLN showed spectra corresponding to a superimposition of their parent products and no significant shift of the major peaks of diazepam. The data indicated that no strong chemical interaction between diazepam and glycerol behenate

5.7.8 Differential scanning calorimetry

Figures 32 and 33 present DSC thermograms of glycerol behenate SLN, diazepam and 0.1-0.9% diazepam loaded SLN. The DSC thermogram of glycerol behenate SLN displayed its endothermic peak at 71.9ºC. The DSC thermogram of diazepam showed endothermic peak at 131.6ºC. Whilst 0.1-0.9% diazepam SLN were melted in range of 71.7-73.1ºC. The melting peak of diazepam disappeared. This suggested that diazepam in lipid matrix was in either molecularly dispersed or amorphous form. Similar finding had been reported by Cavalli, Caputo, and Calotti (1997). They formulated diazepam loaded SLN by microemulsion method and found that diazepam presented in its amorphous form in SLN. Moreover, Cavalli Caputo, and Gasco (2000) prepared paclitaxel-loaded SLN using O/W microemulsion method. The thermal analysis revealed that paclitaxel was in an amorphous form or molecularly dispersed.

5.7.9 Powder X-ray diffractometry

To verify the existence of diazepam in glycerol behenate, physical mixture of diazepam and glycerol behenate was analyzed by powder X-ray

diffractometry. Since the X-ray diffractometry pattern of unequal mixture will contain only stronger peaks of the minor component at greatly reduced intensity, but all of the peaks of the major component are present (Byrn et al., 1999). The physical mixtures of diazepam and glycerol behenate in the same quantity as in formulation of 0.3% and 0.5% diazepam loaded SLN were used to assure that the sharpening peaks of diazepam which was less than 10% of the mass lipid matrix could be detected by powder X-ray diffractometry. Figure 34 shows the X-ray diffraction patterns of glycerol behenate, diazepam and physical mixtures of diazepam and glycerol behenate. It is obvious that glycerol behenate and diazepam exhibited crystalline characteristics. X-ray diffraction pattern of physical mixture of diazepam and glycerol behenate was simply a superimposition of each component with the peaks of lower intensities. The existing peaks of diazepam exhibited at 18.780º and 22.740º. From this data, it can be deduced that major peaks of diazepam in physical mixture could be observed by this technique.

Powder X-ray diffraction patterns of 0.1-0.9% loaded diazepam loaded SLN showed similar pattern to glycerol behenate SLN as depicted in Figures 35 and 36. The peak of diazepam at 22.740º was superimposed to the peak of glycerol behenate SLN whereas the distinguished peak of diazepam at 18.780º disappeared. It was found that the peak at 21.270º showed stronger intensity in formulations of 0.7 and 0.9% diazepam loaded SLN. This was likely to be ascribed to preferred orientation affecting the intensity. The data from both differential scanning calorimetry and powder X-ray diffractometry could be concluded that diazepam in lipid matrix was in either molecularly dispersed or amorphous form.

สถาบันวิทยบริการ
จุฬาลงกรณ์มหาวิทยาลัย

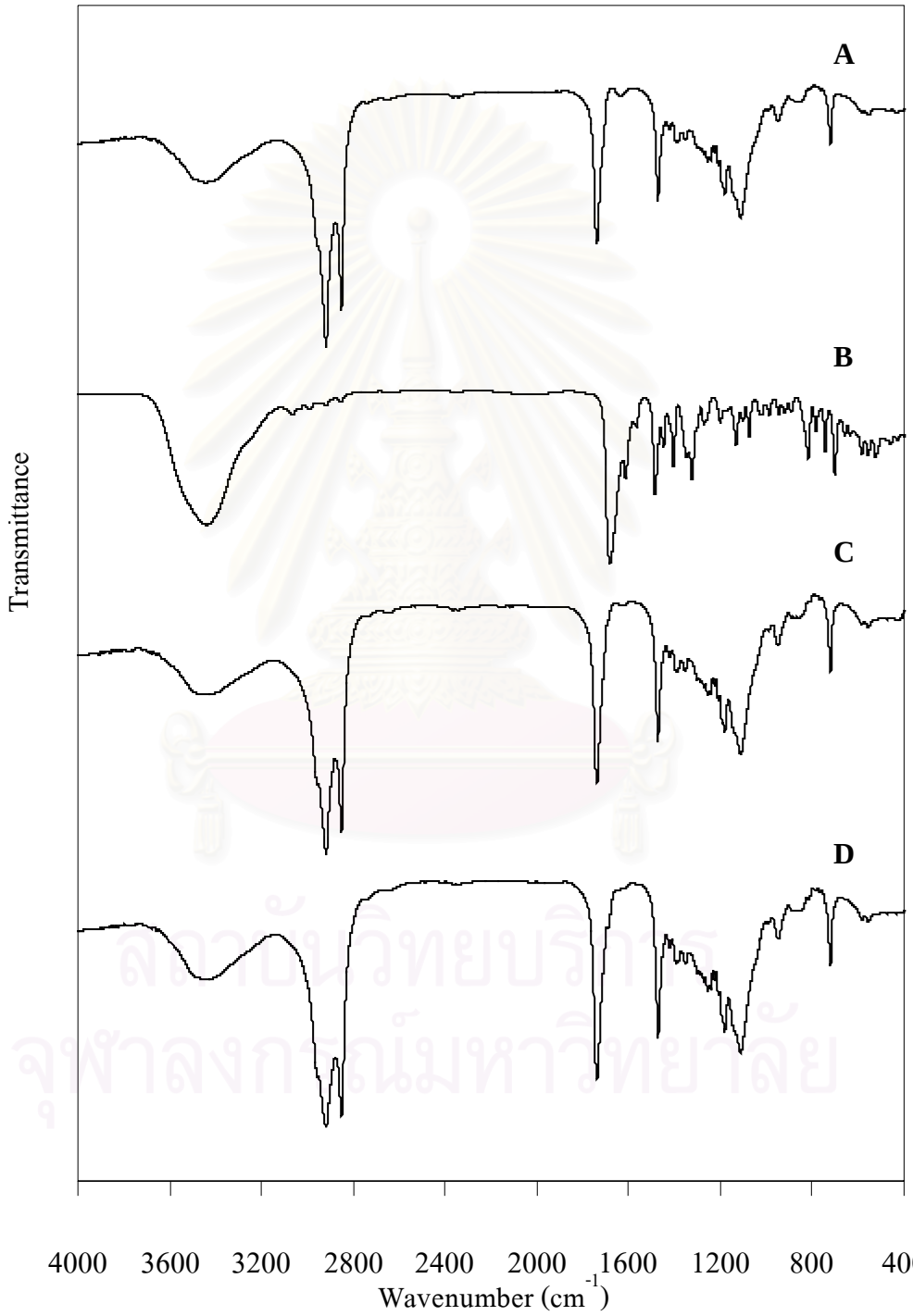

Figure 30 Infrared spectra of (A) glycerol behenate SLN, (B) diazepam, (C) 0.1% diazepam loaded SLN, (D) 0.3% diazepam loaded SLN

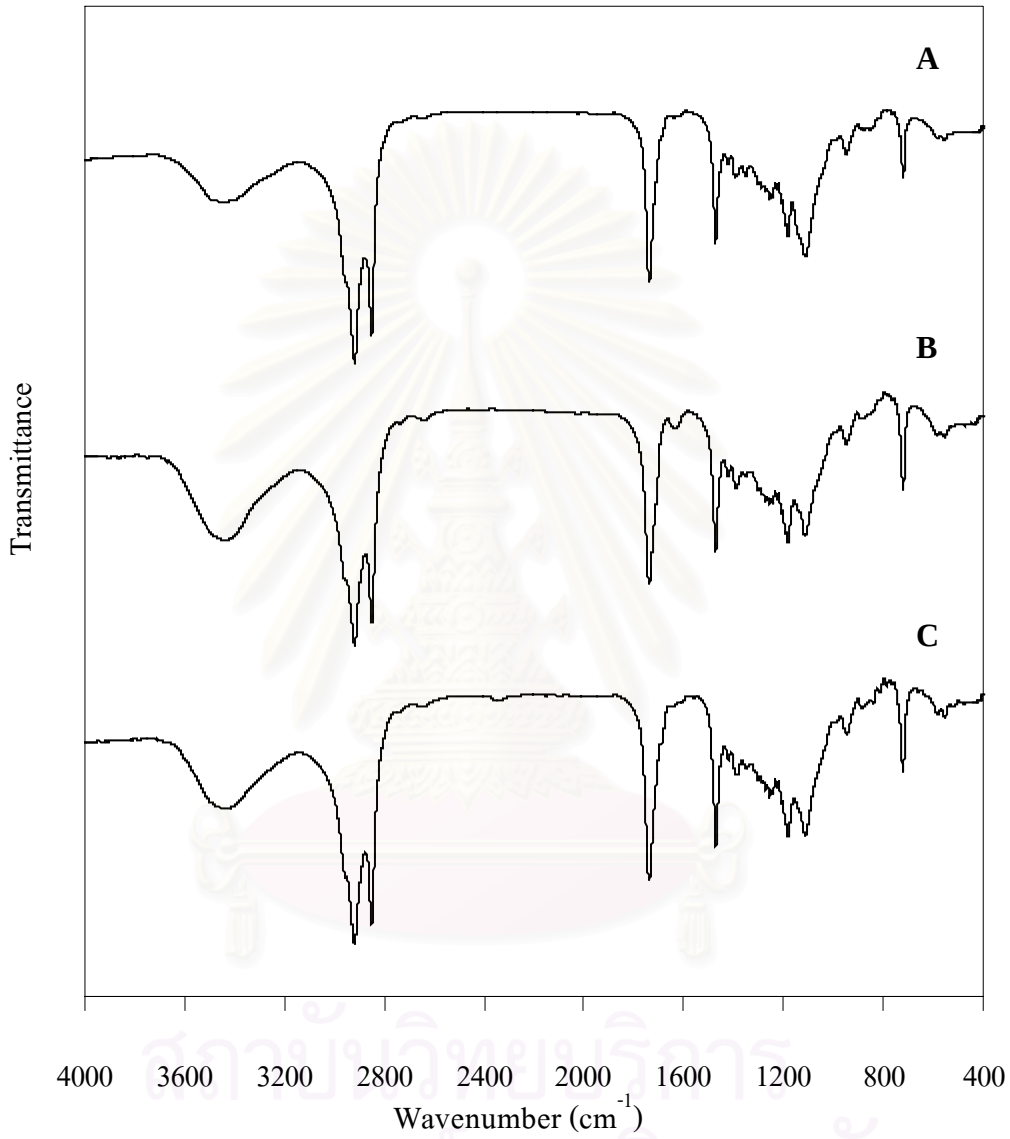

Figure 31 Infrared spectra of (A) 0.5% diazepam loaded SLN, (B) 0.7% diazepam loaded SLN, (C) 0.9% diazepam loaded SLN

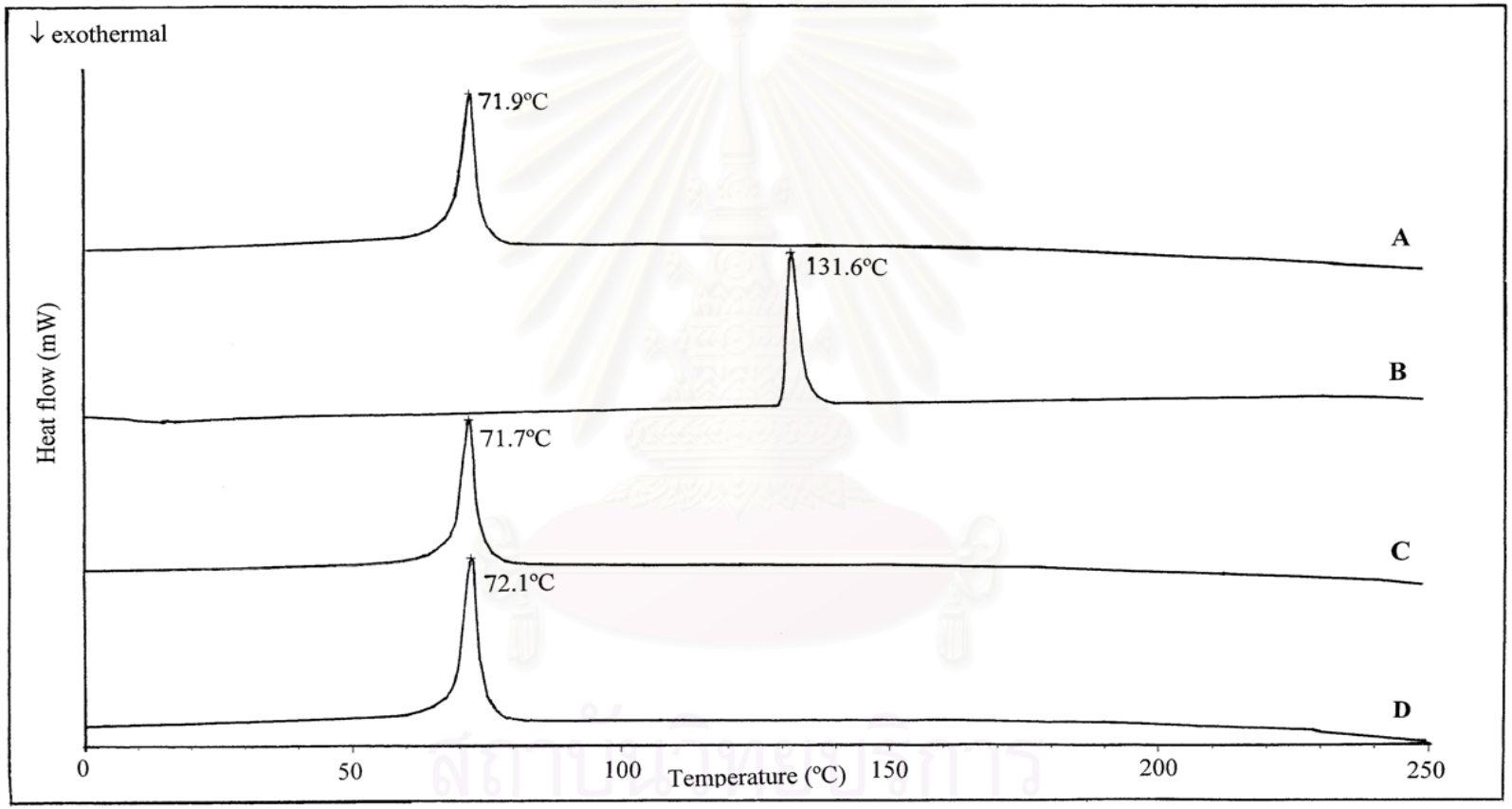

Figure 32 DSC thermograms of (a) glycerol behenate SLN, (b) diazepam, (c) 0.1% diazepam loaded SLN, (d) 0.3% diazepam loaded SLN

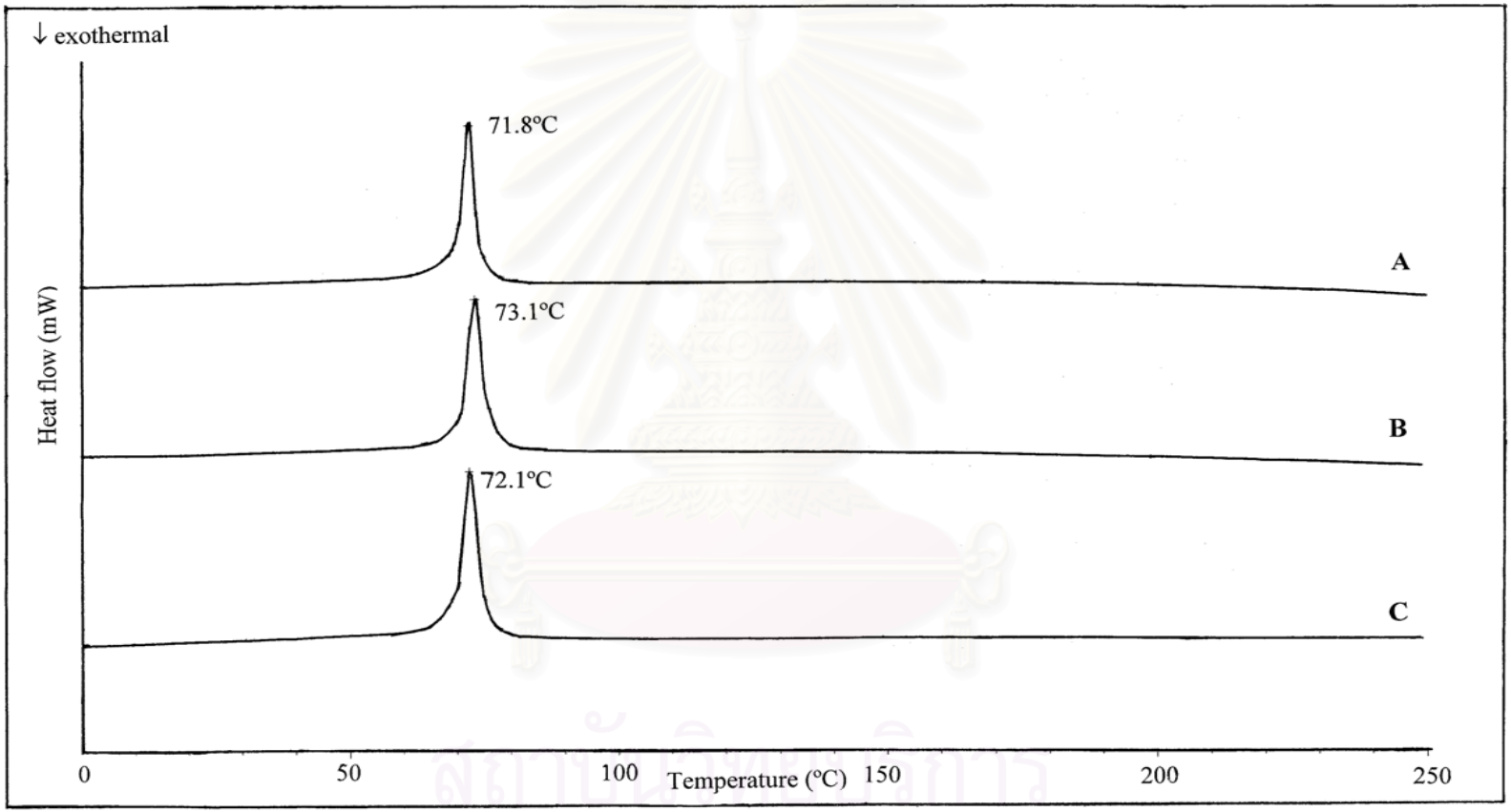

Figure 33 DSC thermograms of (a) 0.5% loaded diazepam loaded, (b) 0.7% diazepam loaded SLN, (C) 0.9% diazepam loaded SLN

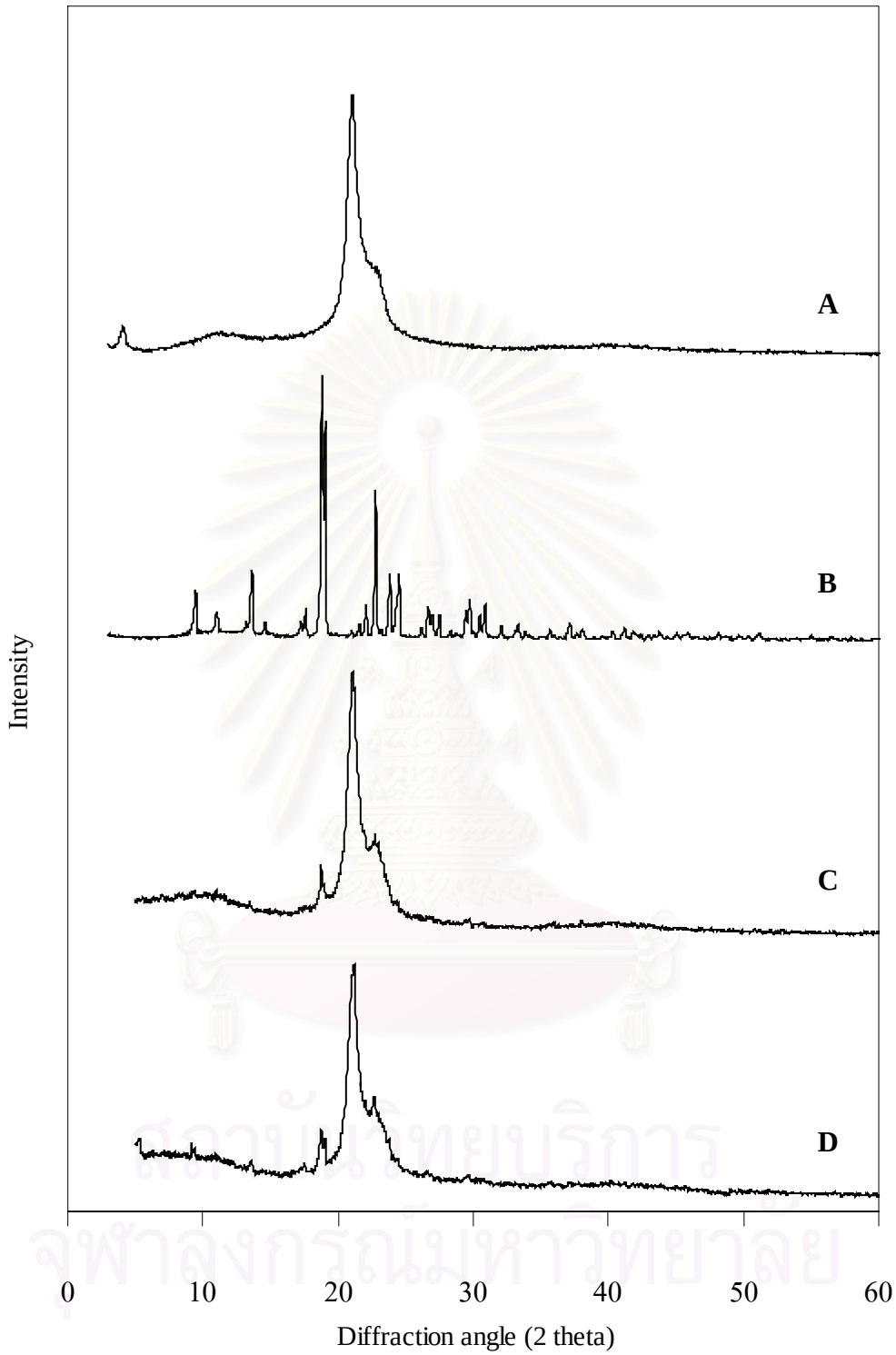

Figure 34 X ray diffractograms of (A) glycerol behenate, (B) diazepam, (C) physical mixing of diazepam and glycerol behenate in the same quantity of 0.3% diazepam loaded SLN, (D) physical mixing of diazepam and glycerol behenate in the same quantity of 0.5% diazepam loaded SLN

สถาบันวิทยบริการ
จุฬาลงกรณ์มหาวิทยาลัย

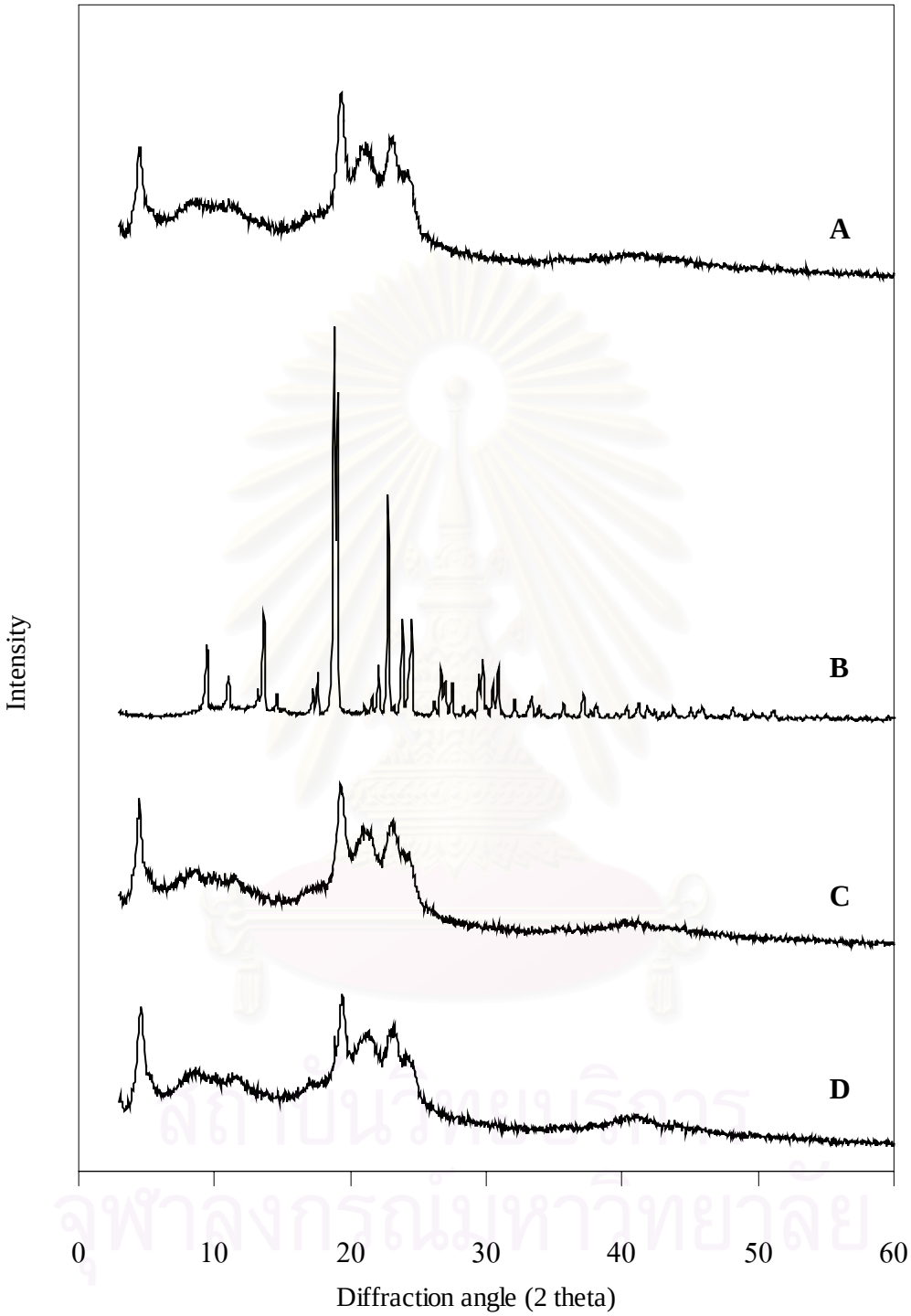

Figure 35 X-ray diffractograms of (A) glycerol behenate SLN, (B) diazepam, (C) 0.1% diazepam loaded SLN, (D) 0.3% diazepam loaded SLN

สถาบันวิทยบริการ
จุฬาลงกรณ์มหาวิทยาลัย

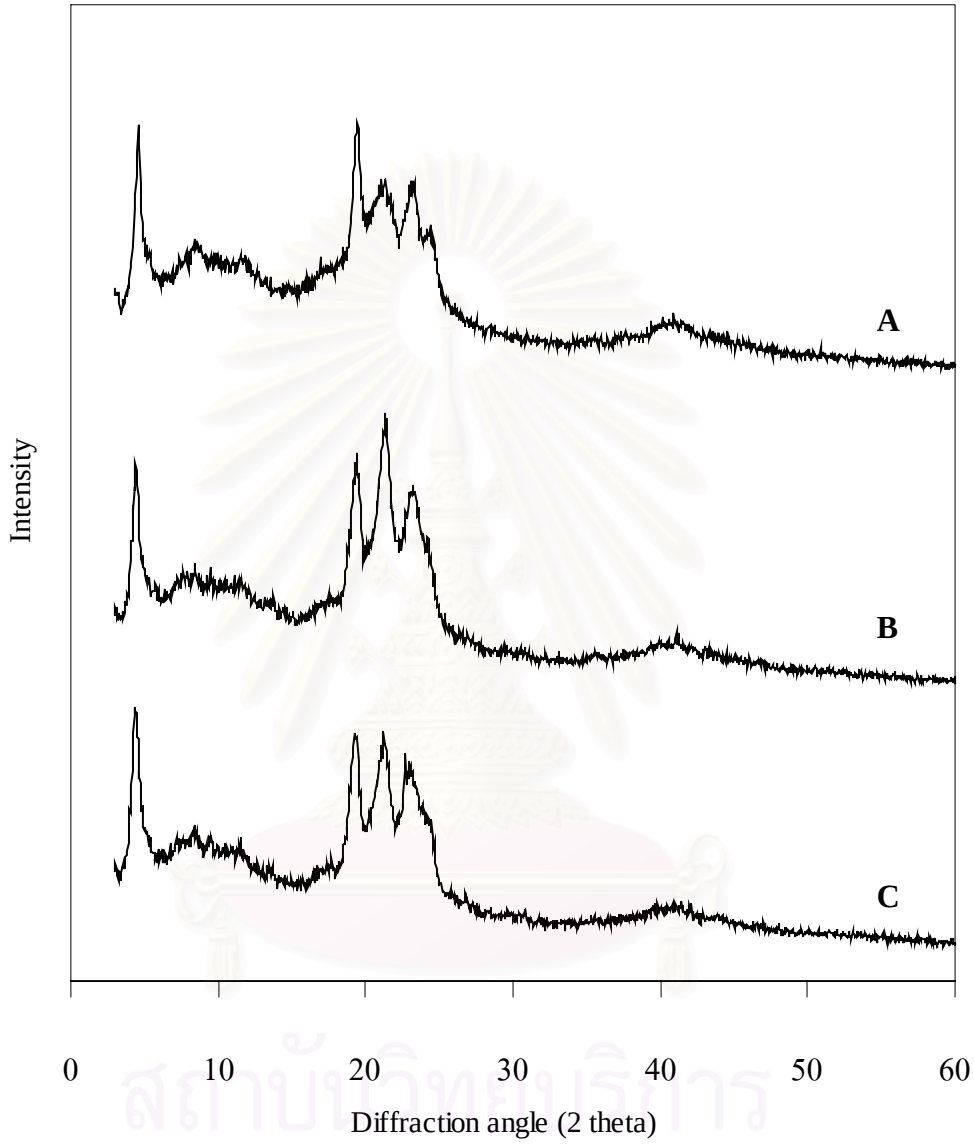

Figure 36 X-ray diffractograms of (A) 0.5% diazepam loaded SLN, (B) 0.7% diazepam loaded SLN, (C) 0.9% diazepam loaded SLN

5.8 Effect of homogenizing condition for 0.5% diazepam loaded SLN

From the data obtained, the particle sizes of all formulations of diazepam loaded SLN were in both micrometer and nanometer size range. However, the formulation which was intended for parenteral applications should has low percentage in micrometer range to prevent the blockage of syringe needle during injection. To minimize particle sizes in micrometer level, the 0.5% diazepam loaded SLN was chosen to determine the optimum homogenizing condition. In this study the homogenizing time used to obtain coarse emulsion was 10 minutes. Three levels of both homogenization pressure and cycle of homogenization were compared to select the most appropriate condition as shown in Table 21.

Table 21 Conditions used in 0.5% diazepam loaded SLN

Formulation	0.5% Diazepam loaded SLN								
Pressure (psi)	10,000			15,000			20,000		
Recycle time (cycles)	5	7	9	5	7	9	5	7	9

Table 22 shows that the bulk population after autoclaving was in nanometer size analyzed by PCS. The D(v,0.5) and the percentage of particle larger than 1, 5 and 10 μm are shown in Table 22. Increasing the homogenization pressure and cycle of homogenization did not affect the mean particle size of SLN. In agreement from both PCS and LD, the z value and D(v,0.5) did not further decrease when increasing homogenization pressure from 10,000 psi to 20,000 psi and cycle of homogenization pressure from 5 to 9 cycles. On the other hand, there was a distinct decrease in percentage of particle larger than 5 μm when increasing homogenization pressure. The percentage of particle larger than 5 μm was also depended largely on homogenization pressure. Interaction effects between pressure and recycle time played importance role as well ($p<0.05$, two-way ANOVA). The statistical analysis is shown in Table 23. Figure 37 shows that the percentage of particle larger than 5 μm was the least at homogenizing condition of 20,000 psi and 5 cycles.

Table 22 Particle sizes of 0.5% diazepam loaded SLN after autoclaving analyzed by PCS and LD

Condition	0.5% diazepam loaded SLN (after autoclaving)								
	Mean particle size (nm)		Volume particle size (μm)				% Particle larger than		
	z value	PI	D(v,0.1)	D(v,0.5)	D(v,0.9)	uniformity	1 μm	5 μm	10 μm
10,000 psi and 5 cycles	152.4	0.163	0.16	0.37	56.24	39.00	34.04	28.08	24.84
10,000 psi and 7 cycles	172.4	0.187	0.17	0.32	3.78	4.48	21.76	8.44	4.67
10,000 psi and 9 cycles	189.4	0.201	0.21	0.38	4.85	6.85	18.74	9.89	7.04
15,000 psi and 5 cycles	155.1	0.163	0.18	0.36	3.91	8.62	19.03	9.04	6.37
15,000 psi and 7 cycles	187.7	0.176	0.21	0.37	2.01	4.76	14.74	6.79	4.74
15,000 psi and 9 cycles	174.4	0.213	0.20	0.37	3.45	9.81	19.12	9.19	7.39
20,000 psi and 5 cycles	157.5	0.148	0.22	0.36	0.77	5.99	8.81	5.28	3.90
20,000 psi and 7 cycles	170.3	0.159	0.22	0.37	10.32	20.62	17.64	12.38	10.11
20,000 psi and 9 cycles	182.4	0.206	0.22	0.37	1.21	5.22	10.86	5.83	4.16

สถาบันวิทยบริการ
จุฬาลงกรณ์มหาวิทยาลัย

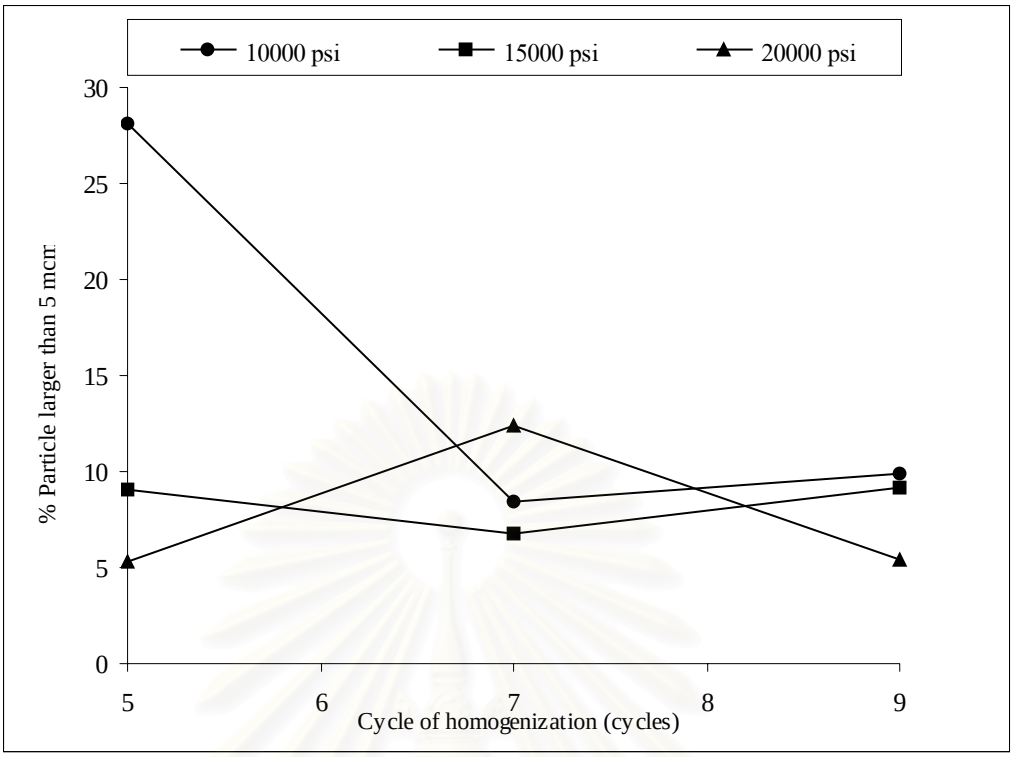

Figure 37 Interactions of homogenization pressure and cycle of homogenization on percentage of particle larger than 5 μm of 0.5% diazepam loaded SLN

Table 23 Statistical analysis of the percentage of particle larger than 5 μm in 0.5% diazepam loaded SLN

Source of variation	Sum of squares	df	Mean square	**F-ratio**	P-value
Pressure	328.169	2	164.085	19.300	.000
Cycle	177.356	2	88.678	10.431	.001
Pressure-cycle	645.749	4	161.437	18.989	.000
Model	1151.274	8	143.909	16.927	.000
Intercept	3002.425	1	3002.425	353.156	.000
Error	153.031	18	8.502		
Total	4306.730	27			
R-squared = 0.883	0.883				
Adjust R-squared = 0.831					

The data also indicated that no further reduction of particle larger than 5 μm was obtained when increasing the homogenizing cycles greater than 5 cycles at 20,000 psi. Thus, It was assumed that the condition with the homogenization pressure of 20,000 psi for 5 cycles was the most appropriate condition to prepare diazepam SLN. The result agreed with a previous study by Müller and Böhm (1998). They varied cycle number of homogenizer (APV homogenizer LAB 40) and found that no further reduction of mean particle size analyzed by PCS. But micrometer particles presented in formulation were removed and led to a reduction of width of the size of distribution.

5.9 Preparation and characterization of diazepam loaded SLN

Diazepam loaded SLN was prepared using Emulsiflex®C-5 operating at pressure of 20,000 psi for 5 cycles to reduce particle in micromerter range. Both formulations of 0.3% and 0.5% w/w diazepam loaded SLN were selected for further study.

5.9.1 Particle size

The particle sizes of 0.3 and 0.5% diazepam loaded SLN which were prepared by Emulsiflex® C-5 operating at pressure of 20,000 psi for 5 cycles are shown in Table 24. The results obtained from PCS demonstrated that the z values of diazepam loaded SLN were larger than that of drug free SLN as aforementioned report. However, the increasing of pressure of high pressure homogenizer from 10,000 psi to 20,000 psi could reduce percentage of particle larger than 1, 5 and 10 μm in preparation of 0.3% diazepam loaded SLN up to 18.05%, 16.09% and 14.60%, respectively. Whilst particles larger than 1, 5 and 10 μm in preparation of 0.5% diazepam loaded SLN could reduce up to 25.23%, 22.80% and 20.94%, respectively as depicted in Figure 38. The result found that not only particle size in micrometer range but also the mean particle size could be reduced in formulation of 0.3% diazepam loaded SLN when increasing pressure up to 20000 psi. This was undoubtedly due to lower drug concentration in formulation than 0.5% diazepam SLN. The polydispersity index and uniformity in diazepam loaded SLN prepared under pressure of 20,000 psi were lower than those of the same formulation prepared

under pressure of 10,000 psi as shown in Figures 39 and 40. This result indicated that pressure of homogenizer impacted on narrow size distribution.

An essential requirement for development of parenteral dosage form is the small particle size that has to be smaller than the inside diameter of hypodermic needle. As ISO standard specification, inside diameters of a 20-25 guage needle were ranging from 0.28 to 1.50 mm (Akers, Fites, and Robinson, 1987). In both of 0.3% and 0.5% diazepam loaded SLN, all particles were less than 103.58 and 222.28 μm, respectively. This indicated that SLN prepared under pressure of 20,000 psi 5 cycles could be easily drawn into syringe through a 20-25 guage needle. However, there were small quantities of particle size larger than 5 μm in both formulations as depicted in Figures 41 and 42. From the result, it was conceivably concluded that the obtained diazepam loaded SLN prepared for parenteral administration was more appropriate for intramuscular and subcutaneous injection.

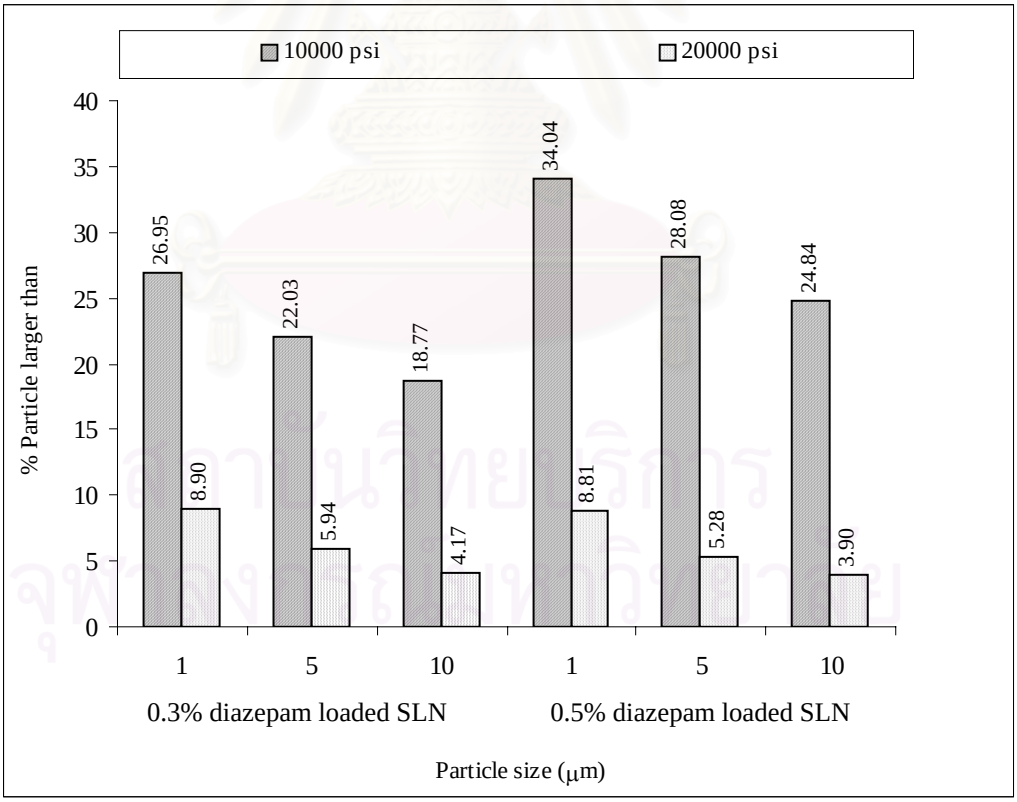

Figure 38 Effect of homogenization pressure on the percentage of particle larger than

1, 5 and 10 μm in formulation of 0.3% and 0.5% diazepam loaded SLN

สถาบันวิทยบริการ
จุฬาลงกรณ์มหาวิทยาลัย

Table 24 Particle sizes of 0.3% and 0.5% diazepam loaded SLN after autoclaving analyzed by PCS and LD (a) operating at 10,000 psi (b) operating at 20,000 psi

Formulation	PCS		LD						
	Mean particle size (nm)		Volume particle size (µm)				% particle larger than		
	Z value	PI	D(v,0.1)	D(v,0.5)	D(v,0.9)	uniformity	1 µm	5 µm	10 µm
0.3 DI + 5 GB + 4 TW80 (a)	156.2	0.161	0.15	0.33	35.72	31.62	26.95	22.03	18.77
0.3 DI + 5 GB + 4 TW80 (b)	148.6	0.161	0.09	0.24	0.76	6.28	8.90	5.94	4.17
0.5 DI + 5 GB + 4 TW80 (a)	152.4	0.163	0.16	0.37	52.24	39.00	34.04	28.08	24.84
0.5 DI + 5 GB + 4 TW80 (b)	157.5	0.148	0.22	0.36	0.77	5.99	8.81	5.28	3.90

สถาบันวิทยบริการ
จุฬาลงกรณ์มหาวิทยาลัย

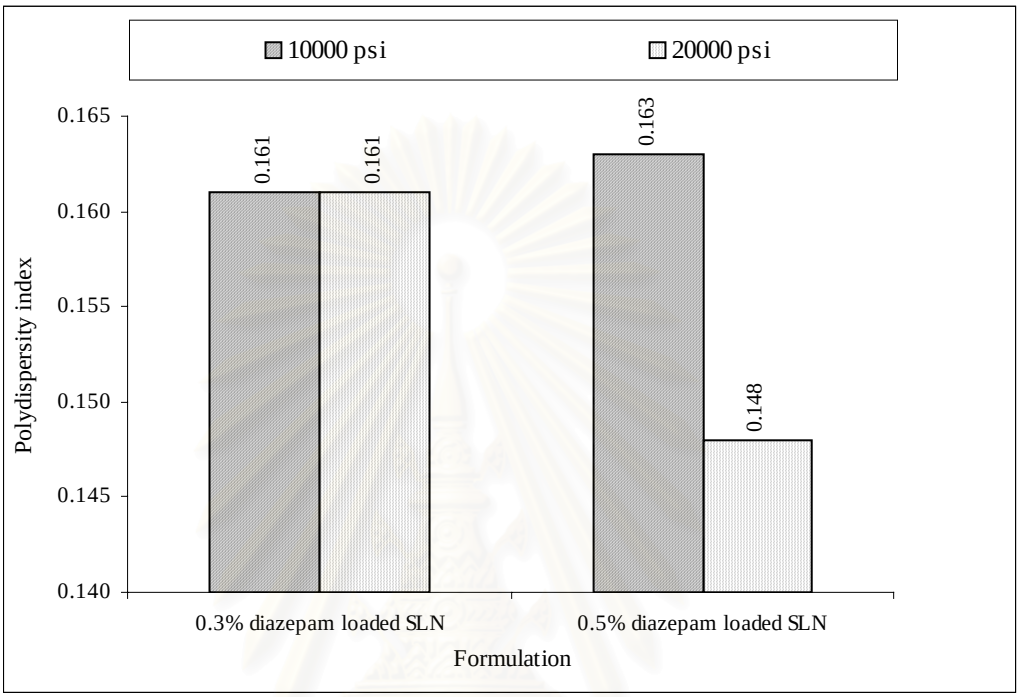

Figure 39 Effect of homogenization pressure on the polydispersity index in formulations of 0.3% and 0.5% diazepam loaded SLN

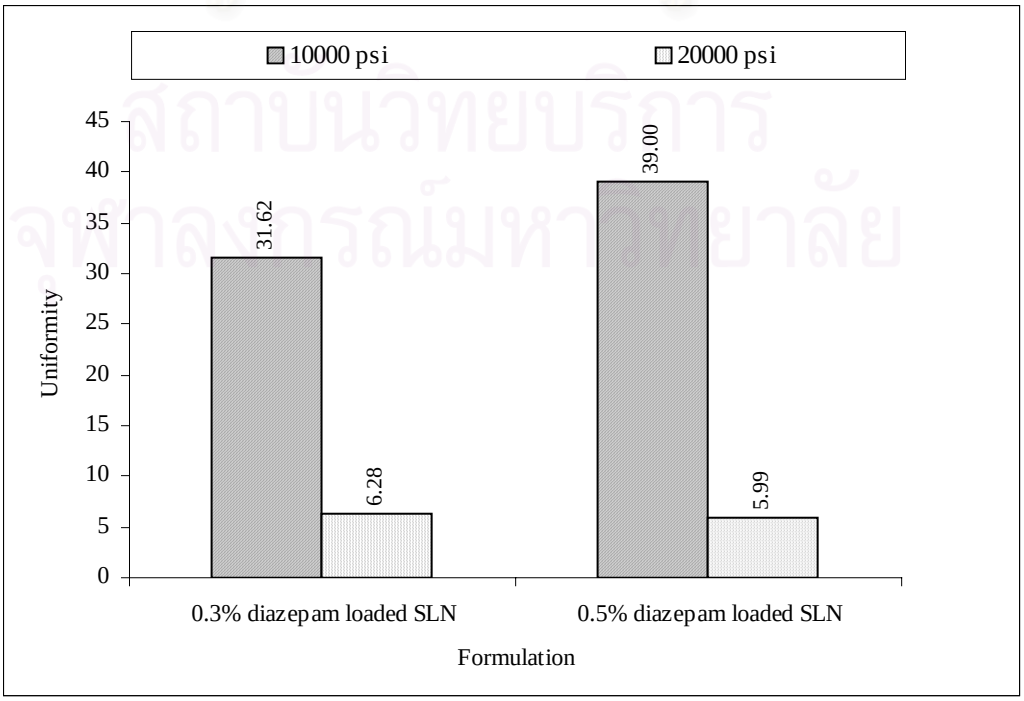

Figure 40 Effect of homogenization pressure on the uniformity in formulations of 0.3% and 0.5% diazepam loaded SLN

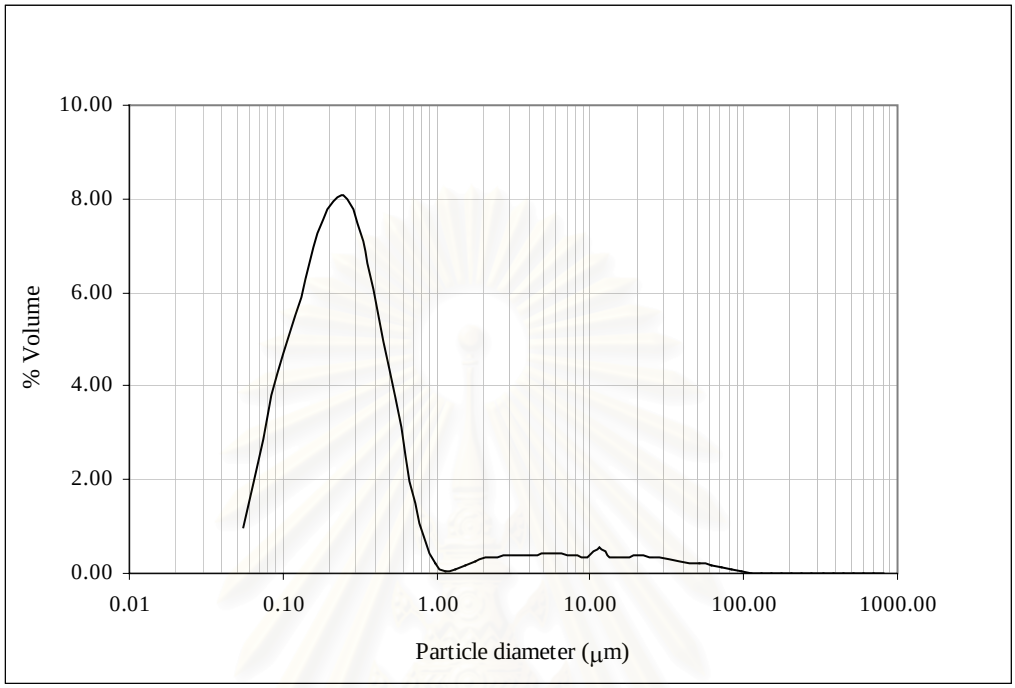

Figure 41 Particle size distribution of formulation of 0.3% diazepam loaded SLN prepared under pressure of 20,000 psi analysed by LD

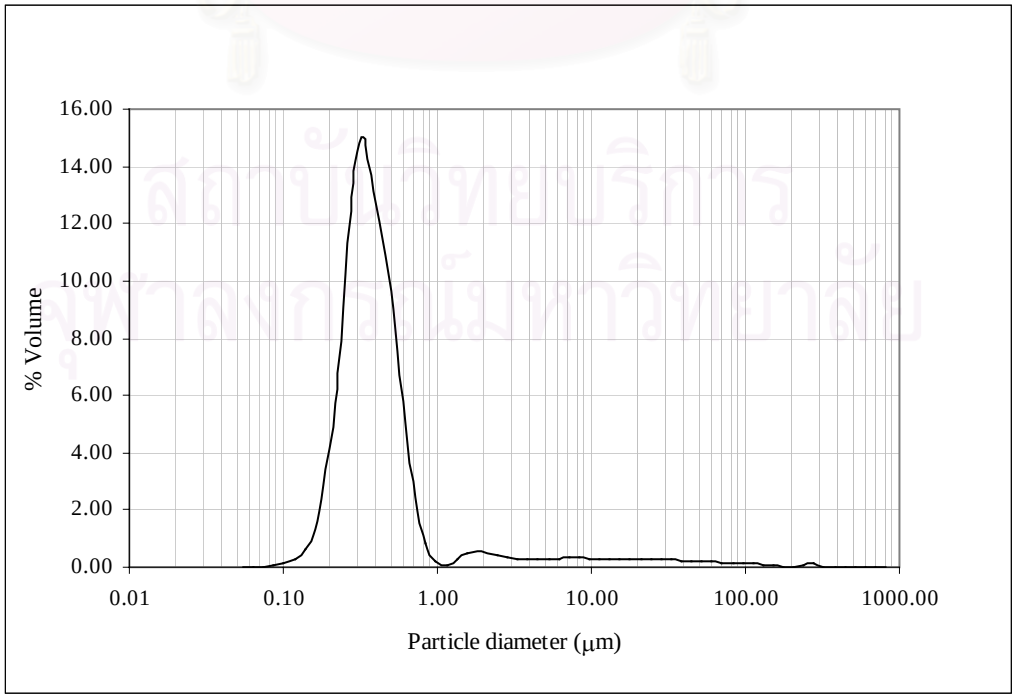

Figure 42 Particle size distribution of formulation of 0.5% diazepam loaded SLN prepared under pressure of 20,000 psi analysed by LD

5.9.2 pH, zeta potential and osmolality

The data presented in Table 25 clearly showed that there was no remarkable change in pH, zeta potential and osmolality upon increasing the pressure of homogenizer in both formulations of 0.3 and 0.5% diazepam loaded SLN. The data obtained implied that the increasing of mechanical input during production highly affected on particle size and particle size distribution but hardly impacted on other physicochemical properties. Furthermore, there was no statistical difference in zeta potential between formulation 0.3% and 0.5% diazepam loaded SLN prepared under pressure of 20,000 psi ($p>0.05$, t-test). This confirmed the previous result that diazepam concentration did not alter surface change of solid lipid particles. Early study has revealed that no change in the zeta potential was obtained with increasing diazepam concentration to the required therapeutics in lipid emulsion (Levy and Benita, 1989).

Table 25 Effect of pressure on pH, zeta potential and osmolality in formulation of 0.3% and 0.5% diazepam loaded SLN after autoclaving (a) operating at 10,000 psi (b) operating at 20,000 psi

Formulation	After autoclaving		
	pH	**Zeta potential** (millivolt)	**Osmolality** (Osmol/kg)
0.3 DI + 5 GB + 4 TW 80 (a)	5.17 ± 0.01	-21.0 ± 0.3	0.026 ± 0.001
0.3 DI + 5 GB + 4 TW 80 (b)	5.20 ± 0.04	-21.2 ± 1.7	0.022 ± 0.005
0.5 DI + 5 GB + 4 TW 80 (a)	5.16 ± 0.01	-21.9 ± 1.7	0.024 ± 0.001
0.5 DI + 5 GB + 4 TW 80 (b)	5.22 ± 0.07	-23.1 ± 0.8	0.025 ± 0.002

5.9.3 Morphology of diazepam loaded SLN

The morphology of two SLN preparations prepared under pressure of 20,000 psi was studied using Cryo-SEM. Electron micrographs showed that most solid lipids were spherical in shape. As depicted in Figures 43 and 44, the particle sizes of solid lipids were mostly smaller than 1 µm. The photomicrograph showed that solid lipids in formulation of 0.5% diazepam loaded SLN were larger than those in formulation of 0.3% diazepam loaded SLN which gave similar result from particle size analysis by PCS. However, surface of solid lipids in this observation could not be seen because increasing magnification of electron microscope resulting in high energy in sample and then caused solid lipids melted.

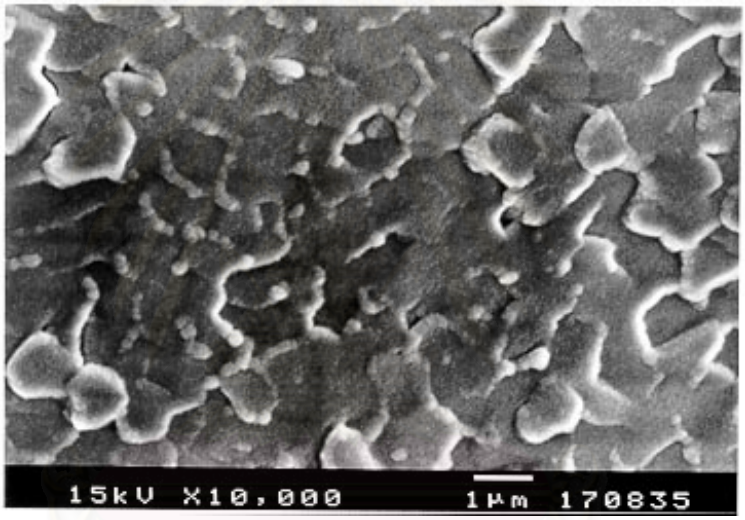

Figure 43 The Cryo-SEM photomicrograph of 0.3% diazepam loaded SLN prepared under pressure of 20,000 psi

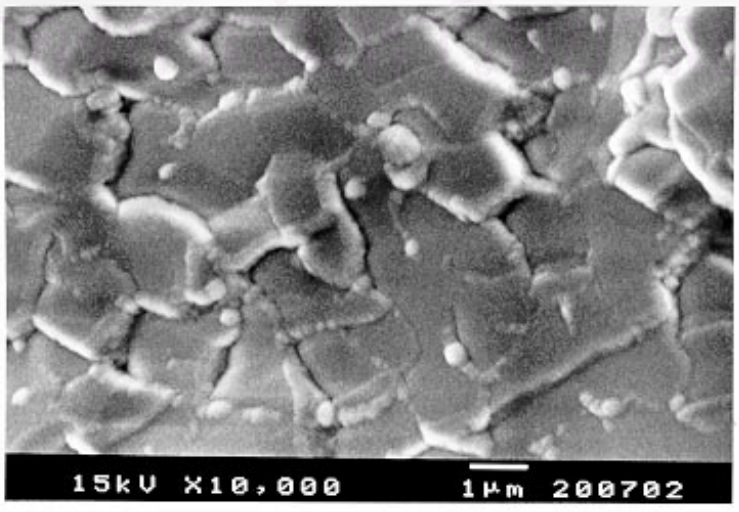

Figure 44 The Cryo-SEM photomicrograph of 0.5% diazepam loaded SLN prepared under pressure of 20,000 psi

5.9.4 Entrapment efficiency

High entrapment of diazepam in SLN prepared under pressure of 20,000 psi was observed as shown in Table 26. Possible explanation of the high entrapment of diazepam in SLN was its high partition coefficient value (log P). This caused the low solubility of diazepam in dispersion medium. Thus most drug could be loaded into lipid matrix and only small amount of drug could partition into aqueous medium.

Table 26 Entrapment efficiency of diazepam in formulations of 0.3% and 0.5% diazepam loaded SLN prepared under pressure of 20,000 psi

Formulation	**% Drug entrapment of diazepam loaded SLN**			
	No. 1	No. 2	No. 3	**Mean ± SD**
0.3 Di + 5 GB + 4 TW 80	88.99	89.40	89.11	89.17 ± 0.21
0.5 Di + 5 GB + 4 TW 80	92.69	92.60	92.67	92.65 ± 0.05

5.9.5 Drug release

In this study, 0.3% and 0.5% diazepam loaded SLN prepared under pressure of 20,000 psi were selected to study. The supernatant of preparations was also studied for comparison. The release profiles of diazepam from SLN and from supernatant are illustrated in Figure 45. Diazepam loaded SLN showed slow release more than 60 hours. While diazepam release from supernatant of both preparations was completely release within 12 hours. Then diazepam was prominently released from lipid matrix. The data obtained suggested that solid lipids could retard diazepam release. This result gave similar release profiles when compared with the preparations prepared under pressure of 10,000 psi in that diazepam released from formulation of 0.3% diazepam loaded SLN faster than that of 0.5% diazepam loaded SLN. The elucidation of drug release kinetics calculated from total amount of diazepam in

formulations and solid lipids is shown in Table 27. It was apparent that diazepam released from SLN followed Higuchi model.

As can be seen from Figure 46, faster release from the formulation of 0.3% diazepam loaded SLN prepared under pressure of 20,000 psi than that prepared under pressure of 10,000 psi could be explained by a short diffusion path due to smaller size analyzed by PCS. In contrast to preparation of 0.5% diazepam loaded SLN, faster diazepam release rate from SLN prepared under pressure of 20,000 psi was not observed. It was likely to ascribe that this difference was resulted from mean particle size. There was no statistical difference in mean particle size (z value) in formulation of 0.5% diazepam loaded SLN prepared under pressure of 20,000 psi and 10000 psi ($p>0.05$, t-test). This might be concluded that release rate of drug from SLN largely depended on particle size in nanometer. Although the microparticle sizes in diazepam loaded SLN were reduced when increasing pressure up to 20,000 psi, the bulk population in SLN were in nanometer range.

The present study showed the slower diazepam release from SLN than that from aqueous solution and supernatant. It was similar to a previous study by Mühen et al. (1998). They stated that the slower prednisolone release from SLN as a result of the presence of a solid solution throughout the particle combined with a slow diffusion of prednisolone from the matrix. Besides the release rate of the drug from SLN is related to other factors such as interactions between drug-lipid molecules, between surfactant-lipid molecules.

Table 27 The coefficient of determinations of diazepam release- from (a) total amount in formulation (b) total amount in solid lipids in formulations- of 0.3% and 0.5% diazepam loaded SLN prepared under pressure of 20,000 psi using different models

Formulation	**Coefficient of determination (R^2)**				
	Zero order model	**First order model**	**Higuchi model**	**Power expression**	**Hixson-Crowell model**

0.3 DI + 5 GB + 4 TW80 (a)	**0.8674**	**0.9684**	**0.9805**	**0.9758**	**0.8674**
0.3 DI + 5 GB + 4 TW80 (b)	**0.8554**	**0.9473**	**0.9766**	**0.9744**	**0.8554**
0.5 DI + 5 GB + 4 TW80 (a)	**0.8971**	**0.9538**	**0.9917**	**0.9872**	**0.8971**
0.5 DI + 5 GB + 4 TW80 (b)	**0.8891**	**0.9423**	**0.9902**	**0.9858**	**0.8891**

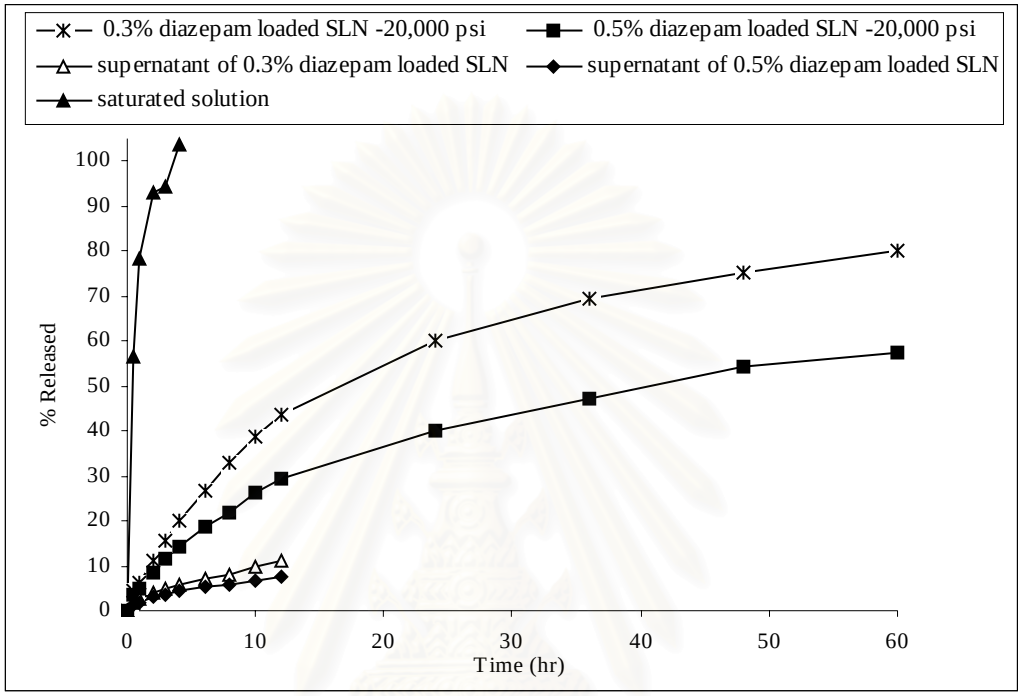

Figure 45 The release profiles of diazepam from saturated solution, 0.3 and 0.5% diazepam loaded SLN prepared under pressure of 20,000 psi and supernatant of both preparations

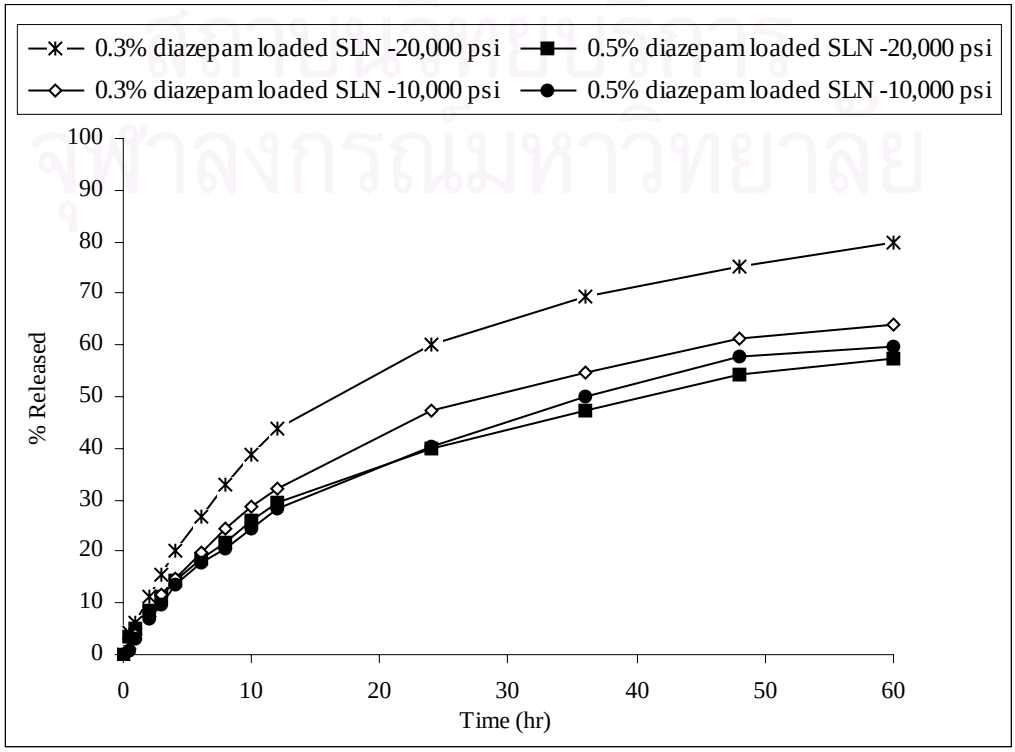

Figure 46 The release profiles of diazepam from 0.3% and 0.5% diazepam loaded SLN prepared under pressure of 10,000 psi and 20,000 psi

5.9.6 Fourier transform infrared spectroscopy

The infrared spectra of 0.3 and 0.5% diazepam loaded SLN prepared under pressure of 20,000 psi exhibited similar pattern to those prepared under pressure of 10,000 psi as depicted in Figure 47. Diazepam loaded SLN showed spectra corresponding to a superimposition of diazepam tween 80 and glycerol behenate. No marked difference of infrared spectrum was noticed. The sharp peaks at 3434, 2918, 2851, 1737, 1472, 1112 and 720 cm^{-1} were observed from the superimposition of diazepam tween 80 and glycerol behenate.

5.9.7 Differential scanning calorimetry

Figure 48 shows the DSC thermograms of 0.3 and 0.5% diazepam loaded SLN prepared under pressure of 20,000 psi. They displayed melting endotherm at 71.6ºC and 71.3ºC, respectively. Whilst the melting peak of diazepam was absent in DSC heating run which was in accordance which the analysis of those prepared under pressure of 10,000 psi.

5.9.8 Powder X-ray diffractometry

No change in powder X-ray diffraction pattern of 0.3 and 0.5% diazepam loaded SLN prepared under pressure of 20,000 psi compared to those prepared under pressure of 10,000 psi as depicted in in Figure 49. The data from thermal analysis and powder X-ray diffractometry revealed that diazepam in lipid matrix was in either molecularly dispersed or amorphous form. Furthermore, this result indicated that the increasing pressure up to 20,000 psi did not further change in polymorphic transition of glycerol behenate in diazepam loaded SLN.

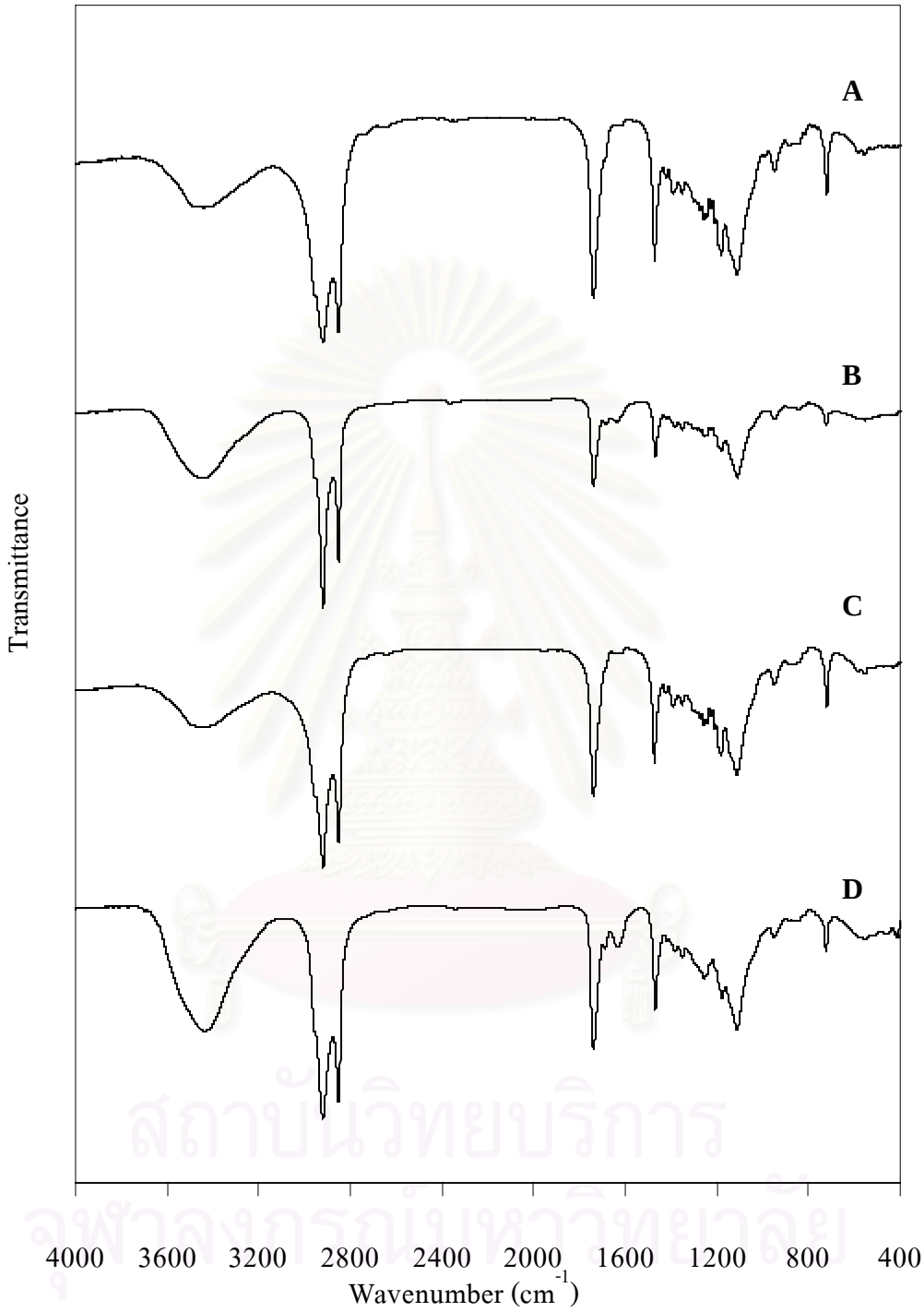

Figure 47 Infrared spectra of (A) 0.3% diazepam loaded SLN –10,000 psi, (B) 0.3% diazepam loaded SLN –20,000 psi, (C) 0.5% diazepam loaded SLN –10,000 psi, (D) 0.5% diazepam loaded SLN –20,000 psi

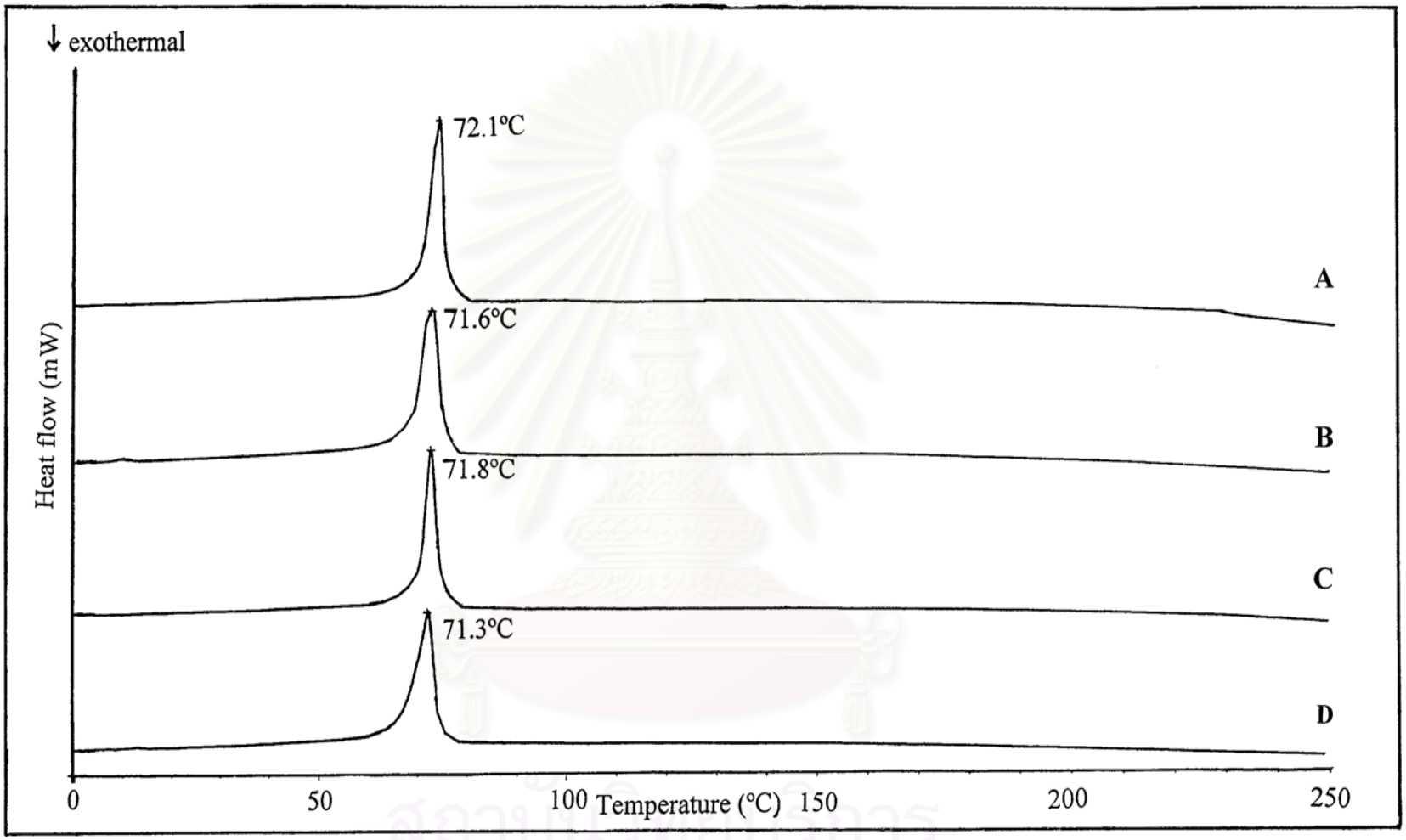

Figure 48 DSC thermograms of (A) 0.3% diazepam loaded SLN- 10,000 psi, (B) 0.3% diazepam loaded SLN- 20,000 psi (C) 0.5% diazepam loaded SLN- 10,000 psi, (D) 0.5% diazepam loaded SLN- 20,000 psi

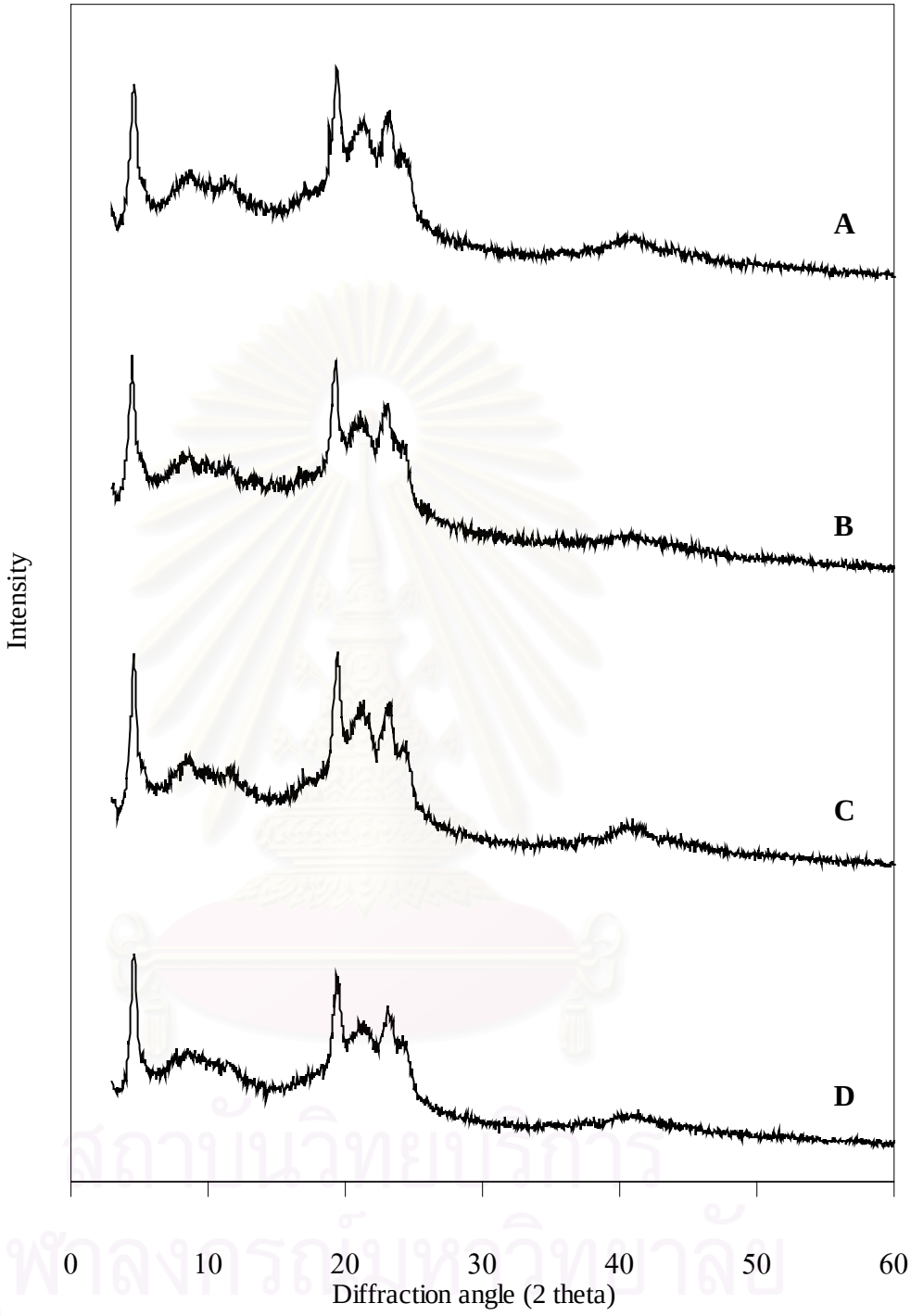

Figure 49 X ray diffractograms of (A) 0.3% diazepam loaded SLN- 10,000 psi, (B) 0.3% diazepam loaded SLN- 20,000 psi, (C) 0.5% diazepam loaded SLN- 10,000 psi, (D) 0.5% diazepam loaded SLN- 20,000 psi,

5.9.9 Stability testing

The preparations of 0.3% and 0.5% diazepam loaded SLN were further examined for the physical stability under accelerated condition. The heating and cooling cycle was performed under storing the samples at 4ºC for 48 hours and at 45ºC for 48 hours for 6 cycles. On exposure of accelerated condition, the white fluid dispersion became yellowish fluid dispersion. The discoloration has been reported in diazepam solution after kept in room temperature. Shah (1991) developed parenteral formulation of diazepam and found that a yellow discoloration occurred during 15 days of storage at room temperature. However, there was no measure loss in diazepam content due to this change. From the data obtained, The significant difference in mean particle size was found after storage under stress condition in both formulations ($p<0.05$, t-test). In addition, the particle size in range of micrometer and particle size distribution obviously increased as shown in Table 28. The relatively increased distribution of particle size was not desirable for good stability. This result might be attributed to the fluctuation of temperature. At cooling interval, temperature in refrigerator was indicative of highly restricted mobility of the solid lipid particles. The energy of system reduced. When the particle came close to adjacent one, there was insufficient energy to repel itself. During elevated temperature at 45ºC, tween 80 might diffuse from interface as a result of higher solubility in aqueous phase. The less of stabilizer adhering to the solid lipids led to particle aggregated and brought about larger particle. As can be seen from Table 29, the accelerated condition has also influenced to pH and zeta potential. The increase in negativity of zeta potential was accompanied with the reduction of pH. This result suggested that the fluctuation of temperature played a important factor to which affected hydrolysis of glycerol behenate. While the osmolality was relatively constant since the osmotic agent was not added in system.

Table 28 Particle sizes of 0.3% and 0.5% diazepam loaded SLN after autoclaving analyzed by PCS and LD (a) before storage under accelerated condition, (b) after storage under accelerated condition

Formulation	PCS		LD						
	Mean particle size (nm)		Volume particle size (µm)				% particle larger than		
	z value	PI	D(v,0.1)	D(v,0.5)	D(v,0.9)	uniformity	1 µm	5 µm	10 µm
0.3 DI + 5 GB + 4 TW80 (a)	148.6	0.161	0.09	0.24	0.76	6.28	8.90	5.94	4.17
0.3 DI + 5 GB + 4 TW80 (b)	258.3	0.213	0.20	0.34	2.05	6.67	12.28	6.39	4.36
0.5 DI + 5 GB + 4 TW80 (a)	157.5	0.148	0.22	0.36	0.77	5.99	8.81	5.28	3.90
0.5 DI + 5 GB + 4 TW80 (b)	348.5	0.233	0.21	0.39	17.72	23.05	23.96	16.76	12.61

สถาบันวิทยบริการ
จุฬาลงกรณ์มหาวิทยาลัย

Table 29 Effect of accelerated condition on pH, zeta potential and osmolality in formulation of 0.3% and 0.5% diazepam loaded SLN (a) before storage under accelerated condition and (b) after storage under accelerated condition

Formulation	After autoclaving		
	pH	Zeta potential (millivolt)	Osmolality (Osmol/kg)
0.3 DI + 5 GB + 4 TW 80 (a)	5.20 ± 0.04	-21.2 ± 1.7	0.022 ± 0.005
0.3 DI + 5 GB + 4 TW 80 (b)	4.90 ± 0.07	-23.8 ± 0.8	0.024 ± 0.002
0.5 DI + 5 GB + 4 TW 80 (a)	5.22 ± 0.07	-23.1 ± 0.8	0.025 ± 0.002
0.5 DI + 5 GB + 4 TW 80 (b)	4.99 ± 0.02	-26.0 ± 0.6	0.023 ± 0.001

6 Tween 20

To compare carbon chain length of fatty acid on polyoxyethylene sorbitan monoester, tween 20 was selected to compare with tween 80. The preparations of SLN containing tween 20 were prepared under pressure of 20,000 psi and 5 cycles.

6.1 particle size measurement

The physical appearances of SLN containing 0.5-5% tween 20 are shown in Table 30. Their particle sizes after autoclaving are presented in Table 31. Precipitation occurred in formulation of 5% glycerol behenate containing 0.5%, 3%, 4% and 5% after autoclaving. Therefore, the particle size analysis could not be determined by PCS due to limitation of instrument. As illustrated in Table 31, the bulk populations in such formulations were mostly in micrometer size range. Since PCS covered a size range from a few nanometer to approximately 3 μm. Hence, particle size of those formulations could be determined only LD.

Table 30 The physical appearances of SLN containing various amounts of tween 20

Formulation	Physical appearances	
	Before autoclaving	After autoclaving
5 GB + 0.5 TW 20	●White fluid dispersion	●White fluid dispersion ●Precipitation ●Gel formation after 2 months storage
5 GB + 1 TW 20	●White fluid dispersion	●White fluid dispersion ●Gel formation after 4 months storage
5 GB + 2 TW 20	●White fluid dispersion	●White fluid dispersion ●Gel formation after 5 months storage
5 GB + 3 TW 20	●White fluid dispersion	●Precipitation within 24 hours after storage
5 GB + 4 TW 20	●White fluid dispersion	●Precipitation within 24 hours after storage
5 GB + 5 TW 20	●White fluid dispersion	●Coalescence ●Precipitation

Table 31 Particle sizes of SLN containing 0.5–5 % tween 20 after autoclaving analyzed by PCS and LD

Formulation	PCS		LD						
	Mean particle size (nm)		Volume particle size (µm)				% particle larger than		
	z value	PI	D(v,0.1)	D(v,0.5)	D(v,0.9)	uniformity	1 µm	5 µm	10 µm
5 GB + 0.5 TW 20	†	†	0.24	0.85	14.42	7.19	45.76	21.41	13.43
5 GB + 1 TW 20	233.8	0.31	0.21	0.37	0.84	5.53	7.49	4.11	3.51
5 GB + 2 TW 20	185.5	0.12	0.21	0.34	11.40	54.38	12.55	10.96	10.17
5 GB + 3 TW 20	†	†	0.44	2.13	4.95	0.87	74.09	9.72	1.09
5 GB + 4 TW 20	†	†	0.28	1.88	28.58	5.25	56.64	41.89	31.20
5 GB + 5 TW 20	†	†	0.33	8.74	65.90	2.40	71.48	57.48	47.60

† - not determined

สถาบันวิทยบริการ
จุฬาลงกรณ์มหาวิทยาลัย

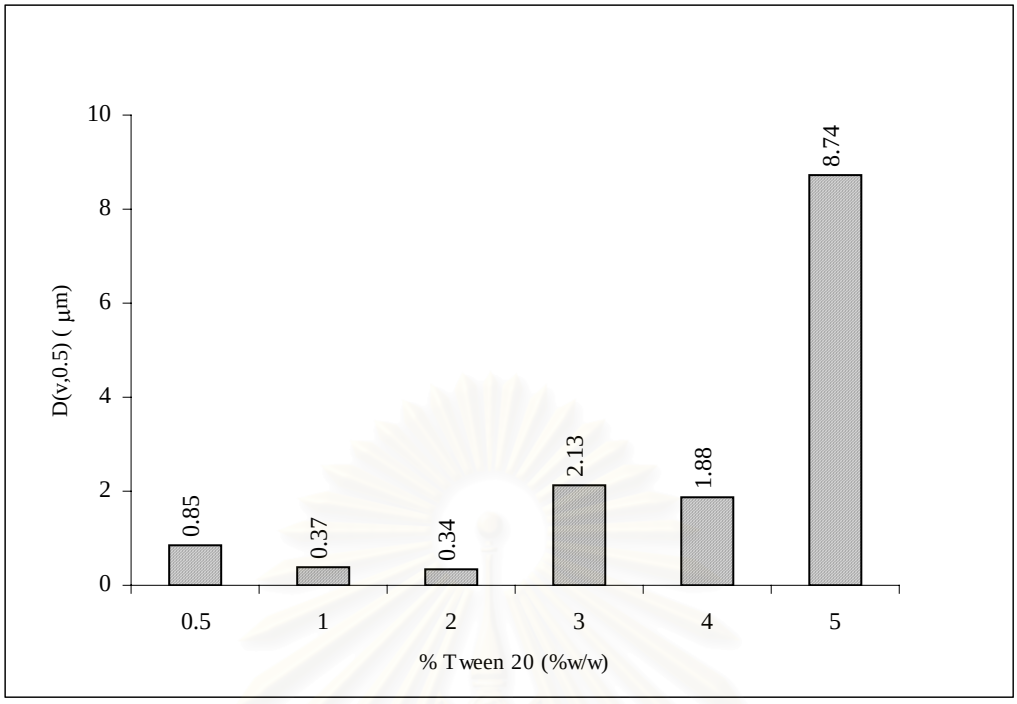

Figure 50 Effect of tween 20 concentration on the particle size of SLN containing 5% glycerol behenate analyzed by LD

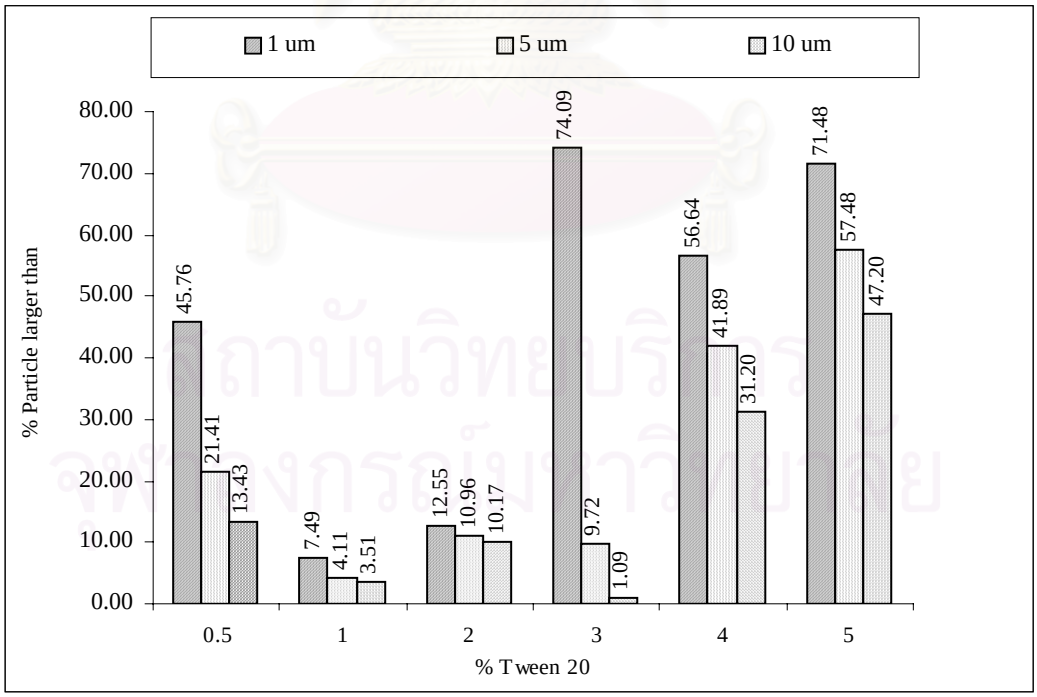

Figure 51 Effect of tween 20 concentration on the percentage of particle larger than 1, 5, 10 µm of SLN containing 5% glycerol behenate analyzed by LD

The formulations which consisted of 1% and 2% tween 20 appeared to be suitable concentrations to prepare SLN in nanometer size range. However, Gel formation occurred within 5 months in both formulations which kept at room temperature and light protection. Unlike tween 80, SLN containing tween 20 obviously displayed instabilities after autoclaving. This difference might attributed to higher HLB value of tween 20 than that of tween 80 which resulted in less of the affinity of tween 20 to solid lipids (Wade and Weller, 1994). The less adhering of tween 20 on solid lipids led to less surface coverage. With incomplete coverage interface, particle aggregation occurred in formulation of SLN containing tween 20 and resulting in coalescence, precipitation and gel formation. Furthermore, it was likely to ascribe that smaller molecule of tween 20 affected instabilities of SLN after autoclaving. Tween 20 could easily diffuse from interface of solid lipids and aqueous phase during autoclaving. Surfactant preferred to solubilize in aqueous phase. Tween 20, therefore, could not reabsorb to the surface of solid lipids and caused instabilities after autoclaving.

6.2 Zeta potential, pH and osmolality

The pH and osmolality of dispersions of SLN containing tween 20 were slightly increased when increasing the concentration of tween 20 as presented in Table 32. The preparations of SLN containing tween 20 showed lower pH and higher osmolality than those containing tween 80 after autoclaving at the same concentration. The lower pH might be attributed to higher free fatty acids as a result of hydrolysis of glycerol behenate. The higher osmolality of preparations containing tween 20 than those containing tween 80 could be also explained from the higher HLB value of tween 20. Tween 20 in favor of aqueous could be more soluble in aqueous phase and increased osmotic pressure than tween 80. It was apparently that the addition of tween 20 affected on zeta potential of SLN. Increasing the concentration of tween 20 could reduce negativity of zeta potential that was similar to SLN containing tween 80. It was possible to explain that the adsorption of alkyl chain of tween 20 onto a hydrophobic portion of the solid lipid surface as a hydrophobic effect and also the association of the ethylene oxide groups with some polar groups at the surface probably by hydrogen bonding. The

polar group of particles was decreased, therefore the negativity of zeta potential decreased (Kayes, 1977).

Table 32 Effect of tween 20 on pH, zeta potential and osmolality in SLN containing 5% glycerol behenate

Formulation	**After autoclaving**		
	pH	**Zeta potential** (millivolt)	**Osmolality** (Osmol/kg)
5 GB + 0.5 TW 20	4.57 ± 0.06	-28.8 ± 2.5	0.007 ± 0.001
5 GB + 1 TW 20	4.67 ± 0.03	-29.4 ± 1.3	0.013 ± 0.004
5 GB + 2 TW 20	4.71 ± 0.01	-28.1 ± 2.0	0.017 ± 0.002
5 GB + 3 TW 20	4.66 ± 0.05	-23.5 ± 3.3	0.024 ± 0.001
5 GB + 4 TW 20	4.72 ± 0.14	-21.5 ± 1.1	0.030 ± 0.002
5 GB + 5 TW 20	4.80 ± 0.03	-21.0 ± 0.1	0.040 ± 0.001

6.3 Diazepam loaded SLN

The preparation of 5% glycerol behenate containing 1% tween 20 was chosen to load diazepam because of the lowest percentage of particle larger than 5 μm. However, gel formation occurred within 24 hours in both formulations of 0.3% and 0.5% diazepam loaded SLN. In regard to this result, it was probable to conclude that the addition of diazepam into SLN could accelerate the physical instability of SLN containing tween 20.

สถาบันวิทยบริการ
จุฬาลงกรณ์มหาวิทยาลัย

CHAPTER V
CONCLUSIONS

Solid lipid nanoparticle (SLN) could be prepared by hot homogenization and showed mean particle sizes in the colloidal size range. The method consisted of two processes; preparing the pre-emulsion using high speed homogenizer and reducing the particle size by high pressure homogenizer. The condition was performed initially using homogenizing time for 10 minutes, pressure at 10,000 psi and 5 recycle times. The data obtained indicated that type and concentration seem to be the crucial factor for producing stable autoclaved SLN. According to the results, neither poloxamers nor lecithins could form stable SLN after autoclaving. The poloxamer 188 and poloxamer 407 provided no sufficient steric stabilization against coalescence after autoclaving. The gel formation in formulation stabilized by poloxamer 407 occurred slower than that stabilized by poloxamer 188. The reasons might attribute to higher molecular weight and more propylene oxide portion in poloxamer 407. This resulted in higher strength of mechanical barrier which could retard instability but could not prevent. Using Phospholipon®80, the phase separation was found after autoclaving while gel formation occurred in preparations which were not autoclaved. Whilst SLN could not be prepared using Epikuron®200 by this method. The results suggested that lecithins had no sufficient both steric and electrostatic stabilization. The dispersions of SLN prepared using tween 20 and tween 80 were white fluid dispersions. Unlike tween 80, SLN containing tween 20 obviously displayed instabilities i.e. coalescence, precipitation and gel formation after autoclaving. This was likely to ascribe that the less adhering of tween 20 on the solid lipids led to incomplete coverage at interface and brought about particle aggregation after exposure high temperature. Whereas tween 80 could stabilize SLN via steric stabilization. Tween 80 in concentration of 4% was found to yield the smallest particle using 5% glycerol behenate as lipid matrix. The mean particle sizes of such formulation both before and after autoclaving were 118.4 and 122.0 nm, respectively, which were insignificantly different ($p>0.05$, t-test). There was no particle of larger than 5 μm which indicated that such formulation was suitable for parenteral applications. The particle size, pH and zeta potential were affected by the amounts of tween 80 and glycerol behenate, while the osmolality value was less influenced. The pH of all preparations decreased and zeta

potential tended to negatively increase after autoclaving. The results obtained can conclude that hydrolysis of glycerol behenate affected pH and zeta potential. Incorporation of diazepam showed high entrapment efficiency. Diazepam loaded SLN exhibited slow release for more than 60 hours. Diazepam diffused from saturated solution through dialysis membrane within 4 hours. These results pointed out that lipid matrix could control diazepam release. The release kinetics of all preparations followed Higuchi model. However, it was found that mean particle sizes of 0.1-0.9% diazepam loaded SLN were larger than those of drug free preparation before and after autoclaving analyzed by PCS. There were large amounts of microparticles at homogenizing condition used. The possible explanation was probable that diazepam had a large particle size leading to particle aggregation. The alternative reason was that the hardness of diazepam loaded into system might require higher mechanical energy input to reduce particle size. Therefore, three levels of both homogenization pressure and cycle of homogenization were compared to select the most appropriate condition. Two-way ANOVA revealed that the content of microparticles was prominently depended upon pressure of homogenization. The evaluation of homogenization process found that the pressure of 20,000 psi with 5 recycle times was the optimal condition for reducing the particle size in diazepam loaded SLN. The data demonstrated that particles of smaller than 103.58 and 222.28 μm could be achieved in formulations of 0.3% and 0.5% diazepam loaded SLN, respectively. This implied that both formulations could be easily drawn into syringe through a hypodermic needle. It was conceivably concluded that the obtained diazepam loaded SLN prepared for parenteral administrations were more appropriate for intramuscular and subcutaneous injection. The IR spectra showed that there was no interaction between diazepam and other components. The DSC thermograms and powder X-ray diffractograms indicated that diazepam in lipid matrix was in either molecularly dispersed or amorphous form.

REFERENCES

Ahlin, A., Kristl, J., Šentjurc, M., Štrancar, J. Pečar, S. 2000. Influence of spin probe structure on its distribution in SLN dispersions. International Journal of Pharmaceutics 196: 241-244.

Akers, M. J., Fites, A. L., and Robinson, R. L. 1987. Formulation design and development of parenteral suspensions. Journal of Parenteral Sciences and Technology Vol. 41, No. 3: 88-96.

Almeida, A. J., Runge, S., and Müller, R. H. 1997. Peptide-loaded solid lipid nanoparticles (SLN): influence of production parameter. International Journal of Pharmaceutics 149: 255-265.

Attwood, D., and Florence, A. T. 1983. Emulsion. Surfactant systems: Their chemistry, pharmacy and biology, pp. 470-471. London: Chapman and Hall.

Avestin. 2000. EmulsiFlex-C5[online]. Available from: http://www.avestin.com [2002, Feb 1].

Bocca, C. Caputo, R., Cavalli, L., Gabrial, L., Miglietta, A., and Gasco, M. R. 1998. Phagocytic uptake of fluorescent stealth and non-stealth solid lipid nanoparticles. International Journal of Pharmaceutics 175: 185-193.

Brandl, M. 1998. High-pressure homogenization techniques for the production of liposome dispersions. In R. H. Müller, S. Benita and B. H. L. Böhm (eds.), Emulsions and Nanosuspensions for the Formulation of Poorly Soluble Drugs, pp. 267-294. Stuttgart: Medpharm.

British Pharmacopoeia Commission. 1993. British Pharmacopoeia 1993. Volume II, p. A197. London: HMSO.

Bugay D. E., and Findlay W. P., eds. 1999. Pharmaceutical exipients: characterization by IR, Raman and NMR spectroscopy, pp. 264-265. London: Marcel Dekker.

Bunjes, H., Siekmann, B., and Westesen, K., 1998. Emulsions of supercooled melts – A novel drug delivery system. In S. Benita (ed.), Submicron Emulsions in Drug Targeting and Delivery, pp. 205-218. Australia: Harwood academic publishers.

Bunjes, H., Westesen, K., and Koch, M. H. J. 1996. Crystallization tendency and polymorphic transitions in triglyceride nanoparticles. International Journal of Pharmaceutics 129: 159-173.

Byrn, S. R., Pfeiffer, R. R., and Stowell, J. G., eds. 1999. The X-ray powder diffraction method. Solid-State Chemistry of Drugs, 2nd edition, pp. 59-67, 81-90, 111-118. West Lafayette, SSCI.

Cavalli, R., Caputo, O., and Gasco, M. R. 2000. Preparation and characterization of solid lipid nanospheres containing paclitaxel. European Journal of Pharmaceutical Sciences 10: 305-309.

Cavalli, R., Caputo, O., Carlotti, M. E., Trotta, M., Scarnecchia, C., and Gasco, M. R. 1997. Sterilization and freeze-drying of drug-free and drug-loaded solid lipid nanoparticles. International Journal of Pharmaceutics 148: 47-54.

Cavalli, R., Gasco, M., Barresi, A. A. and Rovero, G. 2001. Evaporative drying of aqueous dispersions of solid lipid nanoparticles. Drug Development and Industrial Pharmacy 27(9): 919-924.

Cavalli, R., Marengo, E., and Rodriguez, M. R. 1996. Effect of some experimental factors on the production process of solid lipid nanoparticles. European Journal of Pharmaceutics and Biopharmaceutics 43(2): 110-115.

Cavalli, R., Morel, S. Gasco, M. R., Chetoni, P., Saettone, M. F. 1995. Preparation and evaluation *in vitro* of colloidal lipospheres containing pilocarpine as ion pair. International Journal of Pharmaceutics 117: 243-246.

Cavalli, R., Peira, E., Caputo, O., and Gasco, M. R. 1999. Solid lipid nanoparticle as carriers of hydrocortisone and progesterone complexes with β-cyclodextrins. International Journal of Pharmaceutics 182: 59-69.

Chansiri, G., Lyons, R. T., Patel, M. V., and Hem, S. T. 1999. Effect of surface charge on the stability of oil/water emulsions during steam sterilization. Journal of Pharmaceutical Sciences 88: 454-458.

Clas S-D., Dalton C. R., and Hancock, B. C. 1999. Differential scanning calorimetry: applications in drug development. Pharmaceutical Science and Technology Today Vol. 2, No.8: 311-320.

Costa, P., and Lobo, J. 2001. Modeling and comparison of dissolution profiles. European Journal of Pharmaceutical Sciences 13: 123-133.

Danisco, 2001. Ingredients[online]. Available from: http://www.danisco.com[2002, Feb 14].

Dolley, C., ed. 1999. Diazepam. Therapeutic drug, 2nd edition, Vol. 1, pp. D80-84. Edinburgh: Churchill Livingstone.

Domb, A. J. 1993. Lipospheres for controlled delivery of substances. United States Patent 5,188,837.

Duro, R., Gómez-Amoza, J. L., Martínez-Pacheco, R., Souto, C., Concheiro, A. 1998. Adsorption of polysorbate 80 on pyrentel pamoate: effects on suspension stability. International Journal of Pharmaceutics 165: 211-216.

Eastley, R. J., Fell, D., and Smith, G. 1986. A comparative study of diazepam with sustained-release diazepam as oral premedication in minor gynaecological surgery. Current Medical Research and Opinion Vol. 10, No. 4: 235-240.

Eldem, T., Speiser, P., and Altorfer, H. 1991. Polymorphic behavior of spayed lipid micropellets and its evaluation by differntial scanning calorimetry and scanning electron microscopy. Pharmaceutical Research Vol. 8, No. 2: 178-184.

Eldem, T., Speiser, P., and Hincal, A. 1991. Optimization of spray-dried and -congealed lipid micropellettes and characterization of their surface morphology by scanning electron microscopy. Pharmaceutical Research Vol. 8, No. 1: 47-54.

Florey, K., ed. 1972. Diazepam. Analytical Profiles of Drug Substance, Volume I, pp. 81-90. New York: Academic Press.

Floyd, A. G. 1999. Top ten considerations in the development of parenteral emulsions. Pharmaceutical Science and Technology Today Vol. 2, No.4: 134-143.

Floyd, A. G., and Jain, S. 1996. Injectable Emulsions and Suspensions. In H. A. Lieberman, M. M. Rieger, and G. S. Banker (eds.), Pharmaceutical Dosage Forms: Dispersed Systems, Vol. 2, second edition, revised and expanded, pp. 261-318. New York: Marcel Dekker.

Freitas, C. and Müller, R. H. 1998. Effect of light and temperature on zeta potential and physical stability in solid lipid nanoparticle (SLN^{TM}) dispersions. International Journal of Pharmaceutics 168: 221-229.

Freitas, C. and Müller, R. H. 1998. Spray-drying of solid lipid nanoparticles (SLN^{TM}). European Journal of Pharmaceutics and Biopharmaceutics 46: 145-151.

Freitas, C. and Müller, R. H. 1999. Correlation between long-term stability of solid lipid nanoparticles (SLN^{TM}) and crystallinity of the lipid phase. European Journal of Pharmaceutics and Biopharmaceutics 47: 125-132.

Fresenius, W. Huber, J. F. K., Pungor, E. Rechnitz, G. A., Simon, W. and West, Th. S. (eds.) 1989. Tables of spectral data for sturcture determination of organic compounds, 2nd edition, pp. I5-I280. London: Springer-Verlag.

Gasco, M. R. 1993. Method for producing solid lipid microspheres having a narrow size distribution. United States Patent 5,250,236.

Gustafon, J. H., Weissman, L., Weinfeld R. E., Holazo, A. A., Khoo. K-C., and Kaplan, S. A. 1981. Clinical bioavailability evaluation of a controlled release formulation of diazepam. Journal of Pharmacokinnetics and Biopharmaceutics Vol. 9, No. 6: 679-691.

Hashem, H., Phillips, N. C., and Tawashi, R. 1996. Evidence for phospholipid bilayer formation in solid lipid nanoparticles formulated with phospholipid and triglyceride. Pharmaceutical Research Vol. 3, No. 9: 1406-1410.

Heiati, H., Tawashi, R., Shivers, R. R., and Phillips, N. C. 1997. Solid lipid nanoparticles as drug carriers I. Incorporation and retention of the lipophilic product 3′-azido-3′-deoxythymidine palmitate. International Journal of Pharmaceutics 146: 123-131.

Herman, C. J., and Groves, M. J. 1992. Hydrolysis kinetics of phospholipids in thermally stressed intravenous lipid emulsion. Journal of Pharmacy and Pharmacology 44: 539-542.

Hulbert, M. K. 1995. Antianxiety agents. In B. R. Olin (ed.), Drug facts and comparisons, pp. 1369-1370. Missouri: A Wolters Kluwer Company.

Jahnke, S. 1998. The theory of high-pressure homogenization. In R. H. Müller, S. Benita, and B. H. L. Böhm (eds.), Emulsions and Nanosuspensions for the Formulation of Poorly Soluble Drugs, pp.177-200. Stuttgart: Medpharm.

Jenning, V., Gysler, A., Schäfer-Korting, M., and Gohla, S. H. 2000. Vitamin A loaded solid lipid nanoparticles for topical use: occlusive properties and drug targeting to the upper skin. European Journal of Pharmaceutics and Biopharmaceutics 49: 211-218.

Jenning, V., Schäfer-Korting, M., and Gohla, S. 2000. Vitamin A-loaded solid lipid nanoparticles for topical use: drug release properties. Journal of Controlled Release 66: 115-126.

Jenning, V., Thünemann, A. F., and Gohla, S. V. 2000. Characterisation of a novel solid lipid nanoparticles carrier system based on binary mixtures of liquid and solid lipids. International Journal of Pharmaceutics 199: 167-177.

Jones, A. R. 1999. Light scattering for particle characterization. Progress in energy and combustion science 25: 1-53.

Jumaa, M., and Müller, B. W. 1998. The effect of oil components and homogenization conditions on the physicochemical properties and stability of parenteral fat emulsions. International Journal of Pharmaceutics 168: 81-89.

Jumaa, M., and Müller, B. W. 1998. The stabilization of parenteral fat emulsion using nnon-ionic ABC copolymer surfactant. International Journal of Pharmaceutics 174: 29-37.

Kayes, J. B. 1977. Pharmaceutical suspensions: microelectrophoretic properties. Journal of Pharmacy and Pharmacology 29: 163-168.

Krause, K. P., and Müller, R. H. 2001. Production of aqueous shellac dispersions by high pressure homogenisation. International Journal of Pharmaceutics 223: 89-92.

Lippacher, A., Müller, R. H., and Mäder, K. 2000. Investigation on the viscoelastic properties of lipid based colloidal drug carriers. International Journal of Pharmaceutics 196: 227-230.

Levy, M. Y., and benita, S. 1989. Design and characterization of a submicron o/w emulsion of diazepam for parenteral use. International Journal of Pharmaceutics 54: 103-112.

Luck, J. S., Müller, B. W., and Müller, R. H. 1990. Inorganic suspension-interaction with salts and ionic surfactants. International Journal of Pharmaceutics 40: 229-235.

Lukowski, G., Kasbohm, J., Pflegel, P., Illing, A., and Wulff, H. Crystallographic investigation of cetylpalmitate solid lipid nanoparticles. International Journal of Pharmaceutics 196: 201-205.

Lundberg, B. 1992. Preparation of drug-carrier emulsions stabilized with phosphatidylcholine-surfactant mixtures. Journal of Pharmaceutical Sciences 83: 72-75.

Lund, W., ed. 1994. The Pharmaceutical Codex, Twelfth edition, pp. 830-835. London: The Pharmaceutical Press.

Lunn, G., and Schmuff, N., eds. 1997. Diazepam. HPLC methods for pharmaceutical analysis, pp. 458-485. New York, John Wiley & Sons, Inc.

Mastersizer reference manual, Instrumental manual. UK: Malvern instruments Ltd.

Mehnert, W., and Mäder, K. 2001. Solid lipid nanoparticles Production, characterization and applications. Advanced Drug Delivery Reviews 47: 165-196.

Montandon, A., Skreta, M., Riggenbach, H., and Ward, J. 1986. Comparison of controlled-release diazepam capsules and placebo in patients in general practice. Current Medical Research and Opinion Vol. 10, No. 1: 10-16.

Morel, S., Terreno, E., Ugazie, E., Aime, S., and Gasco, M. S. 1998. NMR relaxometric investigations of solid lipid nanoparticles (SLN) containing gadolinium (III) complexs. European Journal of Pharmaceutics and Biopharmaceutics 45: 157-163.

Morel, S., Ugazio, E., Cavalli, R., Gasco, M. R. 1996. Thymopentin in solid lipid nanoparticles. International Journal of Pharmaceutics 132: 259-261.

Mühlen, A., Mühlen, E., Niehus, H., and Mehnert, W. 1996. Atomic force microscopy studies of solid lipid nanoparticles. Pharmaceutical Research Vol. 13, No.9: 1411-1416.

Mühlen, A., Schwarz, C., and Mehnert, W. 1998. Solid lipid nanoparticles (SLN) for controlled drug delivery – Drug release and release mechanism. European Journal of Pharmaceutics and Biopharmaceutics 45: 149-155.

Müller, R. H., and Böhm, B. H. L. 1998. Nanosuspensions. In R. H. Müller, S. Benita and B. H. L. Böhm (eds.), Emulsions and Nanosuspensions for the Formulation of Poorly Soluble Drugs, pp. 149-174. Stuttgart: Medpharm.

Müller, R. H., Lippacher, A., and Gohla, S. 2000. Solid lipid nanoparticles (SLN) as a carrier system for the controlled release of drugs. In D. L. Wise (ed.), Handbook of Pharmaceutical Controlled Release Technology, pp. 377-391. New York: Marcel Dekker.

Müller, R. H., Maassen, S., Schwarz C., Mehnert. 1997. Solid lipid nanoparticles (SLN) as potential carrier for human use: interaction with human granulocytes. Journal of Controlled Release 47: 261-269.

Müller, R. H., Mäder, K., and Gohla, S. 2000. Solid lipid nanoparticles (SLN) for controlled drug delivery- a review of the state of the art. European Journal of Pharmaceutics and Biopharmaceutics 50: 161-177.

Müller, R. H., Mehnert, W., Lucks, J-S., Schwarz, C. Mühlen, A., Weyhers, H. Freitas, C., and Rühl, D. 1995. Solid lipid nanoparticles (SLN) - An alternative colloidal carrier system for controlled drug delivery. European Journal Pharmaceutics and Biopharmaceutics 41(1): 62-69.

Müller, R. H., Rühl, D., Runge, S., Schulze-Forster, K., and Mehnert, W. 1997. Cytotoxicity of solid lipid nanoparticles as a function of the lipid matrix and the surfactant. Pharmaceutical Research Vol. 14, No.4: 458-462.

Nema, S., Washkuhn R. J., and Brendel R. J. 1997. Exipients and their use in injectable products. PDA Journal of Pharmaceutical Science and Technology Vol. 51, No. 4: 166-171.

Observation of water-containing specimens SEM method, JEOL application note. Japan: JEOL.

Schöler, N., Hahn, H., Müller R. H., Liesenfeld, O. 2002. Effect of lipid matrix and size of solid lipid nanoparticles (SLN) on the viability and cytokine production of macrophages. International Journal of Pharmaceutics 231: 167-176.

Schöler, N., Olbrich, C., Tabatt, K., Müller R. H., Hahn, H., and Liesenfeld, O. 2001. Surfactant, but not the size of solid lipid nanoparticles (SLN) influences viability and cytokine production of macrophages. International Journal of Pharmaceutics 221: 57-67.

Schwarz, C., and Mehnert, W. 1997. Freeze-drying of drug-free and drug-loaded solid lipid nanoparticles. International Journal of Pharmaceutics 157: 171-179.

Schwarz, C. Mehnert, W., Lucks, J. S., and Müller R. H. 1994. Solid lipid nanoparticles (SLN) for controlled drug delivery. I Production, characterization and sterilization. Journal of Controlled Release 30: 83-96.

Senior, J. H. 2000. Rationale for sustained-release injectable products. In J. H. Senior and M. Radomsky (eds.), Sustained-release injectable products, pp. 1-11. Denver: Interpharm Press.

Shah, A. K. 1991. Physical, chemical, and bioavailability studies of parenteral diazepam formulations containing propylene glycol and polyethylene glycol 400. Drug Development and Industrial Pharmacy 17(12): 1635-1654.

Sheth, P. R., and Tossounian J. 1984. The hydrodynamically balanced system (HBS^{TM}): A novel drug delivery system for oral use. Drug Development and Industrial Pharmacy 10(2): 313-329.

Siekmann, B., and Westesen, K. 1996. Investigations on solid lipid nanoparticles prepared by precipitation ion o/w emulsions. European Journal Pharmaceutics and Biopharmaceutics 43(2): 104-109.

Siekmann, B., and Westesen, K. 1998. Submicron lipid suspensions (solid lipid nanoparticles) versus lipid nanoparticles: similarities and differences. Submicron Emulsions in Drug Targetting, In S. Benita (ed.), pp. 205-234. Australia: Harwood academic publishers.

Siekmann, B., and Westesen, K. 2001. Solid lipid particles, particles of bioactive agents and methods for the manufacturer and use thereof. United States Patent 6,207,178.

Sjöström, B., and Bergenståhl, B. 1992. Precipitation of submicron drug particles in lecithin-stabilized o/w emulsions I Model studies of the precipitation of cholesteryl acetate. International Journal of Pharmaceutics 88: 53-62.

Speiser, P. 1989. Lipid nano-pellets as exipient system for perorally administered drugs. United States Patent 4,880634.

Suryanarayanan, R. 1995. X-ray powder diffractometry. In H. G. Brittain (ed.), Physical Characterization of Pharmaceutical Solids, pp.187-221. New York: Marcel Dekker.

Swarbrick, J., Rubino, J. T., and Rubino, O. P. 2000. Coarse dispersions. In A. R. Gennaro (eds.), Remington: The Science and Practice of Pharmacy, Vol. 1, 20th edition, pp. 316-334. Philadelphia: Lippincott Williams & Wilkins.

Swartz, M. E., and Krull, I. S. 1998. Validation of chromatographic methods. Pharmaceutical Technology. March: 105-117.

Sznitowska, M., Gajewska, M., Janicki, S., Radwanska, A., and Lukowski, G. 2001. Bioavailability of diazepam from aqueous-organic solution, submicron emulsion and solid lipid nanoparticles after rectal administration in rabbits. European Journal Pharmaceutics and Biopharmaceutics 52: 159-163.

Terumo. 2001. Terumo's cannula internal diameter standard[online]. Available from: http://www.terumo.com[2002, Jan 7].

The Council of Europe. 2001 European Pharmacopoeia. 3rd edition, pp. 897-898. France: Strabourg.

The United States Pharmacopeial Convention, Inc. 2000. The United States Pharmacopeia 24/ The National Formulary 19: USP 24/NF 19. pp. 1920-1924, 2231-2232. Philadelphia: National Publishing.

Ugazio, E., Marengo, E., Pellizzaro, C., Coradini, D. Peiro, E., Daidone, M. G., and Gasco, M. R. 2001. The effect of formulation and concentration of cholesteryl butyrate solid lipid nanospheres (SLN) on NIH-H460 cell proliferation. European Journal Pharmaceutics and Biopharmaceutics 52: 197-202.

Wade, A., and Weller, P. J. 1994. Handbook of Pharmaceutical Exipients. 2nd edition. pp. 211-212, 267-268, 352-354. Washington: American Pharmaceutical Association.

Wade, A., ed. 1986. Clake's isolation and identification of drugs in pharmaceuticals, body fluids, and post-mortum. 2nd edition, pp. 526-527. London: The Pharmaceutical Press.

Wills, R. J. 1984. Pharmacokinetics of diazepam from a controlled release capsule in healthy elderly volunteers. Pharmacokinetics and Drug Disposition 5: 241-249.

Wiwat Pichayakorn. 1999. Solid lipid nanoparticles as colloidal drug carriers for parenteral administration. Master's Thesis, Department of Manufacturing Pharmacy, Graduate School, Chulalongkorn University.

Westesen, K., Bunjes, H., and Koch, M. H. J. 1997. Physicochemical characterization of lipid nanoparticles and evaluation of their drug loading capacity and sustained release potential. Journal of Controlled Release 48: 223-236.

Westesen, K., and Siekmann, B. 1996. Biodegradable Colloidal Drug Carrier Systems Based on Solid Lipids. In S. Benita (ed.), Microencapsulation Methods and Industrial Applications, pp. 214-258. The United States of America: Marcel Dekker.

Westesen, K., and Siekmann, B. 1997. Investigation of the gel formation of phospholipid stabilized solid lipid nanoparticles. International Journal of Pharmaceutics 151: 35-45.

Westesen, K., Siekmann, B., and Koch, M. H. J. 1993. Investigations on the physical state of lipid nanoparticles by synchrotron radiation X-ray diffraction. International Journal of Pharmaceutics 93: 189-199.

Yang, S. C., Lu, L. F., Cai, Y., Zhu, J. B., Liang, B. W., and Yang, C. Z. 1999. Body distribution in mice of intravenously injected camptothecin solid lipid nanoparticles and targeting effect on brain. Journal of Controlled Release 59: 299-307.

Yang, S., Zhu, J., Lu, Y., Liang, B., and Yang, C. 1999. Body distribution of camptothecin solid lipid nanoparticles after oral administration. Pharmaceutical Research Vol. 16, No. 5: 751-757.

Zara, G. P., Cavalli, R., Fundarò, A. Bargoni, A., Caputo, O., Gasco, M. R. 1999. Pharmacokinetics of doxorubicin incorporated in solid lipid nanoparticles (SLN). Pharmaceutical Research 44: 281-286.

Zhang, Q., Yie, G., Li, Y, Yang, Q. and Nagai, T. 2000. Studies on the cyclosporin A loaded stearic acid nanoparticles. International Journal of Pharmaceutics 200: 153-159.

Zimmermann, E., Müller, R. H., and Mäder, K. 2000. Influence of different parameters on reconstitution of lyophilized SLN. International Journal of Pharmaceutics 151: 35-45.

สถาบันวิทยบริการ
จุฬาลงกรณ์มหาวิทยาลัย

APPENDICES

สถาบันวิทยบริการ
จุฬาลงกรณ์มหาวิทยาลัย

APPENDIX A

DETAILS OF SOME SUBSTANCES

1. Diazepam (Lund, 1994, Florey, 1992)

1.1 Chemical name

: 7-Chloro-1,3-dihydro-1-methyl-5-phenyl-1,4-benzodiazepin-2-one,
7-chloro-1,3-dihydro-1-methyl-5-phenyl-2*H*-1,4-benzodiazepin-2-one

1.2 Molecular formula

: $C_{16}H_{13}ClN_2O$

1.3 Molecular weight

: 284.75

1.4 Chemical structure

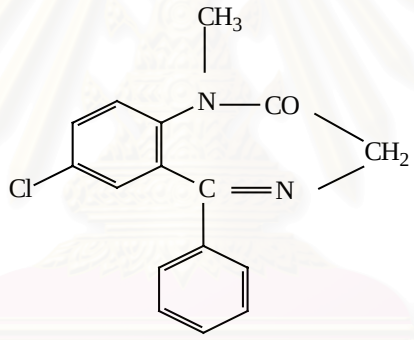

1.5 Appearance

: Off-white to yellow, practically odorless, crystalline power

1.6 Solubility

: Approximate solubility data obtained at room temperature

Solvent	Solubility (mg/ml)
Water	0.05
95% Ethanol	41
Methanol	49
Chloroform	>500

1.7 Typical properties

: Dissociation constant (pK_a) = 3.4

: Partition coefficient (Log *P* octanol/pH7.4) = 2.7

: Melting range = 129-135˚C

2 Glycerol behenate (Compritol® 888 ATO) (The Council of Europe, 2001, Lund, 1994)

2.1 Definition

Glycerol behenate is a mixture of diacylglycerols, mainly dibehenoylglycerol, together with variable quantities of mono and triacylglycerols. It contains 13.0 percent to 21 percent of monoacylglycerols, 40 percent to 60 percent of diacylglycerols and 21 percent to 35 percent of triglycerols, obtained by esterification of glycerol with behenic acid.

Composition of fatty acids

Examine by gas chromatography, the fatty acid fraction of the substance has the following composition:

- palmitic acid: not more than 3.0 percent
- stearic acid: not more than 5.0 percent
- arachidonic acid: not more than 10.0 percent
- behebic acid: not more than 83.0 percent
- lignoceric acid: not more than 3.0 percent
- erunic acid: not more than 3.0 percent

2.2 Chemical name

Glycerobehenate

Glycerol dibehenate

2.3 Molecular formula

$C_{69}H_{134}O_6$

2.4 Molecular weight

160.03

2.5 Structural formula

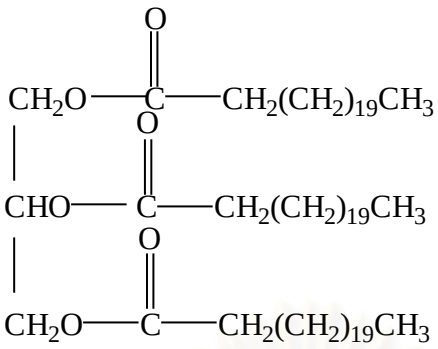

2.6 Appearance

Glycerol behenate is fine powder or white or almost white with a faint odor.

2.7 Solubility

Glycerol behenate is insoluble in water, soluble in methylene chloride and partly soluble in alcohol.

2.8 Typical properties

Melting range = 65-77˚C

Saponification value = 145-164

3 Poloxamer (Wade and Weller, 1994)

3.1 Chemical name

α-Hydro-ω-hydroxypoly(oxyethylene) poly(oxypropylene) poly(oxyethylene) block copolymer

3.2 Molecular formula

$HO(C_2H_4O)_a(C_3H_6O)_b(C_2H_4O)_aH$

3.3 Molecular weight

The poloxamer polyols are a series of closely related block copolymers of ethylene oxide and propylene oxide. Two grades are shown as following.

Poloxamer	Physical form	a	b	Average molecular weight
188	solid	80	27	7680-9510
407	solid	101	56	9840-14600

3.4 Appearance

Both poloxamer 188 and 407 are white-coloured, waxy, free flowing prilled granules or as cast solids.

3.5 Solubility

Both poloxamer 188 and 407 are freely soluble in water and 95% ethanol.

3.6 Typical properties

Poloxamer	Melting point (ºC)	HLB
188	52	29
407	56	22

3.7 Safety

Poloxamers are used in a variety of oral, parenteral and topical pharmaceutical formulations and are generally regarded as nontoxic and nonirritant materials. Poloxamers are not metabolized in body. There is no hemolysis of human blood cells observed over 18 hours at 25˚C, with 0.001-10% w/v poloxamer solution.

4 Soy lecithin (Wade and Weller, 1994)

4.1 Chemical name

The chemical nomenclature and CAS registry numbering of lecithin is complex. The commercially available lecithin, used in cosmetics, pharmaceuticals and food products, although a complex mixture of phospholipids and other materials, may be referred to in some literature sources as 1,2-diacyl-*sn*-glycero-3-phosphocoline (trivial chemical name, phosphatidylcholine) This material is the principal constituent of soy lecithin and has the same CAS registry number.

4.2 Empirical formula

Lecithin is a complex mixture of acetone-insoluble phosphatides, which consist chiefly of phosphatidylcholine, phosphatidylethanolamine, phosphatidylserine and phosphatidylinositol, combined with various amounts of other substances such as triglycerides, fatty acids and carbohydrates as separated from a crude vegetable oil source.

4.3 Empirical formula

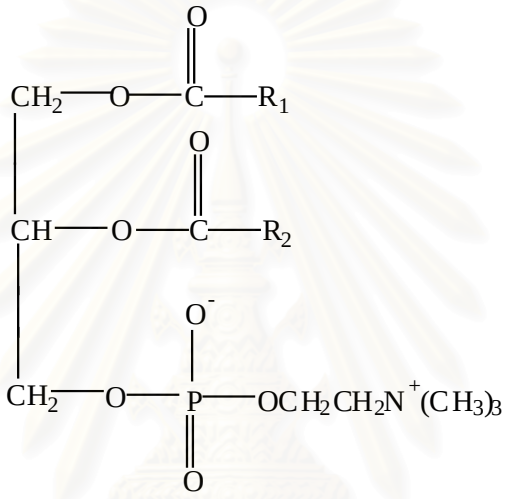

α-phosphatidylcholine

Where, R_1 and R_2 are fatty acids which may be different or identical.

The structure shows phosphatidylcholine, in its α form. In the β-form the phosphorus containing group and the R_2 group exchange positions.

Two commercially available soy lecithins used in this study are shown below.

Components	Phospholipon® 80	Epikuron® 200
Phosphatidylcholine	75.9	96.0
Lysophosphatidylcholine	3.6	2.1

4.4 Appearance

Lecithin is brown to light yellow, depending on whether it is unbleached or unbleached. It has practically no odor. It derived from vegetable sources has a

bland to nut-like taste, similar to soybean oil. In consistency, it may vary from plastic to fluid depending on the free fatty acid content.

4.5 Solubility

Lecithin is soluble in aliphatic and aromatic hydrocarbon, halogenated hydrocarbons, mineral oil and fatty acids. It is practically insoluble in cold vegetable and animal oils, polar solvents and water. When mixed with water however, lecithin hydrates to form emulsions.

4.6 Typical properties

Isoelectric point ≈ 3.5

HLB ≈ 7 (Epikuron 200)

4.7 Safety

Lecithin is a component of cell membranes and its therefore consumed as a normal part of the diet. Although excessive consumption may be harmful, oral doses of up to 80 gram daily have been used therapeutically in the treatment of tardive dyskinesia.

5 Tween 20 (Polysorbate 20)

5.1 Chemical name

Polyoxyethylene 20 laurate

Sorbitan monododecanoate

5.2 Molecular formula

$C_{58}H_{114}O_{26}$

5.3 Molecular weight

1128

ศูนย์วิทยทรัพยากร
จุฬาลงกรณ์มหาวิทยาลัย

5.4 Structural formula

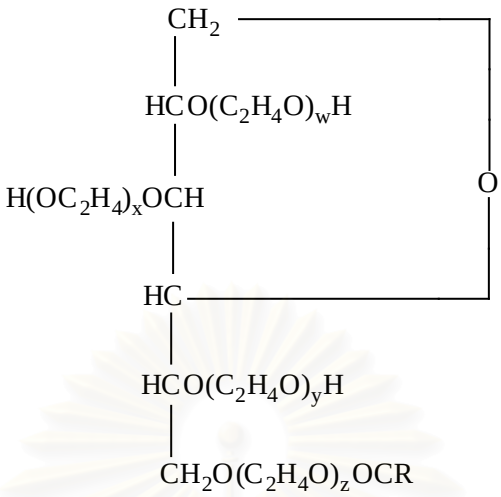

Polyoxyethylene sorbitan monoester

w+x+y+z = 20

R = lauric acid

5.5 Apperance

Tween 20 is yellow oily liquid.

5.6 Solubiltity

Tween 20 is miscible with water and alcohol.

5.7 Typical properties

HLB = 16.7

Specific gravity at 25˚C = 1.1

Viscosity = 400 mPa s

6 Tween 80 (Polysorbate 80)

6.1 Chemical name

Polyoxyethylene 20 oleate

Sorbitan mono-9-octadecanoate

6.2 Molecular formula

$C_{64}H_{124}O_{26}$

6.3 Molecular weight

1310

6.4 Structural formula

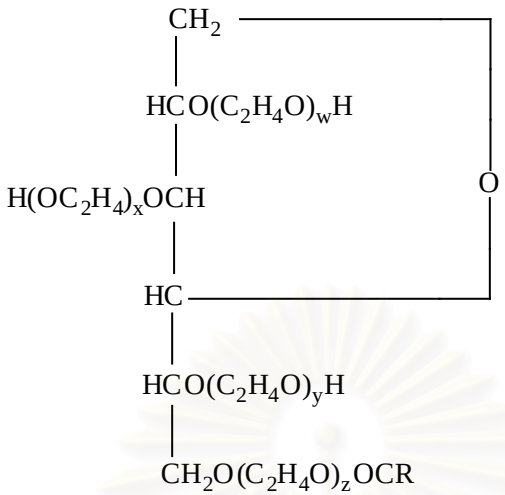

Polyoxyethylene sorbitan monoester

w+x+y+z = 20

R = oleic acid

6.5 Appearance

Tween 80 is yellow oily liquid.

6.6 Solubiltity

Tween 80 is miscible with water and alcohol.

6.7 Typical properties

HLB = 15.0

Specific gravity at 25˚C = 1.08

Viscosity = 425 mPa s

สถาบันวิทยบริการ
จุฬาลงกรณ์มหาวิทยาลัย

APPENDIX B
ANALYSIS OF DIAZEPAM

1 Solubility measurement

The solubility study of diazepam was carried out after equilibrium, approximately 24 hours, using HPLC technique. An aliquot was filtered through a 0.45 μm membrane filter. A portion of the filtrate was adequately diluted and analyzed using detector wavelength of 254 nm. Solubility of diazepam in deionized water and pH 7.4 phosphate buffer is shown in Table b1.

Table b1 Solubility of diazepam

Medium	Solubility (μg/ml) Mean ± SD
Deionized water	64.03 ± 1.27
pH 7.4 phosphate buffer solution	53.19 ± 1.13

2 Method for quantitative analysis of diazepam

2.1 UV-visible assay for diazepam analysis

The maximum absorption wavelength of diazepam in pH 7.4 phosphate buffer was 230 nm shown in Figure b1.

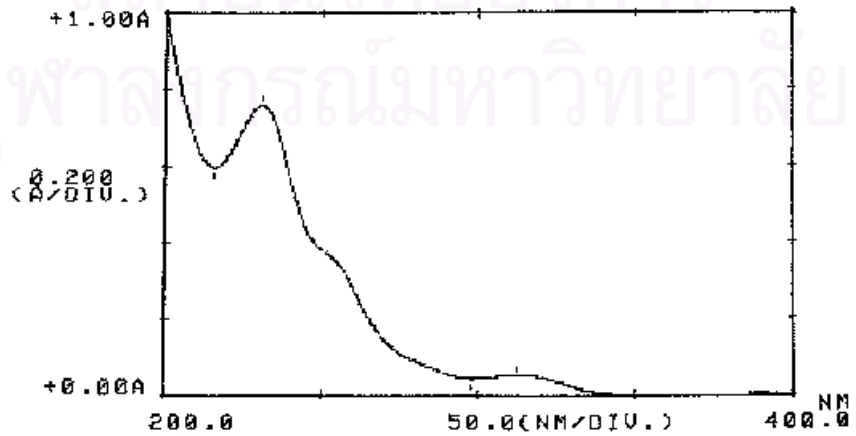

Figure b1 The UV spectrum of diazepam in pH 7.4 phosphate buffer solution

The data and standard curve of diazepam in pH 7.4 phosphate buffer are shown in Table b2 and Figure b2. A typical calibration curve showed a linear relationship between concentration of diazepam and maximum absorption wavelength.

Table b2 The relationship between absorbance and concentrations of diazepam in pH 7.4 phosphate buffer at wavelength of 230 nm

Concentration (μg/ml)	Absorbance					
	No. 1	No. 2	No. 3	Mean	SD	CV
0.5003	0.073	0.072	0.071	0.072	0.001	1.389
1.0005	0.132	0.127	0.129	0.129	0.003	1.946
2.0010	0.252	0.255	0.252	0.253	0.002	0.685
3.0015	0.367	0.371	0.375	0.371	0.004	1.078
4.0020	0.486	0.496	0.498	0.493	0.006	1.303
6.0030	0.744	0.734	0.737	0.738	0.005	0.695
8.0040	0.992	0.973	0.972	0.979	0.011	1.151

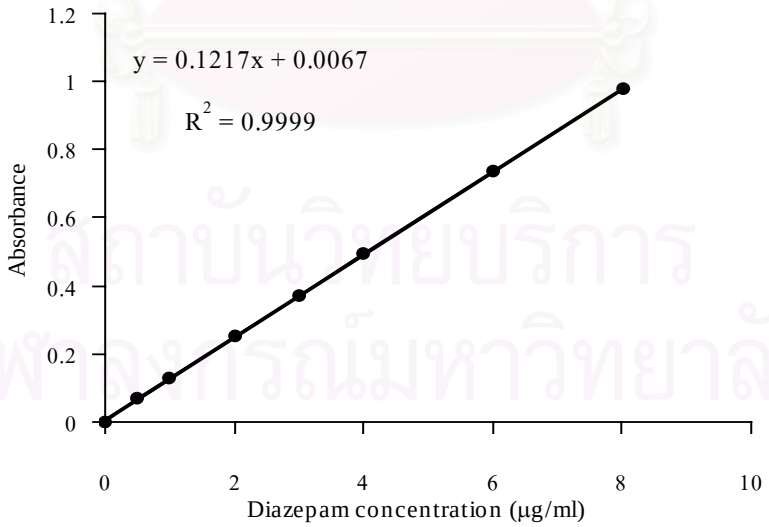

where y = absorbance

x = concentration of diazepam (μg/ml)

Figure b2 A representation of calibration curve of diazepam in pH 7.4 phosphate buffer at 230 nm

2.2 HPLC assay for diazepam analysis

2.2.1 Specificity

Under the chromatographic condition used, the peak of diazepam had to be completely separated from the peak of other components in the sample. Chromatograms of diazepam and lorazepam were eluted at 7.312-7.562 minutes and 5.225-5.295 minutes, respectively. Peaks of phosphate buffer and supernatant from the formulation of 5% glycerol behenate and tween 80 SLN appear in Figure b3. Their retention times were 3.215 and 3.108 minutes, respectively. Peak of tween 80 in mobile phase eluted with a retention time of 3.273 minutes. This indicated that diazepam was not interfered by other components. Hence, HPLC method could be used for analysis of diazepam using 70% MeOH and 30% H_2O at wavelength of 254 nm.

2.2.2 Accuracy

The accuracy of an analytical method is the closeness of test results obtained by that method to the true value. This experiment was conducted to verify that the method used for diazepam analysis was sufficiently accurate. The accuracy was calculated from the test results as percentage of analyte recovered by the assay (The United States Pharmacopeial Convention, 2000). The percentage of recovery within 2% of actual values was required. From the data in Table b3, the percentage of recovery in concentration of 1 µg/ml was out of this range. However, accuracy within 5% of the true value was still acceptable. Table b3 shows percent analytical recovery at each concentration diazepam. The data showed that the mean percent analytical recovery was very high (100.27%) with a low coefficient of variation (1.67%). This indicated that HPLC technique was accurate for quantitative analysis of diazepam in range of concentration studied.

2.2.3 Precision

The precision of an analytical method is the degree of agreement among individual test results when the method is applied repeatedly to multiple samplings of a homogeneous sample. The precision of an analytical method is usually

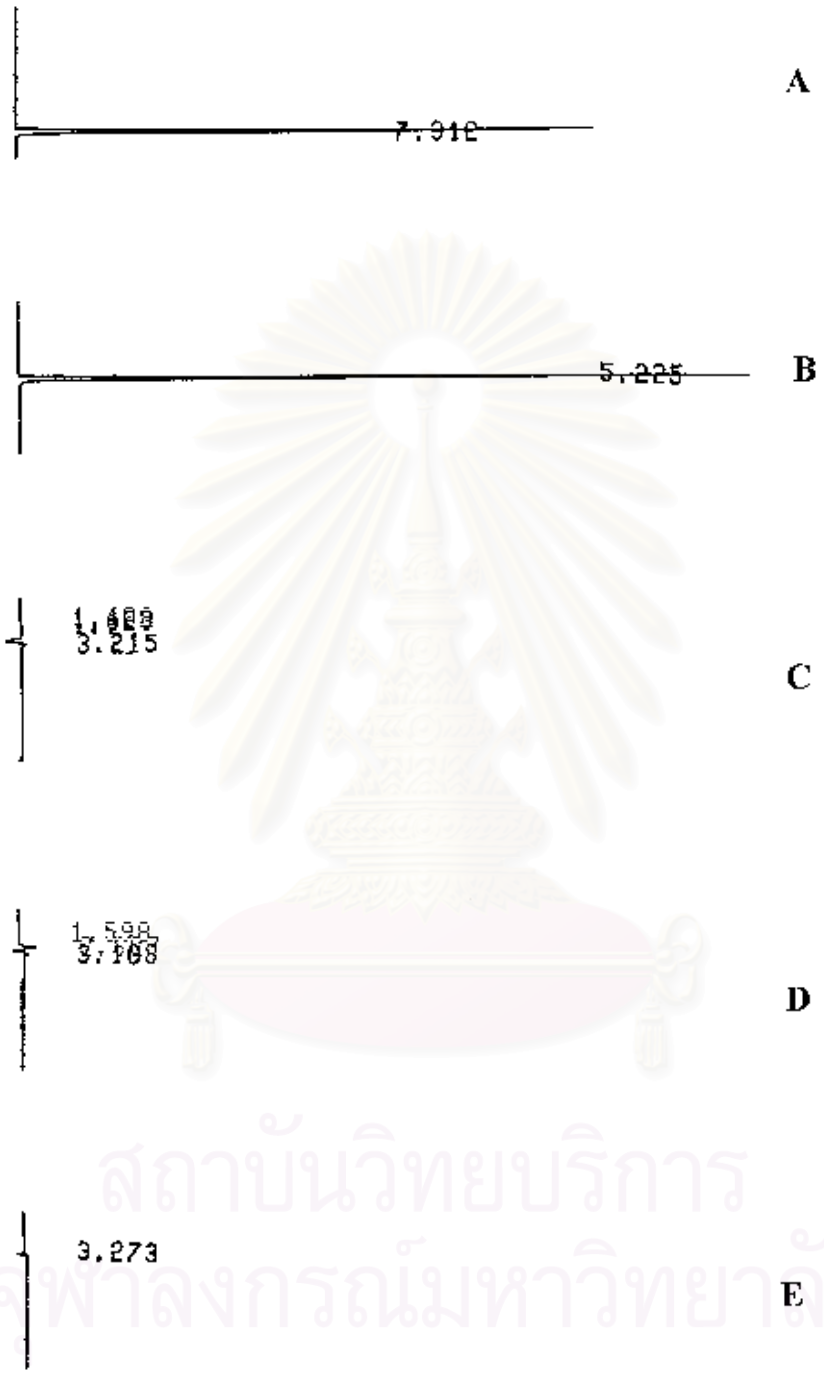

Figure b3 HPLC chromatograms of (A) diazepam (B) lorazepam (C) phosphate buffer (D) supernatant from the formulation of 5% glycerol behenate and tween 80 (E) tween 80

สถาบันวิทยบริการ
จุฬาลงกรณ์มหาวิทยาลัย

Table b3 Accuracy data of diazepam

Actual concentration (μg/ml)	Analytical concentration (μg/ml)	Percentage of recovery (%)	Mean of percent analytical recovery (%)
1	0.9652	96.52	97.45
	0.9712	97.12	
	0.9871	98.71	
5	5.0517	101.03	101.74
	5.1113	102.23	
	5.0984	101.97	
10	10.1302	101.30	101.10
	10.0855	100.86	
	10.1133	101.13	
20	20.2107	101.05	100.79
	20.0596	100.30	
	20.2058	101.03	
25	25.0089	100.04	99.91
	24.9423	97.77	
	24.9801	99.92	
			Mean = 100.02 SD = 1.67 CV = 1.67

สถาบันวิทยบริการ
จุฬาลงกรณ์มหาวิทยาลัย

expressed as the standard deviation or relative standard deviation (coefficient of variation) of series of measurements.

a) Within run precision

Table b4 illustrates the data of within run precision, a measure of degree of repeatability of analytical method under normal operating conditions. The coefficient of variation in range of 2% was required. From the data, coefficient of variation values were in the range of 0.1673-1.7704.

b) Between run precision

Table b5 shows the data of between run precision. Between run precision referred to use analytical procedure on different days. All coefficient of variation values were in range of 0.4034–1.7522. This indicated that the HPLC method used was precise for quantitative analysis of diazepam concentrations in range studied.

2.2.4 Linearity

The linearity of an analytical method is its ability to elicit test results that are directly proportional to the concentration of analyte samples within given range.

a) Calibration curve of diazepam ranging from 1 to 25 μg/ml

The chromatograms of standard solutions and data of calibration curve are shown in Figure b4 and Table b6, respectively. Figure b5 shows that the relationship between peak area ratios and diazepam concentration is linear with coefficient of determination (R^2) value of 1. The result indicated that the HPLC technique was acceptable for quantitative analysis of diazepam solutions in range studied.

b) Calibration curve of diazepam ranging from 50 to 1,000 ng/ml

Data for the calibration curve of diazepam in range of 50-1,000 ng/ml are shown in Table b7. The chromatograms of standard solutions and calibration curve are shown in Figure b6 and b7, respectively. Linear regression was performed with coefficient of determination (R^2) value of 1.

Table b4 Data of within run precision of diazepam assayed by HPLC method

Concentration (μg/ml)	**Peak area ratio**			Mean	SD	%CV
	No. 1	No. 2	No. 3			
1	0.1037	0.1071	0.1041	0.1050	0.0019	1.7704
5	0.5177	0.5084	0.5112	0.5124	0.0048	0.9311
10	1.0055	0.9905	0.9926	0.9962	0.0081	0.8153
20	2.0010	2.0008	2.0067	2.0028	0.0034	0.1673
25	2.5167	2.5275	2.5102	2.5181	0.0081	0.3470

Table b5 Data of between run precision of diazepam assayed by HPLC method

Concentration (μg/ml)	**Peak area ratio**			Mean	SD	%CV
	Day 1	Day 2	Day 3			
1	0.1078	0.1050	0.1043	0.1057	0.0019	1.7502
5	0.5215	0.5124	0.5254	0.5198	0.0067	1.2835
10	1.0267	0.9962	1.0212	1.0147	0.0163	1.6020
20	2.0377	2.0028	2.0243	2.0216	0.0167	0.8709
25	2.5224	2.5181	2.5375	2.5260	0.0102	0.4034

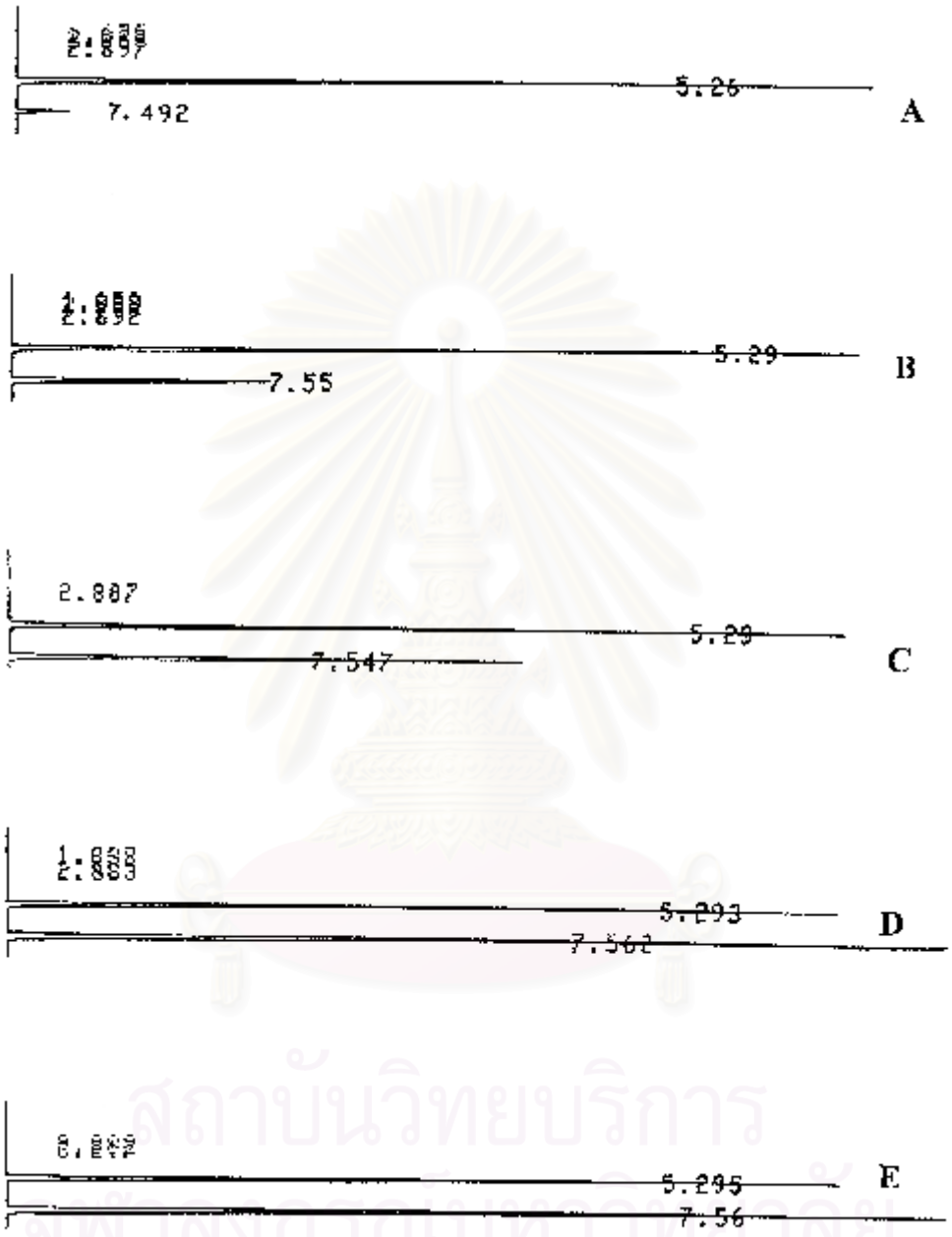

Figure b4 HPLC chromatograms of the standard solutions of diazepam and its internal standard in range of 1-25 μg/ml

Table b6 Data for a calibration curve of standard solutions of diazepam ranging from 1 to 25 μg/ml

Actual concentration (μg/ml)	**Peak area raio of diazepam to lorazepam**
1	0.1057
5	0.5198
10	1.0147
20	2.0216
25	2.5260

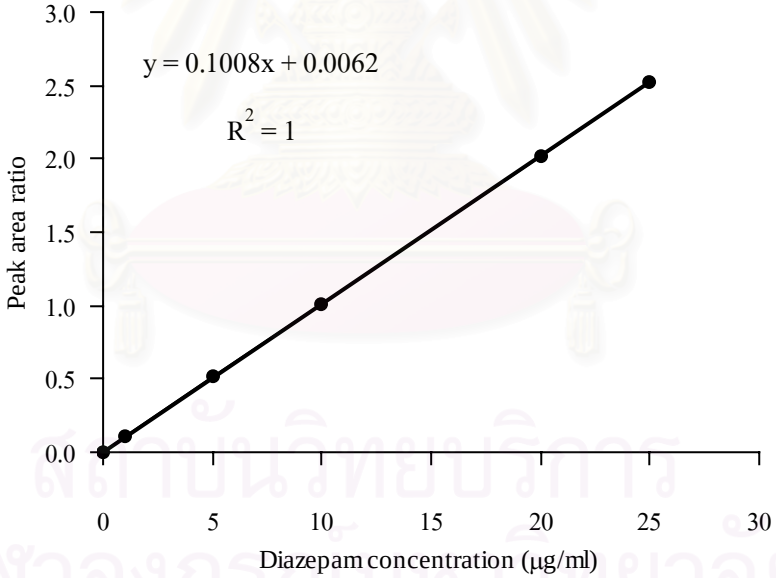

where y = peak area ratio

x = concentration of diazepam (μg/ml)

Figure b5 A representation of calibration curve of standard solutions of diazepam ranging from 1 to 25 μg/ml

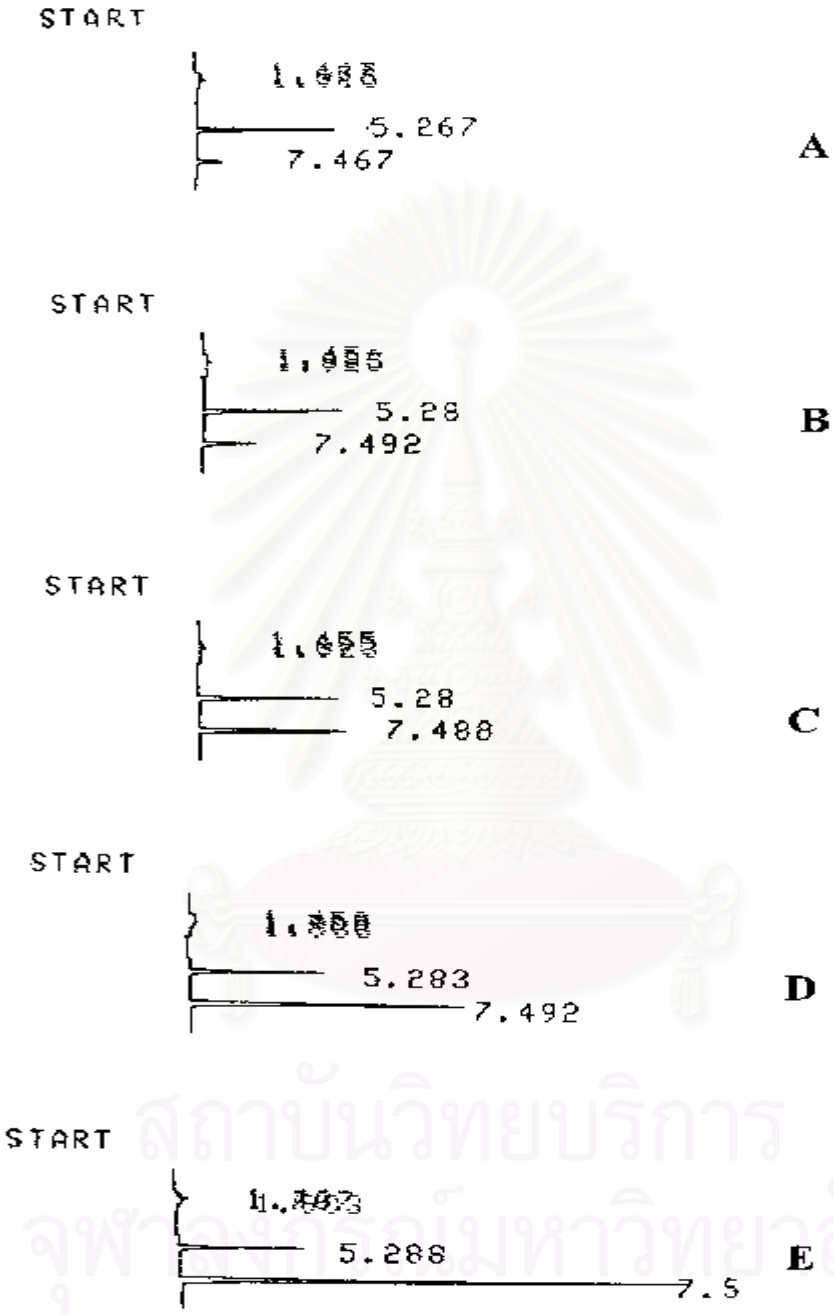

Figure b6 HPLC chromatograms of the standard solutions of diazepam and its internal standard ranging from 50 to 1,000 ng/ml

สถาบันวิทยบริการ
จุฬาลงกรณ์มหาวิทยาลัย

Table b7 Data for a calibration curve of standard solutions of diazepam ranging from 50 to 1,000 ng/ml

Actual concentration (ng/ml)	**Peak area raio of diazepam to lorazepam**
50	0.2716
100	0.5191
250	1.2961
500	2.5508
1,000	5.0905

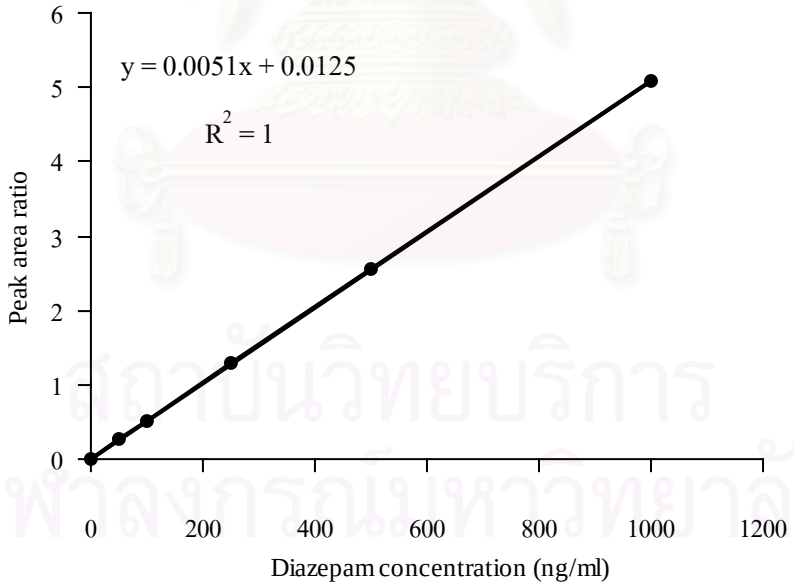

where y = peak area ratio

x = concentration of diazepam (ng/ml)

Figure b7 A representation of calibration curve of standard solutions of diazepam ranging from 50 to 1,000 ng/ml

2.2.5 Resolution

Resolution is specified to measure that closely eluting compound are resolved from each other, to establish the general resolving power of the system (Swartz and Krull, 1998). The requirement of relative standard deviation calculated from the data of five replicate injections was 2.0 or less (The United States Pharmacopeial Convention, 2000). The data in Table b8 show that mean of resolution at concentration of 20 μg/ml diazepam standard solution is 6.83 with a low relative standard deviation (1.86%). Therefore, this condition was suitable for quantitative analysis of diazepam since diazepam was clearly resolved from lorazepam.

Table b8 Resolution of diazepam standard solution at concentration of 20 μg/ml

Concentration (μg/ml)	**Resolution**
20	6.75 6.67 6.93 6.84 6.98
	Mean = 6.83 SD = 0.13 %CV = 1.86

สถาบันวิทยบริการ
จุฬาลงกรณ์มหาวิทยาลัย

2.2.6 Tailing factor

The tailing factor is specified to measure peak symmetry and its value increases as tailing becomes more pronounced. Table b9 illustrates the tailing factor of diazepam and lorazepam calculated by collecting data from replicate injections of standard solution at concentration of 10 μg/ml. Tailing factor data were less than 2 for both diazepam and lorazepam. This indicated that peak symmetry was acceptable and hence precision became reliable.

Table b9 Tailing factor of diazepam and lorazazepam at concentration of 10 and 15 μg/ml

Actual concentration of diazepam (μg/ml)	Tailing factor of diazepam	Tailing factor of lorazepam
10	1.06	1.17
	1.14	1
	1.14	1.19
	1.07	1.07
	1.17	1.17
Mean	1.12	1.12
SD	0.05	0.08

สถาบันวิทยบริการ
จุฬาลงกรณ์มหาวิทยาลัย

APPENDIX C

RELEASE DATA OF DIAZEPAM

Table c1 Release of diazepam from saturated solution

Time(hr)	Diazepam amount (μm)			% Released			Mean	SD
	No. 1	No. 2	No. 3	No. 1	No. 2	No. 3		
0	0.00	0.00	0.00	0.00	0.00	0.00	0.00	0.00
0.25	71.94	65.73	67.93	56.18	51.33	53.05	53.52	2.46
0.5	75.33	67.17	73.79	58.83	52.45	57.63	56.30	3.39
1	93.21	90.53	116.49	72.79	70.70	90.97	78.15	11.15
2	113.52	121.63	122.22	88.65	94.99	95.44	93.03	3.80
3	118.27	118.54	126.33	92.36	92.57	98.65	94.53	3.57
4	128.35	139.73	130.18	100.23	109.15	101.66	103.67	4.77

สถาบันวิทยบริการ
จุฬาลงกรณ์มหาวิทยาลัย

Table c2 Release of diazepam from 0.1% diazepam loaded SLN prepared under pressure of 10,000 psi 5 cycles

Time(hr)	Diazepam amount (µm)			% Released			Mean	SD
	No. 1	No. 2	No. 3	No. 1	No. 2	No. 3		
0	0.00	0.00	0.00	0.00	0.00	0.00	0.00	0.00
0.5	80.86	46.34	51.24	4.04	2.32	2.56	2.98	0.93
1	101.92	106.28	71.85	5.10	5.31	3.59	4.67	0.94
2	182.48	196.78	201.22	9.12	9.84	10.06	9.68	0.49
3	303.80	298.62	313.00	15.19	14.93	15.65	15.26	0.36
4	343.27	382.38	401.94	17.16	19.12	20.10	18.79	1.49
6	472.06	531.55	531.72	23.60	26.58	26.59	25.59	1.72
8	568.40	599.29	643.83	28.42	29.97	32.19	30.19	1.90
10	710.58	786.34	816.83	35.53	39.32	40.84	38.56	2.74
12	835.27	941.84	893.94	41.76	47.09	44.70	44.52	2.70
24	1035.79	1203.25	1243.27	51.79	60.16	62.16	58.04	5.50
36	1347.91	1375.10	1465.08	67.40	68.76	73.25	69.80	3.07
48	1482.53	1544.57	1621.23	74.13	77.23	81.06	77.47	3.47
60	1569.75	1637.62	1725.37	78.49	81.88	86.27	82.21	3.90

สถาบันวิทยบริการ
จุฬาลงกรณ์มหาวิทยาลัย

Table c3 Release of diazepam from 0.3% diazepam loaded SLN prepared under pressure of 10,000 psi 5 cycles

Time (hr)	Diazepam amount (μm)			% Released			Mean	SD
	No. 1	No. 2	No. 3	No. 1	No. 2	No. 3		
0	0.00	0.00	0.00	0.00	0.00	0.00	0.00	0.00
0.5	61.13	70.99	66.06	1.02	1.18	1.10	1.10	0.08
1	229.78	229.94	220.00	3.83	3.83	3.67	3.78	0.10
2	465.31	455.61	425.79	7.76	7.59	7.10	7.48	0.34
3	709.63	714.56	649.73	11.83	11.91	10.83	11.52	0.60
4	864.22	923.47	862.50	14.40	15.39	14.38	14.72	0.58
6	1203.62	1219.47	1132.87	20.06	20.33	18.88	19.76	0.77
8	1454.76	1520.16	1446.95	24.25	25.34	24.12	24.57	0.67
10	1744.27	1697.35	1692.01	29.07	28.29	28.20	28.52	0.48
12	1919.90	1955.97	1921.05	32.00	32.60	32.02	32.21	0.34
24	2857.24	2869.24	2809.17	47.62	47.82	46.82	47.42	0.53
36	3262.45	3245.03	3322.10	54.37	54.08	55.37	54.61	0.67
48	3604.63	3695.35	3709.73	60.08	61.59	61.83	61.17	0.95
60	3813.62	3777.63	3915.57	63.56	62.96	65.26	63.93	1.19

สถาบันวิทยบริการ
จุฬาลงกรณ์มหาวิทยาลัย

Table c4 Release of diazepam from 0.5% diazepam loaded SLN prepared under pressure of 10,000 psi 5 cycles

Time (hr)	Diazepam amount (μm)			% Released			Mean	SD
	No. 1	No. 2	No. 3	No. 1	No. 2	No. 3		
0	0.00	0.00	0.00	0.00	0.00	0.00	0.00	0.00
0.5	80.86	90.72	66.06	0.81	0.91	0.66	0.79	0.12
1	289.27	338.74	274.23	2.89	3.39	2.74	3.01	0.34
2	693.41	689.47	683.06	6.93	6.90	6.83	6.89	0.05
3	971.09	1026.28	940.86	9.71	10.26	9.41	9.79	0.43
4	1337.03	1417.72	1335.88	13.37	14.18	13.36	13.64	0.47
6	1782.74	1864.75	1752.01	17.83	18.65	17.52	18.00	0.58
8	2023.53	2131.50	1952.87	20.24	21.32	19.53	20.36	0.90
10	2386.18	2515.60	2388.32	23.86	25.16	23.88	24.30	0.74
12	2813.49	2905.52	2746.69	28.14	29.06	27.47	28.22	0.80
24	4031.19	4104.90	4002.76	40.31	41.05	40.03	40.46	0.53
36	5036.73	5017.83	5002.96	50.37	50.18	50.03	50.19	0.17
48	5749.33	5720.08	5803.81	57.49	57.20	58.04	57.58	0.43
60	6076.11	5809.55	5963.94	60.76	58.10	59.64	59.50	1.34

สถาบันวิทยบริการ
จุฬาลงกรณ์มหาวิทยาลัย

Table c5 Release of diazepam from 0.7% diazepam loaded SLN prepared under pressure of 10,000 psi 5 cycles

Time (hr)	Diazepam amount (μm)			% Released			Mean	SD
	No. 1	No. 2	No. 3	No. 1	No. 2	No. 3		
0	0.00	0.00	0.00	0.00	0.00	0.00	0.00	0.00
0.5	159.74	159.74	144.95	1.14	1.14	1.04	1.11	0.06
1	458.21	463.14	354.43	3.27	3.31	2.53	3.04	0.44
2	850.35	870.16	700.48	6.07	6.22	5.00	5.76	0.66
3	1268.63	1214.81	1091.64	9.06	8.68	7.80	8.51	0.65
4	1580.25	1525.52	1415.17	11.29	10.90	10.11	10.76	0.60
6	2019.97	2013.64	1876.91	14.43	14.38	13.41	14.07	0.58
8	2437.01	2405.95	2360.76	17.41	17.19	16.86	17.15	0.27
10	2855.53	2897.93	2822.58	20.40	20.70	20.16	20.42	0.27
12	3201.50	3224.91	3163.29	22.87	23.04	22.60	22.83	0.22
24	4479.34	4695.45	4563.98	32.00	33.54	32.60	32.71	0.78
36	5143.63	5412.65	5545.44	36.74	38.66	39.61	38.34	1.46
48	5539.75	6069.58	5968.18	39.57	43.35	42.63	41.85	2.01
60	5783.37	6183.86	6120.43	41.31	44.17	43.72	43.07	1.54

สถาบันวิทยบริการ
จุฬาลงกรณ์มหาวิทยาลัย

Table c6 Release of diazepam from 0.9% diazepam loaded SLN prepared under pressure of 10,000 psi 5 cycles

Time (hr)	Diazepam amount (μm)			% Released			Mean	SD
	No. 1	No. 2	No. 3	No. 1	No. 2	No. 3		
0	0.00	0.00	0.00	0.00	0.00	0.00	0.00	0.00
0.5	361.87	253.41	263.27	2.01	1.41	1.46	1.63	0.33
1	658.78	518.93	524.03	3.66	2.88	2.91	3.15	0.44
2	1103.52	961.36	932.03	6.13	5.34	5.18	5.55	0.51
3	1535.76	1411.03	1366.41	8.53	7.84	7.59	7.99	0.49
4	1881.23	1779.18	1694.38	10.45	9.88	9.41	9.92	0.52
6	2606.74	2429.17	2387.35	14.48	13.50	13.26	13.75	0.65
8	3131.83	2990.91	2879.41	17.40	16.62	16.00	16.67	0.70
10	3664.98	3536.71	3403.68	20.36	19.65	18.91	19.64	0.73
12	4087.86	4031.65	3783.09	22.71	22.40	21.02	22.04	0.90
24	5938.67	5605.72	5496.11	32.99	31.14	30.53	31.55	1.28
36	6653.77	6660.67	6332.49	36.97	37.00	35.18	36.38	1.04
48	7546.85	7376.76	6905.28	41.93	40.98	38.36	40.42	1.85
60	7782.58	7817.09	7387.35	43.23	43.43	41.04	42.57	1.33

สถาบันวิทยบริการ
จุฬาลงกรณ์มหาวิทยาลัย

Table c7 Release of diazepam from 0.3% diazepam loaded SLN prepared under pressure of 20,000 psi 5 cycles

Time (hr)	Diazepam amount (μm)			% Released			Mean	SD
	No. 1	No. 2	No. 3	No. 1	No. 2	No. 3		
0	0.00	0.00	0.00	0.00	0.00	0.00	0.00	0.00
0.5	248.48	268.20	278.06	4.14	4.47	4.63	4.42	0.25
1	356.15	361.41	376.37	5.94	6.02	6.27	6.08	0.18
2	672.62	692.75	658.65	11.21	11.55	10.98	11.25	0.29
3	885.80	965.42	965.26	14.76	16.09	16.09	15.65	0.77
4	1186.16	1198.08	1227.49	19.77	19.97	20.46	20.07	0.36
6	1565.24	1626.62	1646.67	26.09	27.11	27.45	26.88	0.71
8	1901.02	2027.48	1988.69	31.68	33.79	33.15	32.83	1.08
10	2276.49	2340.90	2385.28	37.94	39.02	39.76	38.90	0.91
12	2568.96	2654.08	2640.03	42.82	44.24	44.00	43.68	0.76
24	3432.67	3686.74	3711.88	57.21	61.45	61.87	60.17	2.57
36	4107.97	4242.89	4159.98	68.47	70.72	69.33	69.51	1.13
48	4537.26	4417.86	4555.42	75.62	73.63	75.92	75.06	1.24
60	4790.21	4851.01	4754.22	79.84	80.85	79.24	79.98	0.82

สถาบันวิทยบริการ
จุฬาลงกรณ์มหาวิทยาลัย

Table c8 Release of diazepam from 0.5% diazepam loaded SLN prepared under pressure of 20,000 psi 5 cycles

Time (hr)	Diazepam amount (μm)			% Released			Mean	SD
	No. 1	No. 2	No. 3	No. 1	No. 2	No. 3		
0	0.00	0.00	0.00	0.00	0.00	0.00	0.00	0.00
0.5	337.23	332.29	356.94	3.37	3.32	3.57	3.42	0.13
1	500.61	466.02	496.01	5.01	4.66	4.96	4.88	0.19
2	809.60	838.52	854.22	8.10	8.39	8.54	8.34	0.23
3	1108.81	1162.88	1149.24	11.09	11.63	11.49	11.40	0.28
4	1378.27	1477.62	1448.94	13.78	14.78	14.49	14.35	0.51
6	1819.56	1935.33	1861.79	18.20	19.35	18.62	18.72	0.59
8	2149.50	2232.65	2172.67	21.50	22.33	21.73	21.85	0.43
10	2523.90	2706.97	2616.42	25.24	27.07	26.17	26.16	0.92
12	2830.01	3055.48	2914.15	28.30	30.56	29.14	29.33	1.14
24	3855.43	4138.75	4014.84	38.55	41.39	40.15	40.03	1.42
36	4611.26	4864.59	4699.26	46.11	48.65	46.99	47.25	1.29
48	5439.80	5391.41	5400.94	54.40	53.91	54.01	54.11	0.26
60	5790.90	5731.49	5692.05	57.91	57.32	56.92	57.38	0.50

สถาบันวิทยบริการ
จุฬาลงกรณ์มหาวิทยาลัย

Table c9 Release of diazepam from supernatant of formulation 0.3% diazepam loaded SLN calculated from total amount of diazepam in formulation

Time (hr)	Diazepam amount (μm)			% Released			Mean	SD
	No. 1	No. 2	No. 3	No. 1	No. 2	No. 3		
0	0.00	0.00	0.00	0.00	0.00	0.00	0.00	0.00
0.25	67.68	65.78	74.10	1.13	1.10	1.24	1.15	0.07
0.5	101.53	101.01	93.06	1.69	1.68	1.55	1.64	0.08
1	144.80	156.38	145.70	2.41	2.61	2.43	2.48	0.10
2	243.18	243.89	242.98	4.05	4.06	4.05	4.06	0.01
3	306.05	311.52	301.28	5.10	5.19	5.02	5.10	0.09
4	359.43	364.69	352.79	5.99	6.08	5.88	5.98	0.10
6	423.69	417.40	414.61	7.06	6.96	6.91	6.98	0.08
8	470.16	474.02	465.97	7.84	7.90	7.77	7.83	0.07
10	607.53	617.38	555.45	10.13	10.29	9.26	9.89	0.55
12	646.06	709.92	649.41	10.77	11.83	10.82	11.14	0.60

สถาบันวิทยบริการ
จุฬาลงกรณ์มหาวิทยาลัย

Table c10 Release of diazepam from supernatant of formulation 0.5% diazepam loaded SLN calculated from total amount of diazepam in formulation

Time (hr)	Diazepam amount (μm)			% Released			Mean	SD
	No. 1	No. 2	No. 3	No. 1	No. 2	No. 3		
0	0.00	0.00	0.00	0.00	0.00	0.00	0.00	0.00
0.25	92.14	91.62	91.38	0.92	0.92	0.91	0.92	0.01
0.5	119.89	122.93	125.65	1.20	1.23	1.26	1.23	0.03
1	188.51	198.05	213.19	1.89	1.98	2.13	2.00	0.12
2	338.05	313.16	325.19	3.38	3.13	3.25	3.25	0.12
3	379.65	360.43	385.65	3.80	3.60	3.86	3.75	0.13
4	481.43	441.77	423.56	4.81	4.42	4.24	4.49	0.30
6	514.21	541.46	531.82	5.14	5.41	5.32	5.29	0.14
8	574.18	554.11	611.29	5.74	5.54	6.11	5.80	0.29
10	598.20	740.60	663.47	5.98	7.41	6.63	6.67	0.71
12	741.09	762.01	721.09	7.41	7.62	7.21	7.41	0.20

สถาบันวิทยบริการ
จุฬาลงกรณ์มหาวิทยาลัย

APPENDIX D
PARTICLE SIZE DETERMINATION OF SLN

The particle size of solid lipid nanoparticle (SLN) was determined by Mastersizer S. It is a range of a laser diffraction instrument (Mastersizer reference manual, Instrumental manual). The results reported base on a number of fundamental concepts as followed:

- The result is volume based. This means that when the result lists, for example 11% of the distribution in the size category 6.97-7.75 μm this means that the total volume of all particles with diameters in this range represents 11% of the total volume of all particles in the distribution.
- The result is expressed in terms of equivalent spheres.
- Distribution parameters and derived diameters are calculated from the fundamental distribution using the summation of the contributions from each size band. In performing this calculation the representative diameter for each band is taken to be the geometric mean of the size band limits:

$$X_i = \sqrt{d_{i-1} d_i}$$

The result from the analysis is the relative distribution of volume of particles in the range of size classes. The result tables have listed the percentile sizes for 10%, 50% and 90%. The 50% volume percentile, expressed as D(v,0.5) is the median of the volume distribution. D(v,0.1), the 10% volume percentile, shows that 10% of the distribution is below this value. D(v,0.9), the 90% volume percentile, shows that 90% of the distribution is below this value. From this basic result, the statistics of the distribution are calculated using derived diameter D[m,n]. The span and uniformity are calculated to describe the distribution of the particles. The span gives a description of the width of the distribution which is independent of the median size. The span is a dimensionless number which illustrates whether or not the distribution spread is narrow or wide. The uniformity is a measure of the absolute deviations from the median.

The derived diameters are defined as:

$$D[m,n] = \left[\frac{\sum v_i d_i^{m-3}}{\sum v_i d_i^{n-3}} \right]^{\frac{1}{m-n}}$$

v_i = the relative volume in class *i* with mean class diameter of d_i

m and n = integer values which describe the type of derived diameter

D[4,3] = the volume mean diameter or volume weighted mean

D[3,2] = the surface area mean diameter or surface weighted mean

The span of the distribution is defined as:

$$\text{Span} = \frac{d(v,0.9) - d(v,0.1)}{d(v,0.5)}$$

The uniformity of the distribution is defined as:

$$\text{Uniformity} = \frac{\sum x_i \left| d(x,0.5) - d_i \right|}{d(x,0.5) \sum x_i}$$

where d(v,0.5) = the median size of the distribution

d_i and x_i = the mean diameter of, and result in, size class *i*, respectively.

สถาบันวิทยบริการ
จุฬาลงกรณ์มหาวิทยาลัย

Table d1 Particle size distribution of formulation 5 GB + 1 TW80 before autoclaving

Distribution type: volume	D(v,0.1) = 0.19	D(v,0.5) = 0.40	D(v,0.9) = 1.17
Mean diameter	D[4,3] = 3.62	D[3,2] = 0.35	Span = 2.44
% > 1 μm = 13.02	% > 5 μm = 1.90	% > 10 μm = 0.75	Uniformity = 8.45

size low (μm)	size in %	size high (μm)	under %
0.05	0.10	0.06	0.10
0.06	0.22	0.07	0.32
0.07	0.35	0.08	0.67
0.08	0.52	0.09	1.19
0.09	0.76	0.11	1.95
0.11	1.09	0.13	3.04
0.13	1.59	0.15	4.63
0.15	2.38	0.17	7.01
0.17	3.65	0.20	10.66
0.20	5.55	0.23	16.21
0.23	7.93	0.27	24.14
0.27	9.86	0.31	34.00
0.31	10.19	0.36	44.19
0.36	9.23	0.42	53.42
0.42	8.24	0.49	61.66
0.49	7.51	0.58	69.16
0.58	6.36	0.67	75.52
0.67	5.20	0.78	80.72
0.78	4.21	0.91	84.94
0.91	3.41	1.06	88.35
1.06	2.80	1.24	91.15
1.24	2.29	1.44	93.45
1.44	1.73	1.68	95.17
1.68	1.15	1.95	96.33
1.95	0.70	2.28	97.02
2.28	0.33	2.65	97.35
2.65	0.22	3.09	97.57
3.09	0.13	3.60	97.70
3.60	0.15	4.19	97.85
4.19	0.21	4.88	98.06
4.88	0.25	5.69	98.31
5.69	0.28	6.63	98.59
6.63	0.28	7.72	98.86
7.72	0.25	9.00	99.12
9.00	0.19	10.48	99.31
10.48	0.14	12.21	99.45
12.21	0.09	14.22	99.54
14.22	0.03	16.57	99.57
16.57	0.01	19.31	99.58
19.31	0.00	22.49	99.58
22.49	0.00	26.20	99.58
26.20	0.00	30.53	99.58
30.53	0.00	35.56	99.58
35.56	0.00	41.43	99.58
41.43	0.00	48.27	99.58
48.27	0.00	56.23	99.58
56.23	0.00	65.51	99.58
65.51	0.00	76.32	99.58
76.32	0.00	88.91	99.58
88.91	0.00	103.58	99.58
103.58	0.00	120.67	99.58
120.67	0.00	140.58	99.58
140.58	0.00	163.77	99.58
163.77	0.00	190.80	99.58
190.80	0.00	222.28	99.58
222.28	0.00	258.95	99.58
258.95	0.00	301.68	99.58
301.68	0.00	351.46	99.58
351.46	0.00	409.45	99.58
409.45	0.01	477.01	99.60
477.01	0.03	555.71	99.63
555.71	0.06	647.41	99.69
647.41	0.13	754.23	99.82
754.23	0.18	878.67	100.00

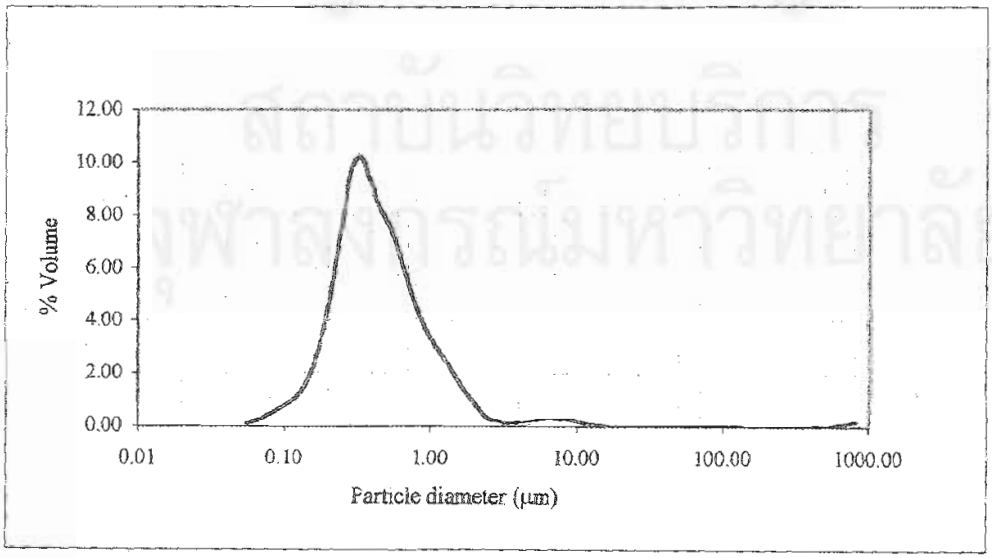

Figure d1 Particle size distribution of formulation 5 GB + 1 TW80 before autoclaving

Table d2 Particle size distribution of formulation 5 GB + 1 TW80 after autoclaving

Distribution type: volume	D(v,0.1) = 0.24	D(v,0.5) = 0.44	D(v,0.9) = 1.10
Mean diameter	D[4,3] = 0.56	D[3,2] = 0.38	Span = 1.96
% > 1 µm = 12.54	% > 5 µm = 0.00	% > 10 µm = 0.00	Uniformity = 0.62

size low (µm)	size in %	size high (µm)	under %	size low (µm)	size in %	size high (µm)	under %
0.05	0.05	0.06	0.05	6.63	0.00	7.72	100.00
0.06	0.10	0.07	0.15	7.72	0.00	9.00	100.00
0.07	0.17	0.08	0.32	9.00	0.00	10.48	100.00
0.08	0.26	0.09	0.58	10.48	0.00	12.21	100.00
0.09	0.39	0.11	0.98	12.21	0.00	14.22	100.00
0.11	0.60	0.13	1.58	14.22	0.00	16.57	100.00
0.13	0.95	0.15	2.52	16.57	0.00	19.31	100.00
0.15	1.55	0.17	4.07	19.31	0.00	22.49	100.00
0.17	2.63	0.20	6.70	22.49	0.00	26.20	100.00
0.20	4.46	0.23	11.17	26.20	0.00	30.53	100.00
0.23	7.09	0.27	18.26	30.53	0.00	35.56	100.00
0.27	9.57	0.31	27.83	35.56	0.00	41.43	100.00
0.31	10.35	0.36	38.18	41.43	0.00	48.27	100.00
0.36	9.57	0.42	47.75	48.27	0.00	56.23	100.00
0.42	8.83	0.49	56.58	56.23	0.00	65.51	100.00
0.49	8.51	0.58	65.09	65.51	0.00	76.32	100.00
0.58	7.58	0.67	72.67	76.32	0.00	88.91	100.00
0.67	6.52	0.78	79.19	88.91	0.00	103.58	100.00
0.78	5.52	0.91	84.72	103.58	0.00	120.67	100.00
0.91	4.57	1.06	89.28	120.67	0.00	140.58	100.00
1.06	3.66	1.24	92.94	140.58	0.00	163.77	100.00
1.24	2.82	1.44	95.77	163.77	0.00	190.80	100.00
1.44	1.98	1.68	97.75	190.80	0.00	222.28	100.00
1.68	1.24	1.95	98.98	222.28	0.00	258.95	100.00
1.95	0.67	2.28	99.65	258.95	0.00	301.68	100.00
2.28	0.29	2.65	99.94	301.68	0.00	351.46	100.00
2.65	0.06	3.09	100.00	351.46	0.00	409.45	100.00
3.09	0.00	3.60	100.00	409.45	0.00	477.01	100.00
3.60	0.00	4.19	100.00	477.01	0.00	555.71	100.00
4.19	0.00	4.88	100.00	555.71	0.00	647.41	100.00
4.88	0.00	5.69	100.00	647.41	0.00	754.23	100.00
5.69	0.00	6.63	100.00	754.23	0.00	878.67	100.00

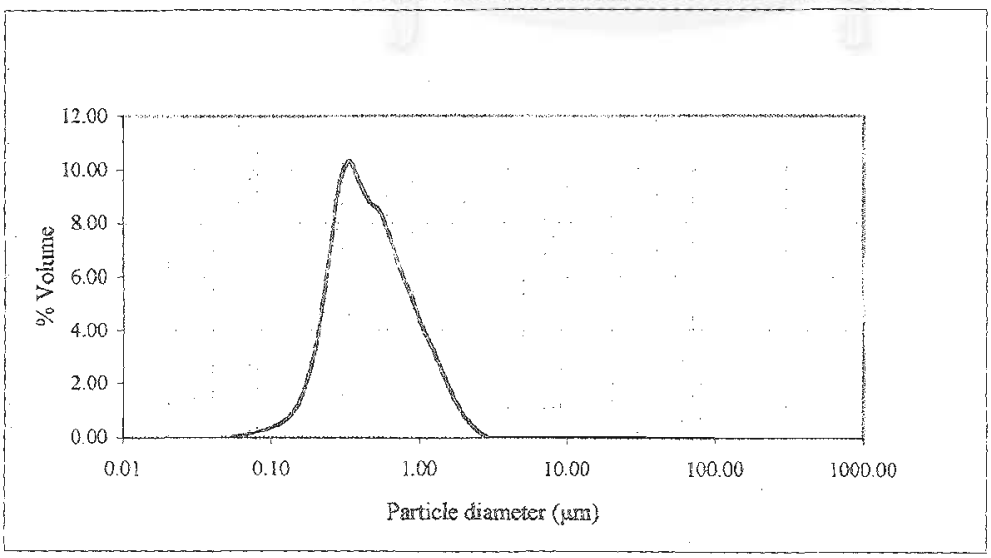

Figure d2 Particle size distribution of formulation 5 GB + 1 TW80 after autoclaving

Table d3 Particle size distribution of formulation 5 GB + 2 TW80 before autoclaving

Distribution type: volume	D(v,0.1) = 0.17	D(v,0.5) = 0.33	D(v,0.9) = 0.64
Mean diameter	D[4,3] = 0.46	D[3,2] = 0.28	Span = 1.44
% > 1 μm = 1.85	% > 5 μm = 0.10	% > 10 μm = 0.05	Uniformity = 0.74

size low (μm)	size in %	size high (μm)	under %	size low (μm)	size in %	size high (μm)	under %
0.05	0.06	0.06	0.06	6.63	0.00	7.72	99.95
0.06	0.18	0.07	0.24	7.72	0.00	9.00	99.95
0.07	0.38	0.08	0.63	9.00	0.00	10.48	99.95
0.08	0.68	0.09	1.31	10.48	0.00	12.21	99.96
0.09	1.10	0.11	2.41	12.21	0.00	14.22	99.96
0.11	1.70	0.13	4.11	14.22	0.00	16.57	99.96
0.13	2.55	0.15	6.65	16.57	0.00	19.31	99.96
0.15	3.77	0.17	10.42	19.31	0.00	22.49	99.96
0.17	5.48	0.20	15.90	22.49	0.00	26.20	99.96
0.20	7.78	0.23	23.68	26.20	0.00	30.53	99.96
0.23	10.32	0.27	34.00	30.53	0.00	35.56	99.96
0.27	12.15	0.31	46.15	35.56	0.00	41.43	99.96
0.31	12.29	0.36	58.44	41.43	0.00	48.27	99.96
0.36	11.00	0.42	69.44	48.27	0.00	56.23	99.96
0.42	9.37	0.49	78.82	56.23	0.00	65.51	99.96
0.49	7.68	0.58	86.50	65.51	0.00	76.32	99.96
0.58	5.58	0.67	92.08	76.32	0.00	88.91	99.96
0.67	3.57	0.78	95.64	88.91	0.00	103.58	99.96
0.78	1.96	0.91	97.61	103.58	0.00	120.67	99.96
0.91	0.90	1.06	98.51	120.67	0.00	140.58	99.96
1.06	0.37	1.24	98.88	140.58	0.00	163.77	99.96
1.24	0.19	1.44	99.07	163.77	0.02	190.80	99.99
1.44	0.16	1.68	99.23	190.80	0.00	222.28	99.99
1.68	0.15	1.95	99.38	222.28	0.01	258.95	100.00
1.95	0.14	2.28	99.52	258.95	0.00	301.68	100.00
2.28	0.13	2.65	99.65	301.68	0.00	351.46	100.00
2.65	0.09	3.09	99.74	351.46	0.00	409.45	100.00
3.09	0.07	3.60	99.81	409.45	0.00	477.01	100.00
3.60	0.05	4.19	99.86	477.01	0.00	555.71	100.00
4.19	0.04	4.88	99.90	555.71	0.00	647.41	100.00
4.88	0.03	5.69	99.92	647.41	0.00	754.23	100.00
5.69	0.02	6.63	99.94	754.23	0.00	878.67	100.00

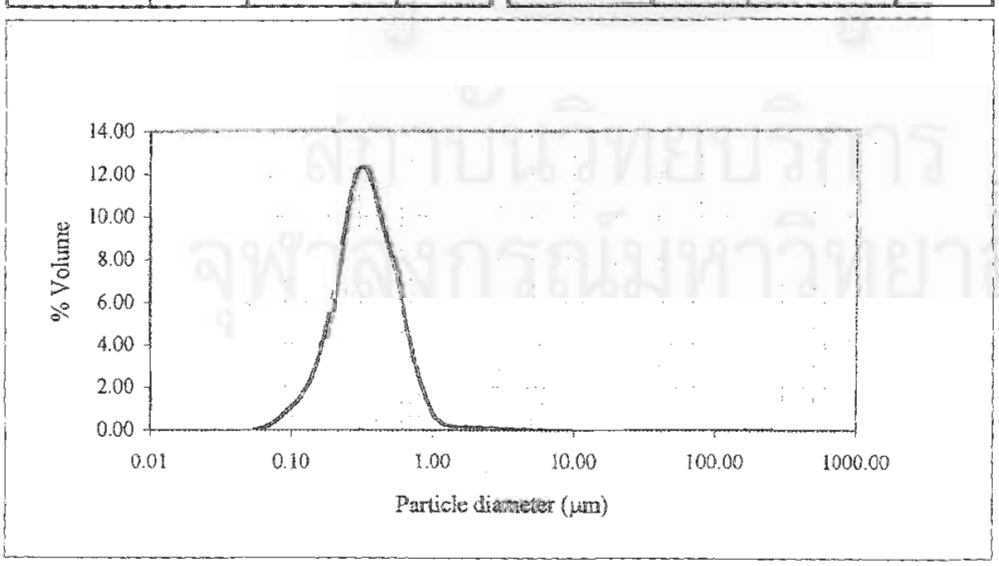

Figure d3 Particle size distribution of formulation 5 GB + 2 TW80 before autoclaving

Table d4 Particle size distribution of formulation 5 GB + 2 TW80 after autoclaving

Distribution type: volume	D(v,0.1) = 0.20	D(v,0.5) = 0.35	D(v,0.9) = 0.66
Mean diameter	D[4,3] = 0.41	D[3,2] = 0.32	Span = 1.31
% > 1 μm = 2.16	% > 5 μm = 0.00	% > 10 μm = 0.00	Uniformity = 0.44

size low (μm)	size in %	size high (μm)	under %	size low (μm)	size in %	size high (μm)	under %
0.05	0.01	0.06	0.01	6.63	0.00	7.72	100.00
0.06	0.05	0.07	0.06	7.72	0.00	9.00	100.00
0.07	0.13	0.08	0.19	9.00	0.00	10.48	100.00
0.08	0.26	0.09	0.45	10.48	0.00	12.21	100.00
0.09	0.48	0.11	0.93	12.21	0.00	14.22	100.00
0.11	0.84	0.13	1.77	14.22	0.00	16.57	100.00
0.13	1.43	0.15	3.20	16.57	0.00	19.31	100.00
0.15	2.40	0.17	5.60	19.31	0.00	22.49	100.00
0.17	4.02	0.20	9.63	22.49	0.00	26.20	100.00
0.20	6.54	0.23	16.17	26.20	0.00	30.53	100.00
0.23	9.82	0.27	25.98	30.53	0.00	35.56	100.00
0.27	12.66	0.31	38.65	35.56	0.00	41.43	100.00
0.31	13.42	0.36	52.06	41.43	0.00	48.27	100.00
0.36	12.21	0.42	64.27	48.27	0.00	56.23	100.00
0.42	10.48	0.49	74.75	56.23	0.00	65.51	100.00
0.49	9.03	0.58	83.78	65.51	0.00	76.32	100.00
0.58	6.59	0.67	90.37	76.32	0.00	88.91	100.00
0.67	4.29	0.78	94.66	88.91	0.00	103.58	100.00
0.78	2.45	0.91	97.12	103.58	0.00	120.67	100.00
0.91	1.21	1.06	98.33	120.67	0.00	140.58	100.00
1.06	0.56	1.24	98.89	140.58	0.00	163.77	100.00
1.24	0.33	1.44	99.22	163.77	0.00	190.80	100.00
1.44	0.25	1.68	99.48	190.80	0.00	222.28	100.00
1.68	0.18	1.95	99.66	222.28	0.00	258.95	100.00
1.95	0.13	2.28	99.78	258.95	0.00	301.68	100.00
2.28	0.08	2.65	99.86	301.68	0.00	351.46	100.00
2.65	0.04	3.09	99.90	351.46	0.00	409.45	100.00
3.09	0.04	3.60	99.94	409.45	0.00	477.01	100.00
3.60	0.06	4.19	100.00	477.01	0.00	555.71	100.00
4.19	0.00	4.88	100.00	555.71	0.00	647.41	100.00
4.88	0.00	5.69	100.00	647.41	0.00	754.23	100.00
5.69	0.00	6.63	100.00	754.23	0.00	878.67	100.00

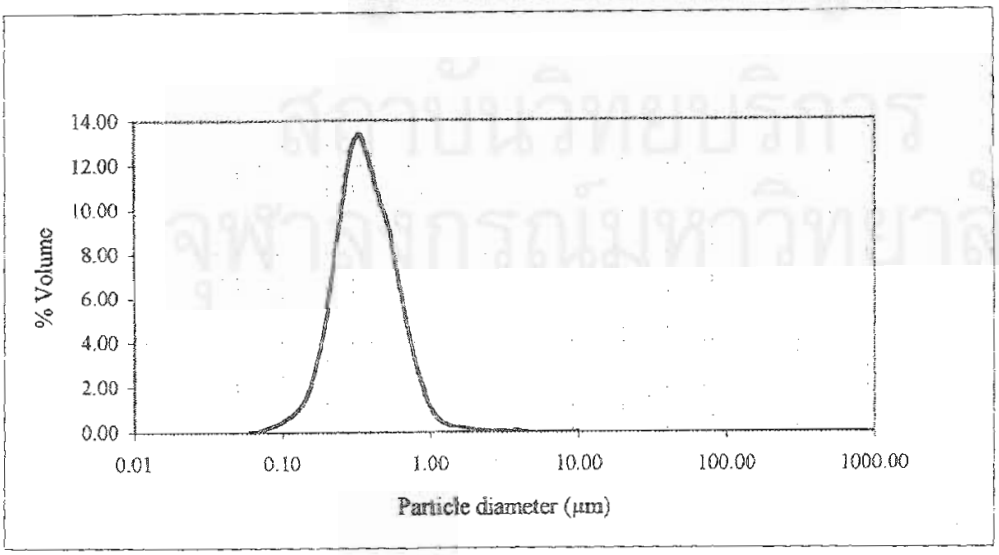

Figure d4 Particle size distribution of formulation 5 GB + 2 TW80 after autoclaving

Table d5 Particle size distribution of formulation 5 GB + 3 TW80 before autoclaving

Distribution type: volume	D(v,0.1) = 0.21	D(v,0.5) = 0.30	D(v,0.9) = 0.46
Mean diameter	D[4,3] = 0.89	D[3,2] = 0.29	Span = 0.83
% > 1 μm = 0.15	% > 5 μm = 0.15	% > 10 μm = 0.15	Uniformity = 2.15

size low (μm)	size in %	size high (μm)	under %	size low (μm)	size in %	size high (μm)	under %
0.05	0.01	0.06	0.01	6.63	0.00	7.72	99.85
0.06	0.04	0.07	0.05	7.72	0.00	9.00	99.85
0.07	0.09	0.08	0.13	9.00	0.00	10.48	99.85
0.08	0.16	0.09	0.30	10.48	0.00	12.21	99.85
0.09	0.31	0.11	0.61	12.21	0.00	14.22	99.85
0.11	0.56	0.13	1.17	14.22	0.00	16.57	99.85
0.13	1.06	0.15	2.23	16.57	0.00	19.31	99.85
0.15	2.07	0.17	4.31	19.31	0.00	22.49	99.85
0.17	4.24	0.20	8.54	22.49	0.00	26.20	99.85
0.20	8.59	0.23	17.13	26.20	0.00	30.53	99.85
0.23	15.48	0.27	32.61	30.53	0.00	35.56	99.85
0.27	21.03	0.31	53.64	35.56	0.00	41.43	99.85
0.31	19.26	0.36	72.90	41.43	0.00	48.27	99.85
0.36	12.90	0.42	85.80	48.27	0.00	56.23	99.85
0.42	7.73	0.49	93.53	56.23	0.00	65.51	99.85
0.49	4.24	0.58	97.77	65.51	0.00	76.32	99.85
0.58	1.64	0.67	99.42	76.32	0.00	88.91	99.85
0.67	0.40	0.78	99.82	88.91	0.00	103.58	99.85
0.78	0.03	0.91	99.85	103.58	0.00	120.67	99.85
0.91	0.00	1.06	99.85	120.67	0.00	140.58	99.85
1.06	0.00	1.24	99.85	140.58	0.00	163.77	99.85
1.24	0.00	1.44	99.85	163.77	0.00	190.80	99.85
1.44	0.00	1.68	99.85	190.80	0.00	222.28	99.85
1.68	0.00	1.95	99.85	222.28	0.00	258.95	99.85
1.95	0.00	2.28	99.85	258.95	0.00	301.68	99.85
2.28	0.00	2.65	99.85	301.68	0.01	351.46	99.86
2.65	0.00	3.09	99.85	351.46	0.14	409.45	100.00
3.09	0.00	3.60	99.85	409.45	0.00	477.01	100.00
3.60	0.00	4.19	99.85	477.01	0.00	555.71	100.00
4.19	0.00	4.88	99.85	555.71	0.00	647.41	100.00
4.88	0.00	5.69	99.85	647.41	0.00	754.23	100.00
5.69	0.00	6.63	99.85	754.23	0.00	878.67	100.00

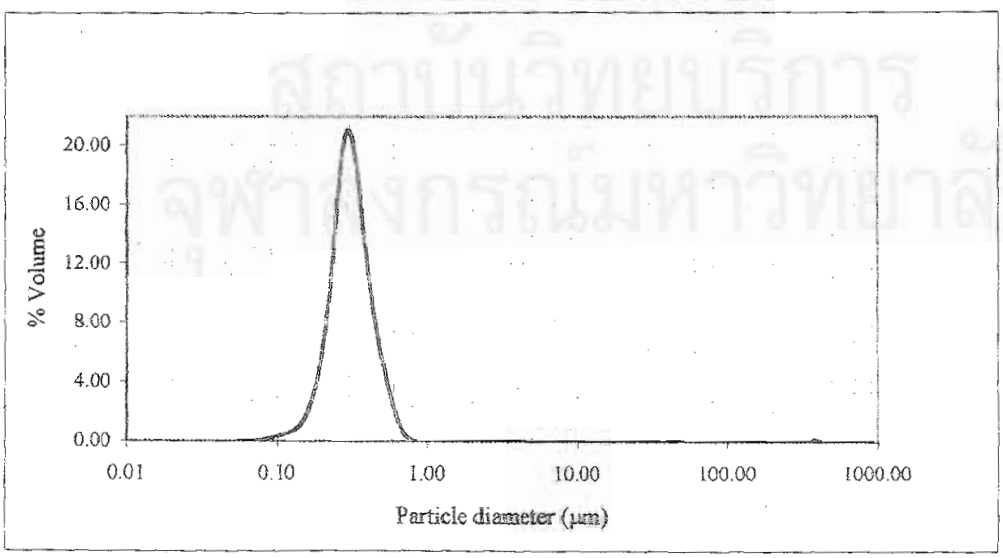

Figure d5 Particle size distribution of formulation 5 GB + 3 TW80 before autoclaving

Table d6 Particle size distribution of formulation 5 GB + 3 TW80 after autoclaving

Distribution type: volume	D(v,0.1) = 0.17	D(v,0.5) = 0.32	D(v,0.9) = 0.59
Mean diameter	D[4,3] = 0.36	D[3,2] = 0.28	Span = 1.31
% > 1 μm = 0.36	% > 5 μm = 0.00	% > 10 μm = 0.00	Uniformity = 0.43

size low (μm)	size in %	size high (μm)	under %	size low (μm)	size in %	size high (μm)	under %
0.05	0.04	0.06	0.04	6.63	0.00	7.72	100.00
0.06	0.16	0.07	0.19	7.72	0.00	9.00	100.00
0.07	0.36	0.08	0.55	9.00	0.00	10.48	100.00
0.08	0.67	0.09	1.22	10.48	0.00	12.21	100.00
0.09	1.12	0.11	2.34	12.21	0.00	14.22	100.00
0.11	1.75	0.13	4.10	14.22	0.00	16.57	100.00
0.13	2.64	0.15	6.74	16.57	0.00	19.31	100.00
0.15	3.90	0.17	10.64	19.31	0.00	22.49	100.00
0.17	5.66	0.20	16.30	22.49	0.00	26.20	100.00
0.20	7.95	0.23	24.26	26.20	0.00	30.53	100.00
0.23	10.49	0.27	34.75	30.53	0.00	35.56	100.00
0.27	12.41	0.31	47.16	35.56	0.00	41.43	100.00
0.31	12.71	0.36	59.87	41.43	0.00	48.27	100.00
0.36	11.60	0.42	71.47	48.27	0.00	56.23	100.00
0.42	9.96	0.49	81.43	56.23	0.00	65.51	100.00
0.49	8.09	0.58	89.52	65.51	0.00	76.32	100.00
0.58	5.65	0.67	95.17	76.32	0.00	88.91	100.00
0.67	3.23	0.78	98.40	88.91	0.00	103.58	100.00
0.78	1.25	0.91	99.64	103.58	0.00	120.67	100.00
0.91	0.00	1.06	99.64	120.67	0.00	140.58	100.00
1.06	0.00	1.24	99.64	140.58	0.00	163.77	100.00
1.24	0.00	1.44	99.64	163.77	0.00	190.80	100.00
1.44	0.00	1.68	99.64	190.80	0.00	222.28	100.00
1.68	0.00	1.95	99.64	222.28	0.00	258.95	100.00
1.95	0.00	2.28	99.64	258.95	0.00	301.68	100.00
2.28	0.00	2.65	99.64	301.68	0.00	351.46	100.00
2.65	0.00	3.09	99.64	351.46	0.00	409.45	100.00
3.09	0.03	3.60	99.68	409.45	0.00	477.01	100.00
3.60	0.04	4.19	99.71	477.01	0.00	555.71	100.00
4.19	0.29	4.88	100.00	555.71	0.00	647.41	100.00
4.88	0.00	5.69	100.00	647.41	0.00	754.23	100.00
5.69	0.00	6.63	100.00	754.23	0.00	878.67	100.00

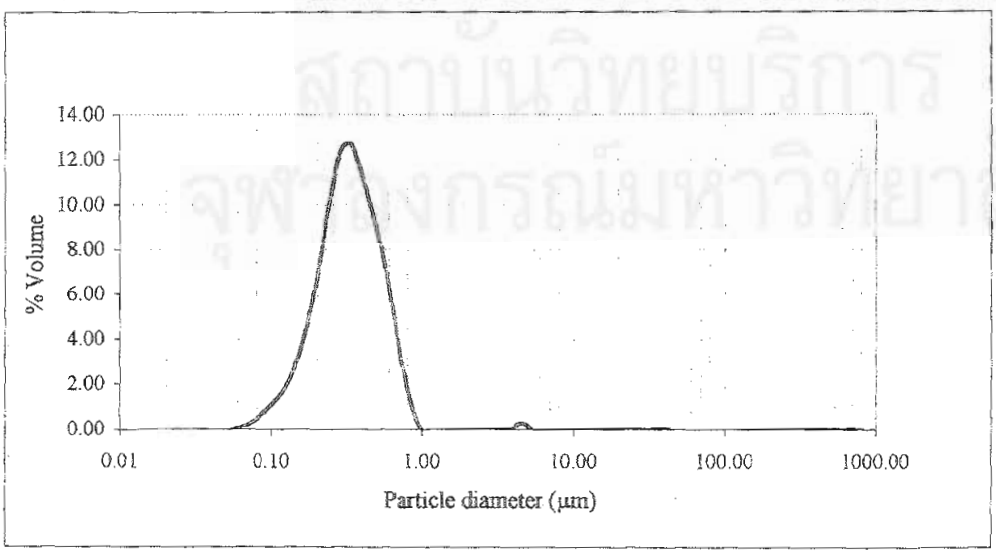

Figure d6 Particle size distribution of formulation 5 GB + 3 TW80 after autoclaving

Table d7 Particle size distribution of formulation 5 GB + 4 TW80 before autoclaving

Distribution type: volume	D(v,0.1) = 0.36	D(v,0.5) = 0.39	D(v,0.9) = 0.92
Mean diameter	D[4,3] = 1.22	D[3,2] = 0.32	Span = 1.42
% > 1 μm = 8.75	% > 5 μm = 2.53	% > 10 μm = 2.20	Uniformity = 2.38

size low (μm)	size in %	size high (μm)	under %	size low (μm)	size in %	size high (μm)	under %
0.05	0.00	0.06	0.00	6.63	0.08	7.72	97.62
0.06	0.03	0.07	0.03	7.72	0.10	9.00	97.72
0.07	0.06	0.08	0.09	9.00	0.12	10.48	97.84
0.08	0.12	0.09	0.21	10.48	0.13	12.21	97.97
0.09	0.24	0.11	0.45	12.21	0.15	14.22	98.12
0.11	0.44	0.13	0.89	14.22	0.17	16.57	98.29
0.13	0.80	0.15	1.69	16.57	0.18	19.31	98.47
0.15	1.49	0.17	3.17	19.31	0.19	22.49	98.66
0.17	2.75	0.20	5.92	22.49	0.19	26.20	98.85
0.20	4.99	0.23	10.91	26.20	0.19	30.53	99.04
0.23	8.28	0.27	19.19	30.53	0.19	35.56	99.23
0.27	11.49	0.31	30.68	35.56	0.18	41.43	99.41
0.31	12.59	0.36	43.27	41.43	0.16	48.27	99.57
0.36	11.57	0.42	54.84	48.27	0.13	56.23	99.70
0.42	10.25	0.49	65.09	56.23	0.11	65.51	99.81
0.49	9.09	0.58	74.18	65.51	0.08	76.32	99.89
0.58	7.13	0.67	81.31	76.32	0.06	88.91	99.95
0.67	5.12	0.78	86.43	88.91	0.05	103.58	100.00
0.78	3.45	0.91	89.89	103.58	0.00	120.67	100.00
0.91	2.27	1.06	92.16	120.67	0.00	140.58	100.00
1.06	1.58	1.24	93.74	140.58	0.00	163.77	100.00
1.24	1.25	1.44	94.99	163.77	0.00	190.80	100.00
1.44	1.02	1.68	96.02	190.80	0.00	222.28	100.00
1.68	0.73	1.95	96.75	222.28	0.00	258.95	100.00
1.95	0.45	2.28	97.20	258.95	0.00	301.68	100.00
2.28	0.20	2.65	97.40	301.68	0.00	351.46	100.00
2.65	0.05	3.09	97.45	351.46	0.00	409.45	100.00
3.09	0.00	3.60	97.45	409.45	0.00	477.01	100.00
3.60	0.00	4.19	97.45	477.01	0.00	555.71	100.00
4.19	0.01	4.88	97.46	555.71	0.00	647.41	100.00
4.88	0.03	5.69	97.49	647.41	0.00	754.23	100.00
5.69	0.05	6.63	97.55	754.23	0.00	878.67	100.00

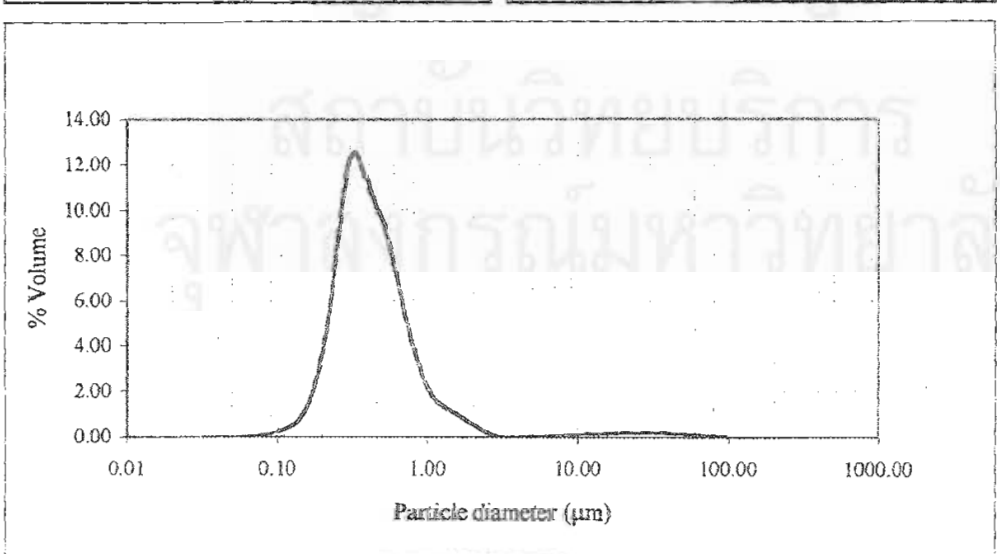

Figure d7 Particle size distribution of formulation 5 GB + 4 TW80 before autoclaving

Table d8 Particle size distribution of formulation 5 GB + 4 TW80 after autoclaving

Distribution type: volume	D(v,0.1) = 0.18	D(v,0.5) = 0.30	D(v,0.9) = 0.47
Mean diameter	D[4,3] = 0.32	D[3,2] = 0.27	Span = 1.01
% > 1 µm = 0.30	% > 5 µm = 0.00	% > 10 µm = 0.00	Uniformity = 0.33

size low (µm)	size in %	size high (µm)	under %	size low (µm)	size in %	size high (µm)	under %
0.05	0.05	0.06	0.05	6.63	0.00	7.72	100.00
0.06	0.15	0.07	0.20	7.72	0.00	9.00	100.00
0.07	0.30	0.08	0.50	9.00	0.00	10.48	100.00
0.08	0.51	0.09	1.01	10.48	0.00	12.21	100.00
0.09	0.83	0.11	1.84	12.21	0.00	14.22	100.00
0.11	1.34	0.13	3.18	14.22	0.00	16.57	100.00
0.13	2.15	0.15	5.33	16.57	0.00	19.31	100.00
0.15	3.56	0.17	8.89	19.31	0.00	22.49	100.00
0.17	5.96	0.20	14.84	22.49	0.00	26.20	100.00
0.20	9.73	0.23	24.57	26.20	0.00	30.53	100.00
0.23	14.40	0.27	38.97	30.53	0.00	35.56	100.00
0.27	17.39	0.31	56.36	35.56	0.00	41.43	100.00
0.31	15.97	0.36	72.33	41.43	0.00	48.27	100.00
0.36	11.75	0.42	84.08	48.27	0.00	56.23	100.00
0.42	7.83	0.49	91.91	56.23	0.00	65.51	100.00
0.49	4.75	0.58	96.67	65.51	0.00	76.32	100.00
0.58	2.14	0.67	98.81	76.32	0.00	88.91	100.00
0.67	0.63	0.78	99.44	88.91	0.00	103.58	100.00
0.78	0.22	0.91	99.66	103.58	0.00	120.67	100.00
0.91	0.06	1.06	99.72	120.67	0.00	140.58	100.00
1.06	0.01	1.24	99.73	140.58	0.00	163.77	100.00
1.24	0.01	1.44	99.74	163.77	0.00	190.80	100.00
1.44	0.00	1.68	99.74	190.80	0.00	222.28	100.00
1.68	0.00	1.95	99.74	222.28	0.00	258.95	100.00
1.95	0.00	2.28	99.74	258.95	0.00	301.68	100.00
2.28	0.02	2.65	99.76	301.68	0.00	351.46	100.00
2.65	0.03	3.09	99.79	351.46	0.00	409.45	100.00
3.09	0.07	3.60	99.86	409.45	0.00	477.01	100.00
3.60	0.14	4.19	100.00	477.01	0.00	555.71	100.00
4.19	0.00	4.88	100.00	555.71	0.00	647.41	100.00
4.88	0.00	5.69	100.00	647.41	0.00	754.23	100.00
5.69	0.00	6.63	100.00	754.23	0.00	878.67	100.00

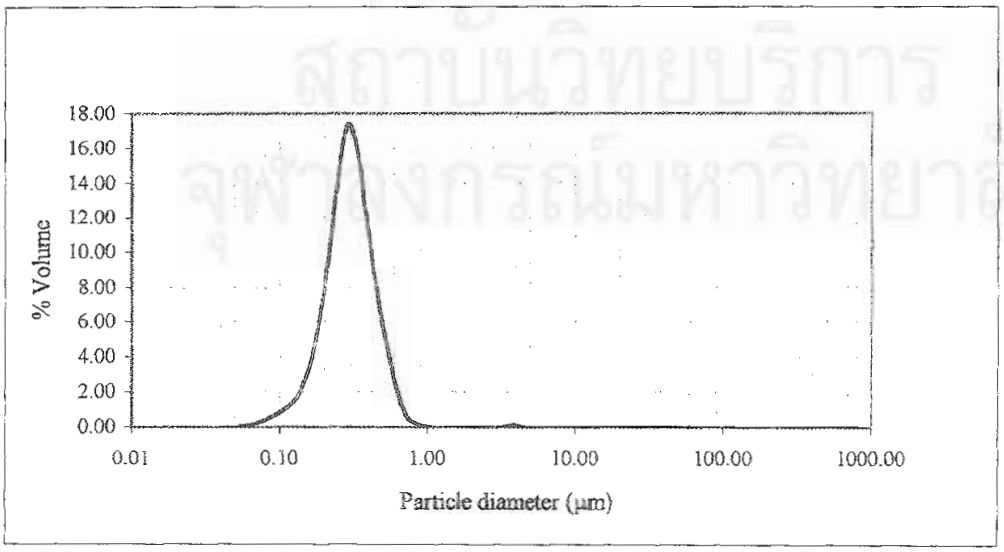

Figure d8 Particle size distribution of formulation 5 GB + 4 TW80 after autoclaving

Table d9 Particle size distribution of formulation 5 GB + 5 TW80 before autoclaving

Distribution type: volume	D(v,0.1) = 0.17	D(v,0.5) = 0.41	D(v,0.9) = 18.82
Mean diameter	D[4,3] = 5.40	D[3,2] = 0.36	Span = 45.14
% > 1 μm = 26.30	% > 5 μm = 15.46	% > 10 μm = 13.16	Uniformity = 12.47

size low (μm)	size in %	size high (μm)	under %
0.05	0.16	0.06	0.16
0.06	0.34	0.07	0.49
0.07	0.54	0.08	1.03
0.08	0.77	0.09	1.80
0.09	1.08	0.11	2.89
0.11	1.49	0.13	4.38
0.13	2.07	0.15	6.44
0.15	2.91	0.17	9.35
0.17	4.15	0.20	13.50
0.20	5.79	0.23	19.29
0.23	7.53	0.27	26.82
0.27	8.54	0.31	35.37
0.31	8.26	0.36	43.62
0.36	7.21	0.42	50.83
0.42	6.24	0.49	57.07
0.49	5.34	0.58	62.41
0.58	4.22	0.67	66.63
0.67	3.29	0.78	69.91
0.78	2.54	0.91	72.45
0.91	2.08	1.06	74.53
1.06	1.83	1.24	76.36
1.24	1.72	1.44	78.07
1.44	1.57	1.68	79.64
1.68	1.34	1.95	80.98
1.95	1.07	2.28	82.06
2.28	0.78	2.65	82.84
2.65	0.55	3.09	83.39
3.09	0.41	3.60	83.80
3.60	0.33	4.19	84.13
4.19	0.35	4.88	84.48
4.88	0.40	5.69	84.89
5.69	0.47	6.63	85.35
6.63	0.52	7.72	85.87
7.72	0.56	9.00	86.43
9.00	0.60	10.48	87.03
10.48	0.65	12.21	87.68
12.21	0.73	14.22	88.41
14.22	0.82	16.57	89.23
16.57	0.94	19.31	90.17
19.31	1.04	22.49	91.20
22.49	1.12	26.20	92.32
26.20	1.16	30.53	93.48
30.53	1.15	35.56	94.63
35.56	1.11	41.43	95.74
41.43	1.04	48.27	96.78
48.27	0.95	56.23	97.72
56.23	0.82	65.51	98.54
65.51	0.64	76.32	99.18
76.32	0.46	88.91	99.64
88.91	0.18	103.58	99.82
103.58	0.18	120.67	100.00
120.67	0.00	140.58	100.00
140.58	0.00	163.77	100.00
163.77	0.00	190.80	100.00
190.80	0.00	222.28	100.00
222.28	0.00	258.95	100.00
258.95	0.00	301.68	100.00
301.68	0.00	351.46	100.00
351.46	0.00	409.45	100.00
409.45	0.00	477.01	100.00
477.01	0.00	555.71	100.00
555.71	0.00	647.41	100.00
647.41	0.00	754.23	100.00
754.23	0.00	878.67	100.00

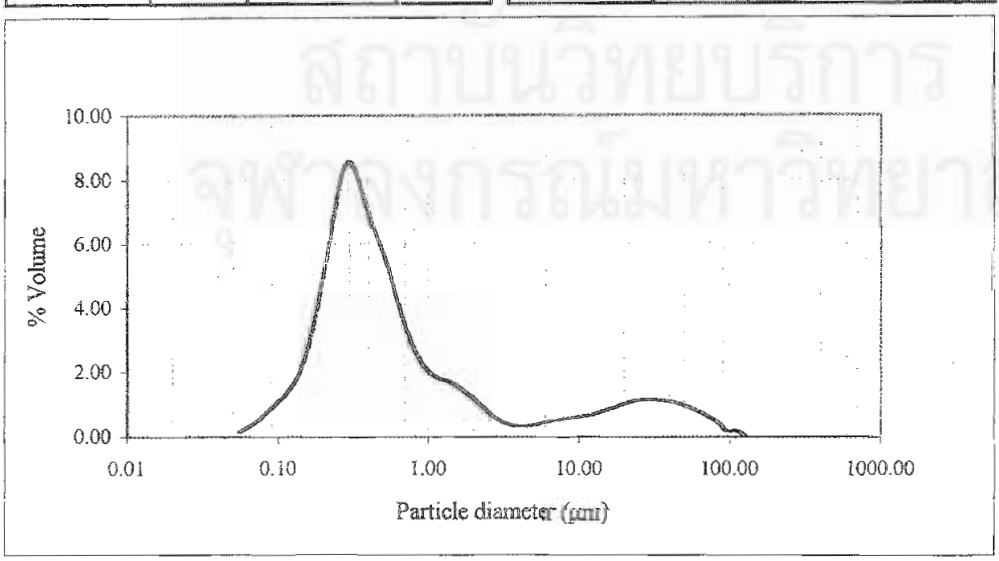

Figure d9 Particle size distribution of formulation 5 GB + 5 TW80 before autoclaving

Table d10 Particle size distribution of formulation 5 GB + 5 TW80 after autoclaving

Distribution type: volume	D(v,0.1) = 0.15	D(v,0.5) = 0.37	D(v,0.9) = 29.41
Mean diameter	D[4,3] = 7.52	D[3,2] = 0.33	Span = 78.87
% > 1 μm = 31.33	% > 5 μm = 23.34	% > 10 μm = 19.61	Uniformity = 19.65

size low (μm)	size in %	size high (μm)	under %	size low (μm)	size in %	size high (μm)	under %
0.05	0.23	0.06	0.23	6.63	0.84	7.72	78.82
0.06	0.51	0.07	0.74	7.72	0.91	9.00	79.73
0.07	0.84	0.08	1.58	9.00	0.97	10.48	80.71
0.08	1.22	0.09	2.81	10.48	1.04	12.21	81.74
0.09	1.68	0.11	4.49	12.21	1.12	14.22	82.87
0.11	2.24	0.13	6.73	14.22	1.23	16.57	84.10
0.13	2.97	0.15	9.71	16.57	1.37	19.31	85.47
0.15	3.92	0.17	13.63	19.31	1.53	22.49	87.00
0.17	5.15	0.20	18.78	22.49	1.68	26.20	88.68
0.20	6.57	0.23	25.35	26.20	1.78	30.53	90.46
0.23	7.83	0.27	33.17	30.53	1.82	35.56	92.28
0.27	8.22	0.31	41.40	35.56	1.76	41.43	94.05
0.31	7.48	0.36	48.88	41.43	1.60	48.27	95.65
0.36	6.11	0.42	54.99	48.27	1.40	56.23	97.05
0.42	4.79	0.49	59.78	56.23	1.13	65.51	98.18
0.49	3.54	0.58	63.32	65.51	0.85	76.32	99.03
0.58	2.31	0.67	65.63	76.32	0.58	88.91	99.61
0.67	1.40	0.78	67.04	88.91	0.27	103.58	99.88
0.78	1.09	0.91	68.13	103.58	0.12	120.67	100.00
0.91	0.90	1.06	69.03	120.67	0.00	140.58	100.00
1.06	0.80	1.24	69.83	140.58	0.00	163.77	100.00
1.24	0.76	1.44	70.59	163.77	0.00	190.80	100.00
1.44	0.96	1.68	71.55	190.80	0.00	222.28	100.00
1.68	0.92	1.95	72.48	222.28	0.00	258.95	100.00
1.95	0.86	2.28	73.33	258.95	0.00	301.68	100.00
2.28	0.76	2.65	74.09	301.68	0.00	351.46	100.00
2.65	0.67	3.09	74.76	351.46	0.00	409.45	100.00
3.09	0.61	3.60	75.37	409.45	0.00	477.01	100.00
3.60	0.59	4.19	75.95	477.01	0.00	555.71	100.00
4.19	0.61	4.88	76.56	555.71	0.00	647.41	100.00
4.88	0.67	5.69	77.23	647.41	0.00	754.23	100.00
5.69	0.75	6.63	77.98	754.23	0.00	878.67	100.00

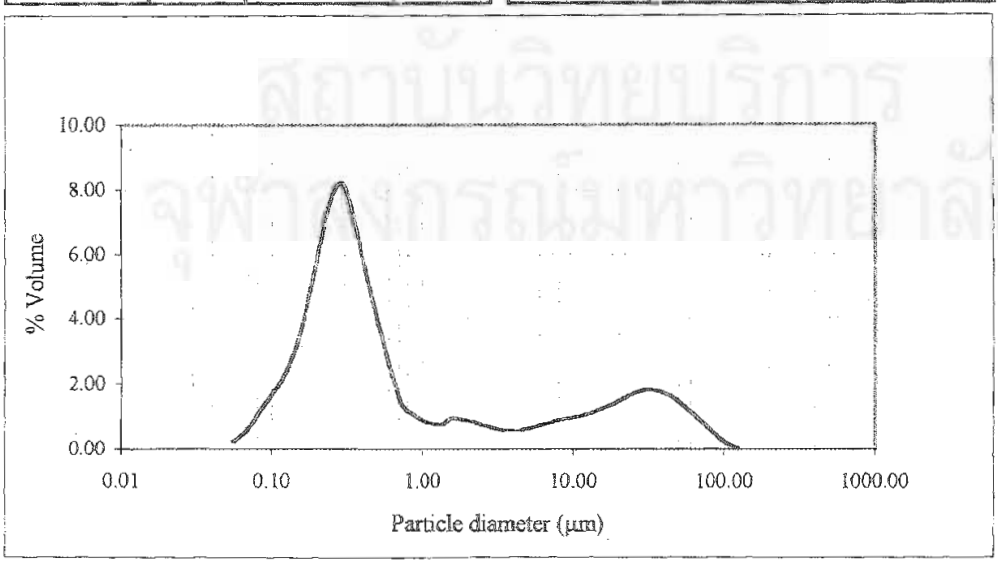

Figure d10 Particle size distribution of formulation 5 GB + 5 TW80 after autoclaving

Table d11 Particle size distribution of formulation 5 GB + 4 TW80 after autoclaving stored at room temperature for 1 month

Distribution type: volume	D(v,0.1) = 0.12	D(v,0.5) = 0.26	D(v,0.9) = 0.48
Mean diameter	D[4,3] = 0.28	D[3,2] = 0.22	Span = 1.38
% > 1 μm = 0.00	% > 5 μm = 0.00	% > 10 μm = 0.00	Uniformity = 0.43

size low (μm)	size in %	size high (μm)	under %	size low (μm)	size in %	size high (μm)	under %
0.05	0.13	0.06	0.13	6.63	0.00	7.72	100.00
0.06	0.53	0.07	0.66	7.72	0.00	9.00	100.00
0.07	1.18	0.08	1.84	9.00	0.00	10.48	100.00
0.08	2.05	0.09	3.89	10.48	0.00	12.21	100.00
0.09	3.14	0.11	7.03	12.21	0.00	14.22	100.00
0.11	4.38	0.13	11.41	14.22	0.00	16.57	100.00
0.13	5.75	0.15	17.17	16.57	0.00	19.31	100.00
0.15	7.18	0.17	24.35	19.31	0.00	22.49	100.00
0.17	8.58	0.20	32.93	22.49	0.00	26.20	100.00
0.20	9.81	0.23	42.73	26.20	0.00	30.53	100.00
0.23	10.65	0.27	53.39	30.53	0.00	35.56	100.00
0.27	10.88	0.31	64.27	35.56	0.00	41.43	100.00
0.31	10.35	0.36	74.62	41.43	0.00	48.27	100.00
0.36	9.13	0.42	83.76	48.27	0.00	56.23	100.00
0.42	7.37	0.49	91.13	56.23	0.00	65.51	100.00
0.49	5.22	0.58	96.35	65.51	0.00	76.32	100.00
0.58	2.88	0.67	99.23	76.32	0.00	88.91	100.00
0.67	0.77	0.78	100.00	88.91	0.00	103.58	100.00
0.78	0.00	0.91	100.00	103.58	0.00	120.67	100.00
0.91	0.00	1.06	100.00	120.67	0.00	140.58	100.00
1.06	0.00	1.24	100.00	140.58	0.00	163.77	100.00
1.24	0.00	1.44	100.00	163.77	0.00	190.80	100.00
1.44	0.00	1.68	100.00	190.80	0.00	222.28	100.00
1.68	0.00	1.95	100.00	222.28	0.00	258.95	100.00
1.95	0.00	2.28	100.00	258.95	0.00	301.68	100.00
2.28	0.00	2.65	100.00	301.68	0.00	351.46	100.00
2.65	0.00	3.09	100.00	351.46	0.00	409.45	100.00
3.09	0.00	3.60	100.00	409.45	0.00	477.01	100.00
3.60	0.00	4.19	100.00	477.01	0.00	555.71	100.00
4.19	0.00	4.88	100.00	555.71	0.00	647.41	100.00
4.88	0.00	5.69	100.00	647.41	0.00	754.23	100.00
5.69	0.00	6.63	100.00	754.23	0.00	878.67	100.00

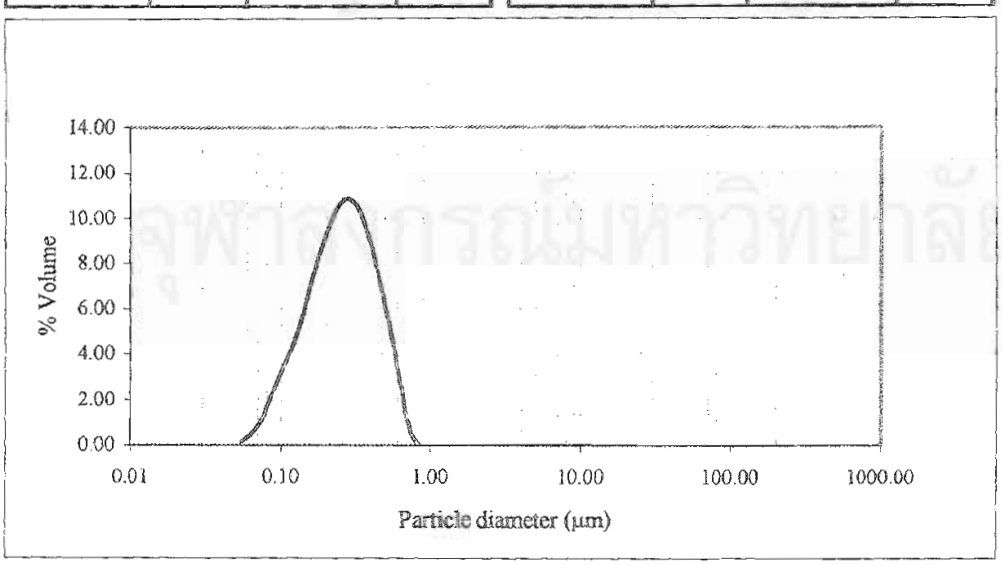

Figure d11 Particle size distribution of formulation 5 GB + 4 TW80 after autoclaving stored at room temperature for 1 month

Table d12 Particle size distribution of formulation 5 GB + 4 TW80 after autoclaving kept in refrigerator for 1 month

Distribution type: volume	D(v,0.1) = 0.15	D(v,0.5) = 0.33	D(v,0.9) = 15.81
Mean diameter	D[4,3] = 5.54	D[3,2] = 0.30	Span = 47.36
% > 1 µm = 24.12	% > 5 µm = 16.28	% > 10 µm = 13.10	Uniformity = 16.11

size low (µm)	size in %	size high (µm)	under %	size low (µm)	size in %	size high (µm)	under %
0.05	0.28	0.06	0.28	6.63	0.71	7.72	85.54
0.06	0.59	0.07	0.87	7.72	0.79	9.00	86.33
0.07	0.92	0.08	1.79	9.00	0.84	10.48	87.17
0.08	1.31	0.09	3.10	10.48	1.21	12.21	88.39
0.09	1.77	0.11	4.87	12.21	0.95	14.22	89.34
0.11	2.37	0.13	7.24	14.22	0.98	16.57	90.32
0.13	3.15	0.15	10.39	16.57	1.00	19.31	91.32
0.15	4.23	0.17	14.62	19.31	1.00	22.49	92.32
0.17	5.67	0.20	20.29	22.49	0.98	26.20	93.29
0.20	7.43	0.23	27.73	26.20	0.93	30.53	94.23
0.23	9.05	0.27	36.77	30.53	0.88	35.56	95.10
0.27	9.62	0.31	46.39	35.56	0.81	41.43	95.91
0.31	8.69	0.36	55.09	41.43	0.75	48.27	96.66
0.36	6.99	0.42	62.07	48.27	0.69	56.23	97.34
0.42	5.34	0.49	67.42	56.23	0.64	65.51	97.99
0.49	3.79	0.58	71.20	65.51	0.42	76.32	98.41
0.58	2.26	0.67	73.46	76.32	0.56	88.91	98.97
0.67	1.13	0.78	74.59	88.91	0.47	103.58	99.44
0.78	0.86	0.91	75.45	103.58	0.34	120.67	99.78
0.91	0.71	1.06	76.16	120.67	0.17	140.58	99.95
1.06	0.71	1.24	76.87	140.58	0.05	163.77	100.00
1.24	0.83	1.44	77.71	163.77	0.00	190.80	100.00
1.44	0.94	1.68	78.65	190.80	0.00	222.28	100.00
1.68	0.97	1.95	79.62	222.28	0.00	258.95	100.00
1.95	0.91	2.28	80.53	258.95	0.00	301.68	100.00
2.28	0.80	2.65	81.33	301.68	0.00	351.46	100.00
2.65	0.69	3.09	82.02	351.46	0.00	409.45	100.00
3.09	0.58	3.60	82.60	409.45	0.00	477.01	100.00
3.60	0.52	4.19	83.12	477.01	0.00	555.71	100.00
4.19	0.52	4.88	83.64	555.71	0.00	647.41	100.00
4.88	0.56	5.69	84.20	647.41	0.00	754.23	100.00
5.69	0.63	6.63	84.83	754.23	0.00	878.67	100.00

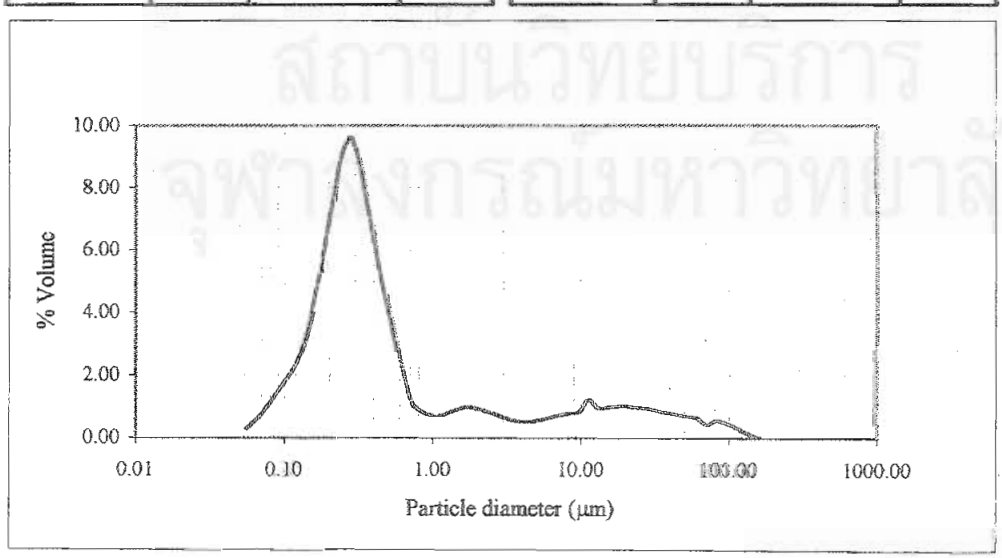

Figure d12 Particle size distribution of formulation 5 GB + 4 TW80 after autoclaving kept in refrigerator for 1 month

Table d13 Particle size distribution of formulation 5 GB + 4 TW80 after autoclaving stored at room temperature for 3 months

Distribution type: volume	D(v,0.1) = 0.12	D(v,0.5) = 0.27	D(v,0.9) = 0.62
Mean diameter	D[4,3] = 0.44	D[3,2] = 0.23	Span = 1.82
% > 1 µm = 7.67	% > 5 µm = 0.00	% > 10 µm = 0.00	Uniformity = 0.94

size low (µm)	size in %	size high (µm)	under %	size low (µm)	size in %	size high (µm)	under %
0.05	0.45	0.06	0.45	6.63	0.00	7.72	100.00
0.06	0.93	0.07	1.38	7.72	0.00	9.00	100.00
0.07	1.46	0.08	2.84	9.00	0.00	10.48	100.00
0.08	2.04	0.09	4.88	10.48	0.00	12.21	100.00
0.09	2.71	0.11	7.59	12.21	0.00	14.22	100.00
0.11	3.53	0.13	11.12	14.22	0.00	16.57	100.00
0.13	4.55	0.15	15.67	16.57	0.00	19.31	100.00
0.15	5.87	0.17	21.54	19.31	0.00	22.49	100.00
0.17	7.52	0.20	29.06	22.49	0.00	26.20	100.00
0.20	9.40	0.23	38.46	26.20	0.00	30.53	100.00
0.23	10.97	0.27	49.44	30.53	0.00	35.56	100.00
0.27	11.31	0.31	60.74	35.56	0.00	41.43	100.00
0.31	10.05	0.36	70.80	41.43	0.00	48.27	100.00
0.36	8.02	0.42	78.82	48.27	0.00	56.23	100.00
0.42	6.07	0.49	84.89	56.23	0.00	65.51	100.00
0.49	4.16	0.58	89.05	65.51	0.00	76.32	100.00
0.58	2.27	0.67	91.32	76.32	0.00	88.91	100.00
0.67	0.85	0.78	92.17	88.91	0.00	103.58	100.00
0.78	0.02	0.91	92.19	103.58	0.00	120.67	100.00
0.91	0.24	1.06	92.42	120.67	0.00	140.58	100.00
1.06	0.47	1.24	92.90	140.58	0.00	163.77	100.00
1.24	0.80	1.44	93.69	163.77	0.00	190.80	100.00
1.44	0.92	1.68	94.61	190.80	0.00	222.28	100.00
1.68	0.95	1.95	95.56	222.28	0.00	258.95	100.00
1.95	0.93	2.28	96.49	258.95	0.00	301.68	100.00
2.28	0.90	2.65	97.39	301.68	0.00	351.46	100.00
2.65	0.87	3.09	98.26	351.46	0.00	409.45	100.00
3.09	0.87	3.60	99.13	409.45	0.00	477.01	100.00
3.60	0.77	4.19	99.90	477.01	0.00	555.71	100.00
4.19	0.10	4.88	100.00	555.71	0.00	647.41	100.00
4.88	0.00	5.69	100.00	647.41	0.00	754.23	100.00
5.69	0.00	6.63	100.00	754.23	0.00	878.67	100.00

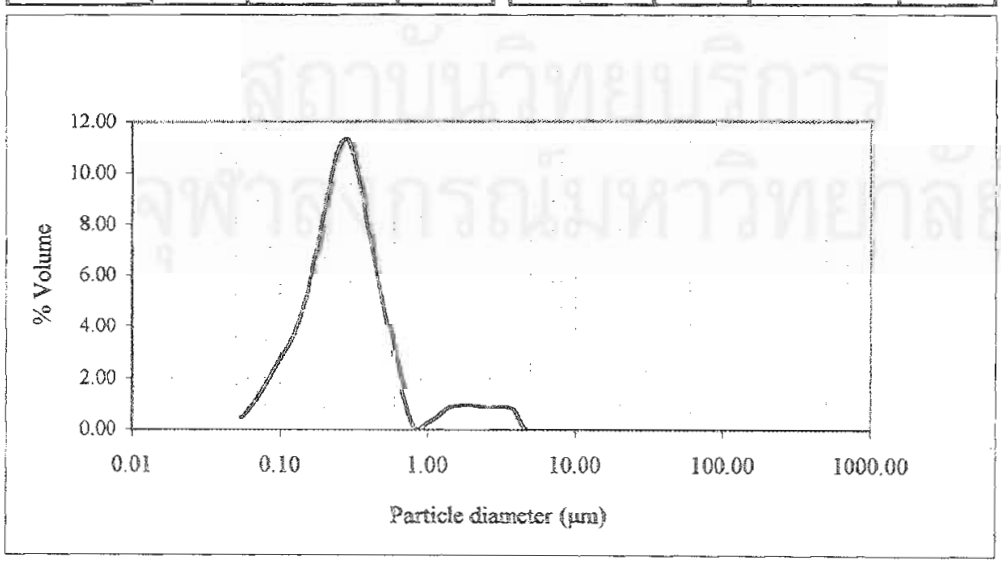

Figure d13 Particle size distribution of formulation 5 GB + 4 TW80 after autoclaving stored at room temperature for 3 months

Table d14 Particle size distribution of formulation 5 GB + 4 TW80 after autoclaving kept in refrigerator for 3 months

Distribution type: volume	D(v,0.1) = 0.24	D(v,0.5) = 0.46	D(v,0.9) = 56.30
Mean diameter	D[4,3] = 15.04	D[3,2] = 0.51	Span = 121.14
% > 1 μm = 42.57	% > 5 μm = 36.13	% > 10 μm = 31.00	Uniformity = 31.84

size low (μm)	size in %	size high (μm)	under %	size low (μm)	size in %	size high (μm)	under %
0.05	0.00	0.06	0.00	6.63	1.15	7.72	66.89
0.06	0.02	0.07	0.02	7.72	1.23	9.00	68.12
0.07	0.03	0.08	0.05	9.00	1.31	10.48	69.43
0.08	0.05	0.09	0.10	10.48	1.88	12.21	71.30
0.09	0.09	0.11	0.19	12.21	1.54	14.22	72.84
0.11	0.17	0.13	0.36	14.22	1.66	16.57	74.50
0.13	0.33	0.15	0.69	16.57	1.76	19.31	76.26
0.15	0.73	0.17	1.41	19.31	1.85	22.49	78.12
0.17	1.75	0.20	3.16	22.49	1.89	26.20	80.00
0.20	4.27	0.23	7.43	26.20	1.90	30.53	81.90
0.23	8.90	0.27	16.33	30.53	1.90	35.56	83.81
0.27	12.55	0.31	28.88	35.56	1.93	41.43	85.74
0.31	10.92	0.36	39.80	41.43	2.03	48.27	87.77
0.36	7.21	0.42	47.02	48.27	2.21	56.23	89.98
0.42	4.88	0.49	51.90	56.23	2.49	65.51	92.47
0.49	3.14	0.58	55.04	65.51	1.94	76.32	94.41
0.58	1.42	0.67	56.46	76.32	3.19	88.91	97.60
0.67	0.55	0.78	57.01	88.91	0.87	103.58	98.47
0.78	0.30	0.91	57.32	103.58	0.69	120.67	99.16
0.91	0.19	1.06	57.51	120.67	0.43	140.58	99.59
1.06	0.17	1.24	57.68	140.58	0.20	163.77	99.79
1.24	0.48	1.44	58.16	163.77	0.08	190.80	99.87
1.44	0.58	1.68	58.73	190.80	0.04	222.28	99.90
1.68	0.63	1.95	59.36	222.28	0.04	258.95	99.94
1.95	0.66	2.28	60.02	258.95	0.06	301.68	100.00
2.28	0.67	2.65	60.70	301.68	0.00	351.46	100.00
2.65	0.69	3.09	61.38	351.46	0.00	409.45	100.00
3.09	0.71	3.60	62.09	409.45	0.00	477.01	100.00
3.60	0.78	4.19	62.87	477.01	0.00	555.71	100.00
4.19	0.86	4.88	63.73	555.71	0.00	647.41	100.00
4.88	0.96	5.69	64.69	647.41	0.00	754.23	100.00
5.69	1.06	6.63	65.74	754.23	0.00	878.67	100.00

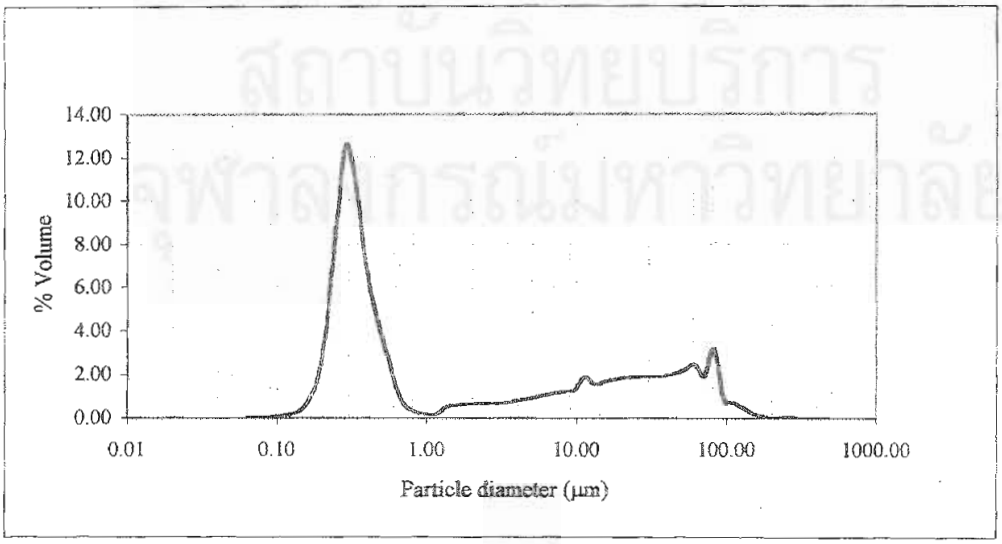

Figure d14 Particle size distribution of formulation 5 GB + 4 TW80 after autoclaving kept in refrigerator for 3 months

Table d15 Particle size distribution of formulation 5 GB + 4 TW80 after autoclaving stored at room temperature for 6 months

Distribution type: volume	D(v,0.1) = 0.15	D(v,0.5) = 0.29	D(v,0.9) = 0.50
Mean diameter	D[4,3] = 0.31	D[3,2] = 0.25	Span = 1.18
% > 1 μm = 0.00	% > 5 μm = 0.00	% > 10 μm = 0.00	Uniformity = 0.35

size low (μm)	size in %	size high (μm)	under %	size low (μm)	size in %	size high (μm)	under %
0.05	0.21	0.06	0.21	6.63	0.00	7.72	100.00
0.06	0.45	0.07	0.65	7.72	0.00	9.00	100.00
0.07	0.72	0.08	1.37	9.00	0.00	10.48	100.00
0.08	1.07	0.09	2.44	10.48	0.00	12.21	100.00
0.09	1.51	0.11	3.94	12.21	0.00	14.22	100.00
0.11	2.13	0.13	6.07	14.22	0.00	16.57	100.00
0.13	3.06	0.15	9.14	16.57	0.00	19.31	100.00
0.15	4.49	0.17	13.62	19.31	0.00	22.49	100.00
0.17	6.67	0.20	20.29	22.49	0.00	26.20	100.00
0.20	9.70	0.23	29.99	26.20	0.00	30.53	100.00
0.23	12.93	0.27	42.93	30.53	0.00	35.56	100.00
0.27	14.54	0.31	57.46	35.56	0.00	41.43	100.00
0.31	13.34	0.36	70.80	41.43	0.00	48.27	100.00
0.36	10.65	0.42	81.45	48.27	0.00	56.23	100.00
0.42	8.15	0.49	89.61	56.23	0.00	65.51	100.00
0.49	5.80	0.58	95.41	65.51	0.00	76.32	100.00
0.58	3.29	0.67	98.70	76.32	0.00	88.91	100.00
0.67	1.30	0.78	100.00	88.91	0.00	103.58	100.00
0.78	0.00	0.91	100.00	103.58	0.00	120.67	100.00
0.91	0.00	1.06	100.00	120.67	0.00	140.58	100.00
1.06	0.00	1.24	100.00	140.58	0.00	163.77	100.00
1.24	0.00	1.44	100.00	163.77	0.00	190.80	100.00
1.44	0.00	1.68	100.00	190.80	0.00	222.28	100.00
1.68	0.00	1.95	100.00	222.28	0.00	258.95	100.00
1.95	0.00	2.28	100.00	258.95	0.00	301.68	100.00
2.28	0.00	2.65	100.00	301.68	0.00	351.46	100.00
2.65	0.00	3.09	100.00	351.46	0.00	409.45	100.00
3.09	0.00	3.60	100.00	409.45	0.00	477.01	100.00
3.60	0.00	4.19	100.00	477.01	0.00	555.71	100.00
4.19	0.00	4.88	100.00	555.71	0.00	647.41	100.00
4.88	0.00	5.69	100.00	647.41	0.00	754.23	100.00
5.69	0.00	6.63	100.00	754.23	0.00	878.67	100.00

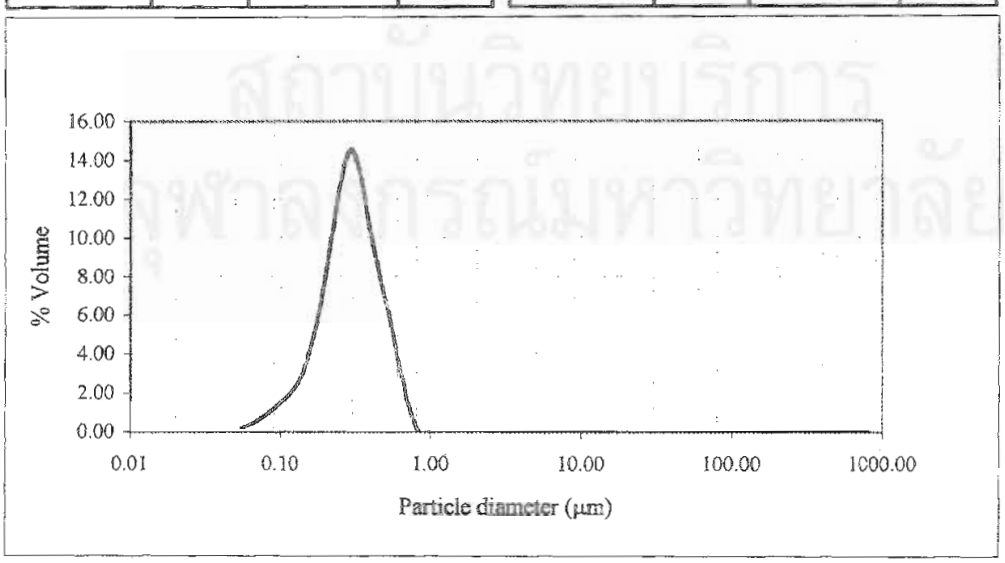

Figure d15 Particle size distribution of formulation 5 GB + 4 TW80 after autoclaving stored at room temperature for 6 months

Table d16 Particle size distribution of formulation 5 GB + 4 TW80 after autoclaving kept in refrigerator for 6 months

Distribution type: volume	D(v,0.1) = 0.16	D(v,0.5) = 0.30	D(v,0.9) = 0.57
Mean diameter	D[4,3] = 0.39	D[3,2] = 0.27	Span = 1.35
% > 1 μm = 3.17	% > 5 μm = 0.00	% > 10 μm = 0.00	Uniformity = 0.58

size low (μm)	size in %	size high (μm)	under %	size low (μm)	size in %	size high (μm)	under %
0.05	0.04	0.06	0.04	6.63	0.00	7.72	100.00
0.06	0.20	0.07	0.24	7.72	0.00	9.00	100.00
0.07	0.45	0.08	0.70	9.00	0.00	10.48	100.00
0.08	0.83	0.09	1.53	10.48	0.00	12.21	100.00
0.09	1.37	0.11	2.90	12.21	0.00	14.22	100.00
0.11	2.12	0.13	5.02	14.22	0.00	16.57	100.00
0.13	3.14	0.15	8.17	16.57	0.00	19.31	100.00
0.15	4.55	0.17	12.72	19.31	0.00	22.49	100.00
0.17	6.47	0.20	19.19	22.49	0.00	26.20	100.00
0.20	8.84	0.23	28.02	26.20	0.00	30.53	100.00
0.23	11.24	0.27	39.27	30.53	0.00	35.56	100.00
0.27	12.67	0.31	51.94	35.56	0.00	41.43	100.00
0.31	12.39	0.36	64.33	41.43	0.00	48.27	100.00
0.36	10.84	0.42	75.17	48.27	0.00	56.23	100.00
0.42	8.92	0.49	84.09	56.23	0.00	65.51	100.00
0.49	6.69	0.58	90.78	65.51	0.00	76.32	100.00
0.58	4.10	0.67	94.88	76.32	0.00	88.91	100.00
0.67	1.82	0.78	96.69	88.91	0.00	103.58	100.00
0.78	0.14	0.91	96.84	103.58	0.00	120.67	100.00
0.91	0.00	1.06	96.83	120.67	0.00	140.58	100.00
1.06	0.00	1.24	96.84	140.58	0.00	163.77	100.00
1.24	0.00	1.44	96.84	163.77	0.00	190.80	100.00
1.44	0.36	1.68	97.20	190.80	0.00	222.28	100.00
1.68	0.58	1.95	97.78	222.28	0.00	258.95	100.00
1.95	0.64	2.28	98.42	258.95	0.00	301.68	100.00
2.28	0.57	2.65	98.99	301.68	0.00	351.46	100.00
2.65	0.44	3.09	99.43	351.46	0.00	409.45	100.00
3.09	0.32	3.60	99.75	409.45	0.00	477.01	100.00
3.60	0.25	4.19	100.00	477.01	0.00	555.71	100.00
4.19	0.00	4.88	100.00	555.71	0.00	647.41	100.00
4.88	0.00	5.69	100.00	647.41	0.00	754.23	100.00
5.69	0.00	6.63	100.00	754.23	0.00	878.67	100.00

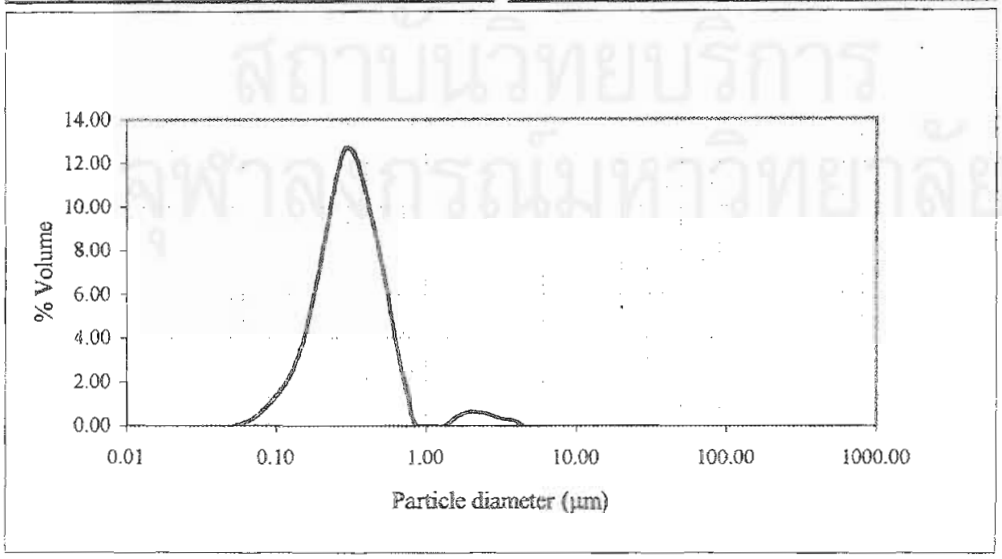

Figure d16 Particle size distribution of formulation 5 GB + 4 TW80 after autoclaving kept in refrigerator for 6 months

Table d17 Particle size distribution of formulation 1 GB + 4 TW80 before autoclaving

Distribution type: volume	D(v,0.1) = 0.18	D(v,0.5) = 0.37	D(v,0.9) = 0.77
Mean diameter	D[4,3] = 0.44	D[3,2] = 0.32	Span = 1.58
% > 1 μm = 3.75	% > 5 μm = 0.00	% > 10 μm = 0.00	Uniformity = 0.50

size low (μm)	size in %	size high (μm)	under %	size low (μm)	size in %	size high (μm)	under %
0.05	0.10	0.06	0.10	6.63	0.00	7.72	100.00
0.06	0.24	0.07	0.34	7.72	0.00	9.00	100.00
0.07	0.40	0.08	0.74	9.00	0.00	10.48	100.00
0.08	0.61	0.09	1.35	10.48	0.00	12.21	100.00
0.09	0.88	0.11	2.22	12.21	0.00	14.22	100.00
0.11	1.26	0.13	3.48	14.22	0.00	16.57	100.00
0.13	1.83	0.15	5.31	16.57	0.00	19.31	100.00
0.15	2.71	0.17	8.02	19.31	0.00	22.49	100.00
0.17	4.08	0.20	12.10	22.49	0.00	26.20	100.00
0.20	6.09	0.23	18.19	26.20	0.00	30.53	100.00
0.23	8.51	0.27	26.70	30.53	0.00	35.56	100.00
0.27	10.34	0.31	37.04	35.56	0.00	41.43	100.00
0.31	10.69	0.36	47.73	41.43	0.00	48.27	100.00
0.36	10.08	0.42	57.81	48.27	0.00	56.23	100.00
0.42	9.62	0.49	67.43	56.23	0.00	65.51	100.00
0.49	9.06	0.58	76.49	65.51	0.00	76.32	100.00
0.58	7.64	0.67	84.13	76.32	0.00	88.91	100.00
0.67	6.16	0.78	90.29	88.91	0.00	103.58	100.00
0.78	4.32	0.91	94.61	103.58	0.00	120.67	100.00
0.91	2.74	1.06	97.35	120.67	0.00	140.58	100.00
1.06	1.50	1.24	98.84	140.58	0.00	163.77	100.00
1.24	0.67	1.44	99.52	163.77	0.00	190.80	100.00
1.44	0.25	1.68	99.76	190.80	0.00	222.28	100.00
1.68	0.10	1.95	99.86	222.28	0.00	258.95	100.00
1.95	0.03	2.28	99.89	258.95	0.00	301.68	100.00
2.28	0.00	2.65	99.89	301.68	0.00	351.46	100.00
2.65	0.02	3.09	99.92	351.46	0.00	409.45	100.00
3.09	0.08	3.60	100.00	409.45	0.00	477.01	100.00
3.60	0.00	4.19	100.00	477.01	0.00	555.71	100.00
4.19	0.00	4.88	100.00	555.71	0.00	647.41	100.00
4.88	0.00	5.69	100.00	647.41	0.00	754.23	100.00
5.69	0.00	6.63	100.00	754.23	0.00	878.67	100.00

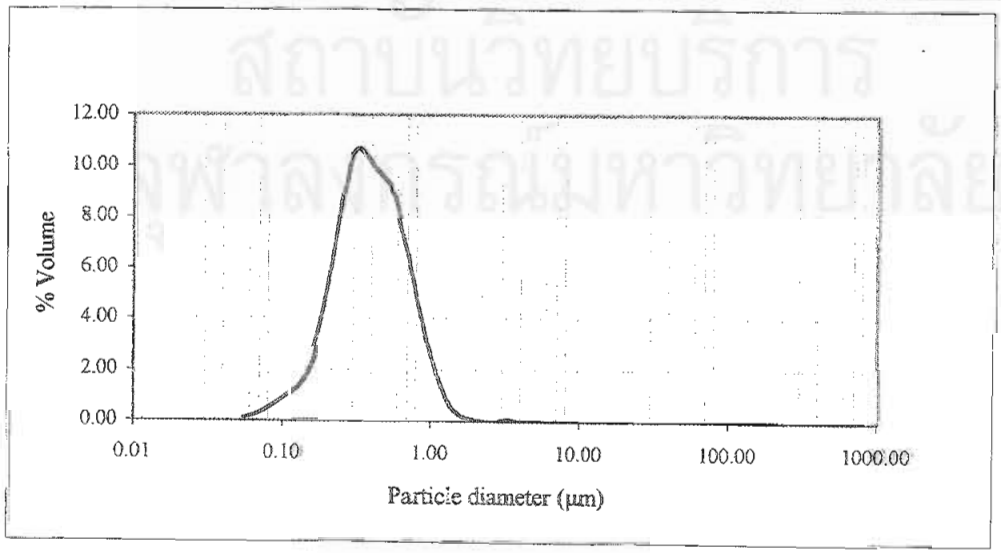

Figure d17 Particle size distribution of formulation 1 GB + 4 TW80 before autoclaving

Table d18 Particle size distribution of formulation 1 GB + 4 TW80 after autoclaving

Distribution type: volume	D(v,0.1) = 0.11	D(v,0.5) = 0.26	D(v,0.9) = 0.60
Mean diameter	D[4,3] = 0.40	D[3,2] = 0.22	Span = 1.85
% > 1 µm = 5.83	% > 5 µm = 0.00	% > 10 µm = 0.00	Uniformity = 0.88

size low (µm)	size in %	size high (µm)	under %	size low (µm)	size in %	size high (µm)	under %
0.05	0.57	0.06	0.57	6.63	0.00	7.72	100.00
0.06	1.16	0.07	1.73	7.72	0.00	9.00	100.00
0.07	1.79	0.08	3.51	9.00	0.00	10.48	100.00
0.08	2.46	0.09	5.97	10.48	0.00	12.21	100.00
0.09	3.20	0.11	9.17	12.21	0.00	14.22	100.00
0.11	4.05	0.13	13.22	14.22	0.00	16.57	100.00
0.13	5.04	0.15	18.26	16.57	0.00	19.31	100.00
0.15	6.24	0.17	24.50	19.31	0.00	22.49	100.00
0.17	7.66	0.20	32.16	22.49	0.00	26.20	100.00
0.20	9.17	0.23	41.33	26.20	0.00	30.53	100.00
0.23	10.35	0.27	51.68	30.53	0.00	35.56	100.00
0.27	10.50	0.31	62.18	35.56	0.00	41.43	100.00
0.31	9.40	0.36	71.58	41.43	0.00	48.27	100.00
0.36	7.65	0.42	79.23	48.27	0.00	56.23	100.00
0.42	5.93	0.49	85.16	56.23	0.00	65.51	100.00
0.49	4.22	0.58	89.38	65.51	0.00	76.32	100.00
0.58	2.52	0.67	91.90	76.32	0.00	88.91	100.00
0.67	1.22	0.78	93.12	88.91	0.00	103.58	100.00
0.78	0.77	0.91	93.89	103.58	0.00	120.67	100.00
0.91	0.47	1.06	94.36	120.67	0.00	140.58	100.00
1.06	0.34	1.24	94.70	140.58	0.00	163.77	100.00
1.24	0.36	1.44	95.06	163.77	0.00	190.80	100.00
1.44	0.47	1.68	95.52	190.80	0.00	222.28	100.00
1.68	0.60	1.95	96.12	222.28	0.00	258.95	100.00
1.95	0.74	2.28	96.87	258.95	0.00	301.68	100.00
2.28	0.87	2.65	97.74	301.68	0.00	351.46	100.00
2.65	1.03	3.09	98.77	351.46	0.00	409.45	100.00
3.09	1.23	3.60	100.00	409.45	0.00	477.01	100.00
3.60	0.00	4.19	100.00	477.01	0.00	555.71	100.00
4.19	0.00	4.88	100.00	555.71	0.00	647.41	100.00
4.88	0.00	5.69	100.00	647.41	0.00	754.23	100.00
5.69	0.00	6.63	100.00	754.23	0.00	878.67	100.00

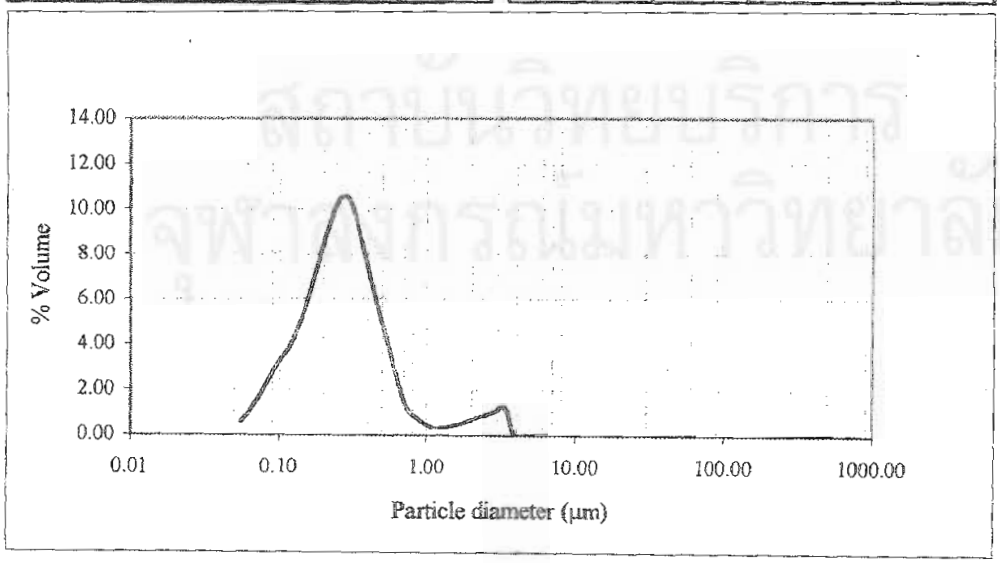

Figure d18 Particle size distribution of formulation 1 GB + 4 TW80 after autoclaving

Table d19 Particle size distribution of formulation 3 GB + 4 TW80 before autoclaving

Distribution type: volume	D(v,0.1) = 0.14	D(v,0.5) = 0.29	D(v,0.9) = 4.67
Mean diameter	D[4,3] = 2.59	D[3,2] = 0.25	Span = 15.90
% > 1 µm = 15.74	% > 5 µm = 9.71	% > 10 µm = 6.75	Uniformity = 8.42

size low (µm)	size in %	size high (µm)	under %	size low (µm)	size in %	size high (µm)	under %
0.05	0.37	0.06	0.37	6.63	0.64	7.72	92.10
0.06	0.74	0.07	1.11	7.72	0.67	9.00	92.77
0.07	1.16	0.08	2.27	9.00	0.72	10.48	93.48
0.08	1.61	0.09	3.88	10.48	0.77	12.21	94.25
0.09	2.16	0.11	6.04	12.21	0.81	14.22	95.07
0.11	2.87	0.13	8.91	14.22	0.83	16.57	95.90
0.13	3.82	0.15	12.73	16.57	0.79	19.31	96.68
0.15	5.17	0.17	17.90	19.31	0.69	22.49	97.38
0.17	7.04	0.20	24.94	22.49	0.56	26.20	97.93
0.20	9.34	0.23	34.27	26.20	0.43	30.53	98.37
0.23	11.34	0.27	45.61	30.53	0.25	35.56	98.62
0.27	11.59	0.31	57.20	35.56	0.23	41.43	98.85
0.31	9.68	0.36	66.89	41.43	0.23	48.27	99.09
0.36	7.04	0.42	73.92	48.27	0.23	56.23	99.32
0.42	4.88	0.49	78.80	56.23	0.21	65.51	99.53
0.49	3.08	0.58	81.88	65.51	0.16	76.32	99.69
0.58	1.50	0.67	83.38	76.32	0.11	88.91	99.80
0.67	0.53	0.78	83.91	88.91	0.06	103.58	99.86
0.78	0.27	0.91	84.18	103.58	0.03	120.67	99.88
0.91	0.13	1.06	84.31	120.67	0.01	140.58	99.89
1.06	0.07	1.24	84.38	140.58	0.00	163.77	99.90
1.24	0.37	1.44	84.76	163.77	0.01	190.80	99.91
1.44	0.51	1.68	85.27	190.80	0.01	222.28	99.92
1.68	0.64	1.95	85.91	222.28	0.02	258.95	99.94
1.95	0.73	2.28	86.64	258.95	0.06	301.68	100.00
2.28	0.76	2.65	87.39	301.68	0.00	351.46	100.00
2.65	0.75	3.09	88.14	351.46	0.00	409.45	100.00
3.09	0.72	3.60	88.86	409.45	0.00	477.01	100.00
3.60	0.68	4.19	89.54	477.01	0.00	555.71	100.00
4.19	0.66	4.88	90.20	555.71	0.00	647.41	100.00
4.88	0.63	5.69	90.83	647.41	0.00	754.23	100.00
5.69	0.63	6.63	91.46	754.23	0.00	878.67	100.00

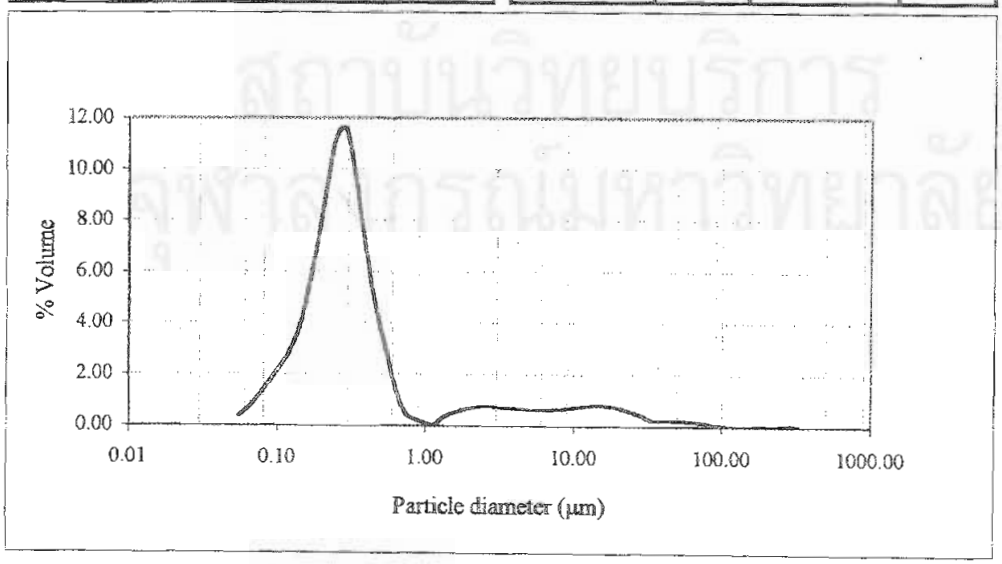

Figure d19 Particle size distribution of formulation 3 GB + 4 TW80 before autoclaving

Table d20 Particle size distribution of formulation 3 GB + 4 TW80 after autoclaving

Distribution type: volume	D(v,0.1) = 0.10	D(v,0.5) = 0.23	D(v,0.9) = 0.42
Mean diameter	D[4,3] = 0.26	D[3,2] = 0.19	Span = 1.36
% > 1 µm = 0.09	% > 5 µm = 0.00	% > 10 µm = 0.00	Uniformity = 0.45

size low (µm)	size in %	size high (µm)	under %	size low (µm)	size in %	size high (µm)	under %
0.05	0.74	0.06	0.74	6.63	0.00	7.72	100.00
0.06	1.46	0.07	2.20	7.72	0.00	9.00	100.00
0.07	2.20	0.08	4.39	9.00	0.00	10.48	100.00
0.08	2.96	0.09	7.35	10.48	0.00	12.21	100.00
0.09	3.79	0.11	11.14	12.21	0.00	14.22	100.00
0.11	4.75	0.13	15.90	14.22	0.00	16.57	100.00
0.13	5.92	0.15	21.82	16.57	0.00	19.31	100.00
0.15	7.38	0.17	29.20	19.31	0.00	22.49	100.00
0.17	9.15	0.20	38.35	22.49	0.00	26.20	100.00
0.20	11.03	0.23	49.38	26.20	0.00	30.53	100.00
0.23	12.27	0.27	61.66	30.53	0.00	35.56	100.00
0.27	11.84	0.31	73.50	35.56	0.00	41.43	100.00
0.31	9.65	0.36	83.14	41.43	0.00	48.27	100.00
0.36	6.95	0.42	90.09	48.27	0.00	56.23	100.00
0.42	4.73	0.49	94.82	56.23	0.00	65.51	100.00
0.49	2.91	0.58	97.73	65.51	0.00	76.32	100.00
0.58	1.40	0.67	99.13	76.32	0.00	88.91	100.00
0.67	0.48	0.78	99.61	88.91	0.00	103.58	100.00
0.78	0.24	0.91	99.85	103.58	0.00	120.67	100.00
0.91	0.10	1.06	99.95	120.67	0.00	140.58	100.00
1.06	0.04	1.24	100.00	140.58	0.00	163.77	100.00
1.24	0.00	1.44	100.00	163.77	0.00	190.80	100.00
1.44	0.00	1.68	100.00	190.80	0.00	222.28	100.00
1.68	0.00	1.95	100.00	222.28	0.00	258.95	100.00
1.95	0.00	2.28	100.00	258.95	0.00	301.68	100.00
2.28	0.00	2.65	100.00	301.68	0.00	351.46	100.00
2.65	0.00	3.09	100.00	351.46	0.00	409.45	100.00
3.09	0.00	3.60	100.00	409.45	0.00	477.01	100.00
3.60	0.00	4.19	100.00	477.01	0.00	555.71	100.00
4.19	0.00	4.88	100.00	555.71	0.00	647.41	100.00
4.88	0.00	5.69	100.00	647.41	0.00	754.23	100.00
5.69	0.00	6.63	100.00	754.23	0.00	878.67	100.00

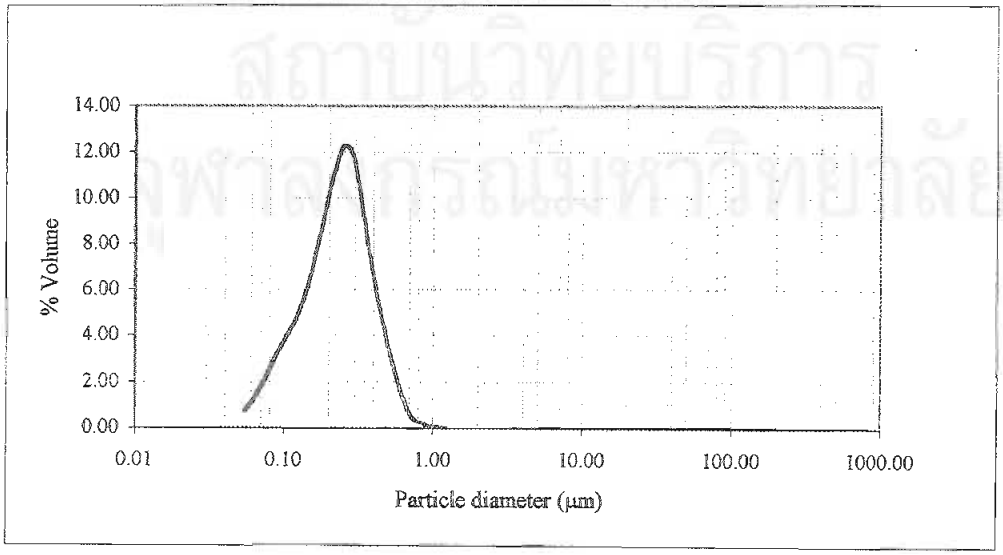

Figure d20 Particle size distribution of formulation 3 GB + 4 TW80 after autoclaving

Table d21 Particle size distribution of formulation 7 GB + 4 TW80 before autoclaving

Distribution type: volume	D(v,0.1) = 0.17	D(v,0.5) = 0.33	D(v,0.9) = 0.65
Mean diameter	D[4,3] = 0.74	D[3,2] = 0.30	Span = 1.45
% > 1 µm = 6.73	% > 5 µm = 2.69	% > 10 µm = 1.34	Uniformity = 1.53

size low (µm)	size in %	size high (µm)	under %
0.05	0.02	0.06	0.02
0.06	0.09	0.07	0.11
0.07	0.23	0.08	0.34
0.08	0.48	0.09	0.82
0.09	0.87	0.11	1.69
0.11	1.46	0.13	3.16
0.13	2.35	0.15	5.50
0.15	3.62	0.17	9.13
0.17	5.44	0.20	14.57
0.20	7.81	0.23	22.38
0.23	10.37	0.27	32.74
0.27	12.17	0.31	44.91
0.31	12.40	0.36	57.31
0.36	11.36	0.42	68.67
0.42	9.78	0.49	78.45
0.49	7.62	0.58	86.07
0.58	4.79	0.67	90.87
0.67	2.19	0.78	93.06
0.78	0.21	0.91	93.27
0.91	0.00	1.06	93.27
1.06	0.00	1.24	93.27
1.24	0.13	1.44	93.41
1.44	0.44	1.68	93.84
1.68	0.60	1.95	94.44
1.95	0.64	2.28	95.09
2.28	0.59	2.65	95.67
2.65	0.50	3.09	96.18
3.09	0.41	3.60	96.59
3.60	0.36	4.19	96.95
4.19	0.32	4.88	97.27
4.88	0.31	5.69	97.57
5.69	0.30	6.63	97.88
6.63	0.30	7.72	98.18
7.72	0.29	9.00	98.47
9.00	0.29	10.48	98.76
10.48	0.27	12.21	99.03
12.21	0.27	14.22	99.30
14.22	0.17	16.57	99.47
16.57	0.17	19.31	99.64
19.31	0.17	22.49	99.81
22.49	0.09	26.20	99.90
26.20	0.10	30.53	100.00
30.53	0.00	35.56	100.00
35.56	0.00	41.43	100.00
41.43	0.00	48.27	100.00
48.27	0.00	56.23	100.00
56.23	0.00	65.51	100.00
65.51	0.00	76.32	100.00
76.32	0.00	88.91	100.00
88.91	0.00	103.58	100.00
103.58	0.00	120.67	100.00
120.67	0.00	140.58	100.00
140.58	0.00	163.77	100.00
163.77	0.00	190.80	100.00
190.80	0.00	222.28	100.00
222.28	0.00	258.95	100.00
258.95	0.00	301.68	100.00
301.68	0.00	351.46	100.00
351.46	0.00	409.45	100.00
409.45	0.00	477.01	100.00
477.01	0.00	555.71	100.00
555.71	0.00	647.41	100.00
647.41	0.00	754.23	100.00
754.23	0.00	878.67	100.00

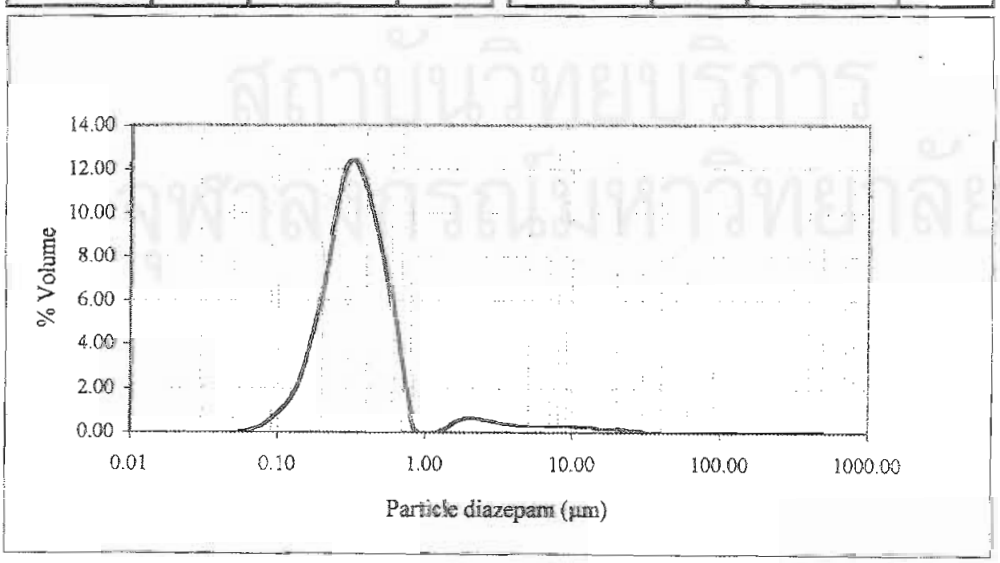

Figure d21 Particle size distribution of formulation 7 GB + 4 TW80 before autoclaving

Table d22 Particle size distribution of formulation 7 GB + 4 TW80 after autoclaving

Distribution type: volume	D(v,0.1) = 0.19	D(v,0.5) = 0.34	D(v,0.9) = 3.09
Mean diameter	D[4,3] = 3.68	D[3,2] = 0.33	Span = 8.56
% > 1 μm = 12.75	% > 5 μm = 9.12	% > 10 μm = 7.49	Uniformity = 10.15

size low (μm)	size in %	size high (μm)	under %
0.05	0.01	0.06	0.01
0.06	0.06	0.07	0.07
0.07	0.15	0.08	0.22
0.08	0.31	0.09	0.52
0.09	0.56	0.11	1.08
0.11	0.98	0.13	2.06
0.13	1.66	0.15	3.72
0.15	2.79	0.17	6.51
0.17	4.68	0.20	11.19
0.20	7.54	0.23	18.74
0.23	10.95	0.27	29.69
0.27	13.18	0.31	42.87
0.31	12.73	0.36	55.60
0.36	10.63	0.42	66.22
0.42	8.52	0.49	74.75
0.49	6.29	0.58	81.04
0.58	3.72	0.67	84.76
0.67	1.82	0.78	86.58
0.78	0.59	0.91	87.17
0.91	0.12	1.06	87.30
1.06	0.11	1.24	87.40
1.24	0.32	1.44	87.72
1.44	0.49	1.68	88.21
1.68	0.54	1.95	88.75
1.95	0.50	2.28	89.25
2.28	0.42	2.65	89.67
2.65	0.34	3.09	90.00
3.09	0.28	3.60	90.28
3.60	0.27	4.19	90.55
4.19	0.28	4.88	90.83
4.88	0.31	5.69	91.14
5.69	0.34	6.63	91.48
6.63	0.37	7.72	91.86
7.72	0.39	9.00	92.25
9.00	0.40	10.48	92.64
10.48	0.57	12.21	93.21
12.21	0.45	14.22	93.66
14.22	0.48	16.57	94.14
16.57	0.51	19.31	94.65
19.31	0.54	22.49	95.18
22.49	0.55	26.20	95.74
26.20	0.55	30.53	96.29
30.53	0.53	35.56	96.82
35.56	0.50	41.43	97.32
41.43	0.47	48.27	97.79
48.27	0.43	56.23	98.22
56.23	0.40	65.51	98.62
65.51	0.22	76.32	98.83
76.32	0.36	88.91	99.19
88.91	0.31	103.58	99.50
103.58	0.24	120.67	99.75
120.67	0.14	140.58	99.88
140.58	0.06	163.77	99.95
163.77	0.02	190.80	99.96
190.80	0.00	222.28	99.96
222.28	0.00	258.95	99.96
258.95	0.04	301.68	100.00
301.68	0.00	351.46	100.00
351.46	0.00	409.45	100.00
409.45	0.00	477.01	100.00
477.01	0.00	555.71	100.00
555.71	0.00	647.41	100.00
647.41	0.00	754.23	100.00
754.23	0.00	878.67	100.00

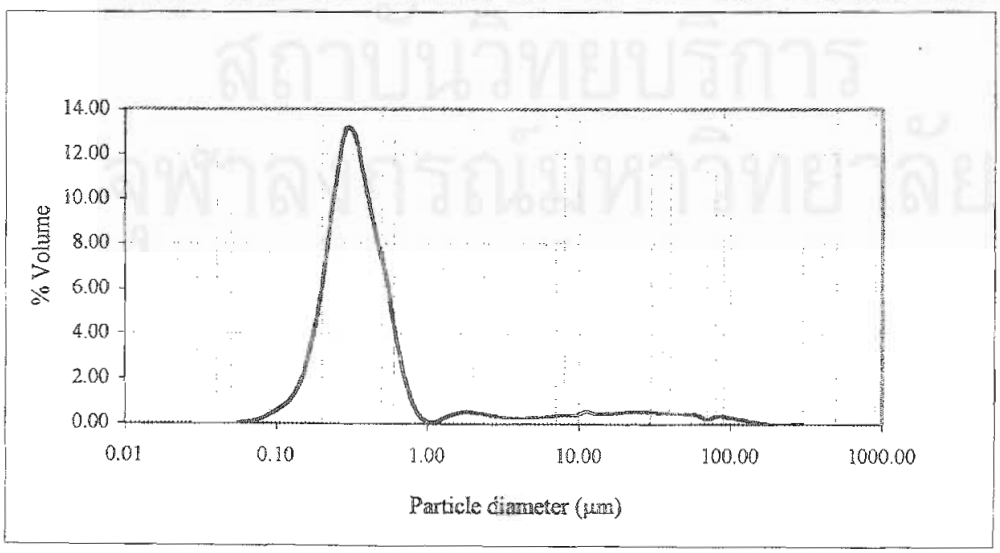

Figure d22 Particle size distribution of formulation 7 GB + 4 TW80 after autoclaving

Table d23 Particle size distribution of formulation 9 GB + 4 TW80 before autoclaving

Distribution type: volume	D(v,0.1) = 0.21	D(v,0.5) = 0.35	D(v,0.9) = 0.87
Mean diameter	D[4,3] = 4.87	D[3,2] = 0.34	Span = 1.87
% > 1 µm = 9.70	% > 5 µm = 5.97	% > 10 µm = 5.02	Uniformity = 13.15

size low (µm)	size in %	size high (µm)	under %	size low (µm)	size in %	size high (µm)	under %
0.05	0.00	0.06	0.00	6.63	0.21	7.72	94.68
0.06	0.02	0.07	0.02	7.72	0.19	9.00	94.87
0.07	0.06	0.08	0.08	9.00	0.17	10.48	95.04
0.08	0.13	0.09	0.21	10.48	0.23	12.21	95.27
0.09	0.25	0.11	0.46	12.21	0.15	14.22	95.42
0.11	0.49	0.13	0.95	14.22	0.08	16.57	95.50
0.13	0.93	0.15	1.88	16.57	0.10	19.31	95.60
0.15	1.79	0.17	3.68	19.31	0.10	22.49	95.70
0.17	3.45	0.20	7.12	22.49	0.11	26.20	95.81
0.20	6.42	0.23	13.54	26.20	0.14	30.53	95.95
0.23	10.64	0.27	24.18	30.53	0.16	35.56	96.11
0.27	14.11	0.31	38.29	35.56	0.18	41.43	96.29
0.31	14.37	0.36	52.66	41.43	0.21	48.27	96.50
0.36	12.31	0.42	64.97	48.27	0.25	56.23	96.75
0.42	10.15	0.49	75.12	56.23	0.29	65.51	97.04
0.49	7.67	0.58	82.79	65.51	0.34	76.32	97.38
0.58	4.53	0.67	87.32	76.32	0.38	88.91	97.76
0.67	2.20	0.78	89.52	88.91	0.42	103.58	98.18
0.78	0.71	0.91	90.22	103.58	0.45	120.67	98.63
0.91	0.12	1.06	90.34	120.67	0.44	140.58	99.06
1.06	0.04	1.24	90.38	140.58	0.38	163.77	99.44
1.24	0.21	1.44	90.59	163.77	0.29	190.80	99.73
1.44	0.41	1.68	91.00	190.80	0.18	222.28	99.91
1.68	0.70	1.95	91.70	222.28	0.08	258.95	99.99
1.95	0.54	2.28	92.24	258.95	0.01	301.68	100.00
2.28	0.49	2.65	92.73	301.68	0.00	351.46	100.00
2.65	0.31	3.09	93.03	351.46	0.00	409.45	100.00
3.09	0.37	3.60	93.40	409.45	0.00	477.01	100.00
3.60	0.31	4.19	93.72	477.01	0.00	555.71	100.00
4.19	0.27	4.88	93.99	555.71	0.00	647.41	100.00
4.88	0.25	5.69	94.24	647.41	0.00	754.23	100.00
5.69	0.22	6.63	94.46	754.23	0.00	878.67	100.00

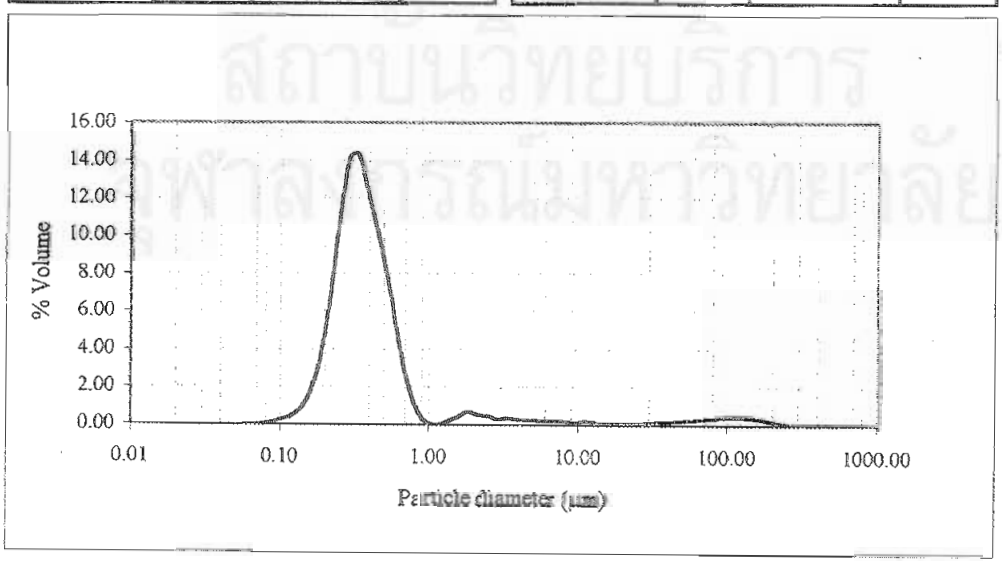

Figure d23 Particle size distribution of formulation 9 GB + 4 TW80 before autoclaving

Table d24 Particle size distribution of formulation 9 GB + 4 TW80 after autoclaving

Distribution type: volume	D(v,0.1) = 0.21	D(v,0.5) = 0.36	D(v,0.9) = 1.19
Mean diameter	D[4,3] = 10.70	D[3,2] = 0.35	Span = 2.73
% > 1 μm = 10.99	% > 5 μm = 6.91	% > 10 μm = 5.97	Uniformity = 29.00

size low (μm)	size in %	size high (μm)	under %
0.05	0.00	0.06	0.00
0.06	0.02	0.07	0.02
0.07	0.06	0.08	0.08
0.08	0.13	0.09	0.21
0.09	0.25	0.11	0.46
0.11	0.49	0.13	0.95
0.13	0.93	0.15	1.88
0.15	1.79	0.17	3.68
0.17	3.45	0.20	7.12
0.20	6.42	0.23	13.54
0.23	10.64	0.27	24.18
0.27	14.11	0.31	38.29
0.31	14.37	0.36	52.66
0.36	12.31	0.42	64.97
0.42	10.15	0.49	75.12
0.49	7.67	0.58	82.79
0.58	4.53	0.67	87.32
0.67	2.20	0.78	89.52
0.78	0.71	0.91	90.22
0.91	0.12	1.06	90.34
1.06	0.04	1.24	90.38
1.24	0.21	1.44	90.59
1.44	0.41	1.68	91.00
1.68	0.70	1.95	91.70
1.95	0.54	2.28	92.24
2.28	0.49	2.65	92.73
2.65	0.31	3.09	93.03
3.09	0.37	3.60	93.40
3.60	0.31	4.19	93.72
4.19	0.27	4.88	93.99
4.88	0.25	5.69	94.24
5.69	0.22	6.63	94.46
6.63	0.21	7.72	94.68
7.72	0.19	9.00	94.87
9.00	0.17	10.48	95.04
10.48	0.23	12.21	95.27
12.21	0.15	14.22	95.42
14.22	0.08	16.57	95.50
16.57	0.10	19.31	95.60
19.31	0.10	22.49	95.70
22.49	0.11	26.20	95.81
26.20	0.14	30.53	95.95
30.53	0.16	35.56	96.11
35.56	0.18	41.43	96.29
41.43	0.21	48.27	96.50
48.27	0.25	56.23	96.75
56.23	0.29	65.51	97.04
65.51	0.34	76.32	97.38
76.32	0.38	88.91	97.76
88.91	0.42	103.58	98.18
103.58	0.45	120.67	98.63
120.67	0.44	140.58	99.06
140.58	0.38	163.77	99.44
163.77	0.29	190.80	99.73
190.80	0.18	222.28	99.91
222.28	0.08	258.95	99.99
258.95	0.01	301.68	100.00
301.68	0.00	351.46	100.00
351.46	0.00	409.45	100.00
409.45	0.00	477.01	100.00
477.01	0.00	555.71	100.00
555.71	0.00	647.41	100.00
647.41	0.00	754.23	100.00
754.23	0.00	878.67	100.00

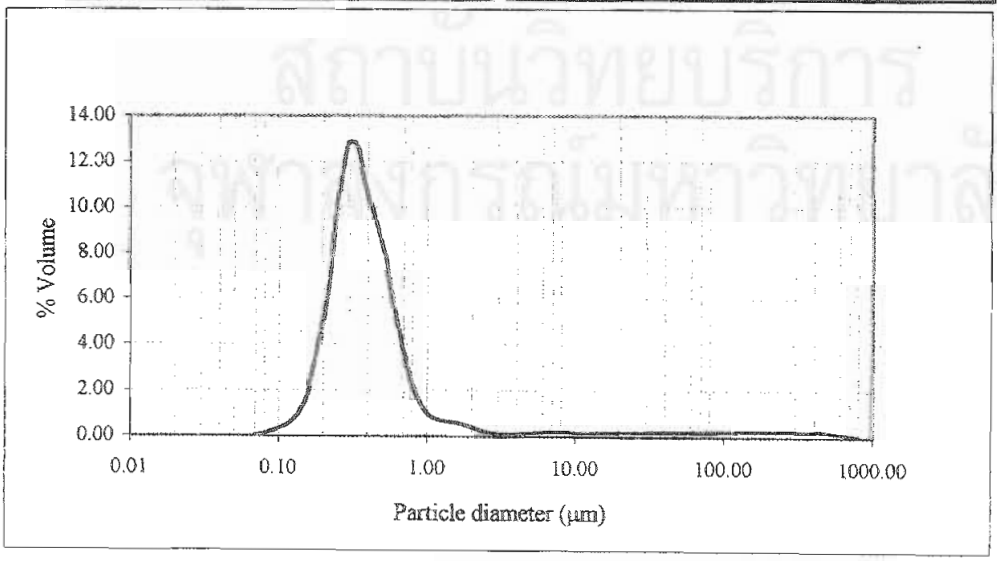

Figure d24 Particle size distribution of formulation 9 GB + 4 TW80 after autoclaving

Table d25 Particle size distribution of formulation 0.1 DI + 5 GB + 4 TW80 before autoclaving

Distribution type: volume	D(v,0.1) = 0.09	D(v,0.5) = 0.25	D(v,0.9) = 11.05
Mean diameter	D[4,3] = 4.95	D[3,2] = 0.21	Span = 44.59
% > 1 µm = 19.05	% > 5 µm = 13.66	% > 10 µm = 10.50	Uniformity = 19.54

size low (µm)	size in %	size high (µm)	under %	size low (µm)	size in %	size high (µm)	under %
0.05	1.00	0.06	1.00	6.63	0.70	7.72	88.27
0.06	1.98	0.07	2.98	7.72	0.72	9.00	88.99
0.07	2.94	0.08	5.92	9.00	0.75	10.48	89.75
0.08	3.85	0.09	9.77	10.48	0.77	12.21	90.51
0.09	4.70	0.11	14.47	12.21	0.79	14.22	91.30
0.11	5.47	0.13	19.94	14.22	0.79	16.57	92.09
0.13	6.14	0.15	26.07	16.57	0.78	19.31	92.87
0.15	6.69	0.17	32.77	19.31	0.75	22.49	93.62
0.17	7.10	0.20	39.86	22.49	0.72	26.20	94.34
0.20	7.29	0.23	47.15	26.20	0.69	30.53	95.04
0.23	7.20	0.27	54.35	30.53	0.67	35.56	95.71
0.27	6.75	0.31	61.10	35.56	0.67	41.43	96.37
0.31	5.96	0.36	67.06	41.43	0.66	48.27	97.03
0.36	4.91	0.42	71.97	48.27	0.65	56.23	97.68
0.42	3.77	0.49	75.74	56.23	0.60	65.51	98.28
0.49	2.60	0.58	78.33	65.51	0.50	76.32	98.78
0.58	1.49	0.67	79.82	76.32	0.38	88.91	99.16
0.67	0.61	0.78	80.43	88.91	0.24	103.58	99.41
0.78	0.40	0.91	80.83	103.58	0.13	120.67	99.54
0.91	0.26	1.06	81.09	120.67	0.06	140.58	99.60
1.06	0.22	1.24	81.31	140.58	0.04	163.77	99.64
1.24	0.29	1.44	81.60	163.77	0.09	190.80	99.74
1.44	0.39	1.68	81.99	190.80	0.26	222.28	100.00
1.68	0.50	1.95	82.50	222.28	0.00	258.95	100.00
1.95	0.58	2.28	83.08	258.95	0.00	301.68	100.00
2.28	0.62	2.65	83.70	301.68	0.00	351.46	100.00
2.65	0.63	3.09	84.34	351.46	0.00	409.45	100.00
3.09	0.63	3.60	84.97	409.45	0.00	477.01	100.00
3.60	0.64	4.19	85.60	477.01	0.00	555.71	100.00
4.19	0.64	4.88	86.24	555.71	0.00	647.41	100.00
4.88	0.65	5.69	86.89	647.41	0.00	754.23	100.00
5.69	0.68	6.63	87.57	754.23	0.00	878.67	100.00

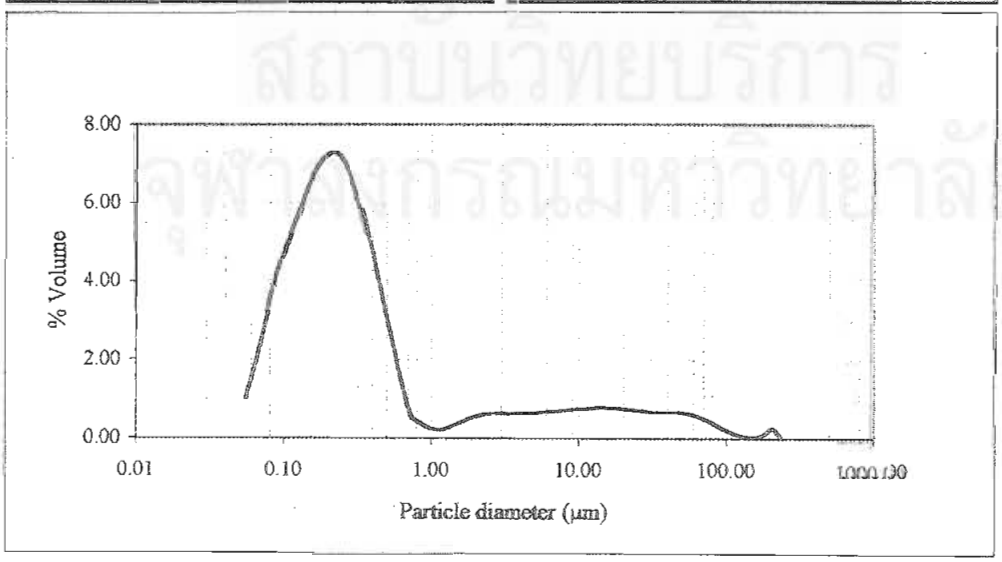

Figure d25 Particle size distribution of formulation 0.1 DI + 5 GB + 4 TW80 before autoclaving

Table d26 Particle size distribution of formulation 0.1 DI + 5 GB + 4 TW80 after autoclaving

Distribution type: volume	D(v,0.1) = 0.14	D(v,0.5) = 0.35	D(v,0.9) = 55.47
Mean diameter	D[4,3] = 18.42	D[3,2] = 0.30	Span = 158.97
% > 1 μm = 30.65	% > 5 μm = 25.08	% > 10 μm = 22.14	Uniformity = 52.30

size low (μm)	size in %	size high (μm)	under %	size low (μm)	size in %	size high (μm)	under %
0.05	0.36	0.06	0.36	6.63	0.67	7.72	76.65
0.06	0.74	0.07	1.10	7.72	0.71	9.00	77.35
0.07	1.15	0.08	2.26	9.00	0.76	10.48	78.11
0.08	1.60	0.09	3.86	10.48	0.80	12.21	78.91
0.09	2.12	0.11	5.98	12.21	0.84	14.22	79.74
0.11	2.72	0.13	8.70	14.22	0.88	16.57	80.62
0.13	3.46	0.15	12.16	16.57	0.94	19.31	81.57
0.15	4.38	0.17	16.54	19.31	1.00	22.49	82.57
0.17	5.52	0.20	22.06	22.49	1.08	26.20	83.65
0.20	6.76	0.23	28.82	26.20	1.15	30.53	84.80
0.23	7.77	0.27	36.59	30.53	1.24	35.56	86.05
0.27	7.97	0.31	44.55	35.56	1.31	41.43	87.36
0.31	7.15	0.36	51.70	41.43	1.37	48.27	88.73
0.36	5.81	0.42	57.51	48.27	1.40	56.23	90.13
0.42	4.52	0.49	62.04	56.23	1.38	65.51	91.52
0.49	3.25	0.58	65.29	65.51	1.33	76.32	92.84
0.58	1.98	0.67	67.27	76.32	1.22	88.91	94.07
0.67	1.03	0.78	68.30	88.91	1.09	103.58	95.15
0.78	0.73	0.91	69.03	103.58	0.94	120.67	96.09
0.91	0.54	1.06	69.57	120.67	0.80	140.58	96.90
1.06	0.46	1.24	70.03	140.58	0.68	163.77	97.58
1.24	0.49	1.44	70.52	163.77	0.56	190.80	98.14
1.44	0.56	1.68	71.08	190.80	0.45	222.28	98.59
1.68	0.60	1.95	71.68	222.28	0.36	258.95	98.96
1.95	0.64	2.28	72.32	258.95	0.26	301.68	99.22
2.28	0.59	2.65	72.92	301.68	0.13	351.46	99.35
2.65	0.52	3.09	73.43	351.46	0.16	409.45	99.51
3.09	0.46	3.60	73.90	409.45	0.14	477.01	99.66
3.60	0.45	4.19	74.35	477.01	0.13	555.71	99.78
4.19	0.49	4.88	74.84	555.71	0.10	647.41	99.89
4.88	0.54	5.69	75.38	647.41	0.07	754.23	99.96
5.69	0.60	6.63	75.98	754.23	0.04	878.67	100.00

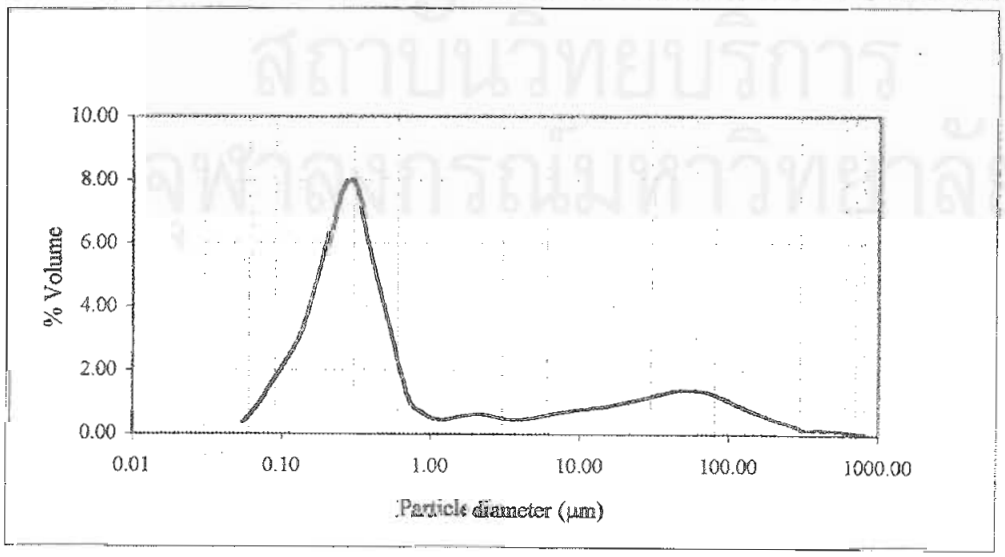

Figure d26 Particle size distribution of formulation 0.1 DI + 5 GB + 4 TW80 after autoclaving

Table d27 Particle size distribution of formulation 0.3 DI + 5 GB + 4 TW80 before autoclaving

Distribution type: volume	D(v,0.1) = 0.15	D(v,0.5) = 0.32	D(v,0.9) = 6.28
Mean diameter	D[4,3] = 3.59	D[3,2] = 0.28	Span = 19.38
% > 1 μm = 13.59	% > 5 μm = 10.47	% > 10 μm = 8.81	Uniformity = 10.67

size low (μm)	size in %	size high (μm)	under %
0.05	0.19	0.06	0.19
0.06	0.43	0.07	0.62
0.07	0.77	0.08	1.39
0.08	1.18	0.09	2.57
0.09	1.72	0.11	4.29
0.11	2.40	0.13	6.69
0.13	3.30	0.15	10.00
0.15	4.49	0.17	14.49
0.17	6.05	0.20	20.54
0.20	7.90	0.23	28.44
0.23	9.66	0.27	38.09
0.27	10.58	0.31	48.68
0.31	10.17	0.36	58.84
0.36	8.84	0.42	67.68
0.42	7.28	0.49	74.96
0.49	5.53	0.58	80.49
0.58	3.55	0.67	84.04
0.67	1.82	0.78	85.86
0.78	0.56	0.91	86.41
0.91	0.00	1.06	86.41
1.06	0.00	1.24	86.41
1.24	0.14	1.44	86.55
1.44	0.37	1.68	86.92
1.68	0.48	1.95	87.40
1.95	0.49	2.28	87.89
2.28	0.43	2.65	88.32
2.65	0.35	3.09	88.67
3.09	0.29	3.60	88.95
3.60	0.26	4.19	89.22
4.19	0.27	4.88	89.49
4.88	0.30	5.69	89.78
5.69	0.34	6.63	90.13
6.63	0.38	7.72	90.51
7.72	0.40	9.00	90.91
9.00	0.40	10.48	91.32
10.48	0.37	12.21	91.69
12.21	0.33	14.22	92.02
14.22	0.42	16.57	92.44
16.57	0.42	19.31	92.85
19.31	0.50	22.49	93.35
22.49	0.68	26.20	94.03
26.20	0.90	30.53	94.93
30.53	1.08	35.56	96.01
35.56	1.14	41.43	97.15
41.43	1.04	48.27	98.18
48.27	0.81	56.23	99.00
56.23	0.54	65.51	99.54
65.51	0.31	76.32	99.85
76.32	0.15	88.91	100.00
88.91	0.00	103.58	100.00
103.58	0.00	120.67	100.00
120.67	0.00	140.58	100.00
140.58	0.00	163.77	100.00
163.77	0.00	190.80	100.00
190.80	0.00	222.28	100.00
222.28	0.00	258.95	100.00
258.95	0.00	301.68	100.00
301.68	0.00	351.46	100.00
351.46	0.00	409.45	100.00
409.45	0.00	477.01	100.00
477.01	0.00	555.71	100.00
555.71	0.00	647.41	100.00
647.41	0.00	754.23	100.00
754.23	0.00	878.67	100.00

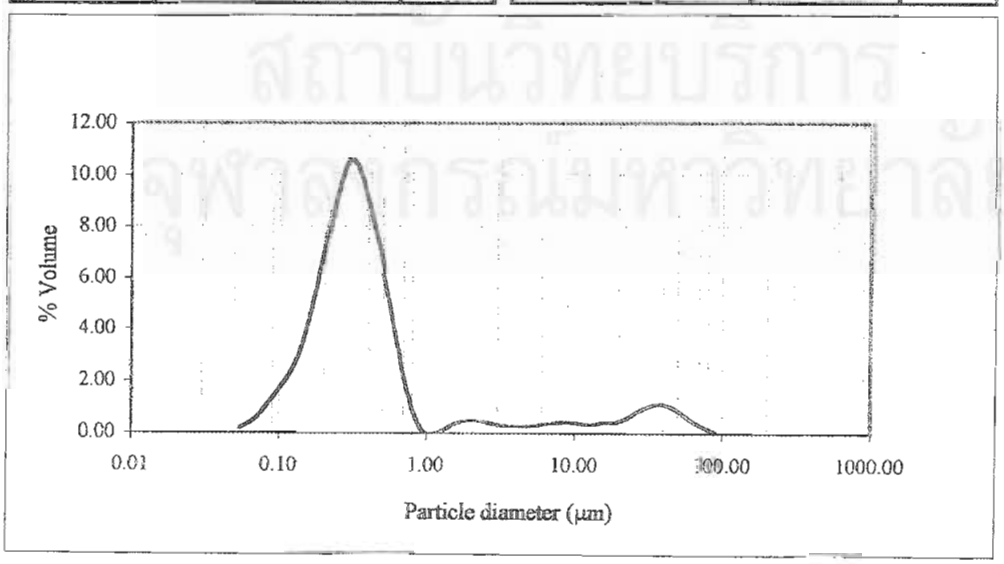

Figure d27 Particle size distribution of formulation 0.3 DI + 5 GB + 4 TW80 before autoclaving

Table d28 Particle size distribution of formulation 0.3 DI + 5 GB + 4 TW80 after autoclaving

Distribution type: volume	D(v,0.1) = 0.15	D(v,0.5) = 0.33	D(v,0.9) = 35.72
Mean diameter	D[4,3] = 10.52	D[3,2] = 0.30	Span = 107.87
% > 1 µm = 26.95	% > 5 µm = 22.03	% > 10 µm = 18.77	Uniformity = 31.26

size low (µm)	size in %	size high (µm)	under %
0.05	0.25	0.06	0.25
0.06	0.56	0.07	0.81
0.07	0.92	0.08	1.72
0.08	1.33	0.09	3.05
0.09	1.83	0.11	4.88
0.11	2.46	0.13	7.33
0.13	3.28	0.15	10.61
0.15	4.36	0.17	14.97
0.17	5.81	0.20	20.78
0.20	7.53	0.23	28.31
0.23	9.01	0.27	37.32
0.27	9.40	0.31	46.73
0.31	8.30	0.36	55.02
0.36	6.51	0.42	61.53
0.42	4.85	0.49	66.38
0.49	3.31	0.58	69.69
0.58	1.84	0.67	71.53
0.67	0.81	0.78	72.34
0.78	0.51	0.91	72.85
0.91	0.32	1.06	73.18
1.06	0.25	1.24	73.43
1.24	0.37	1.44	73.80
1.44	0.45	1.68	74.24
1.68	0.52	1.95	74.76
1.95	0.57	2.28	75.33
2.28	0.57	2.65	75.90
2.65	0.52	3.09	76.41
3.09	0.48	3.60	76.89
3.60	0.48	4.19	77.37
4.19	0.52	4.88	77.88
4.88	0.58	5.69	78.47
5.69	0.66	6.63	79.13
6.63	0.73	7.72	79.86
7.72	0.79	9.00	80.66
9.00	0.84	10.48	81.50
10.48	0.89	12.21	82.39
12.21	0.93	14.22	83.32
14.22	0.98	16.57	84.29
16.57	1.02	19.31	85.32
19.31	1.08	22.49	86.40
22.49	1.14	26.20	87.54
26.20	1.19	30.53	88.73
30.53	1.24	35.56	89.97
35.56	1.26	41.43	91.23
41.43	1.26	48.27	92.48
48.27	1.22	56.23	93.71
56.23	1.16	65.51	94.86
65.51	1.06	76.32	95.92
76.32	0.94	88.91	96.86
88.91	0.81	103.58	97.67
103.58	0.67	120.67	98.34
120.67	0.54	140.58	98.88
140.58	0.43	163.77	99.30
163.77	0.36	190.80	99.66
190.80	0.34	222.28	100.00
222.28	0.00	258.95	100.00
258.95	0.00	301.68	100.00
301.68	0.00	351.46	100.00
351.46	0.00	409.45	100.00
409.45	0.00	477.01	100.00
477.01	0.00	555.71	100.00
555.71	0.00	647.41	100.00
647.41	0.00	754.23	100.00
754.23	0.00	878.67	100.00

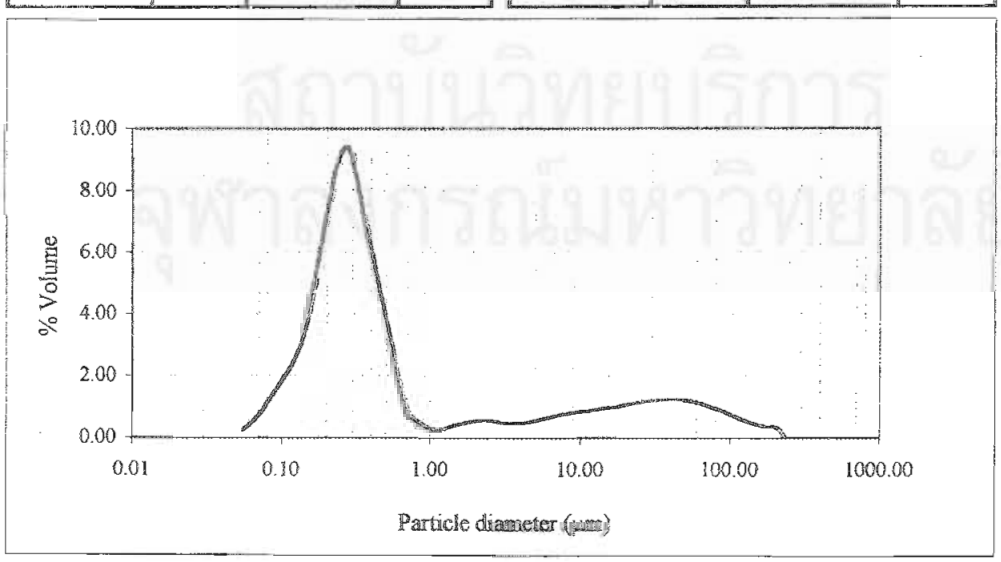

Figure d28 Particle size distribution of formulation 0.3 DI + 5 GB + 4 TW80 after autoclaving

Table d29 Particle size distribution of formulation 0.5 DI + 5 GB + 4 TW80 before autoclaving

Distribution type: volume	D(v,0.1) = 0.15	D(v,0.5) = 0.36	D(v,0.9) = 26.20
Mean diameter	D[4,3] = 9.15	D[3,2] = 0.32	Span = 72.02
% > 1 μm = 25.20	% > 5 μm = 17.22	% > 10 μm = 14.09	Uniformity = 24.68

size low (μm)	size in %	size high (μm)	under %	size low (μm)	size in %	size high (μm)	under %
0.05	0.25	0.06	0.25	6.63	0.72	7.72	84.75
0.06	0.53	0.07	0.78	7.72	0.71	9.00	85.46
0.07	0.83	0.08	1.60	9.00	0.67	10.48	86.13
0.08	1.18	0.09	2.78	10.48	0.64	12.21	86.76
0.09	1.60	0.11	4.38	12.21	0.61	14.22	87.38
0.11	2.13	0.13	6.50	14.22	0.61	16.57	87.99
0.13	2.83	0.15	9.33	16.57	0.64	19.31	88.63
0.15	3.78	0.17	13.11	19.31	0.67	22.49	89.29
0.17	4.07	0.20	17.18	22.49	0.71	26.20	90.00
0.20	7.65	0.23	24.83	26.20	0.75	30.53	90.75
0.23	8.14	0.27	32.97	30.53	0.79	35.56	91.53
0.27	8.75	0.31	41.73	35.56	0.81	41.43	92.34
0.31	8.09	0.36	49.81	41.43	0.83	48.27	93.18
0.36	6.78	0.42	56.59	48.27	0.85	56.23	94.03
0.42	5.59	0.49	62.19	56.23	0.87	65.51	94.90
0.49	4.45	0.58	66.63	65.51	0.89	76.32	95.79
0.58	3.19	0.67	69.82	76.32	0.89	88.91	96.68
0.67	2.25	0.78	72.07	88.91	0.85	103.58	97.53
0.78	1.82	0.91	73.90	103.58	0.78	120.67	98.31
0.91	1.51	1.06	75.40	120.67	0.64	140.58	98.95
1.06	1.28	1.24	76.68	140.58	0.48	163.77	99.43
1.24	1.17	1.44	77.85	163.77	0.33	190.80	99.75
1.44	1.04	1.68	78.89	190.80	0.25	222.28	100.00
1.68	0.85	1.95	79.74	222.28	0.00	258.95	100.00
1.95	0.66	2.28	80.40	258.95	0.00	301.68	100.00
2.28	0.50	2.65	80.90	301.68	0.00	351.46	100.00
2.65	0.39	3.09	81.29	351.46	0.00	409.45	100.00
3.09	0.39	3.60	81.68	409.45	0.00	477.01	100.00
3.60	0.45	4.19	82.13	477.01	0.00	555.71	100.00
4.19	0.55	4.88	82.68	555.71	0.00	647.41	100.00
4.88	0.64	5.69	83.32	647.41	0.00	754.23	100.00
5.69	0.70	6.63	84.02	754.23	0.00	878.67	100.00

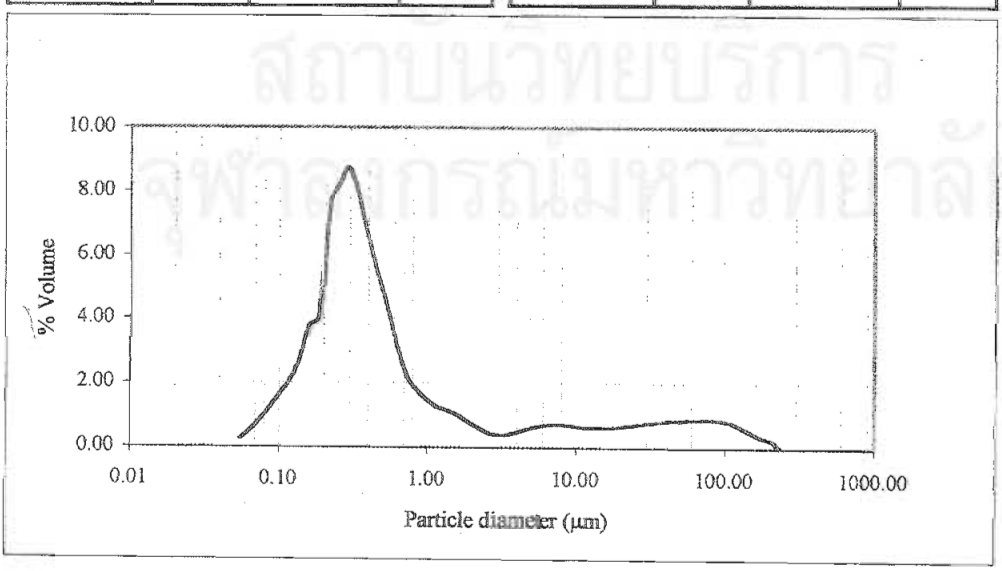

Figure d29 Particle size distribution of formulation 0.5 DI + 5 GB + 4 TW80 before autoclaving

Table d30 Particle size distribution of formulation 0.5 DI + 5 GB + 4 TW80 after autoclaving

Distribution type: volume	D(v,0.1) = 0.16	D(v,0.5) = 0.37	D(v,0.9) = 56.24
Mean diameter	D[4,3] = 14.51	D[3,2] = 0.35	Span = 153.2
% > 1 μm = 34.04	% > 5 μm = 28.08	% > 10 μm = 24.84	Uniformity = 39.00

size low (μm)	size in %	size high (μm)	under %	size low (μm)	size in %	size high (μm)	under %
0.05	0.14	0.06	0.14	6.63	0.72	7.72	73.83
0.06	0.35	0.07	0.49	7.72	0.78	9.00	74.60
0.07	0.60	0.08	1.09	9.00	0.83	10.48	75.43
0.08	0.90	0.09	1.99	10.48	0.90	12.21	76.34
0.09	1.31	0.11	3.30	12.21	0.96	14.22	77.30
0.11	1.84	0.13	5.14	14.22	1.03	16.57	78.33
0.13	2.56	0.15	7.70	16.57	1.11	19.31	79.44
0.15	3.61	0.17	11.31	19.31	1.19	22.49	80.64
0.17	5.08	0.20	16.39	22.49	1.29	26.20	81.93
0.20	6.94	0.23	23.34	26.20	1.40	30.53	83.33
0.23	8.70	0.27	32.03	30.53	1.52	35.56	84.85
0.27	9.24	0.31	41.27	35.56	1.63	41.43	86.48
0.31	8.10	0.36	49.37	41.43	1.73	48.27	88.20
0.36	6.20	0.42	55.58	48.27	1.79	56.23	90.00
0.42	4.53	0.49	60.10	56.23	1.82	65.51	91.82
0.49	3.00	0.58	63.10	65.51	1.79	76.32	93.60
0.58	1.58	0.67	64.69	76.32	1.69	88.91	95.29
0.67	0.67	0.78	65.35	88.91	1.50	103.58	96.79
0.78	0.43	0.91	65.78	103.58	1.24	120.67	98.03
0.91	0.29	1.06	66.07	120.67	0.94	140.58	98.97
1.06	0.27	1.24	66.34	140.58	0.60	163.77	99.57
1.24	0.50	1.44	66.84	163.77	0.30	190.80	99.87
1.44	0.59	1.68	67.43	190.80	0.13	222.28	100.00
1.68	0.66	1.95	68.09	222.28	0.00	258.95	100.00
1.95	0.69	2.28	68.78	258.95	0.00	301.68	100.00
2.28	0.67	2.65	69.45	301.68	0.00	351.46	100.00
2.65	0.63	3.09	70.08	351.46	0.00	409.45	100.00
3.09	0.59	3.60	70.68	409.45	0.00	477.01	100.00
3.60	0.58	4.19	71.25	477.01	0.00	555.71	100.00
4.19	0.58	4.88	71.83	555.71	0.00	647.41	100.00
4.88	0.62	5.69	72.45	647.41	0.00	754.23	100.00
5.69	0.66	6.63	73.11	754.23	0.00	878.67	100.00

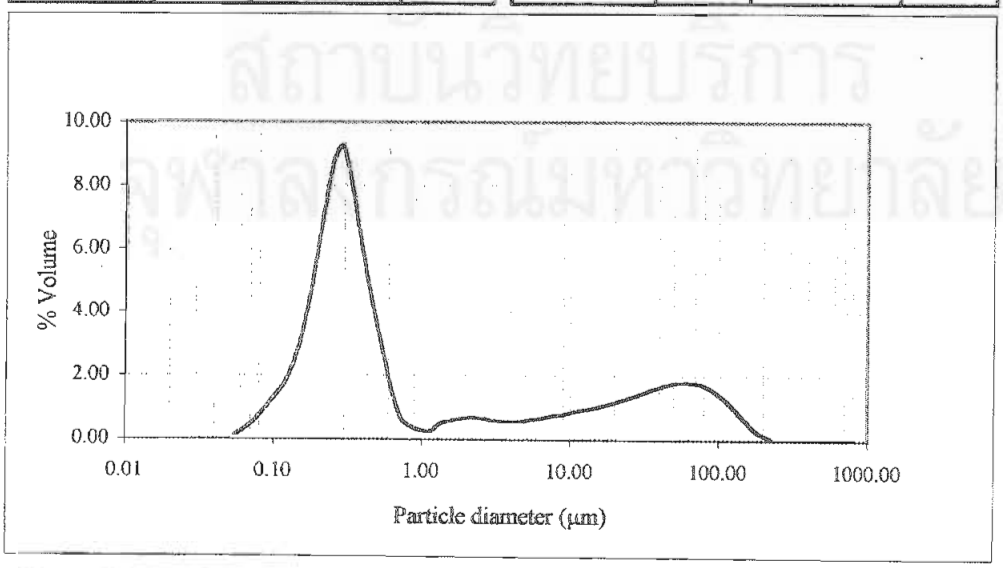

Figure d30 Particle size distribution of formulation 0.5 DI + 5 GB + 4 TW80 after autoclaving

Table d31 Particle size distribution of formulation 0.7 DI + 5 GB + 4 TW80 before autoclaving

Distribution type: volume	D(v,0.1) = 0.21	D(v,0.5) = 0.38	D(v,0.9) = 12.09
Mean diameter	D[4,3] = 6.99	D[3,2] = 0.37	Span = 30.06
% > 1 µm = 22.52	% > 5 µm = 12.93	% > 10 µm = 10.55	Uniformity = 17.51

size low (µm)	size in %	size high (µm)	under %	size low (µm)	size in %	size high (µm)	under %
0.05	0.03	0.06	0.03	6.63	0.55	7.72	88.61
0.06	0.09	0.07	0.12	7.72	0.53	9.00	89.14
0.07	0.17	0.08	0.29	9.00	0.46	10.48	89.60
0.08	0.29	0.09	0.58	10.48	0.43	12.21	90.03
0.09	0.47	0.11	1.04	12.21	0.40	14.22	90.43
0.11	0.76	0.13	1.81	14.22	0.39	16.57	90.82
0.13	1.26	0.15	3.06	16.57	0.41	19.31	91.24
0.15	2.12	0.17	5.18	19.31	0.43	22.49	91.66
0.17	3.64	0.20	8.82	22.49	0.46	26.20	92.12
0.20	6.11	0.23	14.93	26.20	0.49	30.53	92.61
0.23	9.23	0.27	24.16	30.53	0.52	35.56	93.14
0.27	11.35	0.31	35.51	35.56	0.57	41.43	93.70
0.31	10.92	0.36	46.43	41.43	0.62	48.27	94.32
0.36	9.01	0.42	55.43	48.27	0.70	56.23	95.02
0.42	7.35	0.49	62.79	56.23	0.77	65.51	95.80
0.49	5.73	0.58	68.52	65.51	0.85	76.32	96.65
0.58	3.78	0.67	72.30	76.32	0.89	88.91	97.53
0.67	2.43	0.78	74.73	88.91	0.85	103.58	98.39
0.78	1.82	0.91	76.55	103.58	0.73	120.67	99.12
0.91	1.55	1.06	78.10	120.67	0.51	140.58	99.63
1.06	1.41	1.24	79.51	140.58	0.24	163.77	99.87
1.24	1.37	1.44	80.88	163.77	0.07	190.80	99.94
1.44	1.36	1.68	82.24	190.80	0.06	222.28	100.00
1.68	1.23	1.95	83.47	222.28	0.00	258.95	100.00
1.95	0.63	2.28	84.09	258.95	0.00	301.68	100.00
2.28	1.05	2.65	85.14	301.68	0.00	351.46	100.00
2.65	0.53	3.09	85.68	351.46	0.00	409.45	100.00
3.09	0.43	3.60	86.11	409.45	0.00	477.01	100.00
3.60	0.42	4.19	86.53	477.01	0.00	555.71	100.00
4.19	0.46	4.88	87.00	555.71	0.00	647.41	100.00
4.88	0.51	5.69	87.51	647.41	0.00	754.23	100.00
5.69	0.55	6.63	88.06	754.23	0.00	878.67	100.00

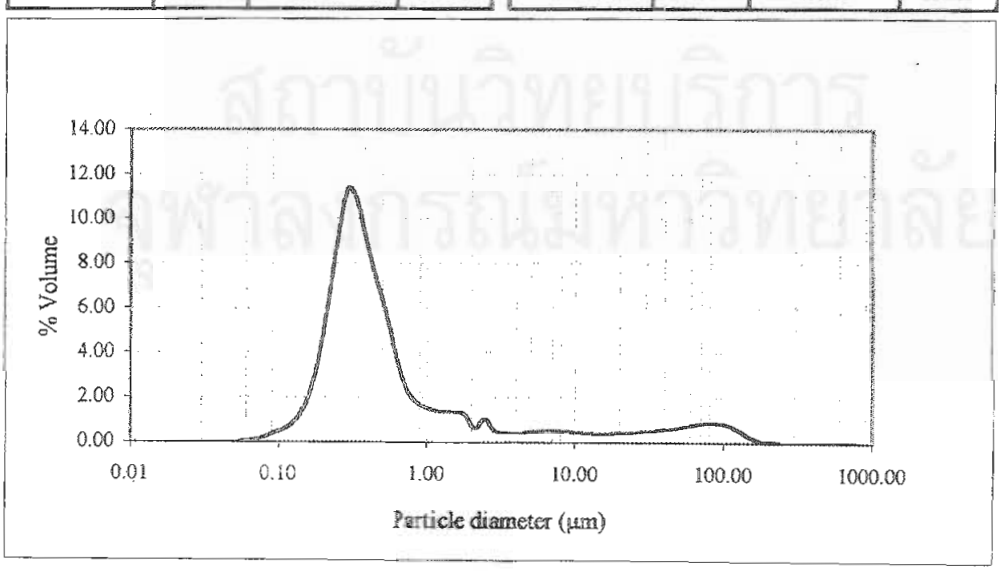

Figure d31 Particle size distribution of formulation 0.7 DI + 5 GB + 4 TW80 before autoclaving

Table d32 Particle size distribution of formulation 0.7 DI + 5 GB + 4 TW80 after autoclaving

Distribution type: volume	D(v,0.1) = 0.17	D(v,0.5) = 0.36	D(v,0.9) = 47.07
Mean diameter	D[4,3] = 12.85	D[3,2] = 0.34	Span = 130.31
% > 1 µm = 31.25	% > 5 µm = 25.37	% > 10 µm = 22.14	Uniformity = 35.06

size low (µm)	size in %	size high (µm)	under %	size low (µm)	size in %	size high (µm)	under %
0.05	0.17	0.06	0.17	6.63	0.71	7.72	76.51
0.06	0.38	0.07	0.55	7.72	0.78	9.00	77.29
0.07	0.61	0.08	1.16	9.00	0.84	10.48	78.13
0.08	0.90	0.09	2.05	10.48	0.90	12.21	79.03
0.09	1.24	0.11	3.30	12.21	0.96	14.22	79.99
0.11	1.72	0.13	5.01	14.22	1.03	16.57	81.01
0.13	2.38	0.15	7.39	16.57	1.11	19.31	82.12
0.15	3.36	0.17	10.75	19.31	1.19	22.49	83.31
0.17	4.83	0.20	15.58	22.49	1.26	26.20	84.57
0.20	6.85	0.23	22.42	26.20	1.34	30.53	85.91
0.23	8.97	0.27	31.39	30.53	1.41	35.56	87.32
0.27	9.86	0.31	41.25	35.56	1.46	41.43	88.78
0.31	8.75	0.36	50.01	41.43	1.48	48.27	90.26
0.36	6.74	0.42	56.75	48.27	1.48	56.23	91.74
0.42	5.01	0.49	61.76	56.23	1.44	65.51	93.18
0.49	3.43	0.58	65.20	65.51	1.38	76.32	94.56
0.58	1.89	0.67	67.09	76.32	1.27	88.91	95.83
0.67	0.86	0.78	67.95	88.91	1.15	103.58	96.98
0.78	0.57	0.91	68.52	103.58	0.99	120.67	97.98
0.91	0.39	1.06	68.91	120.67	0.80	140.58	98.77
1.06	0.34	1.24	69.24	140.58	0.58	163.77	99.35
1.24	0.50	1.44	69.74	163.77	0.38	190.80	99.73
1.44	0.57	1.68	70.31	190.80	0.27	222.28	100.00
1.68	0.64	1.95	70.95	222.28	0.00	258.95	100.00
1.95	0.66	2.28	71.61	258.95	0.00	301.68	100.00
2.28	0.64	2.65	72.25	301.68	0.00	351.46	100.00
2.65	0.60	3.09	72.84	351.46	0.00	409.45	100.00
3.09	0.57	3.60	73.41	409.45	0.00	477.01	100.00
3.60	0.55	4.19	73.97	477.01	0.00	555.71	100.00
4.19	0.57	4.88	74.54	555.71	0.00	647.41	100.00
4.88	0.60	5.69	75.14	647.41	0.00	754.23	100.00
5.69	0.66	6.63	75.80	754.23	0.00	878.67	100.00

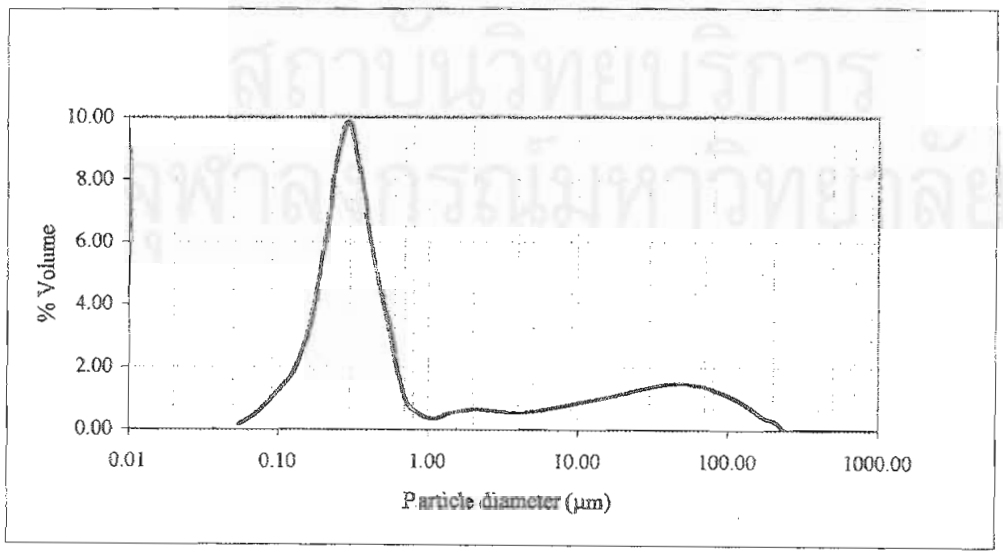

Figure d32 Particle size distribution of formulation 0.7 DI + 5 GB + 4 TW80 after autoclaving

Table d33 Particle size distribution of formulation 0.9 DI + 5 GB + 4 TW80 before autoclaving

Distribution type: volume	D(v,0.1) = 0.19	D(v,0.5) = 0.36	D(v,0.9) = 2.54
Mean diameter	D[4,3] = 1.46	D[3,2] = 0.34	Span = 6.49
% > 1 μm = 17.30	% > 5 μm = 6.35	% > 10 μm = 3.10	Uniformity = 3.36

size low (μm)	size in %	size high (μm)	under %	size low (μm)	size in %	size high (μm)	under %
0.05	0.02	0.06	0.02	6.63	0.74	7.72	95.89
0.06	0.08	0.07	0.09	7.72	0.65	9.00	96.53
0.07	0.18	0.08	0.28	9.00	0.54	10.48	97.08
0.08	0.36	0.09	0.64	10.48	0.44	12.21	97.52
0.09	0.64	0.11	1.28	12.21	0.37	14.22	97.89
0.11	1.06	0.13	2.34	14.22	0.32	16.57	98.21
0.13	1.72	0.15	4.06	16.57	0.29	19.31	98.50
0.15	2.75	0.17	6.80	19.31	0.29	22.49	98.79
0.17	4.38	0.20	11.19	22.49	0.28	26.20	99.08
0.20	6.75	0.23	17.94	26.20	0.27	30.53	99.34
0.23	9.50	0.27	27.44	30.53	0.23	35.56	99.58
0.27	11.32	0.31	38.76	35.56	0.18	41.43	99.76
0.31	11.07	0.36	49.83	41.43	0.13	48.27	99.89
0.36	9.51	0.42	59.33	48.27	0.08	56.23	99.97
0.42	7.93	0.49	67.26	56.23	0.03	65.51	100.00
0.49	6.23	0.58	73.49	65.51	0.00	76.32	100.00
0.58	4.18	0.67	77.67	76.32	0.00	88.91	100.00
0.67	2.64	0.78	80.31	88.91	0.00	103.58	100.00
0.78	1.63	0.91	81.94	103.58	0.00	120.67	100.00
0.91	1.27	1.06	83.20	120.67	0.00	140.58	100.00
1.06	1.03	1.24	84.23	140.58	0.00	163.77	100.00
1.24	1.26	1.44	85.49	163.77	0.00	190.80	100.00
1.44	1.37	1.68	86.86	190.80	0.00	222.28	100.00
1.68	1.31	1.95	88.16	222.28	0.00	258.95	100.00
1.95	1.16	2.28	89.32	258.95	0.00	301.68	100.00
2.28	0.99	2.65	90.31	301.68	0.00	351.46	100.00
2.65	0.85	3.09	91.16	351.46	0.00	409.45	100.00
3.09	0.79	3.60	91.95	409.45	0.00	477.01	100.00
3.60	0.78	4.19	92.73	477.01	0.00	555.71	100.00
4.19	0.80	4.88	93.53	555.71	0.00	647.41	100.00
4.88	0.82	5.69	94.34	647.41	0.00	754.23	100.00
5.69	0.80	6.63	95.15	754.23	0.00	878.67	100.00

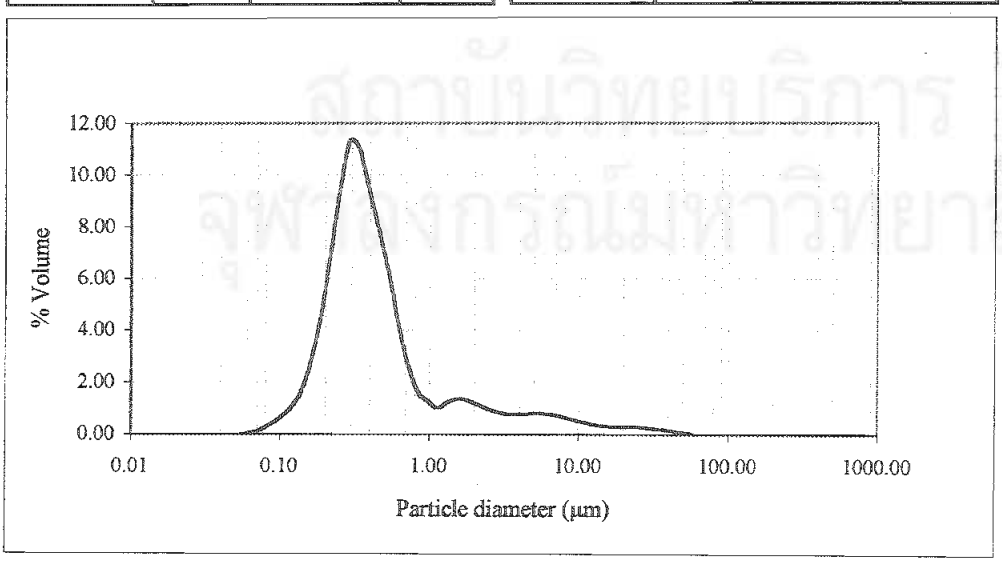

Figure d33 Particle size distribution of formulation 0.9 DI + 5 GB + 4 TW80 before autoclaving

Table d34 Particle size distribution of formulation 0.9 DI + 5 GB + 4 TW80 after autoclaving

Distribution type: volume	D(v,0.1) = 0.17	D(v,0.5) = 0.34	D(v,0.9) = 19.22
Mean diameter	D[4,3] = 8.28	D[3,2] = 0.33	Span = 55.83
% > 1 μm = 22.16	% > 5 μm = 15.58	% > 10 μm = 12.84	Uniformity = 23.59

size low (μm)	size in %	size high (μm)	under %	size low (μm)	size in %	size high (μm)	under %
0.05	0.09	0.06	0.09	6.63	0.61	7.72	86.08
0.06	0.23	0.07	0.33	7.72	0.64	9.00	86.72
0.07	0.42	0.08	0.75	9.00	0.65	10.48	87.37
0.08	0.67	0.09	1.42	10.48	0.66	12.21	88.02
0.09	1.02	0.11	2.44	12.21	0.66	14.22	88.68
0.11	1.51	0.13	3.95	14.22	0.67	16.57	89.35
0.13	2.24	0.15	6.19	16.57	0.67	19.31	90.02
0.15	3.37	0.17	9.56	19.31	0.67	22.49	90.70
0.17	5.10	0.20	14.66	22.49	0.68	26.20	91.38
0.20	7.51	0.23	22.16	26.20	0.69	30.53	92.07
0.23	10.07	0.27	32.23	30.53	0.70	35.56	92.77
0.27	11.33	0.31	43.56	35.56	0.71	41.43	93.48
0.31	10.35	0.36	53.91	41.43	0.73	48.27	94.22
0.36	8.22	0.42	62.13	48.27	0.74	56.23	94.96
0.42	6.29	0.49	68.43	56.23	0.76	65.51	95.71
0.49	4.45	0.58	72.88	65.51	0.74	76.32	96.45
0.58	2.55	0.67	75.43	76.32	0.71	88.91	97.16
0.67	1.25	0.78	76.68	88.91	0.65	103.58	97.81
0.78	0.83	0.91	77.51	103.58	0.55	120.67	98.36
0.91	0.56	1.06	78.07	120.67	0.44	140.58	98.80
1.06	0.41	1.24	78.47	140.58	0.36	163.77	99.16
1.24	0.59	1.44	79.06	163.77	0.35	190.80	99.52
1.44	0.70	1.68	79.76	190.80	0.48	222.28	100.00
1.68	0.76	1.95	80.53	222.28	0.00	258.95	100.00
1.95	0.77	2.28	81.30	258.95	0.00	301.68	100.00
2.28	0.72	2.65	82.02	301.68	0.00	351.46	100.00
2.65	0.65	3.09	82.67	351.46	0.00	409.45	100.00
3.09	0.59	3.60	83.26	409.45	0.00	477.01	100.00
3.60	0.55	4.19	83.80	477.01	0.00	555.71	100.00
4.19	0.53	4.88	84.33	555.71	0.00	647.41	100.00
4.88	0.55	5.69	84.89	647.41	0.00	754.23	100.00
5.69	0.58	6.63	85.47	754.23	0.00	878.67	100.00

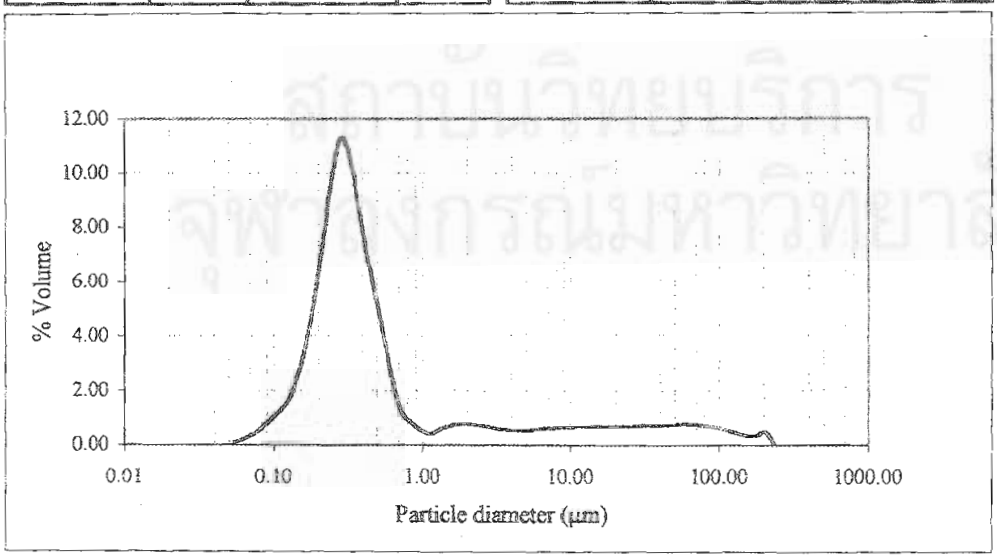

Figure d34 Particle size distribution of formulation 0.9 DI + 5 GB + 4 TW80 after autoclaving

Table d35 Particle size distribution of diazepam powder

Distribution type: volume	D(v,0.1) = 0.39	D(v,0.5) = 23.51	D(v,0.9) = 100.62
Mean diameter	D[4,3] = 42.97	D[3,2] = 1.67	Span = 4.26
% > 1 µm = 84.77	% > 5 µm = 82.88	% > 10 µm = 76.90	Uniformity = 1.40

size low (µm)	size in %	size high (µm)	under %
0.05	0.03	0.06	0.03
0.06	0.05	0.07	0.08
0.07	0.10	0.08	0.18
0.08	0.14	0.09	0.32
0.09	0.20	0.11	0.52
0.11	0.28	0.13	0.80
0.13	0.39	0.15	1.19
0.15	0.57	0.17	1.76
0.17	0.83	0.20	2.59
0.20	1.21	0.23	3.80
0.23	1.62	0.27	5.42
0.27	1.88	0.31	7.30
0.31	1.81	0.36	9.11
0.36	1.56	0.42	10.67
0.42	1.33	0.49	12.01
0.49	1.12	0.58	13.12
0.58	0.84	0.67	13.97
0.67	0.61	0.78	14.58
0.78	0.45	0.91	15.03
0.91	0.33	1.06	15.36
1.06	0.23	1.24	15.59
1.24	0.16	1.44	15.75
1.44	0.12	1.68	15.88
1.68	0.09	1.95	15.97
1.95	0.09	2.28	16.06
2.28	0.11	2.65	16.16
2.65	0.01	3.09	16.18
3.09	0.27	3.60	16.45
3.60	0.24	4.19	16.69
4.19	0.35	4.88	17.04
4.88	0.55	5.69	17.59
5.69	0.84	6.63	18.43
6.63	1.24	7.72	19.66
7.72	1.78	9.00	21.44
9.00	2.46	10.48	23.90
10.48	3.26	12.21	27.16
12.21	4.12	14.22	31.29
14.22	4.98	16.57	36.27
16.57	5.72	19.31	41.99
19.31	6.24	22.49	48.23
22.49	6.46	26.20	54.69
26.20	6.40	30.53	61.09
30.53	6.12	35.56	67.21
35.56	5.53	41.43	72.74
41.43	4.66	48.27	77.39
48.27	3.78	56.23	81.17
56.23	3.07	65.51	84.24
65.51	2.34	76.32	86.58
76.32	2.00	88.91	88.59
88.91	1.77	103.58	90.36
103.58	1.64	120.67	92.00
120.67	1.55	140.58	93.55
140.58	1.43	163.77	94.98
163.77	1.27	190.80	96.25
190.80	1.05	222.28	97.31
222.28	0.81	258.95	98.12
258.95	0.57	301.68	98.68
301.68	0.35	351.46	99.04
351.46	0.27	409.45	99.30
409.45	0.25	477.01	99.55
477.01	0.21	555.71	99.76
555.71	0.14	647.41	99.90
647.41	0.08	754.23	99.98
754.23	0.02	878.67	100.00

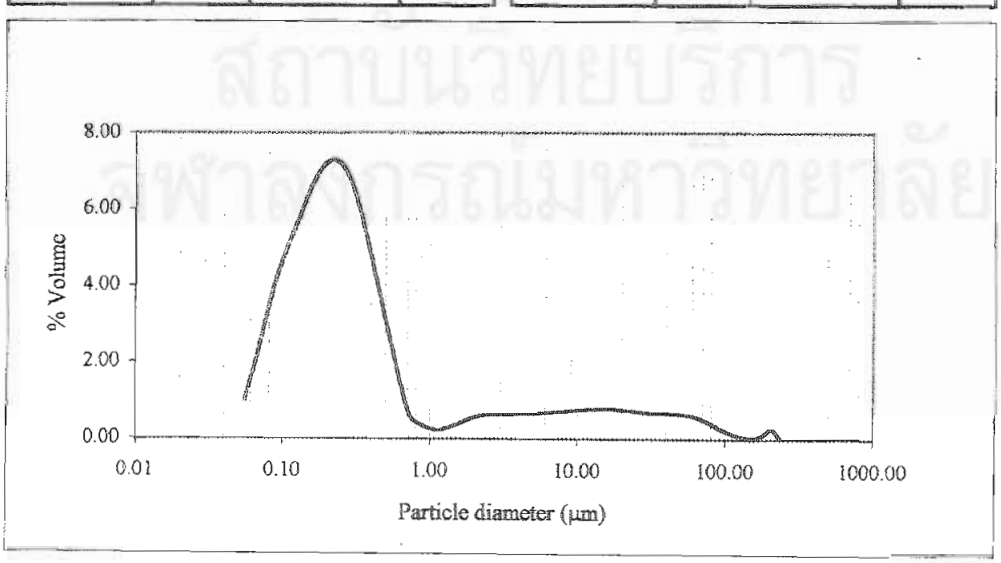

Figure d35 Particle size distribution of diazepam powder

Table d36 Particle size distribution of formulation of 0.5 DI + 5 GB + 4 TW80 prepared under pressure of 10,000 psi 7 cycles

Distribution type: volume	D(v,0.1) = 0.17	D(v,0.5) = 0.32	D(v,0.9) = 3.78
Mean diameter	D[4,3] = 1.67	D[3,2] = 0.31	Span = 11.21
% > 1 μm = 21.76	% > 5 μm = 8.44	% > 10 μm = 4.67	Uniformity = 4.48

size low (μm)	size in %	size high (μm)	under %	size low (μm)	size in %	size high (μm)	under %
0.05	0.14	0.06	0.14	6.63	0.83	7.72	93.88
0.06	0.31	0.07	0.45	7.72	0.86	9.00	94.74
0.07	0.48	0.08	0.93	9.00	0.87	10.48	95.61
0.08	0.70	0.09	1.63	10.48	0.88	12.21	96.49
0.09	1.01	0.11	2.64	12.21	0.85	14.22	97.34
0.11	1.46	0.13	4.10	14.22	0.77	16.57	98.11
0.13	2.18	0.15	6.28	16.57	0.64	19.31	98.74
0.15	3.37	0.17	9.64	19.31	0.47	22.49	99.22
0.17	5.34	0.20	14.99	22.49	0.31	26.20	99.52
0.20	8.29	0.23	23.28	26.20	0.17	30.53	99.70
0.23	11.48	0.27	34.75	30.53	0.10	35.56	99.79
0.27	12.69	0.31	47.45	35.56	0.07	41.43	99.86
0.31	10.75	0.36	58.20	41.43	0.05	48.27	99.91
0.36	7.65	0.42	65.85	48.27	0.04	56.23	99.95
0.42	5.27	0.49	71.13	56.23	0.02	65.51	99.98
0.49	3.45	0.58	74.57	65.51	0.01	76.32	99.99
0.58	1.87	0.67	76.45	76.32	0.00	88.91	99.99
0.67	0.91	0.78	77.35	88.91	0.00	103.58	99.99
0.78	0.52	0.91	77.87	103.58	0.00	120.67	99.99
0.91	0.28	1.06	78.15	120.67	0.00	140.58	99.99
1.06	0.20	1.24	78.35	140.58	0.00	163.77	99.99
1.24	2.01	1.44	80.36	163.77	0.00	190.80	99.99
1.44	2.04	1.68	82.40	190.80	0.00	222.28	99.99
1.68	1.91	1.95	84.32	222.28	0.01	258.95	100.00
1.95	1.72	2.28	86.03	258.95	0.00	301.68	100.00
2.28	1.46	2.65	87.50	301.68	0.00	351.46	100.00
2.65	1.21	3.09	88.71	351.46	0.00	409.45	100.00
3.09	1.02	3.60	89.73	409.45	0.00	477.01	100.00
3.60	0.89	4.19	90.62	477.01	0.00	555.71	100.00
4.19	0.82	4.88	91.44	555.71	0.00	647.41	100.00
4.88	0.80	5.69	92.24	647.41	0.00	754.23	100.00
5.69	0.81	6.63	93.05	754.23	0.00	878.67	100.00

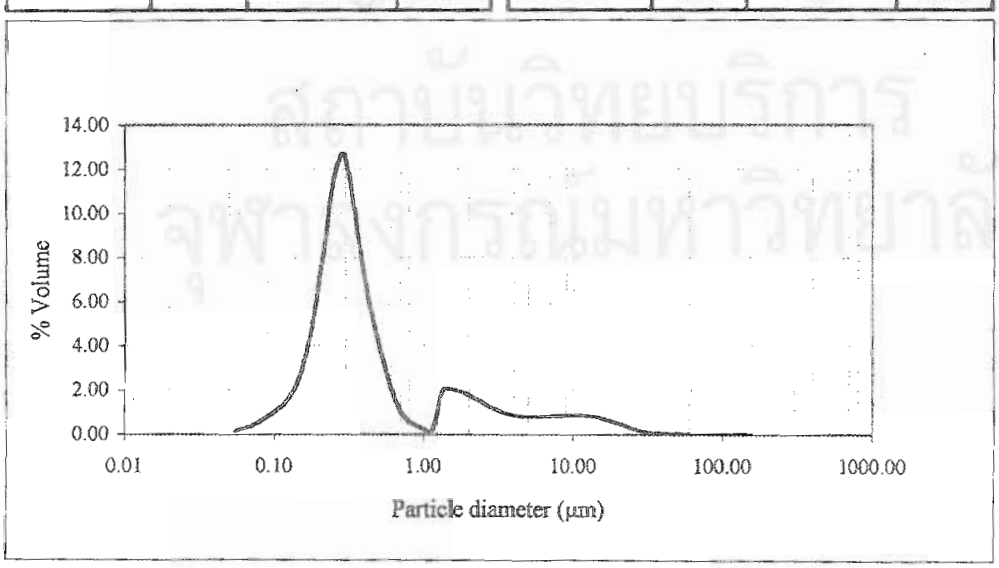

Figure d36 Particle size distribution of formulation of 0.5 DI + 5 GB + 4 TW80 prepared under pressure of 10,000 psi 7 cycles

Table d37 Particle size distribution of formulation of 0.5 DI + 5 GB + 4 TW80 prepared under pressure of 10,000 psi 9 cycles

Distribution type: volume	D(v,0.1) = 0.21	D(v,0.5) = 0.38	D(v,0.9) = 4.85
Mean diameter	D[4,3] = 2.87	D[3,2] = 0.37	Span = 12.21
% > 1 μm = 18.74	% > 5 μm = 9.89	% > 10 μm = 7.04	Uniformity = 6.85

size low (μm)	size in %	size high (μm)	under %
0.05	0.01	0.06	0.01
0.06	0.02	0.07	0.03
0.07	0.08	0.08	0.11
0.08	0.16	0.09	0.27
0.09	0.31	0.11	0.58
0.11	0.56	0.13	1.14
0.13	1.01	0.15	2.15
0.15	1.85	0.17	4.00
0.17	3.38	0.20	7.38
0.20	5.95	0.23	13.33
0.23	9.36	0.27	22.69
0.27	11.96	0.31	34.66
0.31	12.00	0.36	46.66
0.36	10.26	0.42	56.92
0.42	8.48	0.49	65.40
0.49	6.67	0.58	72.07
0.58	4.45	0.67	76.52
0.67	2.68	0.78	79.20
0.78	1.48	0.91	80.69
0.91	0.95	1.06	81.64
1.06	0.92	1.24	82.56
1.24	0.98	1.44	83.54
1.44	1.12	1.68	84.67
1.68	1.11	1.95	85.78
1.95	1.01	2.28	86.79
2.28	0.85	2.65	87.63
2.65	0.70	3.09	88.33
3.09	0.59	3.60	88.92
3.60	0.55	4.19	89.47
4.19	0.55	4.88	90.03
4.88	0.59	5.69	90.61
5.69	0.62	6.63	91.23
6.63	0.64	7.72	91.88
7.72	0.65	9.00	92.53
9.00	0.64	10.48	93.17
10.48	0.63	12.21	93.80
12.21	0.61	14.22	94.41
14.22	0.61	16.57	95.01
16.57	0.60	19.31	95.62
19.31	0.60	22.49	96.22
22.49	0.59	26.20	96.81
26.20	0.58	30.53	97.38
30.53	0.53	35.56	97.92
35.56	0.49	41.43	98.40
41.43	0.42	48.27	98.82
48.27	0.36	56.23	99.18
56.23	0.29	65.51	99.46
65.51	0.22	76.32	99.69
76.32	0.16	88.91	99.84
88.91	0.09	103.58	99.94
103.58	0.04	120.67	99.98
120.67	0.02	140.58	100.00
140.58	0.00	163.77	100.00
163.77	0.00	190.80	100.00
190.80	0.00	222.28	100.00
222.28	0.00	258.95	100.00
258.95	0.00	301.68	100.00
301.68	0.00	351.46	100.00
351.46	0.00	409.45	100.00
409.45	0.00	477.01	100.00
477.01	0.00	555.71	100.00
555.71	0.00	647.41	100.00
647.41	0.00	754.23	100.00
754.23	0.00	878.67	100.00

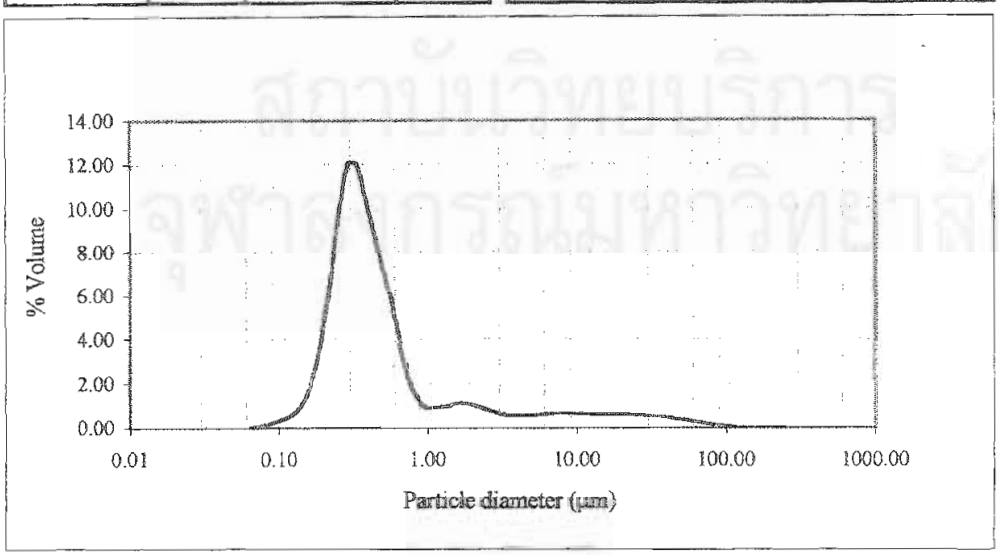

Figure d37 Particle size distribution of formulation of 0.5 DI + 5 GB + 4 TW80 prepared under pressure of 10,000 psi 9 cycles

Table d38 Particle size distribution of formulation of 0.5 DI + 5 GB + 4 TW80 prepared under pressure of 15,000 psi 5 cycles

Distribution type: volume	D(v,0.1) = 0.18	D(v,0.5) = 0.36	D(v,0.9) = 3.91
Mean diameter	D[4,3] = 3.31	D[3,2] = 0.33	Span = 10.47
% > 1 μm = 19.03	% > 5 μm = 9.04	% > 10 μm = 6.37	Uniformity = 8.62

size low (μm)	size in %	size high (μm)	under %	size low (μm)	size in %	size high (μm)	under %
0.05	0.11	0.06	0.11	6.63	0.60	7.72	92.66
0.06	0.23	0.07	0.34	7.72	0.59	9.00	93.25
0.07	0.39	0.08	0.73	9.00	0.57	10.48	93.81
0.08	0.58	0.09	1.31	10.48	0.55	12.21	94.36
0.09	0.85	0.11	2.16	12.21	0.53	14.22	94.89
0.11	1.23	0.13	3.39	14.22	0.51	16.57	95.41
0.13	1.84	0.15	5.23	16.57	0.50	19.31	95.90
0.15	2.82	0.17	8.05	19.31	0.47	22.49	96.37
0.17	4.43	0.20	12.48	22.49	0.43	26.20	96.81
0.20	6.83	0.23	19.31	26.20	0.37	30.53	97.18
0.23	9.61	0.27	28.92	30.53	0.30	35.56	97.48
0.27	11.26	0.31	40.18	35.56	0.25	41.43	97.73
0.31	10.62	0.36	50.80	41.43	0.22	48.27	97.95
0.36	8.71	0.42	59.51	48.27	0.23	56.23	98.18
0.42	7.02	0.49	66.53	56.23	0.28	65.51	98.46
0.49	5.50	0.58	72.04	65.51	0.35	76.32	98.82
0.58	3.76	0.67	75.80	76.32	0.41	88.91	99.22
0.67	2.43	0.78	78.23	88.91	0.39	103.58	99.62
0.78	1.86	0.91	80.09	103.58	0.29	120.67	99.91
0.91	1.47	1.06	81.56	120.67	0.09	140.58	100.00
1.06	1.28	1.24	82.84	140.58	0.00	163.77	100.00
1.24	1.17	1.44	84.01	163.77	0.00	190.80	100.00
1.44	1.24	1.68	85.25	190.80	0.00	222.28	100.00
1.68	1.11	1.95	86.36	222.28	0.00	258.95	100.00
1.95	1.01	2.28	87.37	258.95	0.00	301.68	100.00
2.28	0.89	2.65	88.26	301.68	0.00	351.46	100.00
2.65	0.77	3.09	89.02	351.46	0.00	409.45	100.00
3.09	0.66	3.60	89.68	409.45	0.00	477.01	100.00
3.60	0.60	4.19	90.28	477.01	0.00	555.71	100.00
4.19	0.59	4.88	90.87	555.71	0.00	647.41	100.00
4.88	0.59	5.69	91.46	647.41	0.00	754.23	100.00
5.69	0.60	6.63	92.06	754.23	0.00	878.67	100.00

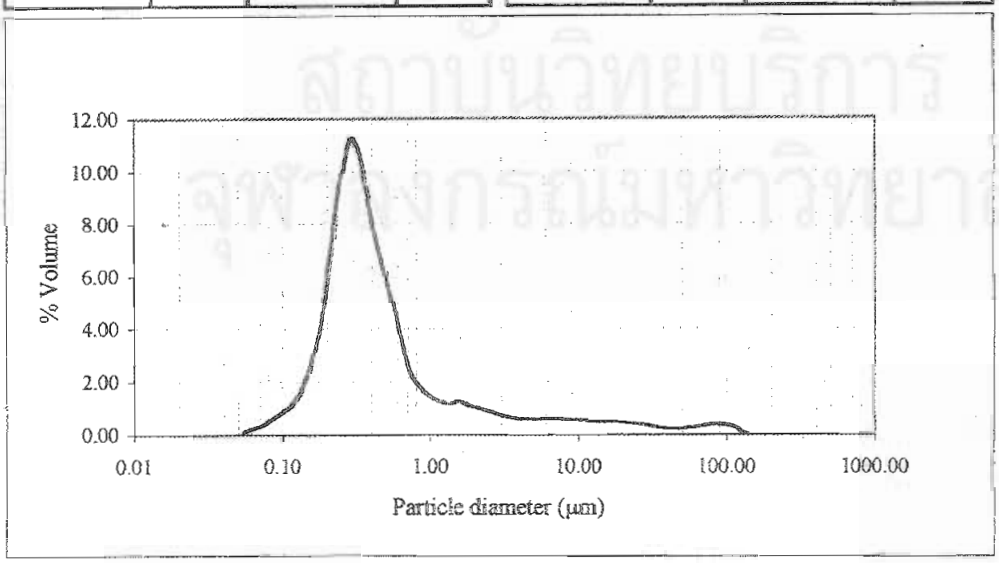

Figure d38 Particle size distribution of formulation of 0.5 DI + 5 GB + 4 TW80 prepared under pressure of 15,000 psi 5 cycles

Table d39 Particle size distribution of formulation of 0.5 DI + 5 GB + 4 TW80 prepared under pressure of 15,000 psi 7 cycles

Distribution type: volume	D(v,0.1) = 0.21	D(v,0.5) = 0.37	D(v,0.9) = 2.01
Mean diameter	D[4,3] = 2.01	D[3,2] = 0.36	Span = 4.89
% > 1 μm = 14.74	% > 5 μm = 6.79	% > 10 μm = 4.74	Uniformity = 4.76

size low (μm)	size in %	size high (μm)	under %	size low (μm)	size in %	size high (μm)	under %
0.05	0.01	0.06	0.01	6.63	0.47	7.72	94.46
0.06	0.03	0.07	0.04	7.72	0.48	9.00	94.94
0.07	0.07	0.08	0.11	9.00	0.48	10.48	95.42
0.08	0.17	0.09	0.28	10.48	0.47	12.21	95.89
0.09	0.32	0.11	0.60	12.21	0.46	14.22	96.35
0.11	0.59	0.13	1.19	14.22	0.45	16.57	96.80
0.13	1.06	0.15	2.25	16.57	0.44	19.31	97.24
0.15	1.93	0.17	4.18	19.31	0.42	22.49	97.66
0.17	3.53	0.20	7.70	22.49	0.40	26.20	98.07
0.20	6.21	0.23	13.92	26.20	0.37	30.53	98.43
0.23	9.77	0.27	23.69	30.53	0.33	35.56	98.76
0.27	12.50	0.31	36.19	35.56	0.29	41.43	99.05
0.31	12.55	0.36	48.74	41.43	0.24	48.27	99.29
0.36	10.74	0.42	59.48	48.27	0.20	56.23	99.49
0.42	8.90	0.49	68.38	56.23	0.17	65.51	99.66
0.49	7.03	0.58	75.41	65.51	0.14	76.32	99.80
0.58	4.71	0.67	80.12	76.32	0.11	88.91	99.91
0.67	2.88	0.78	83.00	88.91	0.07	103.58	99.98
0.78	1.63	0.91	84.63	103.58	0.02	120.67	100.00
0.91	1.05	1.06	85.68	120.67	0.00	140.58	100.00
1.06	1.00	1.24	86.68	140.58	0.00	163.77	100.00
1.24	1.01	1.44	87.69	163.77	0.00	190.80	100.00
1.44	1.11	1.68	88.80	190.80	0.00	222.28	100.00
1.68	1.05	1.95	89.85	222.28	0.00	258.95	100.00
1.95	0.89	2.28	90.74	258.95	0.00	301.68	100.00
2.28	0.70	2.65	91.45	301.68	0.00	351.46	100.00
2.65	0.54	3.09	91.99	351.46	0.00	409.45	100.00
3.09	0.42	3.60	92.41	409.45	0.00	477.01	100.00
3.60	0.37	4.19	92.78	477.01	0.00	555.71	100.00
4.19	0.37	4.88	93.15	555.71	0.00	647.41	100.00
4.88	0.40	5.69	93.55	647.41	0.00	754.23	100.00
5.69	0.44	6.63	94.00	754.23	0.00	878.67	100.00

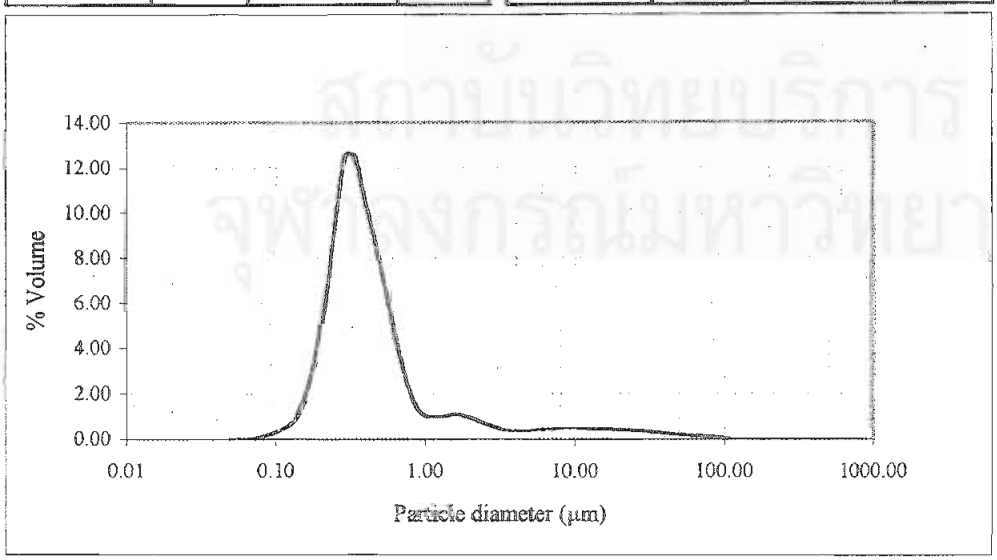

Figure d39 Particle size distribution of formulation of 0.5 DI + 5 GB + 4 TW80 prepared under pressure of 15,000 psi 7 cycles

Table d40 Particle size distribution of formulation of 0.5 DI + 5 GB + 4 TW80 prepared under pressure of 15,000 psi 9 cycles

Distribution type: volume	D(v,0.1) = 0.20	D(v,0.5) = 0.37	D(v,0.9) = 3.45
Mean diameter	D[4,3] = 3.91	D[3,2] = 0.35	Span = 8.73
% > 1 μm = 19.12	% > 5 μm = 9.19	% > 10 μm = 7.39	Uniformity = 9.81

size low (μm)	size in %	size high (μm)	under %	size low (μm)	size in %	size high (μm)	under %
0.05	0.08	0.06	0.08	6.63	0.41	7.72	91.88
0.06	0.17	0.07	0.26	7.72	0.43	9.00	92.31
0.07	0.29	0.08	0.55	9.00	0.45	10.48	92.76
0.08	0.45	0.09	1.00	10.48	0.46	12.21	93.22
0.09	0.65	0.11	1.64	12.21	0.49	14.22	93.71
0.11	0.96	0.13	2.60	14.22	0.52	16.57	94.22
0.13	1.46	0.15	4.06	16.57	0.55	19.31	94.77
0.15	2.30	0.17	6.36	19.31	0.58	22.49	95.36
0.17	3.78	0.20	10.14	22.49	0.60	26.20	95.96
0.20	6.20	0.23	16.34	26.20	0.61	30.53	96.57
0.23	9.31	0.27	25.65	30.53	0.60	35.56	97.17
0.27	11.46	0.31	37.11	35.56	0.55	41.43	97.72
0.31	10.99	0.36	48.10	41.43	0.48	48.27	98.20
0.36	9.04	0.42	57.14	48.27	0.39	56.23	98.60
0.42	7.40	0.49	64.54	56.23	0.29	65.51	98.89
0.49	5.99	0.58	70.53	65.51	0.21	76.32	99.10
0.58	4.27	0.67	74.80	76.32	0.14	88.91	99.24
0.67	2.95	0.78	77.75	88.91	0.14	103.58	99.38
0.78	2.13	0.91	79.88	103.58	0.08	120.67	99.46
0.91	1.66	1.06	81.54	120.67	0.10	140.58	99.56
1.06	1.47	1.24	83.01	140.58	0.11	163.77	99.67
1.24	1.44	1.44	84.45	163.77	0.10	190.80	99.77
1.44	1.37	1.68	85.81	190.80	0.09	222.28	99.86
1.68	1.21	1.95	87.02	222.28	0.07	258.95	99.93
1.95	1.02	2.28	88.04	258.95	0.04	301.68	99.97
2.28	0.84	2.65	88.88	301.68	0.02	351.46	99.99
2.65	0.68	3.09	89.57	351.46	0.01	409.45	100.00
3.09	0.61	3.60	90.18	409.45	0.00	477.01	100.00
3.60	0.28	4.19	90.46	477.01	0.00	555.71	100.00
4.19	0.30	4.88	90.76	555.71	0.00	647.41	100.00
4.88	0.34	5.69	91.10	647.41	0.00	754.23	100.00
5.69	0.38	6.63	91.47	754.23	0.00	878.67	100.00

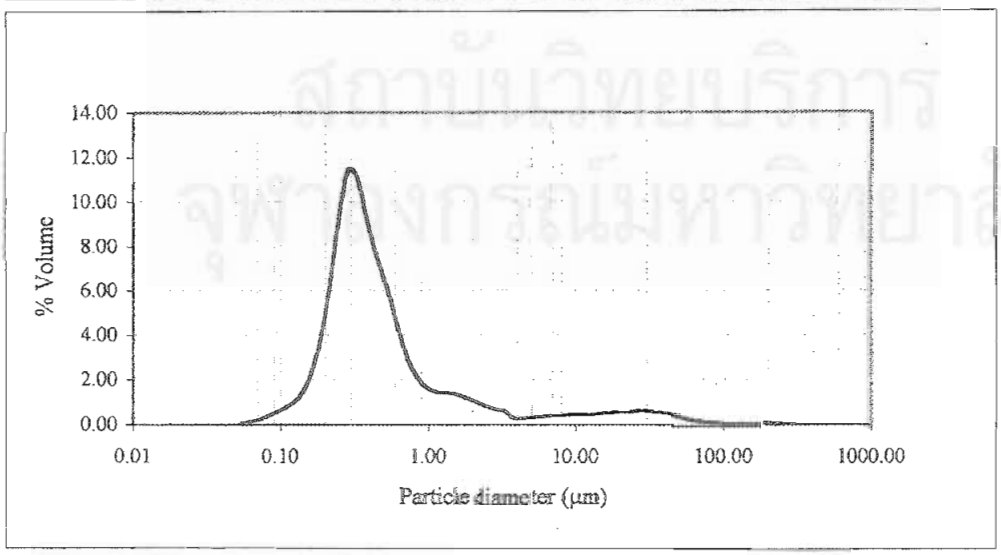

Figure d40 Particle size distribution of formulation of 0.5 DI + 5 GB + 4 TW80 prepared under pressure of 15,000 psi 9 cycles

Table d41 Particle size distribution of formulation of 0.5 DI + 5 GB + 4 TW80 prepared under pressure of 20,000 psi 5 cycles

Distribution type: volume	D(v,0.1) = 0.22	D(v,0.5) = 0.36	D(v,0.9) = 0.77
Mean diameter	D[4,3] = 2.42	D[3,2] = 0.35	Span = 1.52
% > 1 μm = 8.81	% > 5 μm = 5.28	% > 10 μm = 3.90	Uniformity = 5.99

size low (μm)	size in %	size high (μm)	under %	size low (μm)	size in %	size high (μm)	under %
0.05	0.00	0.06	0.00	6.63	0.32	7.72	95.58
0.06	0.00	0.07	0.00	7.72	0.32	9.00	95.89
0.07	0.02	0.08	0.02	9.00	0.31	10.48	96.20
0.08	0.05	0.09	0.07	10.48	0.29	12.21	96.49
0.09	0.12	0.11	0.19	12.21	0.27	14.22	96.76
0.11	0.27	0.13	0.46	14.22	0.26	16.57	97.02
0.13	0.61	0.15	1.07	16.57	0.26	19.31	97.28
0.15	1.33	0.17	2.40	19.31	0.26	22.49	97.54
0.17	2.85	0.20	5.25	22.49	0.25	26.20	97.79
0.20	5.76	0.23	11.01	26.20	0.25	30.53	98.04
0.23	10.19	0.27	21.20	30.53	0.25	35.56	98.29
0.27	14.20	0.31	35.40	35.56	0.23	41.43	98.52
0.31	15.02	0.36	50.42	41.43	0.21	48.27	98.74
0.36	13.16	0.42	63.58	48.27	0.20	56.23	98.94
0.42	10.89	0.49	74.47	56.23	0.18	65.51	99.11
0.49	8.30	0.58	82.76	65.51	0.16	76.32	99.28
0.58	5.01	0.67	87.77	76.32	0.14	88.91	99.42
0.67	2.45	0.78	90.22	88.91	0.13	103.58	99.55
0.78	0.85	0.91	91.07	103.58	0.11	120.67	99.66
0.91	0.19	1.06	91.26	120.67	0.08	140.58	99.74
1.06	0.09	1.24	91.35	140.58	0.05	163.77	99.79
1.24	0.29	1.44	91.64	163.77	0.10	190.80	99.89
1.44	0.46	1.68	92.10	190.80	0.11	222.28	100.00
1.68	0.53	1.95	92.62	222.28	0.00	258.95	100.00
1.95	0.51	2.28	93.13	258.95	0.00	301.68	100.00
2.28	0.42	2.65	93.55	301.68	0.00	351.46	100.00
2.65	0.34	3.09	93.89	351.46	0.00	409.45	100.00
3.09	0.28	3.60	94.17	409.45	0.00	477.01	100.00
3.60	0.25	4.19	94.42	477.01	0.00	555.71	100.00
4.19	0.26	4.88	94.68	555.71	0.00	647.41	100.00
4.88	0.28	5.69	94.96	647.41	0.00	754.23	100.00
5.69	0.30	6.63	95.26	754.23	0.00	878.67	100.00

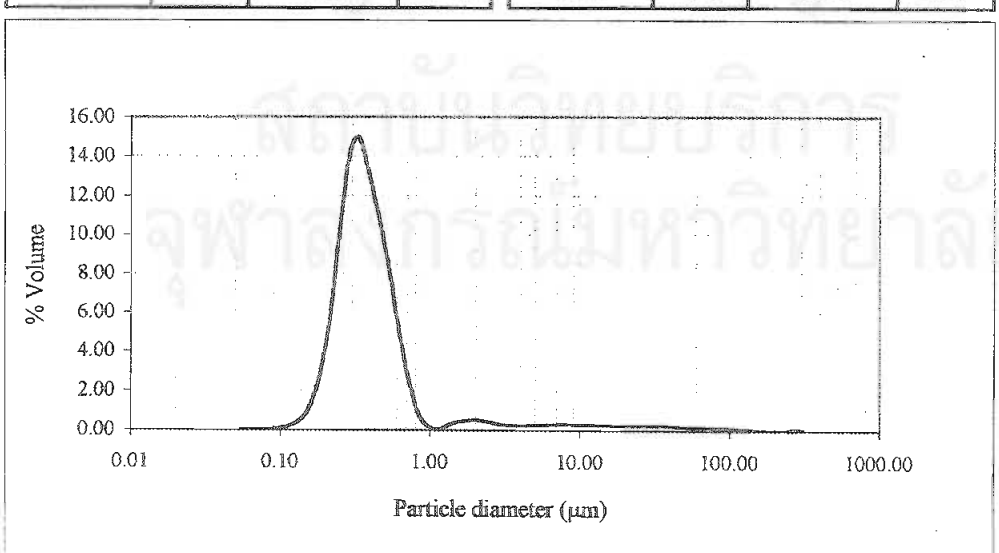

Figure d41 Particle size distribution of formulation of 0.5 DI + 5 GB + 4 TW80 prepared under pressure of 20,000 psi 5 cycles

Table d42 Particle size distribution of formulation of 0.5 DI + 5 GB + 4 TW80 prepared under pressure of 20,000 psi 7 cycles

Distribution type: volume	D(v,0.1) = 0.22	D(v,0.5) = 0.37	D(v,0.9) = 10.32
Mean diameter	D[4,3] = 7.82	D[3,2] = 0.37	Span = 27.59
% > 1 μm = 17.64	% > 5 μm = 12.38	% > 10 μm = 10.11	Uniformity = 20.62

size low (μm)	size in %	size high (μm)	under %	size low (μm)	size in %	size high (μm)	under %
0.05	0.00	0.06	0.00	6.63	0.52	7.72	89.00
0.06	0.03	0.07	0.03	7.72	0.53	9.00	89.53
0.07	0.06	0.08	0.08	9.00	0.53	10.48	90.06
0.08	0.13	0.09	0.21	10.48	0.52	12.21	90.58
0.09	0.24	0.11	0.45	12.21	0.51	14.22	91.09
0.11	0.47	0.13	0.93	14.22	0.51	16.57	91.60
0.13	0.88	0.15	1.81	16.57	0.51	19.31	92.11
0.15	1.68	0.17	3.49	19.31	0.52	22.49	92.63
0.17	3.26	0.20	6.75	22.49	0.52	26.20	93.15
0.20	6.05	0.23	12.80	26.20	0.51	30.53	93.67
0.23	9.97	0.27	22.77	30.53	0.50	35.56	94.17
0.27	13.06	0.31	35.83	35.56	0.48	41.43	94.65
0.31	13.03	0.36	48.86	41.43	0.44	48.27	95.09
0.36	10.90	0.42	59.76	48.27	0.42	56.23	95.51
0.42	8.77	0.49	68.53	56.23	0.40	65.51	95.91
0.49	6.65	0.58	75.18	65.51	0.43	76.32	96.35
0.58	4.08	0.67	79.26	76.32	0.46	88.91	96.81
0.67	2.11	0.78	81.37	88.91	0.52	103.58	97.33
0.78	0.82	0.91	82.20	103.58	0.57	120.67	97.90
0.91	0.27	1.06	82.47	120.67	0.57	140.58	98.47
1.06	0.23	1.24	82.70	140.58	0.51	163.77	98.98
1.24	0.46	1.44	83.15	163.77	0.39	190.80	99.37
1.44	0.68	1.68	83.83	190.80	0.25	222.28	99.62
1.68	0.74	1.95	84.57	222.28	0.18	258.95	99.81
1.95	0.70	2.28	85.27	258.95	0.19	301.68	100.00
2.28	0.59	2.65	85.87	301.68	0.00	351.46	100.00
2.65	0.49	3.09	86.36	351.46	0.00	409.45	100.00
3.09	0.41	3.60	86.77	409.45	0.00	477.01	100.00
3.60	0.39	4.19	87.15	477.01	0.00	555.71	100.00
4.19	0.40	4.88	87.56	555.71	0.00	647.41	100.00
4.88	0.44	5.69	88.00	647.41	0.00	754.23	100.00
5.69	0.49	6.63	88.48	754.23	0.00	878.67	100.00

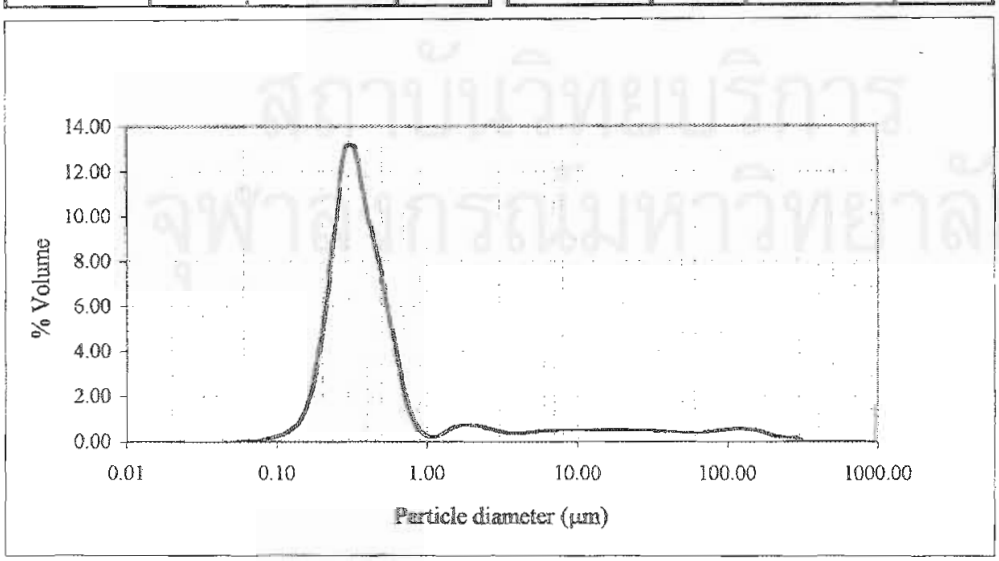

Figure d42 Particle size distribution of formulation of 0.5 DI + 5 GB + 4 TW80 prepared under pressure of 20,000 psi 7 cycles

Table d43 Particle size distribution of formulation of 0.5 DI + 5 GB + 4 TW80 prepared under pressure of 20,000 psi 9 cycles

Distribution type: volume	D(v,0.1) = 0.22	D(v,0.5) = 0.37	D(v,0.9) = 1.21
Mean diameter	D[4,3] = 1.92	D[3,2] = 0.36	Span = 2.69
% > 1 μm = 10.86	% > 5 μm = 5.83	% > 10 μm = 4.16	Uniformity = 5.22

size low (μm)	size in %	size high (μm)	under %	size low (μm)	size in %	size high (μm)	under %
0.05	0.00	0.06	0.00	6.63	0.38	7.72	95.20
0.06	0.02	0.07	0.02	7.72	0.39	9.00	95.59
0.07	0.04	0.08	0.06	9.00	0.37	10.48	95.96
0.08	0.09	0.09	0.16	10.48	0.37	12.21	96.33
0.09	0.19	0.11	0.34	12.21	0.36	14.22	96.69
0.11	0.36	0.13	0.71	14.22	0.36	16.57	97.04
0.13	0.71	0.15	1.42	16.57	0.36	19.31	97.40
0.15	1.43	0.17	2.85	19.31	0.36	22.49	97.77
0.17	2.89	0.20	5.74	22.49	0.36	26.20	98.13
0.20	5.69	0.23	11.43	26.20	0.34	30.53	98.47
0.23	9.88	0.27	21.31	30.53	0.32	35.56	98.79
0.27	13.43	0.31	34.74	35.56	0.27	41.43	99.06
0.31	13.76	0.36	48.50	41.43	0.23	48.27	99.29
0.36	11.77	0.42	60.27	48.27	0.19	56.23	99.48
0.42	9.87	0.49	70.14	56.23	0.16	65.51	99.64
0.49	7.99	0.58	78.13	65.51	0.11	76.32	99.75
0.58	5.40	0.67	83.53	76.32	0.10	88.91	99.85
0.67	3.31	0.78	86.84	88.91	0.08	103.58	99.93
0.78	1.75	0.91	88.59	103.58	0.04	120.67	99.97
0.91	0.91	1.06	89.50	120.67	0.00	140.58	99.97
1.06	0.59	1.24	90.09	140.58	0.00	163.77	99.97
1.24	0.60	1.44	90.69	163.77	0.00	190.80	99.97
1.44	0.62	1.68	91.32	190.80	0.00	222.28	99.97
1.68	0.60	1.95	91.92	222.28	0.00	258.95	99.97
1.95	0.54	2.28	92.46	258.95	0.03	301.68	100.00
2.28	0.44	2.65	92.89	301.68	0.00	351.46	100.00
2.65	0.36	3.09	93.25	351.46	0.00	409.45	100.00
3.09	0.29	3.60	93.54	409.45	0.00	477.01	100.00
3.60	0.28	4.19	93.83	477.01	0.00	555.71	100.00
4.19	0.30	4.88	94.12	555.71	0.00	647.41	100.00
4.88	0.34	5.69	94.46	647.41	0.00	754.23	100.00
5.69	0.36	6.63	94.82	754.23	0.00	878.67	100.00

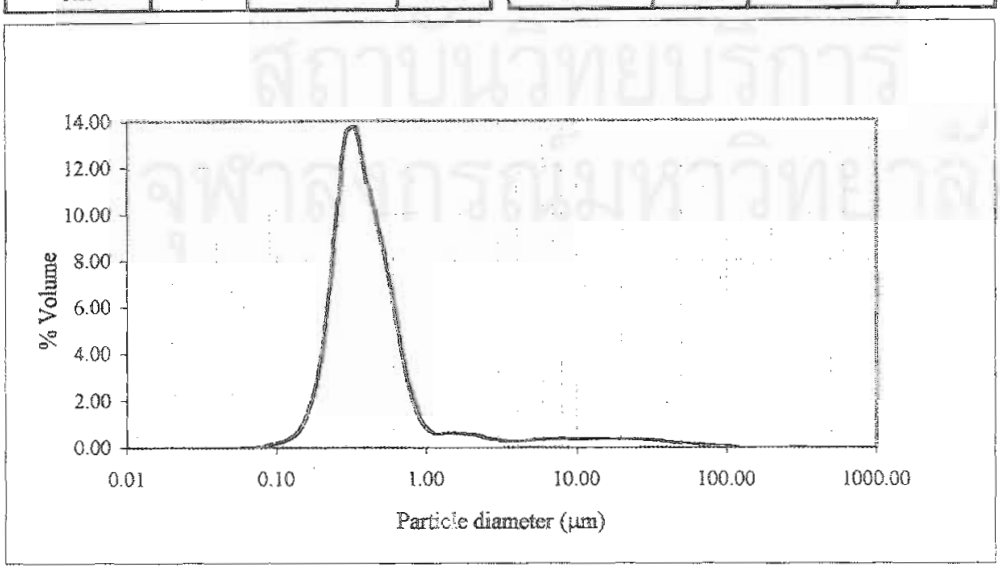

Figure d43 Particle size distribution of formulation of 0.5 DI + 5 GB + 4 TW80 prepared under pressure of 20,000 psi 9 cycles

Table d44 Particle size distribution of formulation of 0.3 DI + 5 GB + 4 TW80 prepared under pressure of 20,000 psi 5 cycles

Distribution type: volume	D(v,0.1) = 0.09	D(v,0.5) = 0.24	D(v,0.9) = 0.76
Mean diameter	D[4,3] = 1.64	D[3,2] = 0.19	Span = 2.81
% > 1 μm = 8.90	% > 5 μm = 5.94	% > 10 μm = 4.17	Uniformity = 6.28

size low (μm)	size in %	size high (μm)	under %	size low (μm)	size in %	size high (μm)	under %
0.05	0.97	0.06	0.97	6.63	0.40	7.72	95.22
0.06	1.93	0.07	2.91	7.72	0.38	9.00	95.60
0.07	2.88	0.08	5.79	9.00	0.35	10.48	95.94
0.08	3.80	0.09	9.59	10.48	0.34	12.21	96.49
0.09	4.68	0.11	14.27	12.21	0.35	14.22	96.84
0.11	5.51	0.13	19.79	14.22	0.35	16.57	97.18
0.13	6.28	0.15	26.06	16.57	0.35	19.31	97.54
0.15	6.97	0.17	33.03	19.31	0.37	22.49	97.90
0.17	7.55	0.20	40.59	22.49	0.36	26.20	98.26
0.20	7.96	0.23	48.55	26.20	0.34	30.53	98.60
0.23	8.08	0.27	56.62	30.53	0.31	35.56	98.91
0.27	7.79	0.31	64.42	35.56	0.26	41.43	99.17
0.31	7.08	0.36	71.50	41.43	0.23	48.27	99.40
0.36	6.08	0.42	77.58	48.27	0.20	56.23	99.59
0.42	4.95	0.49	82.52	56.23	0.16	65.51	99.76
0.49	3.75	0.58	86.27	65.51	0.13	76.32	99.89
0.58	2.54	0.67	88.81	76.32	0.08	88.91	99.97
0.67	1.48	0.78	90.29	88.91	0.03	103.58	100.00
0.78	0.69	0.91	90.98	103.58	0.00	120.67	100.00
0.91	0.21	1.06	91.19	120.67	0.00	140.58	100.00
1.06	0.04	1.24	91.23	140.58	0.00	163.77	100.00
1.24	0.08	1.44	91.31	163.77	0.00	190.80	100.00
1.44	0.18	1.68	91.49	190.80	0.00	222.28	100.00
1.68	0.27	1.95	91.76	222.28	0.00	258.95	100.00
1.95	0.34	2.28	92.10	258.95	0.00	301.68	100.00
2.28	0.36	2.65	92.46	301.68	0.00	351.46	100.00
2.65	0.37	3.09	92.83	351.46	0.00	409.45	100.00
3.09	0.38	3.60	93.20	409.45	0.00	477.01	100.00
3.60	0.39	4.19	93.60	477.01	0.00	555.71	100.00
4.19	0.40	4.88	94.00	555.71	0.00	647.41	100.00
4.88	0.41	5.69	94.41	647.41	0.00	754.23	100.00
5.69	0.41	6.63	94.82	754.23	0.00	878.67	100.00

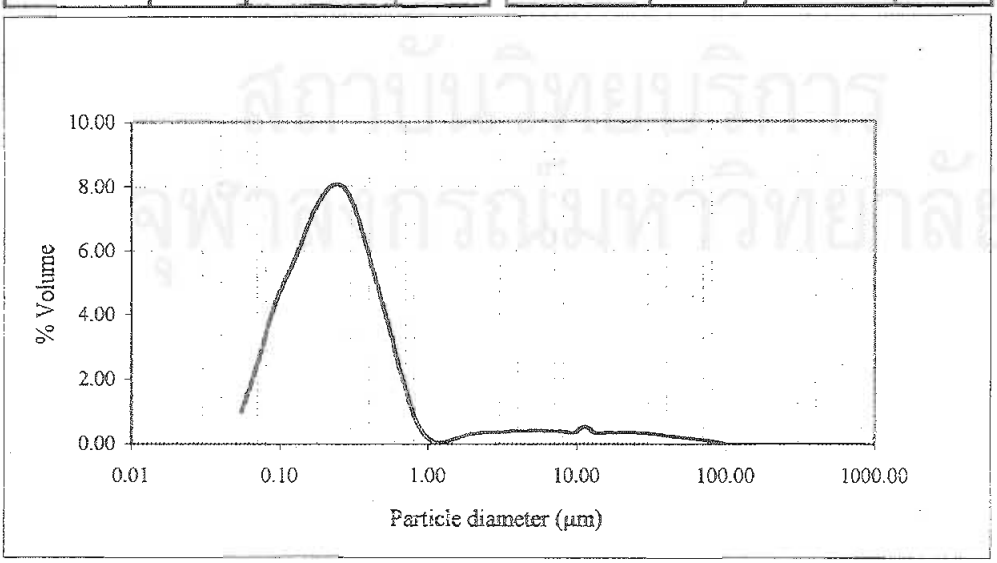

Figure d44 Particle size distribution of formulation of 0.3 DI + 5 GB + 4 TW80 prepared under pressure of 20,000 psi 5 cycles

Table d45 Particle size distribution of formulation of 0.3 DI + 5 GB + 4 TW80 after storage under accelerated condition

Distribution type: volume	D(v,0.1) = 0.20	D(v,0.5) = 0.34	D(v,0.9) = 2.05
Mean diameter	D[4,3] = 2.50	D[3,2] = 0.33	Span = 5.49
% > 1 μm = 12.28	% > 5 μm = 6.39	% > 10 μm = 4.36	Uniformity = 6.67

size low (μm)	size in %	size high (μm)	under %	size low (μm)	size in %	size high (μm)	under %
0.05	0.01	0.06	0.01	6.63	0.46	7.72	94.98
0.06	0.04	0.07	0.05	7.72	0.41	9.00	95.39
0.07	0.11	0.08	0.17	9.00	0.36	10.48	95.75
0.08	0.24	0.09	0.41	10.48	0.32	12.21	96.08
0.09	0.45	0.11	0.85	12.21	0.20	14.22	96.27
0.11	0.80	0.13	1.65	14.22	0.20	16.57	96.48
0.13	1.42	0.15	3.07	16.57	0.32	19.31	96.80
0.15	2.50	0.17	5.57	19.31	0.30	22.49	97.10
0.17	4.39	0.20	9.96	22.49	0.19	26.20	97.29
0.20	7.42	0.23	17.39	26.20	0.35	30.53	97.64
0.23	11.21	0.27	28.60	30.53	0.29	35.56	97.93
0.27	13.86	0.31	42.45	35.56	0.25	41.43	98.19
0.31	13.51	0.36	55.97	41.43	0.25	48.27	98.44
0.36	11.17	0.42	67.14	48.27	0.32	56.23	98.75
0.42	8.74	0.49	75.87	56.23	0.30	65.51	99.05
0.49	6.26	0.58	82.13	65.51	0.28	76.32	99.33
0.58	3.54	0.67	85.67	76.32	0.23	88.91	99.56
0.67	1.51	0.78	87.18	88.91	0.18	103.58	99.73
0.78	0.49	0.91	87.68	103.58	0.15	120.67	99.88
0.91	0.07	1.06	87.75	120.67	0.07	140.58	99.95
1.06	0.03	1.24	87.78	140.58	0.04	163.77	99.99
1.24	0.39	1.44	88.17	163.77	0.01	190.80	100.00
1.44	0.72	1.68	88.89	190.80	0.00	222.28	100.00
1.68	0.84	1.95	89.73	222.28	0.00	258.95	100.00
1.95	0.84	2.28	90.58	258.95	0.00	301.68	100.00
2.28	0.75	2.65	91.32	301.68	0.00	351.46	100.00
2.65	0.64	3.09	91.96	351.46	0.00	409.45	100.00
3.09	0.56	3.60	92.52	409.45	0.00	477.01	100.00
3.60	0.52	4.19	93.04	477.01	0.00	555.71	100.00
4.19	0.50	4.88	93.54	555.71	0.00	647.41	100.00
4.88	0.49	5.69	94.03	647.41	0.00	754.23	100.00
5.69	0.49	6.63	94.52	754.23	0.00	878.67	100.00

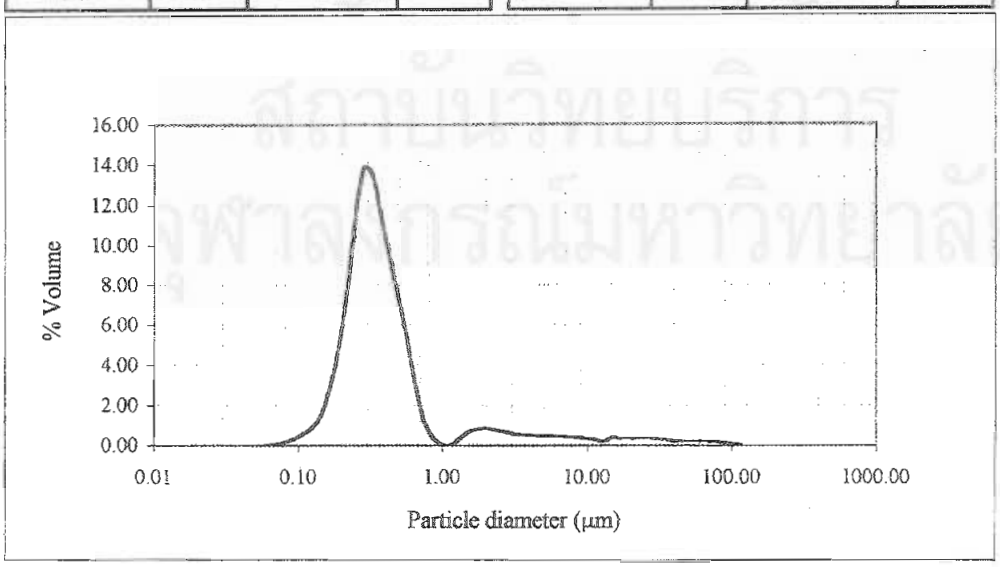

Figure d45 Particle size distribution of formulation of 0.3 DI + 5 GB + 4 TW80 after storage under accelerated condition

Table d46 Particle size distribution of formulation of 0.5 DI + 5 GB + 4 TW80 after storage under accelerated condition

Distribution type: volume	D(v,0.1) = 0.21	D(v,0.5) = 0.39	D(v,0.9) = 17.02
Mean diameter	D[4,3] = 9.25	D[3,2] = 0.39	Span = 43.12
% > 1 μm = 23.96	% > 5 μm = 16.76	% > 10 μm = 12.61	Uniformity = 23.05

size low (μm)	size in %	size high (μm)	under %	size low (μm)	size in %	size high (μm)	under %
0.05	0.01	0.06	0.01	6.63	0.92	7.72	85.98
0.06	0.03	0.07	0.04	7.72	0.86	9.00	86.84
0.07	0.09	0.08	0.13	9.00	0.81	10.48	87.65
0.08	0.19	0.09	0.33	10.48	0.77	12.21	88.42
0.09	0.37	0.11	0.69	12.21	0.74	14.22	89.16
0.11	0.65	0.13	1.35	14.22	0.73	16.57	89.88
0.13	1.14	0.15	2.49	16.57	0.71	19.31	90.60
0.15	2.01	0.17	4.49	19.31	0.69	22.49	91.29
0.17	3.51	0.20	8.01	22.49	0.67	26.20	91.96
0.20	5.95	0.23	13.95	26.20	0.64	30.53	92.60
0.23	9.04	0.27	22.99	30.53	0.60	35.56	93.20
0.27	11.24	0.31	34.24	35.56	0.55	41.43	93.75
0.31	11.08	0.36	45.32	41.43	0.55	48.27	94.30
0.36	9.42	0.42	54.74	48.27	0.51	56.23	94.81
0.42	7.83	0.49	62.57	56.23	0.50	65.51	95.31
0.49	6.11	0.58	68.68	65.51	0.50	76.32	95.81
0.58	3.92	0.67	72.60	76.32	0.66	88.91	96.46
0.67	2.22	0.78	74.82	88.91	0.53	103.58	96.99
0.78	0.99	0.91	75.81	103.58	0.53	120.67	97.53
0.91	0.39	1.06	76.19	120.67	0.52	140.58	98.05
1.06	0.21	1.24	76.41	140.58	0.47	163.77	98.52
1.24	0.31	1.44	76.72	163.77	0.88	190.80	99.40
1.44	0.48	1.68	77.20	190.80	0.31	222.28	99.71
1.68	0.62	1.95	77.81	222.28	0.20	258.95	99.91
1.95	0.73	2.28	78.54	258.95	0.09	301.68	100.00
2.28	0.80	2.65	79.34	301.68	0.00	351.46	100.00
2.65	0.87	3.09	80.21	351.46	0.00	409.45	100.00
3.09	0.92	3.60	81.13	409.45	0.00	477.01	100.00
3.60	0.97	4.19	82.10	477.01	0.00	555.71	100.00
4.19	0.99	4.88	83.09	555.71	0.00	647.41	100.00
4.88	1.00	5.69	84.09	647.41	0.00	754.23	100.00
5.69	0.97	6.63	85.06	754.23	0.00	878.67	100.00

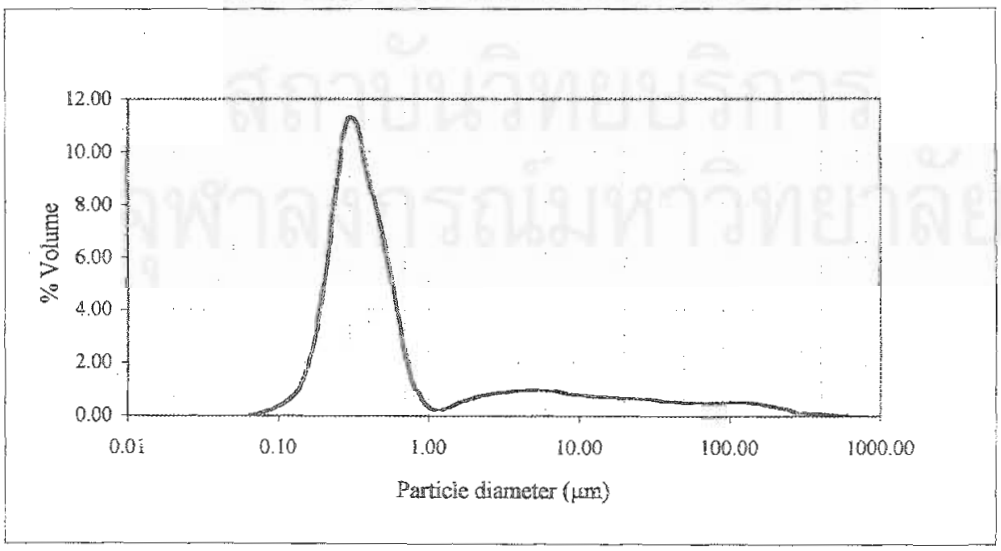

Figure d46 Particle size distribution of formulation of 0.5 DI + 5 GB + 4 TW80 after storage under accelerated condition

Table d47 Particle size distribution of formulation of 5 GB + 0.5 TW20 after autoclaving

Distribution type: volume	D(v,0.1) = 0.24	D(v,0.5) = 0.85	D(v,0.9) = 14.42
Mean diameter	D[4,3] = 6.48	D[3,2] = 0.56	Span = 16.78
% > 1 µm = 45.76	% > 5 µm = 21.41	% > 10 µm = 13.43	Uniformity = 7.19

size low (µm)	size in %	size high (µm)	under %	size low (µm)	size in %	size high (µm)	under %
0.05	0.05	0.06	0.05	6.63	1.84	7.72	83.66
0.06	0.12	0.07	0.17	7.72	1.79	9.00	85.45
0.07	0.19	0.08	0.36	9.00	1.66	10.48	87.11
0.08	0.29	0.09	0.65	10.48	1.48	12.21	88.60
0.09	0.41	0.11	1.06	12.21	1.31	14.22	89.90
0.11	0.59	0.13	1.66	14.22	1.15	16.57	91.05
0.13	0.87	0.15	2.53	16.57	1.02	19.31	92.07
0.15	1.32	0.17	3.85	19.31	0.94	22.49	93.02
0.17	2.03	0.20	5.88	22.49	0.90	26.20	93.92
0.20	3.12	0.23	9.00	26.20	0.87	30.53	94.79
0.23	4.40	0.27	13.40	30.53	0.85	35.56	95.63
0.27	5.41	0.31	18.81	35.56	0.80	41.43	96.44
0.31	5.56	0.36	24.37	41.43	0.75	48.27	97.18
0.36	5.20	0.42	29.57	48.27	0.65	56.23	97.83
0.42	4.95	0.49	34.52	56.23	0.55	65.51	98.38
0.49	4.83	0.58	39.35	65.51	0.42	76.32	98.81
0.58	4.46	0.67	43.81	76.32	0.32	88.91	99.13
0.67	4.20	0.78	48.02	88.91	0.22	103.58	99.34
0.78	3.96	0.91	51.98	103.58	0.14	120.67	99.49
0.91	3.77	1.06	55.75	120.67	0.10	140.58	99.59
1.06	3.58	1.24	59.33	140.58	0.05	163.77	99.64
1.24	3.35	1.44	62.68	163.77	0.05	190.80	99.68
1.44	3.04	1.68	65.72	190.80	0.05	222.28	99.74
1.68	2.66	1.95	68.37	222.28	0.07	258.95	99.80
1.95	2.27	2.28	70.65	258.95	0.07	301.68	99.87
2.28	1.89	2.65	72.54	301.68	0.06	351.46	99.94
2.65	1.52	3.09	74.05	351.46	0.04	409.45	99.98
3.09	1.38	3.60	75.43	409.45	0.02	477.01	100.00
3.60	1.40	4.19	76.83	477.01	0.00	555.71	100.00
4.19	1.51	4.88	78.34	555.71	0.00	647.41	100.00
4.88	1.68	5.69	80.02	647.41	0.00	754.23	100.00
5.69	1.80	6.63	81.82	754.23	0.00	878.67	100.00

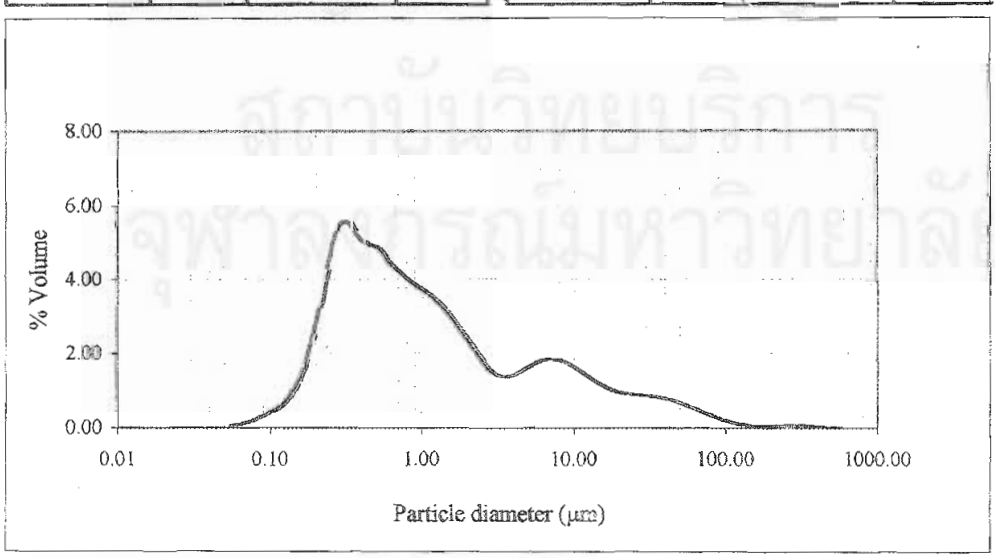

Figure d47 Particle size distribution of formulation of 5 GB + 0.5 TW20 after autoclaving

Table d48 Particle size distribution of formulation of 5 GB + 1 TW20 after autoclaving

Distribution type: volume	D(v,0.1) = 0.21	D(v,0.5) = 0.37	D(v,0.9) = 0.84
Mean diameter	D[4,3] = 2.32	D[3,2] = 0.35	Span = 1.67
% > 1 μm = 7.49	% > 5 μm = 4.11	% > 10 μm = 3.51	Uniformity = 5.53

size low (μm)	size in %	size high (μm)	under %	size low (μm)	size in %	size high (μm)	under %
0.05	0.01	0.06	0.01	6.63	0.14	7.72	96.27
0.06	0.02	0.07	0.03	7.72	0.13	9.00	96.41
0.07	0.07	0.08	0.10	9.00	0.13	10.48	96.54
0.08	0.15	0.09	0.25	10.48	0.13	12.21	96.67
0.09	0.29	0.11	0.54	12.21	0.15	14.22	96.81
0.11	0.54	0.13	1.08	14.22	0.16	16.57	96.97
0.13	0.97	0.15	2.05	16.57	0.19	19.31	97.16
0.15	1.79	0.17	3.84	19.31	0.22	22.49	97.38
0.17	3.31	0.20	7.15	22.49	0.25	26.20	97.63
0.20	5.91	0.23	13.05	26.20	0.27	30.53	97.89
0.23	9.48	0.27	22.53	30.53	0.27	35.56	98.17
0.27	12.42	0.31	34.96	35.56	0.27	41.43	98.44
0.31	12.88	0.36	47.83	41.43	0.25	48.27	98.69
0.36	11.51	0.42	59.34	48.27	0.23	56.23	98.93
0.42	10.10	0.49	69.44	56.23	0.20	65.51	99.13
0.49	8.62	0.58	78.06	65.51	0.18	76.32	99.31
0.58	6.39	0.67	84.45	76.32	0.15	88.91	99.46
0.67	4.40	0.78	88.85	88.91	0.13	103.58	99.59
0.78	2.72	0.91	91.57	103.58	0.11	120.67	99.69
0.91	1.58	1.06	93.15	120.67	0.09	140.58	99.79
1.06	0.92	1.24	94.07	140.58	0.07	163.77	99.86
1.24	0.57	1.44	94.64	163.77	0.06	190.80	99.92
1.44	0.38	1.68	95.01	190.80	0.03	222.28	99.95
1.68	0.25	1.95	95.26	222.28	0.02	258.95	99.97
1.95	0.17	2.28	95.43	258.95	0.02	301.68	99.99
2.28	0.10	2.65	95.53	301.68	0.01	351.46	100.00
2.65	0.08	3.09	95.61	351.46	0.00	409.45	100.00
3.09	0.07	3.60	95.68	409.45	0.00	477.01	100.00
3.60	0.09	4.19	95.76	477.01	0.00	555.71	100.00
4.19	0.11	4.88	95.87	555.71	0.00	647.41	100.00
4.88	0.13	5.69	96.00	647.41	0.00	754.23	100.00
5.69	0.13	6.63	96.13	754.23	0.00	878.67	100.00

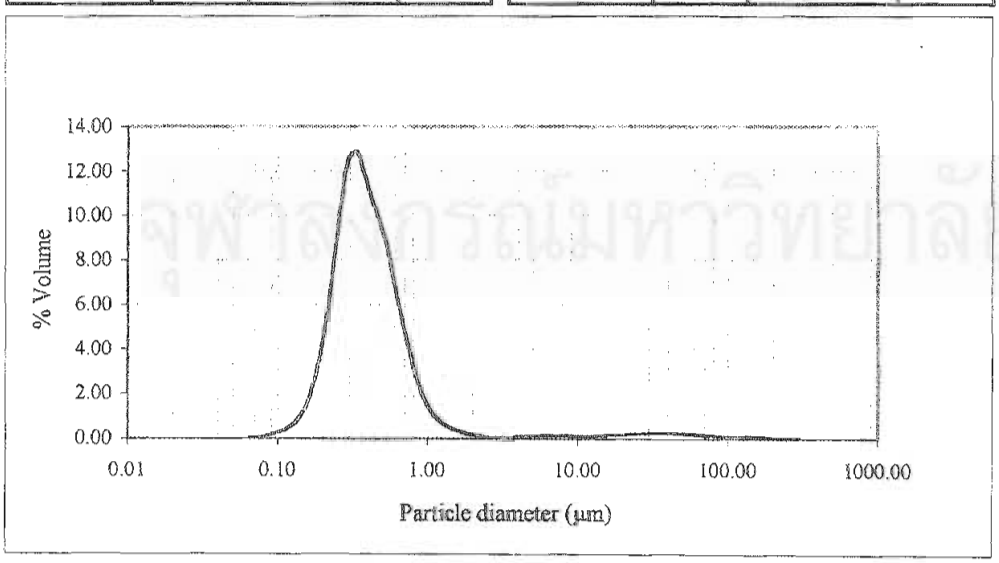

Figure d48 Particle size distribution of formulation of 5 GB + 1 TW20 after autoclaving

Table d49 Particle size distribution of formulation of 5 GB + 2 TW20 after autoclaving

Distribution type: volume	D(v,0.1) = 0.21	D(v,0.5) = 0.34	D(v,0.9) = 11.40
Mean diameter	D[4,3] = 18.97	D[3,2] = 0.34	Span = 32.53
% > 1 µm = 12.55	% > 5 µm = 10.96	% > 10 µm = 10.17	Uniformity = 54.38

size low (µm)	size in %	size high (µm)	under %	size low (µm)	size in %	size high (µm)	under %
0.05	0.00	0.06	0.00	6.63	0.18	7.72	89.50
0.06	0.02	0.07	0.02	7.72	0.20	9.00	89.70
0.07	0.05	0.08	0.07	9.00	0.20	10.48	89.90
0.08	0.12	0.09	0.19	10.48	0.19	12.21	90.09
0.09	0.25	0.11	0.44	12.21	0.19	14.22	90.28
0.11	0.48	0.13	0.92	14.22	0.18	16.57	90.46
0.13	0.94	0.15	1.86	16.57	0.19	19.31	90.64
0.15	1.85	0.17	3.71	19.31	0.30	22.49	90.94
0.17	3.63	0.20	7.34	22.49	0.31	26.20	91.26
0.20	6.80	0.23	14.15	26.20	0.32	30.53	91.57
0.23	11.23	0.27	25.38	30.53	0.32	35.56	91.90
0.27	14.68	0.31	40.06	35.56	0.32	41.43	92.22
0.31	14.59	0.36	54.65	41.43	0.33	48.27	92.55
0.36	12.00	0.42	66.65	48.27	0.34	56.23	92.89
0.42	9.28	0.49	75.93	56.23	0.37	65.51	93.26
0.49	6.51	0.58	82.44	65.51	0.41	76.32	93.67
0.58	3.47	0.67	85.91	76.32	0.47	88.91	94.14
0.67	1.33	0.78	87.24	88.91	0.53	103.58	94.68
0.78	0.19	0.91	87.43	103.58	0.59	120.67	95.27
0.91	0.03	1.06	87.46	120.67	0.60	140.58	95.86
1.06	0.13	1.24	87.58	140.58	0.55	163.77	96.42
1.24	0.18	1.44	87.76	163.77	0.47	190.80	96.89
1.44	0.27	1.68	88.03	190.80	0.37	222.28	97.26
1.68	0.28	1.95	88.31	222.28	0.29	258.95	97.56
1.95	0.25	2.28	88.56	258.95	0.28	301.68	97.83
2.28	0.19	2.65	88.75	301.68	0.28	351.46	98.11
2.65	0.14	3.09	88.89	351.46	0.33	409.45	98.44
3.09	0.05	3.60	88.94	409.45	0.40	477.01	98.84
3.60	0.04	4.19	88.98	477.01	0.44	555.71	99.28
4.19	0.04	4.88	89.02	555.71	0.40	647.41	99.68
4.88	0.14	5.69	89.15	647.41	0.25	754.23	99.93
5.69	0.17	6.63	89.32	754.23	0.07	878.67	100.00

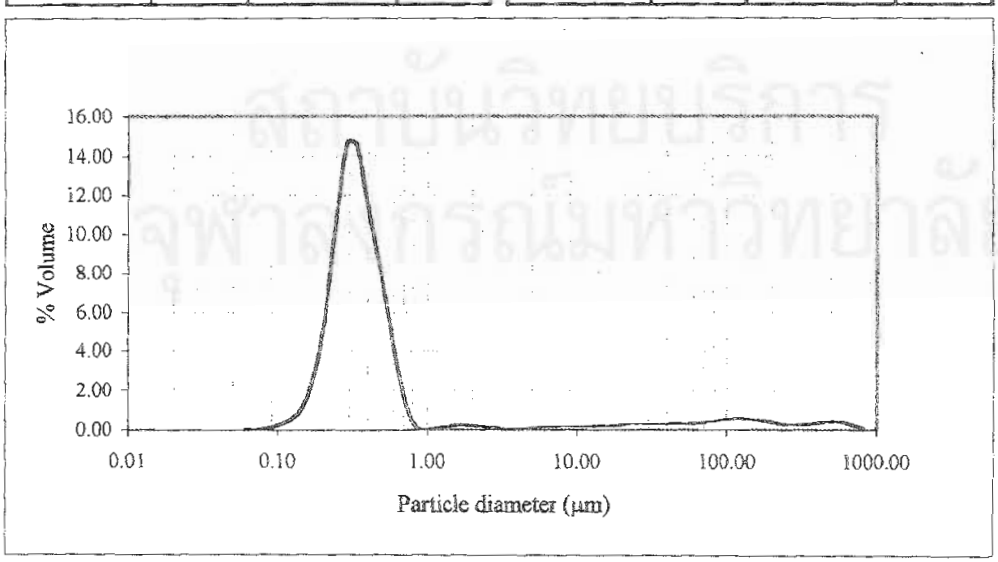

Figure d49 Particle size distribution of formulation of 5 GB + 2 TW20 after autoclaving

Table d50 Particle size distribution of formulation of 5 GB + 3 TW20 after autoclaving

Distribution type: volume	D(v,0.1) = 0.44	D(v,0.5) = 2.13	D(v,0.9) = 4.95
Mean diameter	D[4,3] = 2.89	D[3,2] = 1.14	Span = 2.12
% > 1 μm = 74.09	% > 5 μm = 9.72	% > 10 μm = 1.09	Uniformity = 0.87

size low (μm)	size in %	size high (μm)	under %	size low (μm)	size in %	size high (μm)	under %
0.05	0.00	0.06	0.00	6.63	1.53	7.72	98.30
0.06	0.00	0.07	0.00	7.72	0.60	9.00	98.90
0.07	0.00	0.08	0.00	9.00	0.02	10.48	98.91
0.08	0.00	0.09	0.01	10.48	0.00	12.21	98.91
0.09	0.01	0.11	0.02	12.21	0.00	14.22	98.91
0.11	0.01	0.13	0.03	14.22	0.00	16.57	98.91
0.13	0.03	0.15	0.06	16.57	0.00	19.31	98.91
0.15	0.07	0.17	0.13	19.31	0.05	22.49	98.97
0.17	0.20	0.20	0.33	22.49	0.13	26.20	99.10
0.20	0.53	0.23	0.86	26.20	0.19	30.53	99.28
0.23	1.27	0.27	2.13	30.53	0.20	35.56	99.48
0.27	2.18	0.31	4.31	35.56	0.18	41.43	99.66
0.31	2.55	0.36	6.85	41.43	0.14	48.27	99.80
0.36	2.44	0.42	9.29	48.27	0.08	56.23	99.88
0.42	2.53	0.49	11.82	56.23	0.05	65.51	99.93
0.49	2.85	0.58	14.67	65.51	0.01	76.32	99.94
0.58	2.87	0.67	17.54	76.32	0.00	88.91	99.94
0.67	3.03	0.78	20.57	88.91	0.00	103.58	99.94
0.78	3.22	0.91	23.79	103.58	0.00	120.67	99.94
0.91	3.54	1.06	27.33	120.67	0.00	140.58	99.94
1.06	3.92	1.24	31.24	140.58	0.00	163.77	99.94
1.24	4.43	1.44	35.67	163.77	0.00	190.80	99.94
1.44	5.02	1.68	40.69	190.80	0.01	222.28	99.95
1.68	5.72	1.95	46.41	222.28	0.02	258.95	99.97
1.95	6.59	2.28	53.00	258.95	0.03	301.68	100.00
2.28	7.39	2.65	60.39	301.68	0.00	351.46	100.00
2.65	8.14	3.09	68.52	351.46	0.00	409.45	100.00
3.09	8.06	3.60	76.58	409.45	0.00	477.01	100.00
3.60	7.21	4.19	83.79	477.01	0.00	555.71	100.00
4.19	5.85	4.88	89.65	555.71	0.00	647.41	100.00
4.88	4.31	5.69	93.95	647.41	0.00	754.23	100.00
5.69	2.81	6.63	96.77	754.23	0.00	878.67	100.00

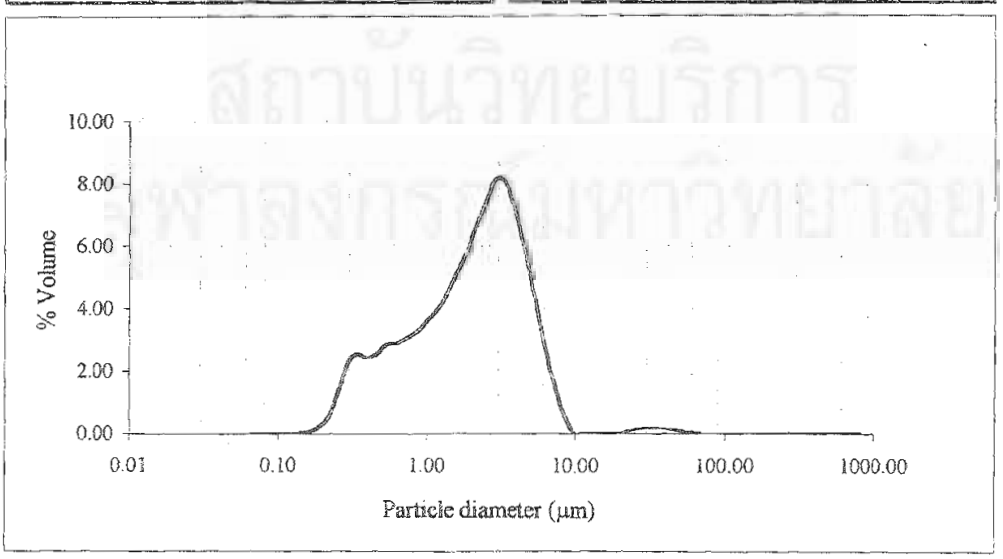

Figure d50 Particle size distribution of formulation of 5 GB + 3 TW20 after autoclaving

Table d51 Particle size distribution of formulation of 5 GB + 4 TW20 after autoclaving

Distribution type: volume	D(v,0.1) = 0.28	D(v,0.5) = 1.88	D(v,0.9) = 28.58
Mean diameter	D[4,3] = 10.43	D[3,2] = 0.73	Span = 15.04
% > 1 µm = 56.64	% > 5 µm = 41.89	% > 10 µm = 31.20	Uniformity = 5.25

size low (µm)	size in %	size high (µm)	under %
0.05	0.01	0.06	0.01
0.06	0.03	0.07	0.04
0.07	0.05	0.08	0.09
0.08	0.08	0.09	0.17
0.09	0.13	0.11	0.30
0.11	0.21	0.13	0.51
0.13	0.36	0.15	0.87
0.15	0.66	0.17	1.54
0.17	1.26	0.20	2.80
0.20	2.40	0.23	5.20
0.23	4.08	0.27	9.28
0.27	5.48	0.31	14.76
0.31	5.60	0.36	20.36
0.36	4.89	0.42	25.25
0.42	4.39	0.49	29.64
0.49	4.04	0.58	33.69
0.58	3.34	0.67	37.03
0.67	2.78	0.78	39.81
0.78	2.34	0.91	42.15
0.91	2.01	1.06	44.17
1.06	1.77	1.24	45.93
1.24	1.60	1.44	47.54
1.44	1.47	1.68	49.00
1.68	1.33	1.95	50.34
1.95	1.24	2.28	51.58
2.28	1.17	2.65	52.74
2.65	1.14	3.09	53.88
3.09	1.18	3.60	55.07
3.60	1.30	4.19	56.36
4.19	1.49	4.88	57.85
4.88	1.74	5.69	59.59
5.69	2.04	6.63	61.63
6.63	2.37	7.72	64.00
7.72	2.72	9.00	66.72
9.00	3.07	10.48	69.80
10.48	3.36	12.21	73.16
12.21	3.50	14.22	76.66
14.22	3.46	16.57	80.11
16.57	3.26	19.31	83.37
19.31	2.92	22.49	86.29
22.49	2.53	26.20	88.83
26.20	2.14	30.53	90.96
30.53	1.79	35.56	92.75
35.56	1.50	41.43	94.25
41.43	1.27	48.27	95.52
48.27	1.08	56.23	96.60
56.23	0.91	65.51	97.52
65.51	0.75	76.32	98.27
76.32	0.60	88.91	98.86
88.91	0.45	103.58	99.32
103.58	0.32	120.67	99.63
120.67	0.20	140.58	99.83
140.58	0.11	163.77	99.94
163.77	0.04	190.80	99.98
190.80	0.01	222.28	99.98
222.28	0.00	258.95	99.98
258.95	0.02	301.68	100.00
301.68	0.00	351.46	100.00
351.46	0.00	409.45	100.00
409.45	0.00	477.01	100.00
477.01	0.00	555.71	100.00
555.71	0.00	647.41	100.00
647.41	0.00	754.23	100.00
754.23	0.00	878.67	100.00

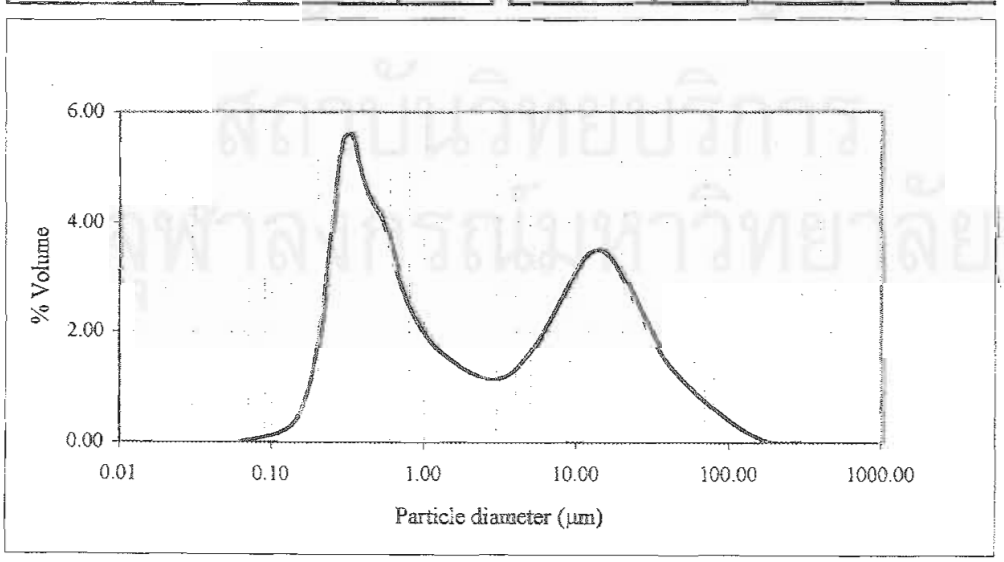

Figure d51 Particle size distribution of formulation of 5 GB + 4 TW20 after autoclaving

Table d52 Particle size distribution of formulation of 5 GB + 5 TW20 after autoclaving

Distribution type: volume	D(v,0.1) = 0.33	D(v,0.5) = 8.74	D(v,0.9) = 65.90
Mean diameter	D[4,3] = 22.95	D[3,2] = 1.09	Span = 7.50
% > 1 μm = 71.48	% > 5 μm = 57.48	% > 10 μm = 47.60	Uniformity = 2.40

size low (μm)	size in %	size high (μm)	under %	size low (μm)	size in %	size high (μm)	under %
0.05	0.02	0.06	0.02	6.63	2.20	7.72	48.00
0.06	0.04	0.07	0.06	7.72	2.51	9.00	50.51
0.07	0.07	0.08	0.13	9.00	2.79	10.48	53.30
0.08	0.11	0.09	0.24	10.48	3.03	12.21	56.33
0.09	0.15	0.11	0.39	12.21	3.18	14.22	59.50
0.11	0.23	0.13	0.63	14.22	3.23	16.57	62.74
0.13	0.35	0.15	0.98	16.57	3.21	19.31	65.94
0.15	0.56	0.17	1.54	19.31	3.11	22.49	69.06
0.17	0.90	0.20	2.44	22.49	3.00	26.20	72.06
0.20	1.46	0.23	3.90	26.20	2.88	30.53	74.94
0.23	2.19	0.27	6.09	30.53	2.89	35.56	77.82
0.27	2.80	0.31	8.89	35.56	2.96	41.43	80.79
0.31	2.96	0.36	11.85	41.43	3.06	48.27	83.85
0.36	2.82	0.42	14.67	48.27	3.09	56.23	86.94
0.42	2.76	0.49	17.43	56.23	2.97	65.51	89.90
0.49	2.75	0.58	20.18	65.51	2.68	76.32	92.58
0.58	2.57	0.67	22.75	76.32	2.23	88.91	94.82
0.67	2.41	0.78	25.16	88.91	1.72	103.58	96.54
0.78	2.18	0.91	27.34	103.58	1.21	120.67	97.75
0.91	1.97	1.06	29.31	120.67	0.79	140.58	98.54
1.06	1.76	1.24	31.07	140.58	0.48	163.77	99.02
1.24	1.58	1.44	32.65	163.77	0.30	190.80	99.32
1.44	1.40	1.68	34.05	190.80	0.22	222.28	99.54
1.68	1.25	1.95	35.30	222.28	0.19	258.95	99.73
1.95	1.15	2.28	36.45	258.95	0.15	301.68	99.88
2.28	1.07	2.65	37.52	301.68	0.09	351.46	99.97
2.65	1.06	3.09	38.58	351.46	0.03	409.45	100.00
3.09	1.10	3.60	39.68	409.45	0.00	477.01	100.00
3.60	1.22	4.19	40.89	477.01	0.00	555.71	100.00
4.19	1.39	4.88	42.28	555.71	0.00	647.41	100.00
4.88	1.62	5.69	43.91	647.41	0.00	754.23	100.00
5.69	1.90	6.63	45.80	754.23	0.00	878.67	100.00

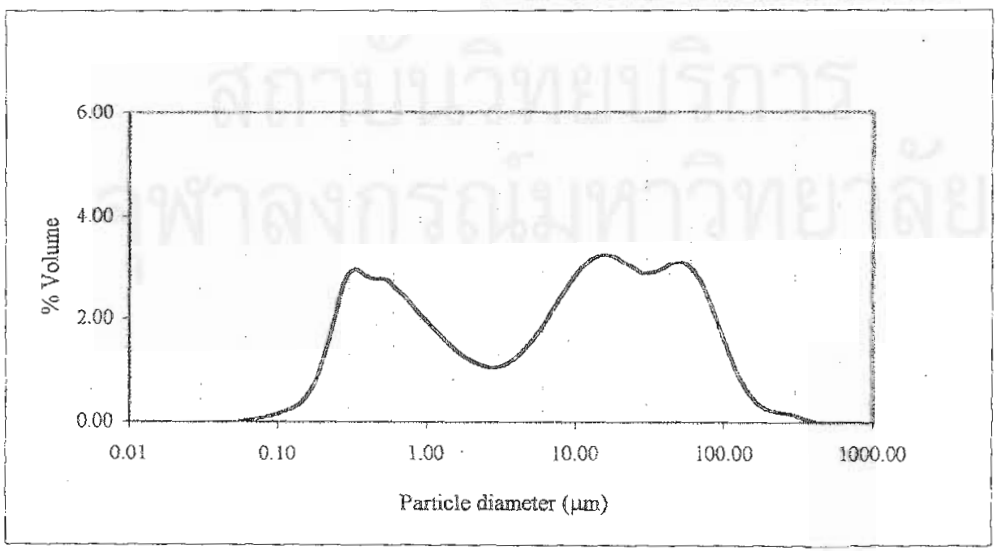

Figure d52 Particle size distribution of formulation of 5 GB + 5 TW20 after autoclaving

VITA

Mrs. Amornrat Viriyaroj was born on March 7, 1974 in Sri Sa Ket, Thailand. She received the Bachelor of Science in Pharmacy from Faculty of Pharmaceutical Sciences, Chulalongkorn University in 1996. After graduation, she had worked at Srinagarind Hospital, Faculty of Medicine, Khon Kaen University. Since 1998 she has been working for Department of Pharmaceutical Technology, Faculty of Pharmaceutical Sciences, Khon Kaen University.

จุฬาลงกรณ์มหาวิทยาลัย